Analysis of human holocytochrome c synthase (*HCCS*) as a candidate gene for X-linked oncocytic cardiomyopathy

By

Quenten P. Schwarz (BSc. Hons.)

University of Adelaide
School of Molecular and Biomedical Science
Discipline of Genetics

February, 2004

The work contained in this thesis contains no material that has been accepted for the award of any other degree or diploma in any University or other tertiary institution and, to the best of my knowledge and belief, contains no material previously published except where due reference has been made.

I give consent to this copy of my thesis, when deposited in the University Library, being available for loan and copying.

Quenten P. Schwarz (Bsc. Hons.)

Acknowledgements.

I would like to thank a number of the people that have had a major influence on me throughout the entirety of this PhD. First of all I must mention a great friend of mine that I have the utmost respect for. Luckily for me he has also been my primary supervisor for the past 5 years. Tim, you have always been there whenever I have needed advice on this project and have also been a fantastic mentor in every aspect of my life. I can't thank you enough for having me in your lab ("Hail to the chief", JFK). I also want to thank Liza for being around during the tough times and being a great person to learn from. Without your guidance this PhD may have taken even longer than it has. We should definitely open that bottle of wine now!

Needless to say but many an idea (not great but hey!) has come over a few bevies at the Unibar. One of the stalwarts of the Thursday afternoon schnitzel deserves a big thanks for being both an inspirational mate and a fantastic colleague (we never did get around to writing a paper together). Kieran, you have been a solid shoulder throughout and now that you are almost married all I have left to say to you is "go forth and multiply". While on the subject of the bar, I would also like to thank Dave (and Sas) for being there for all these years. It's been a long slog, but well worth the effort. I must also thank the other member of the "terrible threesome" frisbee throwers. Blair, you have been a great Post Doc to have in the lab, and a great listener to all of the nonsense that seems to conjure up in my head. I must also thank another fantastic person, Paul. Your endless hours fixing all of the "stuff" that goes wrong anywhere in the building have been most appreciated and it's been great to have you as a partner in crime out of work too.

To the rest of the members of the "Cox Lab" throughout my PhD (Julie, Bel, Saidi, Lillian, Leila, Sonia, Nathan and Annette) – You have all played a huge part in the work presented in this thesis and for that I thank you immensely. You have also made "work-time" really enjoyable (well sometimes anyhow), but just as important, you have been fantastic mates during "playtime". I only hope that you take the time to keep Bob in his most handsome state.

My family also deserve a big thanks for being so supportive and really, just for being a great bunch of people (you can so tell I am one of them!). Mum, Dad, Darren, Kim, Sharee, Mick, Witley, Talyn and the pets, thanks for everything, you guys make me who I am and make life worth living.

Lastly, but perhaps most importantly, I would like to thank the most beautiful girl in the world. Gen, you have been there for me in possibly the most frustrating period of my life. You have kept everything running smoothly, kept me motivated, cooked endlessly, which I must say doesn't necessarily have to stop now, and been the best a boy could have. Thanks for everything, can I watch TV now? To leave by adding a little bit of my own to a famous Groucho Marx quote "I've had a great time, but writing this wasn't it".

Table of Contents.

Amendments to thesis

Spelling and Grammatical errors

Fig1.1 - Replace BA333 in the figure with BA337. The scale bar in this figure is only approximately 10kb.
p17, P2, L5 - Replace dissorder with disorder.
p17, P4, L3 - Replace Morea s with Morea's.
Fig1.2 - Complex II is composed of 4 nuclear encoded subunits not 2.
Fig1.2 - Replace "immer-membrane" with "inner membrane".
Fig1.2 - Replace mitochondria with mitochondrial.
p19, P2, L8 - Replace supplies with supply.
p19, P4, L3 - Replace "is then" with "are then".
p21, P2, L1 - Replace complexes with complex.
p21, P2, L10 - Replace "by a numerous" with "by numerous".
p22, P2, L14 - Replace uncommen with uncommon.
Fig1.4 - Replace "where is then able" with "where it is then able".
p24, P1, L11 - Replace "previously used" with "suitable for".
p24, P2, L14 - Replace consereved with conserved.
p26, P1, L20 - Replace oportunity with opportunity.
p27, P3, L7 - Replace lilt with little.
p55, P2, L4 - Replace mM with mg/ml.
Fig 3.5 - Replace shrter with shorter.
p58, P3, L7 - Replace Cyc2p with Cyt2p.
p71, P3, L2 - Replace matutration with maturation.
p71, P4, L5 - Replace "This data" with "These data".
p74, P3, L3 - Replace Cyc2p with Cyt2p.
p74, P3, L4 - Replace "able catalyse" with "able to catalyse".
p77, P2, L10 - Replace 4.3B with 4.2B.
p78, P1, L3 - Replace Cyc2p with Cyt2p.
p78, P2, L13 - Replace Cyc2p with Cyt2p.
p90, P1, L5 - Replace Cyc2p with Cyt2p.
p91, P1, L7 - Replace cytoplasm's with cytoplasms.
p96, P3, L6 - Replace unsuccesfull with unsuccessfull.
p98, P2, L2 - Replace hundred's with hundreds.
p99, P1, L12 - Replace "unable detect" with "unable to detect".
p99, P2, L11 - Replace dulbeco's with Dulbecco's.
p106, P1, L3 - Replace support with supports
p110, P3, L1 - Replace fascilitate with facilitate.
p112, P1, L12 - Replace flase with false.
p114, P1, L7 - Replace "toapproximately" with "to approximately".
p114, P2, L4 - This sentence should read, "… promoter region, while an …".
p115, P1, L6 - Replace homolgy with homology.
p126, P3, L9 - Replace "were then" with "was then".
p127, P1 L1 - Replace sitre with site.
p130, P2, L1 - Replace aplification with amplification.
p130, P2, L1 - Replace "without G418 resistance" with "without G418".
p135, P1, L9 - Replace Cyc2p with Cyt2p.
p136, P1, L18 - Replace "there differences" with "these differences".
p138, P3, L1 - Replace Chapter 6 with Chapter 5
p143, Ref13 - Remove duplicated reference.
p146, Ref15 - Replace Newpert with Neupert, and Translocation with Translocation.

Further points of discussion

Chapter Three

3.2.5.1 - Several reasons were discussed for the lack of an interaction between CYTC and HCCS in the Y2H analysis. Further to this, it is also possible that the fusion proteins are localized to the mitochondria via mitochondrial targeting signals. As the three reporter systems of this assay rely on protein interactions within the nucleus, these signals may therefore interfere with the identification of any interaction.

Fig 3.4 - The data presented in this figure are representative of several immunoprecipitation experiments completed with anti-HCCS antibody.

Chapter Five

Table 5.3 - Replaced with a table showing corrected data.

5.2.3.1 - Given that patients HC1 and HC2 have differing polymorphisms in the *cytochrome b* sequence, it is unlikely that the two are indeed siblings. This has no influence on the discussions of sequence variations identified in this study.

5.2.3.2 - Upon examination, it was noted that the Human Mitochondrial Genome Database lists the G15431A variant and the C15452A variant in 10 of 746 and 90 of 746 human mitochondrial DNA sequences, respectively (see http://www.genpat.uu.se/mtDB). Although this may suggest that they are benign variants, the C1542A variant remains exciting as it is associated with respiratory deficiencies (Marin-Garcia *et al*, 1996). While perhaps unlikely, it is also possible that the identified non-coding variations are pathogenic based on alterations of internal regulatory sequences within the gene.

5.2.3.5 - The coding mutations were suggested to be heteroplasmic, however, the results should be more correctly referred to as homoplasmic.

Exon / Frag.	HB	HC1	HC2	HC3	HC4	HC5	Wang
HCCS							
1	++	+	+	+	+	+	+
2	+	+	+	?	+	+	+
3	+	++	+	+	+	+	+
4	+	+	+			++	+
5	+	+	+	+	+	++	+
6	++	++	+	+	+	+	+
7	+	+		+	+	+	?
Cytochrome b							
1	?	?	+	+		+	+
2	?	?	?	?	+	?	++
3	+	+	+	+	?	?	+
4	+	?	?	?	+	+	+

Chapter One: General Introduction.

1.1 Abnormalities of the short arm of the X chromosome.

At the onset of the work presented in this thesis, the distal short arm of the X chromosome (Xp) was one of the most well characterised regions within the human genome. A significant factor contributing to this has been the elevated frequency of genomic rearrangements within this region. The vast numbers of published Xp structural anomalies usually occur via X/Y translocations, X/autosomal translocations, duplications and deletions (interstitial and terminal) and more rarely, inversions. These alterations arise as a result of the region containing large numbers of locally repeated sequences and the region of sequence identity with the Y chromosome (pseudo-autosomal region), the main site at which the X and Y chromosomes pair during meiosis (Ballabio & Andria, 1992). Such anomalies in males result in nullisomy[1] of the X chromosome that promote the clinical presentation of numerous disease phenotypes often referred to as contiguous gene syndromes. In males, the clinical features usually correspond to the size of the chromosome anomaly. This phenomenon is unique to the X chromosome and has played an instrumental role in the positioning of a number of disease loci in the region (Ballabio & Andria, 1992): Short stature (SS) (De Rosa *et al*, 1997), chondrodysplasia punctata (Franco *et al*, 1995), ichthyosis (Bonifas *et al*, 1987), Kallmann syndrome (Lee *et al*, 1993), ocular albinism (type 1) (Bassi *et al*, 1995) and Opitz syndrome (Quaderi *et al*, 1998). Given that these disorders are predominantly recessive, the phenotype among females with similar disruptions to the X chromosome is highly variable, presumably because of the random nature of X-inactivation.

1.2 A recently identified X-linked disorder: MIDAS syndrome.

1.2.1 Morphological characteristics.

More recently, another developmental disorder that arises from defects involving the short arm of the X chromosome has been described (Happle *et al*, 1993). This disorder, referred to as both MIDAS syndrome and microphthalmia with linear skin defects (or MLS),

[1] Nullisomy is the complete absence of a chromosomal region.

is believed to be a contiguous gene syndrome with embryonic lethality in males as it is almost without exception found associated with monosomy of Xp22.3 in karyotypically female patients. The term MIDAS was coined to represent the diagnostic features of the syndrome. These include Microphthalmia[2], Dermal Aplasia that is restricted to the head and neck, and Sclerocornea[3]. While the title MLS also refers to the diagnostic features of Microphthalmia and Linear skin defects the term MIDAS is preferred due to the correct representation of the characteristic skin lesions. In this definition the skin abnormalities are described as hypoplastic erythematous lesions resembling scratches or abrasions that are predominantly refined to the face and neck, but are occasionally found on the torso (Happle *et al*, 1993). Due to MIDAS syndrome resulting from monosomy of a region that encodes a number of disease loci, many additional features are seen among affected patients. While the associated findings vary immensely between individuals a few are seen to be recurring. These include agenesis of the corpus callosum, hydrocephaly, infantile seizures, mental retardation and congenital heart defects such as oncocytic cardiomyopathy (OC) and defects of septation (Kayserili *et al*, 2001; Table 1.1).

The clinical features of MIDAS syndrome partially overlap with the phenotype of two other X-linked dominant disorders known as Aicardi syndrome (agenesis of corpus callosum and infantile seizures) (Aicardi & Chevrie, 1994) and Goltz syndrome (focal dermal hypoplasia, microphthalmia and skeletal anomalies) (Temple *et al*, 1990). Naritomi *et al* (1992) initially suggested that MIDAS syndrome results from the deletion of both the Goltz and Aicardi syndrome genes. However, this idea remains unlikely as the skin lesions associated with the Goltz phenotype may be distributed over the entire body (Lindsay *et al*, 1994). Alternatively, as recently suggested by Van den Veyver (2002) the three syndromes may be caused by the same gene(s) with phenotypic differences resulting from variable patterns of X chromosome inactivation (Lindsay *et al*, 1994). Although familial cases of these disorders are very rare, this hypothesis also remains unlikely as none of these syndromes have presented as alternating phenotypes within the few familial examples that have been reported (Happle *et al*, 1993).

[2] Microphthalmia is a phenotype of small eyes that usually occurs as a result of developmental defects.
[3] Sclerocornea is a congenital anomaly in which the cornea and sclera from together such that the cornea is opaque.

With the exception of two patients (Bird *et al*, 1994; Cox *et al*, 1998), all reported cases of MIDAS syndrome have resulted from microscopically visible cytogenetic abnormalities involving Xp22.3-pter. Assuming both of the apparent "non-deletion" patients do not represent phenocopies of MIDAS syndrome they provide a unique opportunity to assist with the identification of the gene(s) involved in this disorder as only minimal regions of the chromosome are likely to be affected. The first of these patients, reported by Bird *et al* (1994), presented with the unique and characteristic facial skin lesions of dermal aplasia as well as the specific heart disorder of OC. The second patient identified had only the typical facial skin lesions (Cox *et al*, 1998). High resolution physical mapping of the Xp22.3 region from both patients has revealed that neither have deletions over 100kb within and around the MIDAS critical region, however, a smaller deletion in this region can not yet be excluded (Cox *et al*, 1998). That these patients do not have the full spectrum of MIDAS features supports the notion that this syndrome is a multigene disorder. Further support for this proposal may be found in two patients reported by Siber (1984) and Duker (1985). Both cases show related features seen in Opitz syndrome with the additional features of microphthalmia, however, no other diagnostic MIDAS features have been reported (i.e. sclerocornea or dermal aplasia). As the gene responsible for the Opitz syndrome (*MID1*) has now been identified directly telomeric to the MIDAS critical region (Quaderi *et al*, 1998, Cox *et al*, 2001), these patients may indirectly suggest that MIDAS syndrome results from the deficiency of more than one gene. However, variable patterns of X-inactivation of a monogenic disorder giving rise to only one feature (i.e. variable expressivity) can not be completely disregarded on the basis of this data.

1.2.2 The role of X-inactivation in disease presentation.

Evidence strongly suggests that monosomy for the proposed MIDAS critical region in otherwise XX individuals leads to the disease phenotype, while nullisomy in hemizygous males leads to embryonic lethality. Given that vastly different features are seen among reported patients with apparently similar breakpoints suggests that X-inactivation is complicating the presenting disease phenotype (Ballabio & Andria, 1992). In attempts to clarify this finding, chromosome replication studies using cultured lymphocytes have shown

the affected chromosome to be late replicating in each case, suggesting that it is inactive in these cells. However, as it is possible that these lymphocytes are the subject of skewed X-inactivation[4], it is not possible to extrapolate this study to all tissues and/or cells.

X-chromosome inactivation is initiated by the X-inactivation centre (XIC) that is suggested to be necessary for chromosome counting and occurs as a dosage compensation mechanism within females (Lyon, 1961; Brown *et al*, 1992). The inactivation process is thought to be random in all somatic cells soon after fertilisation (Brown *et al*, 1992). The mechanism underpinning this process is mediated by the *XIST* gene which expresses a *cis*-acting structural RNA from only one of the X chromosomes. The *cis*-acting RNA then coats the inactivated X chromosome(s) (Willard, 1996). Timing of X-inactivation is the subject of much debate as it is detected at different times in various tissues of an individual and is also thought to vary between species (Migeon, 1998).

As X-inactivation is a largely random process, individuals that have monosomy of the MIDAS critical interval will have a mixture of cells that have the abnormal and the normal X chromosome in an active state. The ratio of cells that harbour an active mutant X chromosome will affect the extent of the disease phenotype (Lindsay *et al*, 1994). Further evidence in support of X-inactivation complicating the disease phenotype is presented by the only two familial cases of the disorder. In the first, a mother with only mild linear skin defects gave birth to a child with microphthalmia and pronounced linear skin lesions (Allanson & Richter, 1991). Similarly, the second case involved transmission from a mother with only mild MIDAS related features to an aborted fetus that had grossly underdeveloped cranial structure (exencephaly; Lindsay *et al*, 1994). In both cases the mother and affected offspring had the same chromosomal abnormality (Allanson & Richter, 1991; Lindsay *et al*, 1994).

1.2.3 Defining the critical region for the MIDAS disease gene(s).

The first recognition of MIDAS syndrome was presented by Al-Gazali *et al* (1990) and to date there have been over 30 additional cases reported in the literature (Table 1.1). In attempts to identify the gene(s) involved in MIDAS syndrome, Wapenaar *et al* (1993 &

[4] Skewed X-inactivation occurs as a result of secondary selection against cells with the defective X active. This results in only the normal X chromosome being in an active state in all cells.

1994) and Cox *et al* (1998) correlated the extent of patient Xp22 anomalies to their associated phenotypes to define a minimal region (critical interval) that must contain the gene(s) causing the syndrome (Fig 1.1). Two female patients (BA325 and BA384) represent the smallest cytological abnormalities of Xp that still present with the complete MIDAS phenotype. Detailed molecular characterisation of the chromosome abnormalities in these patients has precisely positioned the breakpoints within Xp22.3, therefore defining the proximal boundary for the critical interval. Likewise, the distal boundary for the critical interval was initially determined from the identification and subsequent molecular characterisation of chromosome breakpoints for two female patients (BA95 & BA333) that have the largest known deletions resulting in Xp22 monosomy with none of the characteristic MIDAS features. Further analysis by these researchers allowed the cloning of a near complete 1.7Mb cosmid contig which encompasses the entire region. The assembly of this contig initially allowed the size of the critical region to be estimated at approximately 600kb (Wapenaar *et al* 1993; Wapenaar *et al* 1994). Through attempts to isolate the gene(s) responsible for MIDAS syndrome, a number of partial cDNA clones, putative exons and full length cDNA clones have been isolated from within this originally described critical region (T. Cox, personal communication). The full length genes include: 1) *Midline 1* (*MID1*), a member of the RBCC gene family, 2) the putative mammalian holocytochrome c-type synthase (*CTS*), an integral component of oxidative phosphorylation, 3) a Rho-type GTPase activating protein (*ARHGAP6*), and 4) a major organic constituent of tooth enamel, *Amelogenin* (*AMG*). Given that *MID1* is responsible for Opitz syndrome and that removal of *ARHGAP6* has no phenotype in mice it seems unlikely that they would have a role in the presentation of the diagnostic features of the MIDAS phenotype. Indeed, Kayserili *et al* (2001) proposed the refinement of the MIDAS critical interval to an ~260 kb region bounded distally by the *MID1* gene and proximally by *ARHGAP6*. As discussed later, the putative human *CTS* gene is the only notable ORF encoded within this refined critical interval that presents as an interesting candidate.

Reference	Sex	MI	DA	S	OC	Karyotype
Ropers *et al* (1982)	F	+	-	+	-	t(X;3)p22.2
Friedman *et al* (1988)	F	+	+	+	-	Del Xp22.3-pter
Temple *et al* (1990)	F	+	+	+	-	Del Xp22.2-pter
Donnenfeld *et al* (1990)	F	+	_	+	-	t(X;3)p22.2
Al-Gazali *et al* (1990) case 1	F	+	+	+	-	t(X;Y)p22.3
Al-Gazali *et al* (1990) case 2	F	+	+	+	-	t(X;Y)p22.3
Thies *et al* (1991)	F	+	?	+	-	Del Xp22-pter
Allanson *et al* (1991) case 1	F	+	+	+	-	Del Xp22.2-pter
Allanson *et al* (1991) case 2 (Mother)	F	-	+	-	-	Del Xp22.2-pter
Gericke *et al* (1991)	F	-	+	+	-	t(X;2)p22.1
Naritomi *et al* (1992) case 1	F	+	+	+	-	Del Xp22.2-Xp22.31
Naritomi *et al* (1992) case 2	F	+	+	+	-	Del Xp22.3-pter
Lindor *et al* (1992)	F	+	+	+	+	+derXp22.3
Happle *et al* (1993)	F	+	+	-	+	XX?
Lindsay *et al* (1994) case 1	F	+	+	+	-	Del Xp22.2-pter
Lindsay *et al* (1994) case 2 (fetus)	F	N/A	N/A	N/A	-	Del Xp22.2-pter
Lindsay *et al* (1994) case 3	M	+	+	-	-	t(X;Y)p22.2
Lindsay *et al* (1994) case 4 (Mother of 2)	F	-	+	+	-	45, X/del p22.2
McLeod *et al* (1994)	F	+	+	+	-	Del Xp22.1-pter
Bird *et al* (1994)	F	-	+	-	+	XX
Mucke *et al* (1995) case 1	F	+	+	+	-	t(X;Y)p22.3?
Mucke *et al* (1995) case 2 (Mother of 1)	F	+	+	-	-	t(X;Y)p22.3?
Kulharya *et al* (1995)	F	-	-	-	-	t(X;3)p22.3
Tar *et al* (1995)	F	-	-	-	-	Del Xp21.1-pter
Paulger *et al* (1997)	M	+	+	+	-	t(X;Y)p22.3?
Cox *et al* (1998) BA529	F	-	+	-	-	XX
Cox *et al* (1998) BA389	F	+	+	-	-	Del Xp22.3-pter
Kayserili *et al* (2001) BA530	F	+	+	+	-	Del Xp22.3-pter
Kutsche *et al* (2002)	M	-	+	-	+	Inv Xp22.13-Xp22.32
Enright *et al* (2003)	F	+	+	-	-	denovo Del Xp22.3
Kherbaoui-Redouani *et al* (2003)	F	-	+	-	+	Not determined

Table 1.1 Clinical features reported in MIDAS patients. MI, microphthalmia; DA, dermal aplasia S, sclerocornea; OC, oncocytic cardiomyopathy. + indicates the presence of the feature, - indicates absence of the feature, N/A indicates not applicable. Karyotypes determined for each individual are indicated.

Figure 1.1

Defining the MIDAS critical interval

The MIDAS critical region was initially defined from correlation of patient phenotypes with the extent of their corresponding chromosome abnormality. The smallest deletions (BA325 & 389) to have the full MIDAS phenotype marked the proximal boundary (centromeric side) while the largest deletions (BA95 & 337) without the MIDAS phenotype marked the distal boundary (telomeric side). That mouse KO's removing the *ARHGAP6* gene or *MID1* gene present no MIDAS related features has allowed refinement of the interval to the shaded region between *MID1* and *ARHGAP6*. Arrows represent genes with their relative orientation. Labelled yellow circles indicate informative microsatellite markers over the region. This figure has been modified from Kayserili *et al* (2001).

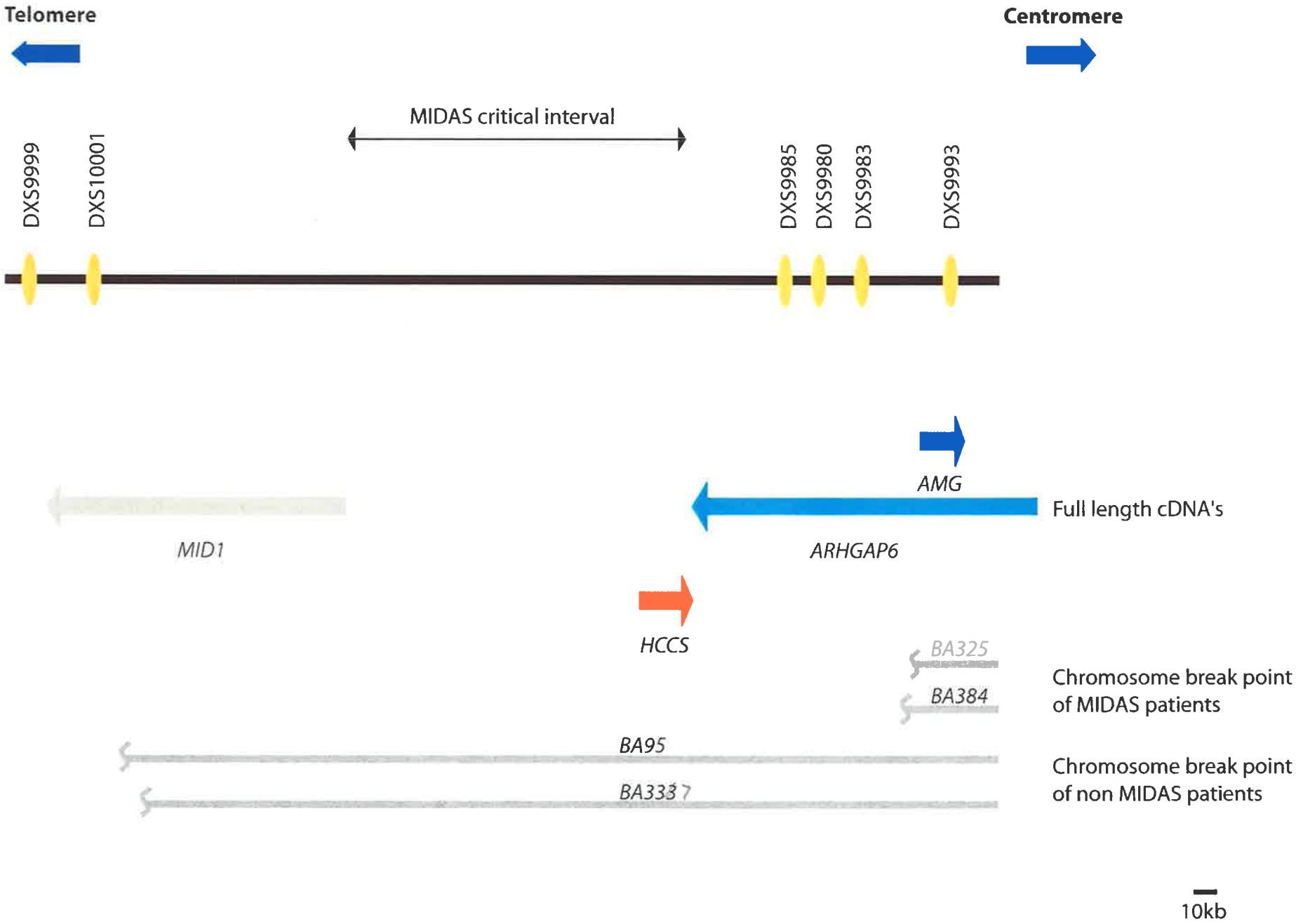
Telomere
Centromere
MIDAS critical interval
DXS9999
DXS10001
DXS9985
DXS9980
DXS9983
DXS9993
AMG
Full length cDNA's
MID1
ARHGAP6
HCCS
BA325
BA384
Chromosome break point of MIDAS patients
BA95
BA333 7
Chromosome break point of non MIDAS patients
10kb

1.3 Oncocytic Cardiomyopathy.

1.3.1 Morphological characteristics.

A distinct clinicopathologic disorder has been defined among infants and is usually manifested by fatal cardiac arrhythmias (Ferrans *et al*, 1976). Approximately seventy separate cases of this distinct disorder have now been reported under variably descriptive names such as histiocytoid cardiomyopathy, isolated cardiac lipidosis, infantile cardiomyopathy, infantile xanthomatous cardiomyopathy, multifocal purkinje-like tumour of the heart, conduction system hamartoma and congenital glycogenic tumours of the heart (see Shehata *et al*, 1998 for recent review). However, due to the characteristic histological features of oncocytic metaplasia (Franciosi & Singh, 1988; Bird *et al*, 1994), the preferred name for this cardiac lesion is oncocytic cardiomyopathy (OC).

Morphologically, OC is characterised by the presence of yellowish nodules (foci) within the heart that are composed of large, spherical cells which frequently have excess amounts of lipid storage. Ultrastructurally, these cells are found to be severely altered cardiac ventricle cells, muscle cells or valve cells that show granular cytoplasms resulting from excessive amounts of mitochondria (mitochondrial hyperplasia). In a number of cases these characteristic unstructured cells have also been noticed in other tissues apart from the heart (Franciosi & Singh, 1988; Bird *et al*, 1994). In addition to the mitochondrial hyperplasia, these cells usually lack myofibrils and are suggested to have lost their contractile ability (Ferrans *et al*, 1976). This functional loss could feasibly give rise to the arrhythmia in the heart and hence the sudden and unexpected death among infants (Ferrans *et al*, 1976). Interestingly, in some cases an excess of intra-mitochondrial glycogen storage has also been demonstrated (McKusick *et al*, 1995).

Although the etiology of the disorder is unknown several researchers have suggested the disorder may arise as a result of a developmental defect of the atrioventricular (AV) conduction system (Boissy *et al*, 1997) or the Purkinje cells (Kauffman *et al*, 1972; Zimmermann *et al*, 1982; Malhotra *et al*, 1994). Indeed, Shehata et al (1998) in their review suggested that the conduction system is invloved in most cases. In contrast, strong support has also been obtained for the muscular origin of the disorder in the form of immunohistochemical staining. The affected cells in this case were found to be reactive

against common markers of muscle cells (i.e. actin, desmin and myoglobin) (Gelb *et al*, 1993; Andreu *et al*, 2000).

1.3.2 Clues to the pathogenesis of OC.

The identification of a number of familial cases of OC (Bahig Shehata, personal communication) and also the lack of male cases documented in the literature may give some insight to the cause of this disorder. Support for an X-linked basis may also be obtained from the finding of a number of patients that suffer from both OC and the X-linked deletion defined dissorder, MIDAS syndrome. The first and perhaps most significant of these is a patient presented by Bird *et al* (1994) that was reported with OC along with the diagnostic and unique facial skin lesions of MIDAS syndrome. Of particular interest to this project, no chromosome abnormality has been identified in this patient (Bird *et al*, 1995; Cox *et al*, 1998).

Adding further support to the co-existence of the two disorders is the finding of at least three other cases presenting with both disorders (Happle *et al*, 1993; Lindor *et al*, 1992; Kutsche *et al*, 2002). Furthermore, retrospective investigations have now found that over 10% of patients solely diagnosed with OC have features that fall into the array of clinical features associated with MIDAS syndrome (i.e. microphthalmia and sclerocornea) (Bird *et al*, 1994). Considered together, these findings support the notion that OC may be an X-linked disorder that results in embryonic male lethality (also characteristic of MIDAS phenotype), supporting the original claims by both Bruton *et al* (1977) and Silver *et al* (1980).

1.3.3 OC and the mitochondrial respiratory chain.

The cellular phenotype with OC is strikingly similar to the morphological changes of the well characterised mitochondrial myopathies that result from disturbances of the mitochondrial respiratory chain (reviewed in DiMauro & Morae s, 1993). Although there is some uncertainty as to the aetiology of OC, not surprisingly, deficiencies in the respiratory chain and specifically of complex III and IV have been detailed in three separate cases (Bohles et al, 1987; Papadimitriou et al, 1984; Otani et al, 1995). Moreover, one of these

patients has now been shown to harbour a mutation within the mitochondrial encoded *cytochrome b* gene (Andreu et al, 2000). The variation in this case was a G to A transition at nucletide 15498 that results in the substitution of glycine with aspartic acid at amino acid 251 that has not been previously reported as a neutral polymorphism. RFLP analysis of the mutation in this patient showed it to be heteroplasmic in all tissues analysed. The replacement of a neutral amino acid with an acidic residue in close proximity to the ubiquinone binding site of cytochrome b would be expected to have a structural effect on the binding site and potentially impair hydroquinone binding. Based on these findings, as well as the documented deficiency in complex III, this mutation has been considered to be pathogenic.

1.3.3.1 Cytochrome b.

Cytochrome b is the only mitochondrial encoded protein of the 11 sub-units that form the ubiquinol cytochrome c reductase complex (complex III) of the mitochondrial respiratory chain. Mutations in cytochrome b have now been reported in a number of human mitochondrial disorders including Leber's hereditary optic neuropathy (LHON) (Johns *et al*, 1993), cardiomyopathy (Valnot *et al*, 1999; Andreu *et al*, 2000), exercise intolerance (Dumoulin *et al*, 1996) and myopathy (Andreu *et al*, 1999). As the mitochondrial genome is represented many times within each cell (up to 100's / cell) the level of mutation heteroplasmy[5] is likely to have an impact on the presentation of the associated disorder. This complicated feature of mitochondrial genetics also allows the presentation of different clinical abnormalities from the same genetic defect (DiMauro & Schon, 2001). Indeed, in all of the above cases, the severity of the mitochondrial respiratory chain deficiency is directly correlated to the proportion of affected mitochondria.

The *cytochrome b* gene encodes a 380 amino acid protein that is an integral hydrophobic membrane protein. Recent elucidation of the crystal structure of both chicken and bovine complex III have allowed analysis of many of the identified pathogenic mutations found in humans and yeast (Fisher & Meunier, 2001). These studies have identified several regions of the protein, which if mutated, will abolish formation / function of complex III.

[5] Heteroplasmy refers to the mixture of both wild-type and mutant mtDNA within the same cell.

Indeed, protein sequence alignments of all species shows the highly conserved nature of the protein (Esposti, 1993).

1.3.4 Defects of the mitochondrial respiratory chain.

The mitochondrial respiratory chain is composed of five major enzyme complexes that produce the majority of the energy required by eukaryotic cells. The process of oxidative phosphorylation (OXPHOS) is completed by a series of electron carriers (cytochrome complexes I-V) that are located within the inner membrane of the mitochondria. Energy in the form of ATP is liberated by an electrochemical gradient established over the mitochondrial inner membrane which is produced by the transfer of electrons along the respiratory chain. In active, aerobic cells, that have high energy demands (such as myocytes and ocular tissues), the mitochondria supplies most of the energy. Correspondingly, these cells also have increased levels of mitochondria.

The enzyme complexes that constitute the respiratory chain are made up of approximately 85 proteins (Darley Usmar & Schapira, 1994; Shoubridge, 2001), 13 of which are encoded within the mitochondrial genome (Fig 1.2). As protein subunits are encoded within both the nucleus and the mitochondria, genetic defects giving rise to deficiencies within the respiratory chain can feasibly occur within either genome. Furthermore, as the vast majority of genes are encoded in the nucleus, most defects are suggested to arise from this genome (Darley Usmar & Schapira, 1994). In fact, the prevalence of mitochondrial disease has been estimated to affect around 1:8500 live births (Chinnery *et al*, 2001). Despite this, surprisingly few deficiencies that arise from nuclear encoded mitochondrial respiratory chain genes have so far been described (Wallace, 2000). In comparison, more than 100 different point mutations and deletions have been detailed in mtDNA, although not all affect the respiratory chain (Chinnery, 2002).

Complex I of the mitochondrial respiratory chain accepts electrons from NADH while complex two receives electrons from FADH. Both complex I and II then transfer electrons to ubiquinone (CoQ) that is then passed to complex III. Cytochrome c mediates traffic of the electron from complex III to complex IV, catalysing the reduction of molecular oxygen. The final enzyme complex (V) is responsible for proton translocation across the inner membrane to synthesise ATP.

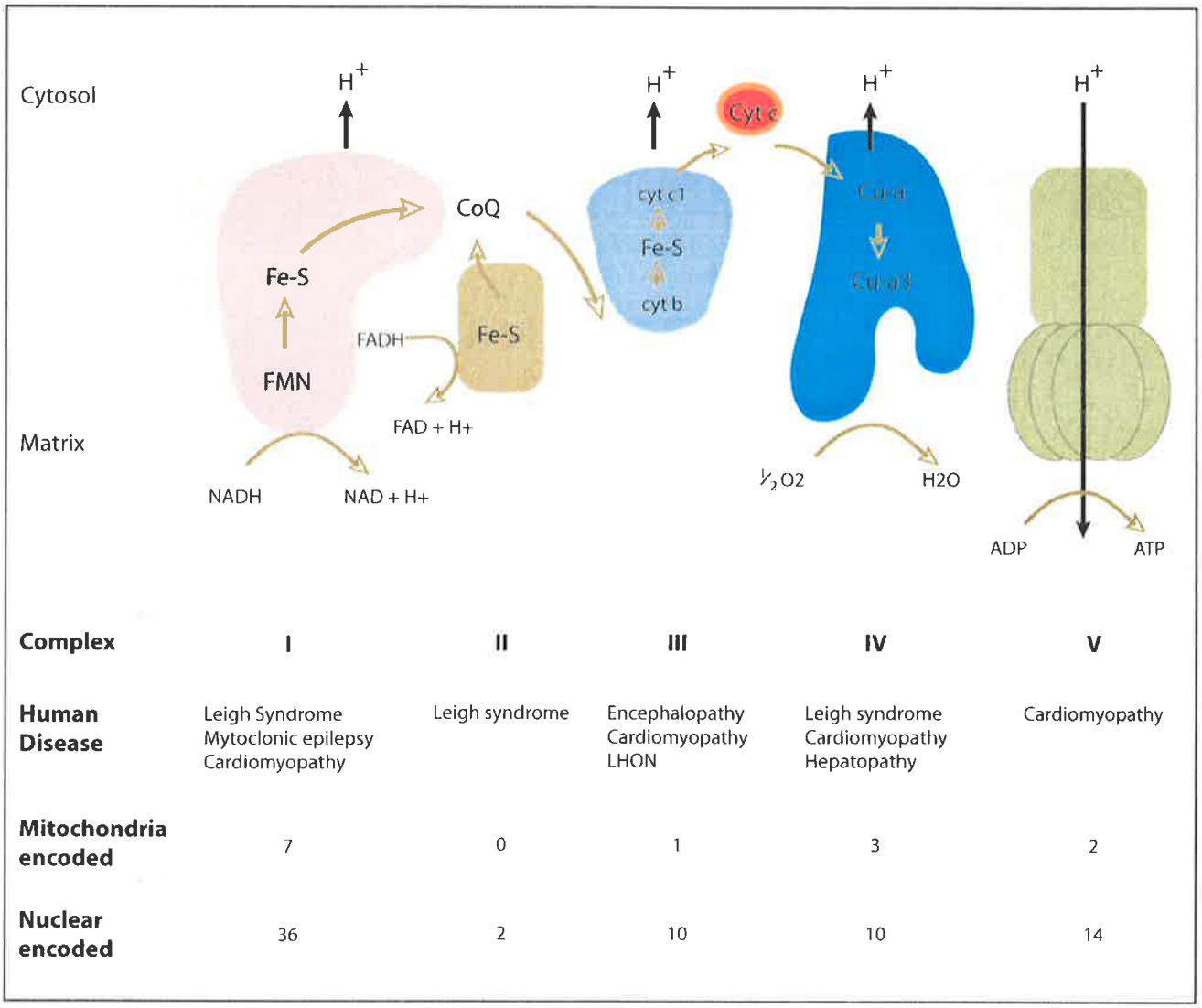

Complex	I	II	III	IV	V
Human Disease	Leigh Syndrome Mytoclonic epilepsy Cardiomyopathy	Leigh syndrome	Encephalopathy Cardiomyopathy LHON	Leigh syndrome Cardiomyopathy Hepatopathy	Cardiomyopathy
Mitochondria encoded	7	0	1	3	2
Nuclear encoded	36	2	10	10	14

Figure 1.2

The mitochondria respiratory chain

The five enzyme complexes representing the electron transport chain are shown within the mitochondrial inner-membrane with the matrix side of the membrane at the bottom. The flow of electrons from NADH / FADH to molecular oxygen (brown arrows) facilitates the production of a proton gradient across the inner membrane (black arrows). Synthesis of the majority of ATP is then correlated with the movement of protons through the ATP synthase complex. Human diseases associated with each of the respiratory complexes is indicated below the corresponding complex. The number of sub-units encoded by the nuclear and mitochondria genomes are also shown. This figure has been modified from Shoubridge (2001).

Mutations of any of the subunits that lead to deficiencies within the mitochondrial respiratory chain give rise to the characteristic and diagnostic mitochondrial myopathies. The morphological features of these myopathies vary immensely, however, they all have the same underlying characteristic feature (Steiner *et al*, 1995); ultrastructurally, the cells that are affected have an excess of abnormal mitochondria that often have increased levels of glycogen and lipid storage (Bleistein & Zierz, 1989). The mitochondrial hyperplasia in these cells is thought to be a compensatory mechanism to account for the decreased capacity of energy production (Papadimitriou *et al*, 1984). These myopathies are most commonly associated with tissues requiring high levels of energy and therefore present as defects of the cardiac and skeletal muscle. In addition, anomalies of ocular and brain tissue are also frequently observed.

1.3.4.1 Respiratory complex III and IV.

As mentioned, complex III of the mitochondrial respiratory chain receives electrons from ubiquinol and catalyses the reduction of cytochrome c that subsequently transfers electrons to complex IV. Like other respiratory complexes, both are composed of mitochondrial and nuclear encoded subunits and hence defects in either complex can also occur as a result of mutations in either genome. Complex III is composed of 11 subunits, of which only one is encoded by the mitochondrial genome (*cytochrome b*). The catalytic core of the enzyme complex is formed by the interaction of cytochrome b, cytochrome c1 and the iron sulphur protein (ISP). In contrast, complex IV is composed of 13 separate subunits, three of which are encoded by the mitochondrial genome. Interestingly, both of these complexes also contain various tissue specific subunits (McKusick *et al*, 1995), hence it could be envisaged that deficiencies of some subunits could also specifically affect only certain tissues.

For correct functioning of all enzyme complexes, the nuclear genes encoding these proteins must be correctly transcribed, translated and then targeted to the mitochondria. Targeting to their correct mitochondrial sub-compartment is usually mediated by specific signal sequences in N-terminal extensions that form positively charged amphiphilic helices that are recognised by the translocase machinery of the outer and inner membrane (TOM and TIM complexes, respectively) (reviewed in Pfanner & Geissler, 2001). Inefficiencies of such machinery could also feasibly give rise to similar deficiencies, although this would perhaps

result in a more severe phenotype because other mitochondrial functions may also be affected.

As each enzyme complex is composed of multiple subunits the clinical definition of distinct mitochondrial myopathies associated with deficiencies of each subunit is likely to be impossible (ie. deficiencies in different proteins in the same complex could generate the same phenotype). Indeed, a number of genetically heterogeneous mitochondrial myopathies have been documented (McKusick *et al*, 1995). Due to the recent support of OC arising from a deficiency in the mitochondrial respiratory chain it may also result from defects in more than one gene (i.e. genetically heterogeneous). Furthermore, if deficiencies of complex III or IV do give rise to the disorder then any of the genes encoding these proteins could potentially be involved. The finding of sporadic male cases that present with diverse clinical malformations and variable associated phenotypes by a numerous researchers further supports this suggestion. As OC has previously co-presented with MIDAS syndrome it therefore remains feasible that at least some cases may arise from mutation(s) within the MIDAS critical interval.

1.3.5 A candidate gene for X-linked OC.

As mentioned previously, an ~260 kb interval on the short arm of the X chromosome between the *Mid1* gene and *Arhgap6* gene defines a region that is likely to encode the gene(s) responsible for the diagnostic features of MIDAS syndrome. In view of the recent co-presentation of MIDAS-like features and OC in a patient with no apparent cytogenetic abnormality, it is also likely to encode the gene(s) affected in X-linked OC. Of note, only one known gene maps entirely within this region. The predicted amino acid sequence of this gene product shows approximately 69% and 68% amino acid sequence similarity (38% and 35% identity, respectively) with the yeast mitochondrial respiratory chain enzymes, holocytochrome c synthase (HCCS; Cyc3p) and holocytochrome c1 synthase (HCC1S; Cyt2p), respectively (Fig 1.3), and is therefore thought to encode a putative human holocytochrome c-type synthase (human CTS) (Schaefer *et al*, 1996). Northern analysis on human and mouse adult tissue identified transcripts in all tissues examined with strongest expression in the heart and skeletal muscle, as well as in the adult retina and fetal brain

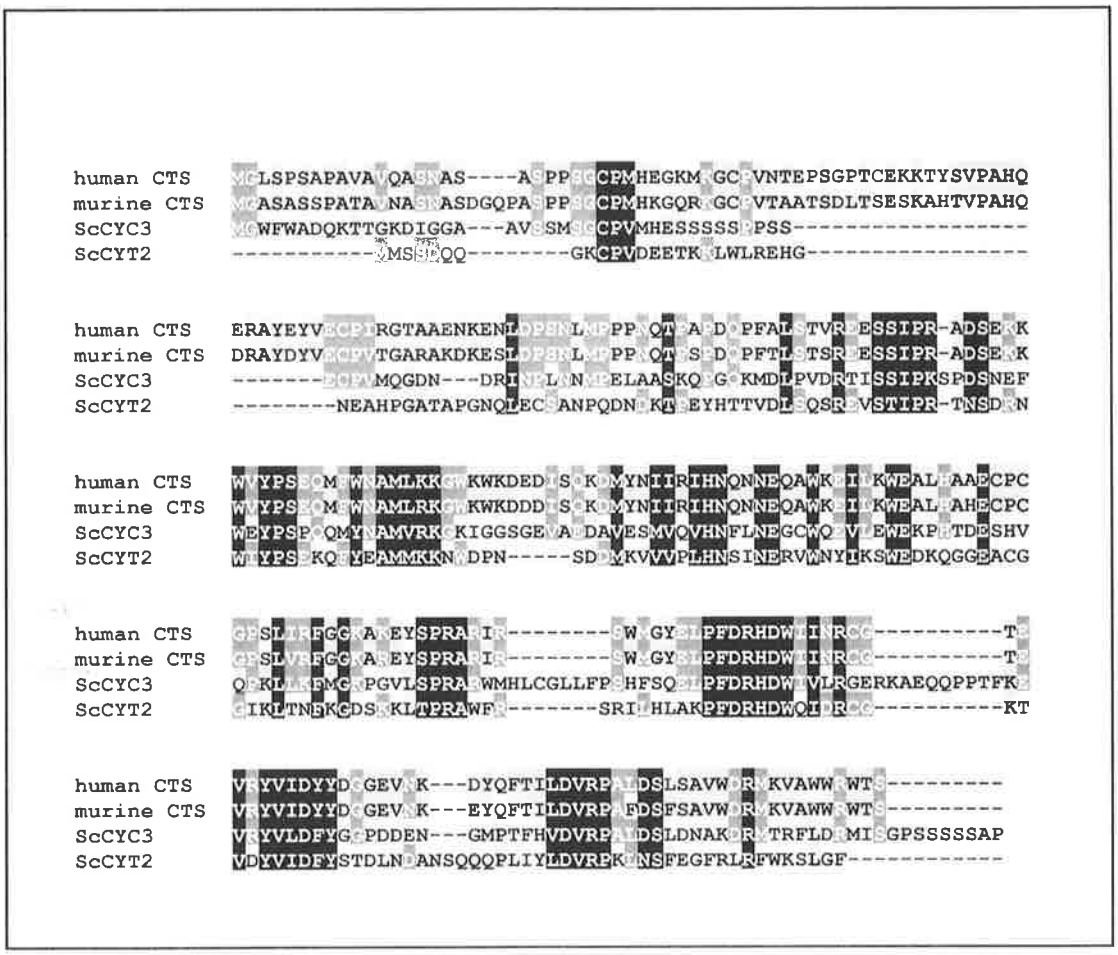

Figure 1.3

Amino acid sequence alignment of the mammalian and S.cerevisiae CTS's
Sequences were obtained from the following accession numbers: human CTS - P53701; murine CTS - P53702; ScCYC3 - P06182; ScCYT2 - Q00873. Black boxes highlight complete conservation between all c-type synthases, dark grey boxes represent similarity between 3 species, light grey boxes indicate similarity between 2 species. Dashed lines indicate a gap in the alignment generated using the ClustalW program (Thompson *et al*, 1994).

(Schaefer *et al*, 1996; Schwarz & Cox, 2002). As a consequence of extensive studies in yeast, these CTS's have been shown to catalyse the covalent addition of a heme moiety into either apocytochrome c or apocytochrome c1, respectively. This prosthetic heme is essential for the electron transport function of the two cytochromes; in cytochrome c for mediating transfer of electrons between complexes III and IV of the respiratory chain, and in cytochrome c1 between reduced ubiquinone and cytochrome c. Interestingly, at the time of writing this thesis it had been shown that neither CTS is able to complement the function of the other, therefore suggesting that each is specifically adapted to its target cytochrome (Dumont *et al*, 1987). The level of sequence similarity of the putative human CTS and the yeast enzymes provides no clue as to the specific target of the hCTS, if any.

As mentioned, deficiencies in both of these complexes (III and IV) have been documented in three separate cases of OC (Bohles *et al*, 1987; Papadimitriou *et al*, 1984; Otani *et al*, 1995) and now also confirmed by mutational analysis of *cytochrome b* (Andreu *et al*, 2000). The human *CTS* is therefore an excellent candidate for the X linked OC associated with MIDAS syndrome and also likely to be responsible for the male lethality, although an XY patient recently presented by Kutsche *et al* (2002) could be seen to argue against this. However, in this case a mosaic inversion of the X chromosome (Xp22.13-Xp22.32) was found in only 15% of peripheral blood lymphocytes. It is therefore conceivable that a reduction to 85% of cells with normal levels of CTS and therefore c-type cytochromes, may still permit the production of sufficient energy levels amongst all tissues to allow survival through development. Interestingly, the inversion breakpoint was mapped to the region spanned by the yeast artificial chromosome harbouring the entire *CTS* gene, exons 2-16 of *ARHGAP6* and the complete *Amg* gene. Although the breakpoint itself was located within *ARHGAP6*, positional effects on neighbouring genes are not uncommon. Such a mechanism would be consistent with the lack of phenotype in *Arhgap6* null mice. Further analysis of this case may be useful in addressing the involvement of *CTS* and / or *ARHGAP6*.

Interestingly, the *CTS* gene has previously been considered as a candidate for other phenotypes, although the evidence to support these considerations is limited. Van den Veyver *et al* (1998) analysed karyotypically normal Aicardi and Goltz patients for mutations within human CTS on the basis of some overlapping clinical features with MIDAS syndrome. As mentioned, it remains unlikely that the three disorders do involve the same

genes and it is therefore not surprising that no mutations were identified in this screen. These same researchers were also unable to detect mutations in *CTS* from Rett syndrome patients (Van den Veyver *et al*, 1998): Their rationale for analysing the gene was based on scientific reports that the disorder mapped to the region Xp22.2 – Xp22.33 (Ellison *et al*, 1992; Schanen *et al*, 1997). The mouse CTS homologue has also been analysed for a causative role in X-linked polydactyly (*Xpl*) and Patchy-fur (*Paf*) mutant mice. Both phenotypes map to the same region as mCTS (i.e. proximal to the PAR) and were suggested to share features with MIDAS syndrome in humans, however, no alterations were identified within the gene (Cormier *et al*, 2001).

1.3.5.1 Cytochrome C and C1 function.

In yeast, cytochrome c and c1 have been shown to be essential electron carriers of the mitochondrial respiratory chain (Fig 1.4). As mentioned, cytochrome c1 (Cyc1p) is an integral sub-unit of the catalytic site of complex III catalysing the transfer of electrons from ubiquinone to cytochrome c (Cyc7p). Subsequently, cytochrome c, a soluble inter-membrane space protein, transfers electrons to complex IV (see Schagger, 2002 for recent review).

Both cytochrome c and c1 are encoded in the nucleus, synthesised on cytosolic ribosomes and translocated to their active site within the mitochondria (Gonzales & Neupert, 1990). Apocytochrome c1 is targeted and attached to the outer surface of the inner-membrane within the inter-membrane space by a mechanism involving the use of a bipartite signalling motif. Matrix targeting signals initially direct the pre-protein to the IM where it is removed by the matrix processing peptidase (MPP). The intermediate protein is then exported to its final destination within the mitochondria by an internal sorting sequence. Cleavage of the internal sorting signal is then thought to occur either at the same time as covalent addition of heme by HCC1S (Dumont *et al*, 1991). In comparison, cytochrome c does not encode any identifiable mitochondrial localisation signal. Indeed, little is known about the mechanism of apocytochrome c transport to the inter-membrane space. Evidence suggests, however, that the protein is able to reversibly cross the outer mitochondrial membrane and is only sequestered in this region following an interaction with HCCS (Dumont *et al*, 1995; Wang *et al*, 1996). In yeast, both CTS's are essential for correct localisation of their apocytochromes (Dumont *et al*, 1991; Mayer *et al* 1995).

Figure 1.4

Biogenesis of *S.cerevisiae* Cytochrome C and C1
Both apocytochrome c and c1 are encoded in the nucleus, synthesised on cytosolic ribosomes and translocated to the mitochondrial inter-membrane space (IMS). Apocytochrome c1 (A) is targeted to the mitochondrial IMS space through the use of a bipartite signalling motif consisting of a typical mitochondrial matrix localisation signal (black line) and an internal sorting sequence (yellow box). The matrix targeting signal initially directs the pre-protein to the receptors of the transfer machinery of the outer membrane (TOM). The protein then passes through the general import pore (GIP) of the outer membrane (OM) to the transfer machinery of the inner membrane (TIM). As the pre-protein is translocated through the inner-membrane (IM) the sorting signal is withheld in the TIM complex, stopping further translocation of the protein into the matrix until the matrix targeting sequence is cleaved by matrix processing peptidase (MPP). The intermediate protein is then directed back to the IMS where HCC1S catalyses the covalent addition of heme (H) that occurs concomitantly with the removal of the sorting signal. The mature cytochrome c1 can then form part of the functional domain within complex III of the mitochondrial respiratory chain. In contrast, cytochrome c (B) contains no characteristic mitochondrial localisation signals but is nevertheless recognised by the receptors of TOM. The precursor protein is then able to reversibly cross the OM also through the GIP. Upon the covalent addition of heme that is catalysed by HCCS, the mature cytochrome c is sequestered in the IMS where is then able to transfer electrons between complex III and IV of the mitochondrial respiratory chain.

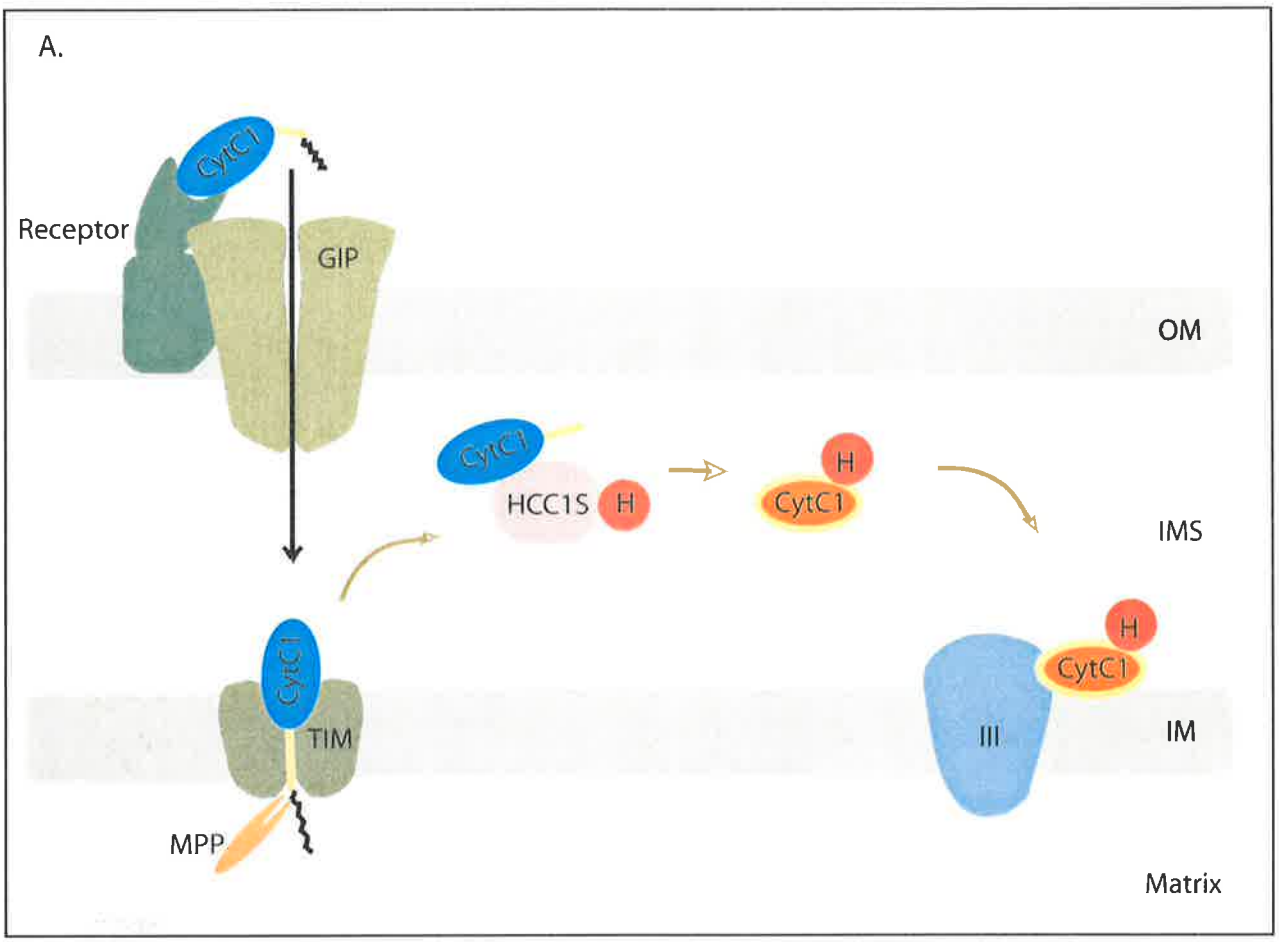
A.
CytC1
Receptor
GIP
OM
CytC1
HCC1S
H
H
CytC1
IMS
H
CytC1
CytC1
TIM
III
IM
MPP
Matrix

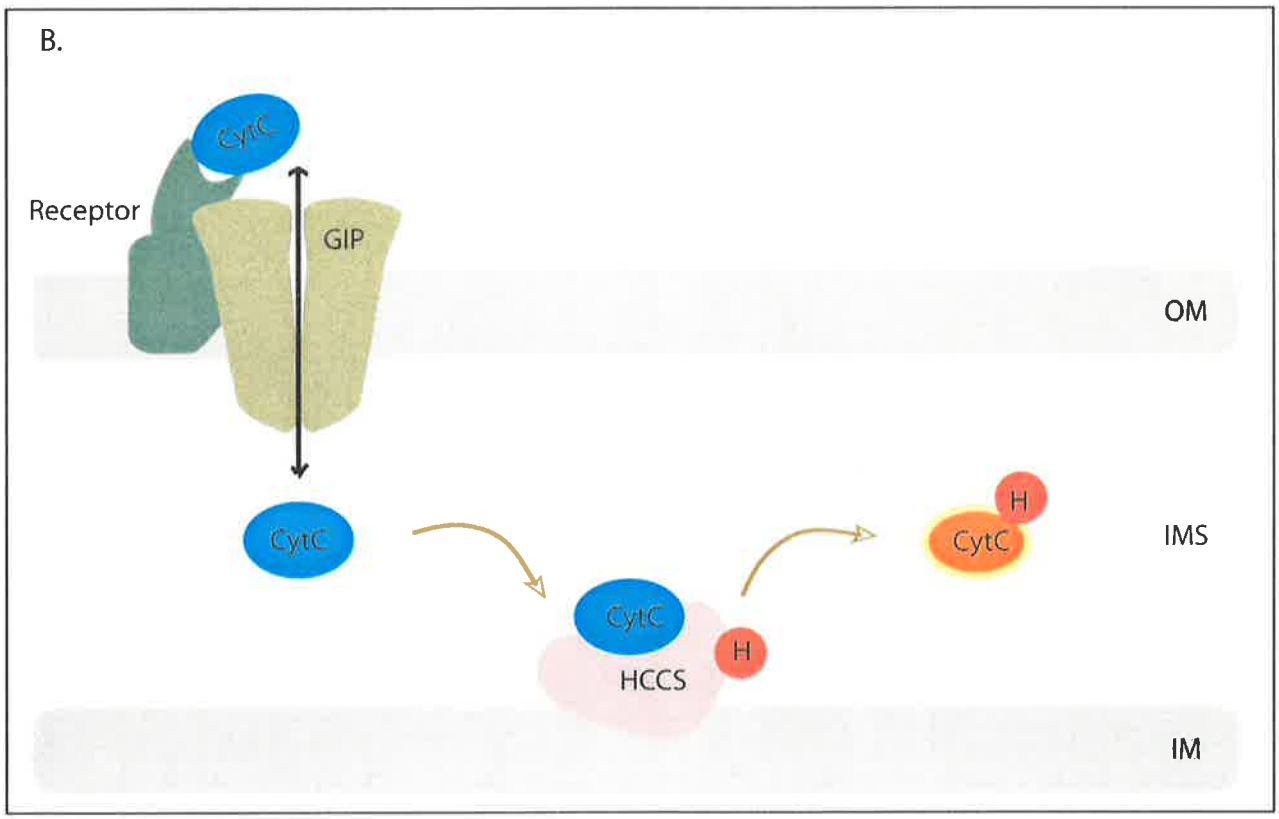
B.
CytC
Receptor
GIP
OM
CytC
H
CytC
IMS
CytC
HCCS
H
IM

Cytochrome c has also been the topic of recent research due to its secondary involvement in apoptosis. Cytochrome c is relocated to the cytosol from the inter-membrane space following the initiation of apoptotic signalling cascades usually resulting from cell stress. From the interaction with apoptotic protease activating factor 1 (Apaf1) and pro-caspase 9, cytochrome c indirectly promotes cleavage of the effector caspases (caspase-3, -6 and –7) that activate substrates required for apoptotic degradation (reviewed in Green & Kroemer, 1998). To study the removal of cytochrome c in the apoptotic signalling pathway, Li *et al* (2000) knocked out mouse cytochrome c. As expected from the removal of an integral OXPHOS enzyme, homozygous $cytc^{-/-}$ mice died *in utero* at mid gestation (embryonic day 10.5). Cultured fibroblasts established from these mice were able to be maintained in supplemented media previously used for growth of cells lacking mitochondrial DNA (Rho^{O} cells) (King & Attardi, 1984). Indeed, these cells also adopt many of the characteristics of these Rho^{O} cells, including the expected deficiencies in OXPHOS (Li *et al*, 2000).

1.3.5.2 Mammalian CTS.

Amino acid alignment of the cytochrome c-type synthases from all species identifies a number of conserved sequences that are expected to be essential for protein function. Most notably, the C-terminal half of the protein shows the highest levels of similarity and has previously been suggested to encode the catalytic domain of the enzyme (Tong & Margoliash, 1998). Also of note is the presence of two conserved CPX heme binding motifs within the first 50 aa of all species (Steiner *et al*, 1996). While the significance of this remains unknown, both human and mouse CTS encode an additional CPX motif in the first 70 amino acids of the protein that is not found in lower eukaryotes. Upon removal of the two CPX motifs in yeast Steiner *et al* (1996) found that both CTS's are unable to catalyse the covalent addition of heme to their corresponding apocytochromes. Furthermore, the researchers were then able to show through *in vitro* binding assays that these residues indeed allow direct binding with heme. Given that these residues are also conserved in the putative mammalian holocytochrome c-type synthases, mutations in this region could feasibly have a similar effect in altering correct gene function. Likewise, mutation in any of the consereved amino acids in the c-terminal half of the protein might be expected to inactivate the enzyme.

1.3.5.2-1 Localisation to the mitochondria.

Similar to their substrates, both holocytochrome c-type synthases in yeast are encoded in the nucleus and are only active once translocated to the mitochondrial inter-membrane space where they catalyse the addition of heme to their corresponding apocytochromes. As mentioned, HCCS also has the additional function of acting as a high affinity binding site for the correct import of apocytochrome c (Mayer *et al*, 1995). Unlike the majority of nuclear encoded mitochondrial enzymes, proteins of the CTS family do not contain any characteristic targeting signals (Steiner *et al*, 1995). In yeast, CTS's are localised to the mitochondria through a unique mechanism that requires the general import machinery and TOM 22 as a receptor protein. This localisation path does not require any external ATP, the requirement of TIM, or the $(\Delta)\Psi$ established by the proton gradient over the mitochondrial inner-membrane (Lill *et al*, 1992; Segui-Real *et al*, 1993). Indeed, *in vitro* studies have also shown that movement across the outer membrane can occur in the native folded state (Steiner *et al*, 1995). Recently, Diekert *et al* (1999) reported the identification of a mitochondrial localisation signal within the third quarter of *N.crassa* HCC1S. Protein alignments of mammalian CTS and the c-type synthases of *N.crassa* highlight a major difference over this region, possibly suggesting that the mammalian CTS is localised to the mitochondria through an alternative signal. In this regard, it is worthy to note that both mouse and human appear to have a specific N-terminal region unlike the CTS sequences of yeast and other lower eukaryotes (see Fig 1.3).

1.4 Mouse models of disease.

Mouse models of human disease have been instrumental in studying the pathogenic nature of complete gene deletions and also specific mutations. The resources underpinning the controlled modification of the mouse genome were first recognised with the extraction of mouse pluripotent embryonic stem (ES) cells that could be maintained in cell culture without the loss of pluripotency (Evans & Kaufman, 1981). Importantly, following introduction to blastocysts these same cells were also shown to contribute to all cell types including the germline. The second technique that allowed specific gene targeting came from the finding that exogenous DNA introduced to ES cells was able to homologously recombine at low

efficiency (Thomas & Capecchi, 1987). Until recently, traditional gene silencing required the removal of an entire gene or coding exon that results in a null allele. While this technique has been invaluable in the studies of disease pathogenesis, it is unable to be utilised for genes that are essential for organism survival as complete removal of these genes is usually severely detrimental to embryonic development and survival. However, recent advances in mouse knock-out (KO) technology now allow gene removal in both a temporal and spatial manner. This is possible through the use of target sequence-specific exogenous recombinases to facilitate conditional silencing of target genes. Two systems that are currently used in mice require the adaptation of the cre / loxP recombination system of coliphage P1 and / or the flp / frt recombination system of yeast. Both cre and flp recombinase are able to recognise similarly oriented recognition sequences (loxP and frt, respectively) and promote recombination without the need for co-factors (Gu *et al*, 1993; Panigrahi *et al*, 1992). This technique therefore allows the engineering of two independent mouse lines such that following crossing of the lines, the target gene is removed in only regions (tissues) expressing the recombinase while remaining present (active) in all other tissues. This approach has the advantage of overcoming any deleterious effects of gene deletion prior to the appropriate developmental stage or within the tissue of interest and therefore facilitates otherwise impossible investigations of gene function. Given that the removal of a *CTS* gene from mouse is likely to present with a similar phenotype to the cytc $^{-/-}$ KO (i.e. early embryonic lethal), the conditional approach offers an ideal oportunity to model the deletion of *CTS* in specific tissues relevant to the presentation of OC and the MIDAS phenotype in humans.

1.5 Summary.

Oncocytic cardiomyopathy is a severe disorder that morphologically resembles the well characterised mitochondrial myopathies (i.e. mitochondrial hyperplasia in affected tissue). Indeed, the finding of decreased activity of respiratory complexes III and/or IV in a number of cases support the conclusion that a primary respiratory chain defect underlies the disorder. Support for such a defect has now been obtained from the identification of a *cytochrome b* mutation in one affected individual (Andreu *et al*, 2000) although there is some question as to whether this is a true example of OC (Bahig Shehata, personal

communication). Like most disorders resulting from deficiencies within the respiratory chain it must be considered that OC is also genetically heterogeneous. Indeed, a total of 24 proteins are required for the transfer of electrons between complex III and IV which if mutated could conceivably give rise to similar clinical manifestations.

However, it must be noted that OC presents predominantly in females (not a common finding in defects of the mitochondrial genome) and often results in sudden infant death that has led to the hypothesis that is consistent with an X-linked mode of inheritance (Bruton *et al*, 1992).

Convincing evidence in support of an X chromosome localisation for the OC locus was published by Bird *et al* (1994). The reported female patient presented with both OC and the facially-restricted skin lesions that are unique to the phenotype of MIDAS syndrome (Happle *et al*, 1993). As mentioned, a retrospective review of the clinical findings in all published cases of OC has now revealed that over 10% of patients also show non-cardiac features that are peculiar to the MIDAS phenotype. These observations infer that coexistence of the two conditions is not a chance finding and supports the notion that a / the genetic locus responsible for OC localises to this same genomic interval (Bird *et al*, 1994).

Correlations between various X chromosome abnormalities and patient phenotypes were initially used to delineate a small chromosomal segment that is likely to contain the causative gene(s) for the MIDAS (and therefore OC) phenotype. Refinement of this region by Kayserili *et al* (2001) to an ~260 kb interval between MID1 and ARHGAP6 gene has identified the putative human *CTS* gene as the only full length gene so far located within the critical region. The two other genes located within the original MIDAS critical interval (*MID1* and *ARHGAP6*) have already partially been investigated with little evidence that either might contribute to the unique features of this syndrome (Kayserili *et al,* 2001; Schaefer *et al,* 1997).

The putative human CTS was originally identified by its sequence similarity to the yeast HCCS and HCC1S that are both involved in the transfer of electrons between complex III and IV of the mitochondrial respiratory chain. Based on this sequence similarity and a presumed conserved function in higher eukaryotes the human CTS poses as an excellent candidate for the associated MIDAS feature of oncocytic cardiomyopathy.

1.6 Aims and approaches.

The overall aim of this thesis is to investigate the hypothesis that defects in the putative human *CTS* gene play a causative role in the pathogenesis of OC associated with MIDAS syndrome. This hypothesis is based initially on the sequence similarity between the human CTS and holocytochrome c-type synthases of yeast and the apparent reduced complex III and IV activities in a number of cases. The specific aims therefore include; 1) evidence to provide support that the human gene indeed encodes a cytochrome c-type synthase consistent with the high sequence similarity to the yeast genes and 2) to detect and study any role this gene may have in the presentation of a cardiomyopathic phenotype resembling OC.

To provide support for a conserved mitochondrial function of human CTS-like protein, localisation within mammalian cells was analysed. In addition, a phenotypic growth rescue with CTS in various yeast strains defective in either HCCS or HCC1S has also been completed (chapter 3). That CTS is localised to the mitochondria and is able to specifically replace HCCS and not HCC1S suggests that this is the human orthologue of holocytochrome c synthase.

To study the intra-mitochondrial localisation of CTS, techniques were developed for cell fractionation and sub-fractionation of the mitochondria (chapter 4). These same techniques with the aid of Myc-tagged deletion constructs were also used to delineate a minimal region required for the correct localisation of CTS to the inter-membrane space of the mitochondria.

Samples from a cohort of OC patients were also screened by direct sequencing of the human CTS or *cytochrome b* genes for potential mutations that might be causative of the phenotype (chapter 5). Studies to address any role that human CTS may have in the presentation of the OC associated with MIDAS syndrome was also initiated with the production of a conditional mouse KO (chapter 6).

Chapter Two: Materials and Methods.

2.1 Abbreviations.

APS: ammonium persulfate

bisacrylamide: N,N′-methylene-bisacrylamide

BSA: bovine serum albumin

bp: base pairs

CIP: alkaline calf intestinal phosphatase

DMEM: Dulbecco's minimal essential medium

DNA: deoxyribonucleic acid

dNTP: deoxyribonucleoside triphosphate

DTT: dithiothreitol

EDTA: ethylene-diamine-tetra-acetic acid

EtOH: ethanol

FBS: fetal bovine serum

GST: glutathione-S-transferase

HFB: human fetal brain cDNA library

Hours: hrs

HSV*tk*: herpes simplex virus thymidine kinase

HWE: human whole embryo (8-10 week gestation) cDNA library

IPTG: isopropyl β-D-thiogalactopyranoside

kb: kilobase pairs

Minutes: mins

Neo^r: neomycin resistance

pBSK: pBluescript KS+

PBX: phosphate buffered saline with 0.1% Triton X

PBS: phosphate buffered saline

PBST: phosphate buffered saline with 0.1% Tween 20

PCR: polymerase chain reaction

PEG: polyethyleneglycol

PGK-1: Phosphoglucokinase-1

PMSF: phenylmethanesulfonyl fluoride

RNase: ribonuclease

rpm: revolutions per min

SDS: sodium dodecyl sulphate

Seconds: sec

UV: ultraviolet light

X-gal: 5 Bromo-4-Chloro-3-indoyl β-D-galactopyranoside

2.2 Materials.

2.2.1 Chemical and reagents.

General laboratory chemicals were of analytical research grade and were purchased from a range of manufacturers. Specialist reagents and their sources are listed below:

DMSO	BDH.
IPTG	Boehringer Mannheim.
PEG 8000	Sigma.
Spermidine	Sigma.
TEMED	BDH.
LiOAc	BDH.
Mineral oil	Sigma.
Yeast Extract	Oxoid.
DMEM	GibcoBRL.
FBS	GibcoBRL.
Colcemid	Sigma.

2.2.2 Stains and dyes.

Bromophenol blue	Sigma.
Ethidium bromide	Sigma.
Xylene Cyenol	Sigma.
Coomassie blue	Sigma.
Poncaue S	Sigma.
Giemsa	Sigma.

2.2.3 Enzymes.

All restriction endonucleases and buffers were purchased from New England Biolabs. Modifying enzymes were bought from the following manufacturers:

Lysozyme	Geneworks.
RNaseA	Sigma.
T4 DNA ligase	Geneworks.
T4 (PNK)	Geneworks.
Taq DNA polymerase	Geneworks.
Calf Intestinal Phosphatase	Boehringer Mannheim.
Proteinase K	Sigma.
Aprotinin	Sigma.
Leupeptin	Sigma.
Benzamidine	Sigma.
PMSF	Sigma.
Sodium Orthovanadate	Sigma.
Pfx Polymerase	Invitrogen.
Digitonin	Boehringer Mannheim.
Pefabloc	Boehringer Mannheim.

Appropriate reaction buffers (either 5 X or 10 X) and additional supplements were supplied with all enzymes.

2.2.4 Antibiotics and indicators.

Ampicillin	Sigma.
X-gal	Sigma.
Kanamycin	Sigma.
IPTG	Sigma.
Penicillin/Streptomycin	Invitrogen.

2.2.5 Kits and miscellaneous materials.

Kits and other materials used in this project were obtained from the following manufacturers:

Glass beads, 150-212 μm	Sigma.
Hybond™ -N+nylon membrane	Amersham.
Hybond™ -C nylon membrane	Amersham.
Sequagel concentrate	National Diagnotics.
Sequagel buffer	National Diagnotics.
Sequagel diluent	National Diagnotics.
Sephadex G-25	Sigma.
Sepharose CL-6B	Pharmacia.
Sequenase Version 2.0 DNA Sequencing Kit	USB.
Hyperfilm™	Amersham.
Qiaex™ gel purification kit	Qiagen.
Megaprime Labelling Kit	Geneworks.
Qiagen DNA mini kit	Qiagen.
Qiagen DNA midi kit	Qiagen.

2.2.6 Solutions and buffers.

1 X SSC

0.15M Sodium chloride

0.015M Sodium citrate

Adjusted to pH 7.2 with sodium hydroxide.

Phenol/chloroform

50% (w/v) Phenol

48% (v/v) Chloroform

2% (v/v) Isoamyl alcohol, buffered with an equal volume of Tris-HCl, pH 8.0

0.2% (v/v) β-mercaptoethanol.

Denaturing Solution

1.5M Sodium chloride

0.5M Sodium hydroxide.

Neutralising Solution

1.5M Sodium chloride

1M Tris-HCl, pH 7.2

1mM EDTA.

1 X TE

10mM Tris-HCl, pH 8.0

1mM EDTA, pH 8.0.

1 X TAE

40mM Tris HCl

20mM Sodium actetate

2mM EDTA

adjusted to pH 7.8 with glacial acetic acid.

1 X TBE

0.9M Tris-borate

2mM EDTA, pH 8.0.

SM Buffer

100mM Sodium chloride

10mM Magnesium sulphate

50mM Tris-HCl, pH 7.5

2% (w/v) Gelatin.

10 X SD

300mM Tris-HCl, pH 7.8

300mM 625mM KAc

100-mM MgAc

40mM Spermidine

5mM DTE.

Solution 1

5 X SSC

50% (v/v) Formamide

0.1% (v/v) Triton X-100

0.5% (w/v) CHAPS.

Buffer A

20mM HEPES, pH 8.0

10mM KCl

1.5mM $MgCl_2$

1mM EDTA

1mM EGTA

250mM Sucrose

1mM DTT

1mM PMSF

10µg/ml Leupeptin

10µg/ml Aprotinin

10mM Benzamidine

0.2mM Sodium orthovanadate.

Buffer B

20mM Hepes, pH 7.5

220mM Mannitol

70mM Sucrose

1mM EDTA

1mM Pefabloc.

Mitochondria buffer

20mM Hepes, pH 7.5

220mM Mannitol

70mM Sucrose

1mM EDTA

0.5% (w/v) BSA.

Mitochondria lysis buffer

10mM Tris-HCl, pH 7.4

150mM NaCl,

5mM EDTA

0.5% (v/v) Triton X-100

10μg/ml Aprotinin

1mM PMSF

1mM Orthovanadate.

Non-denaturing lysis buffer

1% (v/v) Triton X-100

50mM Tris-HCl, pH7.4

300mM NaCl

5mM EDTA

0.02% (w/v) Sodium Azide

Added just prior to use:

10mM Iodoacetamide

1mM PMSF

2μg/ml Leupeptin.

5% Blotto

1 X PBS

5% Milk powder.

DMEM

28mM NaHCO3

19mM Glucose

20mM HEPES, pH 7.3.

2.2.7 Radionucleotides.

α-^{32}P-ATP (specific activity, 3000Ci/mmole, concentration 5mCi/ml): Geneworks.

2.2.8 Nucleic acid and protein molecular weight standards.

1kb ladder	GibcoBRL
HyperLadder I	Bioline.
BENCHMARK™ Prestained	
Protein Ladder	GibcoBRL.

2.2.9 Cloning and expression vectors.

All pBluescript (pBS) cloning vectors and the pRC/RSV mammalian expression vector were obtained from Dr. T. Cox (University of Adelaide, South Australia). Both p*loxPneo*^{r} and p#18 were obtained from Dr. P. Koopman (Centre for Molecular and Cellular Biology, University of Queensland). Both constructs were cloned into pBSII that carries the *lacZ* gene (with a nuclear localisation signal mP1 intron, 3' UTR and polyA signal) and two *loxP* sites separated by the *neo*^{r} gene under a PGK-1 promoter. The p#18 construct also contains the HSV-*tk* gene which has a mutant polyoma virus enhancer. pMC-Cre was obtained from Dr. R. Slattery (Australian National University, Australian Capital Territory). The pGEMT PCR cloning vector was purchased from Stratagene and the pGEM7 cloning vector obtained from Prof. R. Saint (University of Adelaide, South Australia).

2.2.10 Bacterial strains.

Strain	Genotype
DH5α	*supE*44Δ*lac*U169(ϕ80*lacZ*ΔM15)*hsdR*17*recA*1*endA*1*gyrA*96*thi*-1*relA*1
LE392	*supE*44*supF*58*hsdR*514*galK*2*galT*22*metB*1*trpR*55*lacY*1
GM33	LAM^{-}IN(*rrnD-rrnE*)1*dam*-3*sup*-85

2.2.11 Bacterial media.

Luria broth (L-Broth)

1% (w/v) Tryptone

1% (w/v) Sodium chloride

0.5% (w/v) Yeast extract

adjusted to pH 7.2 with sodium hydroxide.

Luria Agar (L-Agar)

Luria broth with the addition of 1% (w/v) bacteriological agar No$_{1}$.

TB top agarose

1% (w/v) Tryptone

0.5% (w/v) Sodium chloride

0.01M Magnesium sulphate

0.7% (w/v) Agarose.

2.2.12 Yeast strains.

B-8025: *MATα, can1-100, cyc3Δ1, cyc7::CYH2, cyh2, his3-Δ1, leu2-3, 112, trp1-289, ura3-52. Kindly donated by Prof. F. Sherman (University of Rochester, New York).*

YS-10: *MATα, ade2-1, his3-11,15, leu2-3, 112 trp1-1, ura3-1, can1-100, CYT2::LEU2. Kindly donated by Prof. R. Lill (Marburg, Germany).*

YS-51: *MATα, ade2-1, his3-11,15, leu2-3, 112 trp1-1, ura3-1, can1-100, CYT2::LEU2 (ARSH4-CEN6-URA3-CYT2). Kindly donated by Prof. R. Lill (Marburg, Germany).*

EGY-191: *MATα, trp1, his3, ura3, 2ops-LEU2.*

2.2.13 Yeast media.

2.2.13.1 Amino acids and carbon source.

Tryptophan, Histidine, Leucine and Uracil were obtained from Sigma. Glucose was obtained from the central services unit (CSU) and Lactic acid (DL) was obtained from BDH.

2.2.13.2 Liquid media.

The composition of the media is given per litre. The appropriate amino acids and carbon source, obtained from sterile solutions, were added after autoclaving. Minimal media: yeast nitrogen base (1.7g), ammonium sulphate (5g) made up to 900mls with water, and autoclaved. Complete Media (YPD): yeast extract (10g), bactopeptone (20g), K_2HPO_4 (0.5g) and KH_2PO_4 (0.5g). Water was added to 900mls and autoclaved.

2.2.13.3 Solid media.

Yeast minimal media plates and complete media plates were made with either yeast minimal media or yeast complete media (respectively) with 2% bactoagar. The appropriate carbon source and amino acids were added prior to plate pouring

2.2.14 Libraries.

The male mouse (129Sv) genomic phage library was kindly supplied by Dr. T. Cox (University of Adelaide, South Australia). The RPCI-23 genomic BAC library (Roswell Park Cancer Institute, Buffalo, New York) constructed from a female C57BL/6J mouse was kindly supplied and screened by Dr. P. Farley (Murdoch Children's Research Institute, Victoria) following standard procedures (Kim *et al*, 1994).

2.2.15 Tissue culture cell lines and media.

2.2.15.1 Cell lines.

Cos-1, Monkey Kidney cells (ATCC CRL-1650)

HeLa, Human Epithelial-like cells (ATCC CRL-2)

HEK-293T, Human Embryonal Kidney cells (ATCC CRL-1573)

NIH-3T3, Murine Swiss Embryo Fibroblast cells (ATCC CRL-1658)

2.2.15.2 Media.

All cells were grown in DMEM (Gibco) supplemented with 5-10% (v/v) FBS.

2.2.16 Antibodies.

anti GFP	Clontech.
anti TOM20	Gift from Dr. B. Wattenberg (Hanson Research Centre, Institute of Medical and Veterinary Science, South Australia).
anti Cytochrome C	Santa Cruz.
anti CPN60	Gift from Prof. N. Hoogenraad (LaTrobe University, Victoria)

2.2.17 Oligonucleotides.

PRIMER	SEQUENCE (5′ → 3′)	ANNEAL TEMP.	SOURCE
Vector primers			
T3	CGAATTAACCCTCACTAAAGGG	51	Geneworks.
T7	GTAATACGACTCACTATAGGGC	51	Geneworks.
λgt-F	CTTTTGAGCAAGTTCAGCCTGGTTAAG	51	Geneworks.
λgt-R	GAGGTGGCTTATGAGTATTTCTTCCAGG	51	Geneworks.
USP	GTAAAACGACGGCCAGT	51	Geneworks
PGK-p2	TCCATTTGTCACGTCCTGCAC	51,59	Pacific Oligos
loxP-for	GCTCTAGATCTCCGATCATATTCAATAACCC	53	Pacific Oligos
pgkneo#2	GCTTTGCTCCTTCGCTTTCTG	54	Sigma Genosys.
pgkneo#3	GTGATATTGCTGAAGAGCTTG	52	Sigma Genosys.
TK2	CACGCTGTTGACGCTGTTAAG	58	Sigma Genosys.
TK3'	CAGGGAGAGAAACTCAGC	54	Sigma Genosys.
EGFP-60r	GTTTACGTCGCCGTCCAGCTC	54	Sigma Genosys.
hHCCS			
CCHL-1	GTGAAGTCACTGCTGCTCTGG	53	Geneworks.
CCHL-2	TCATTCTGTCCCATACTGCCG	51	Geneworks.
CCHL-3	GTGAATTCAGCGTCCCCACCTTCAG	50	Geneworks.
CCHL-4	GCATTTGAGGCCTGAACTGC	53	Geneworks.
CCHL-5	GTGAAGTCAACAAGGACTACCAG	51	Geneworks.
HKpnI	GGGGTACCCGAGGTCCAACGCCACCAAG	55	Genset.
HKpn(aa48)	ATGTGGTACCCTCACAGGTTGGGCCAGAT	55	Sigma Genosys.
HKpn(aa115)	CCCAGGTACCCTCTGAATCTGCTCTCGGA	56	Sigma Genosys.
HBam(aa48)	CGGGATCCGAATGGAGAAGAAAACATACTCTGTGC	54	Sigma Genosys.
HBam(aa115)	TCGGGATCCGAATGGAGAAAAAGTGGGTTTACCCTTCC	54	Sigma Genosys.
HXho(aa48)	CCGCTCGAGCTCTGAATCTGCTCTCGGA	54	Sigma Genosys.
HXho(aa115)	CCGCTCGAGCTCACAGGTTGGGCCAGAT	54	Sigma Genosys.
aa48-stop	GTGGTACCTTACTCAACAGGTTGGGCCAGATGGCT	56	Sigma Genosys.
aa115-stop	CAGGTACCTTACTCTGAATCTGCTCTCGGAATG	55	Sigma Genosys.
m13-stop	GTGGTACCTTAGATATTATACATATCCTTCTGAC	54	Sigma Genosys.
hHCCS-stop	CTTTACGAGGTCCAACGCCACCAA	54	Sigma Genosys.
CxM40a	CACAGGCTGCTGTCCAGTGTC	55	Geneworks.
CxM40b	CAAAGTCCATTTAGGTCAGCC	55	Geneworks.
mHCCS			
mHCCS	ACGCTCAGTAATGTGACGATAGCTG	53	Operon Technologies.
mHCCS1	TTATGCATCGGGCATCCTGAAG	54	Operon Technologies.
mHCCS2	CTGCGCAGTGAGTTCGGCTG	54	Operon Technologies.
mHCCS3	GTGAATTCCAAGAGCTGACTCTGAG	53	Operon Technologies.
mHCCS4	AATCTCCTTCCACGCTTGCTC	51	Operon Technologies.
mHCCS5	CAGCCGAACTCACTGCGCAG	53	Pacific Oligos.
mHCCS6	CCTGTGATTCCAGCCATGGGT	54	Sigma Genosys.
mHCCS7	CACCGCTAACGTCGGTCACAGC	57	Sigma Genosys.

mHCCS8	CTGTGACCGACGTTAGCGGTG	56	Sigma Genosys.
mHCCS9	TGTTGCTGCAGTCACTGGAC	55	Sigma Genosys.
mHCCS10	CAGAATAACGAGCAGGCTTG	50	Sigma Genosys.
mHCCS11	CGGGATCCTGTTTCCAGCCATGGGTTTG	57	Sigma Genosys.
mHCCS12	CGGGATCCAGAAGGATATGTATAATATCATTAG	52	Sigma Genosys.
mHCCS13	GTGGTACCCGATATTATACATATCCTTCTGAC	52	Sigma Genosys.
mHCCS14	GTGGTACCCTATGATCCAATCGTGCCTATC	54	Sigma Genosys.
mHCCS15	GTTTGAAGGATCGAGGCTCTCC	54	Sigma Genosys.
mHCCS16	CAATCAGAATAATGAGCAAGC	50	Sigma Genosys.
mHCCS17	CAAACACTGTAGCTGAGGACTG	52	Sigma Genosys.
mHCCS18	GGACTCGAGCATTTAGAGTGGCAACAAAC	54	Sigma Genosys.
mHCCS19	ATGGAATTCCAGAACATCTGTTCAG	53	Sigma Genosys.
mHCCS20	CAGCTTTCTCAGGAAAAAAGTTTCAC	51	Sigma Genosys.
5'probeHind	TCCCAGCTTCCGCCCGAGCCTTCTCTC	57	Sigma Genosys.
5'probeXho	TTGTGAATTCCCTCGAGTACACTCACAAC	52	Sigma Genosys.
Ex1-2Xho	TCGACCTCGAGGCCTCGGAGCGGAAG	57	Sigma Genosys.
Ex1-2Hind	TCCCAAGCTTGAGAGAAAGAGGAATGGTG	52	Sigma Genosys.
5'Ex1-2-mHCCS	GATACCGTCGACAAGCTTGCCTCGGAGC	58	Sigma Genosys.
Other genes			
5'Sal-CytC	CATGTCGACTATGGGTGATGTTGAGAAA	55	Sigma Genosys.
3'BglII-CytC	AATAGATCTTCATTAGTAGCTTTTTTGAG	55	Sigma Genosys.
Alas2-aa55	CATGCCATGGGTGGATTTGAGAACAGTTTG	54	Sigma Genosys.
Alas2-XbATG	GCTCTAGAATGGTGACTGCAGCCATGC	56	Sigma Genosys.

2.3 Methods.

2.3.1 Ethanol precipitation of nucleic acids.

Samples were adjusted to 0.3M NaAc pH 5.2 using a 3M stock solution. Three volumes of redistilled EtOH was then added, mixed thoroughly by vortexing, and chilled at -20°C for at least 30 min. The precipitated nucleic acid was then pelleted by centrifugation at 15,000 X g for 15 min. The supernatant was carefully removed and the pellet then washed in 70% (v/v) EtOH. The samples were dried *in vacuo* then resuspended in water.

2.3.2 Restriction endonuclease digestions.

All restriction endonuclease digestions of DNA dissolved in water (or TE) were carried out in the supplied 10 X restriction buffer with addition of BSA. Analytical digests of DNA (up to 2μg) were carried out using 2 units of enzyme in a reaction volume of 15μl for 1-2 hrs at 37°C. Preparative digests of DNA (> 2μg) were carried out using 2-3 units of enzyme for each μg of DNA, in a reaction volume of 50-100μl, and allowed to proceed for at least 2-3 hrs at 37°C.

2.3.3 Agarose gel electrophoresis of DNA.

Electrophoresis of DNA was carried out in agarose gels of appropriate percentage and size. Molten agarose in 1 X TAE was poured into plastic trays provided with the electrophoresis tanks with plastic combs to provide the wells. The gels were submerged in TAE in an electrophoresis tank and the DNA samples containing an appropriate amount of loading buffer (final concentration 1 X) were loaded into the wells. 60-80V was applied until the dye had moved to the required distance. The DNA was visualised under long or medium wave UV light after staining with ethidium bromide (10mg/ml) for approximately 10 min.

2.3.4 Extraction of DNA fragments from agarose gels.

Following electrophoresis on an appropriate percentage agarose gel, DNA was isolated by staining the gel with ethidium bromide and excising the band of DNA with a scalpel under long wave UV light. DNA was then isolated from the gel slice using the Qiaex II^{TM} gel extraction kit following the suppliers protocol.

2.3.5 Preparation of electroporation competent bacterial cells.

Single bacterial cells were inoculated in 10ml of luria broth and grown in a shaking incubator overnight at 37°C. 5 ml of each culture was used to seed 500ml of luria broth. Large cultures were grown with shaking at 37°C until an OD_{600} of approximately 0.6-0.8 was obtained. The cultures were placed on ice for 15 min, then centrifuged in a JA14 rotor at 7,000rpm. Cell pellets were resuspended in 500 ml of ice cold Milli-Q water and re-pelleted by centrifugation at 7,000rpm in a JA14 rotor at 4°C for 15 min. Cell re-suspension and pelleting was repeated a further two times before final resuspension in 2ml of ice cold 10% glycerol per 50ml of original culture. Cells were stored in 80µl aliquots at -80°C.

2.3.6 Sub-cloning restriction fragments into plasmid DNA vectors.

2.3.6.1 Preparation of vectors and restriction fragments.

Linearised vector DNA and restriction fragments were prepared by digestion with the appropriate restriction enzymes. The 5′-terminal phosphate group from the linearised vector was removed using calf intestinal phosphatase (CIP) essentially as described by Maniatis *et al* (1989). The vector DNA and the restriction fragments were purified from agarose gels (as described above).

2.3.6.2 Ligation of restriction fragments in to vector DNA.

DNA fragments to be ligated were placed in excess (approximately 3 volumes) within a mix containing 0.1 volumes of 10 X ligation buffer and 1 unit of T4 ligase in a total volume of 10µl. The reaction was incubated at room temperature for 1 hour.

2.3.6.3 Transformation of competent bacterial cell by electroporation.

Ligation reactions were ethanol precipitated and resuspended in 20µl Milli-Q water. To this, 40µl of electroporation competent cells were added and the mixture stored on ice for 5 min. The ligation mixture was then transferred into sterile cuvettes and subjected to a 2.5kV pulse (25µFD) in the Gene Pulser before 200µl SOC medium was used to wash the cells out into another 800 µl of the medium. The transformed cells were incubated at 37°C for

approximately 30 min and spun at 350 X *g* in a centrifuge for 5 min. The pellet was resuspended in 100µl Milli-Q water.

2.3.6.4 Plating of transformed cells.

Using a sterile glass spreader, transformed cells were plated onto L-agar containing 100µg/ml ampicillin or 50µg/ml kanamycin and left overnight at 37°C. For vectors facilitating blue/white colour selection 4µl IPTG (200mg/ml) and 20µl X-gal (20mg/ml) were added to cells immediately prior to plating.

2.3.7 Determination of DNA concentration.

The concentration of DNA samples was estimated by comparing their intensity to bands of known concentration on an agarose gel. For more accurate estimation of DNA concentration, UV absorbance at 260nm was determined using a UV-visible spectrophotometer (50µg/ml of DNA per absorbance unit).

2.3.8 Radiolabelling of DNA.

DNA was labelled with α-^{32}P-ATP using random nonamers as primers from the Amersham Megaprime kit according to the protocol provided. Radio-labelled DNA was separated from the unincorporated radioactive nucleotide by spin-column chromatography. To prepare the columns, a 1.5ml microfuge tube was pierced at the bottom with a 21 gauge needle and placed in a 2ml microfuge tube. Approximately 25µl of acid washed glass beads were placed in the bottom of the 0.5ml tube and approximately 600µl of Sepharose CL6B (Pharmacia) [for fragments over 50bp] or Sephadex G-25 (Sigma) [for fragments under 50bp] equilibrated in TE was added on top of the glass beads. The tubes were centrifuged at 1800rpm for 3 min in a bench centrifuge. The 2ml microfuge tube was replaced with a 1.5ml eppendorf and the labelling mix was loaded onto the column and centrifuged as above.

2.3.9 Plasmid transformation into yeast.

A single yeast colony was inoculated into 5ml of YPD and incubated overnight at 30°C with shaking. The starting culture was then diluted to an OD_{600} of 0.3 in 5ml of fresh YPD and grown for 3-4 hrs at 30°C with shaking. Yeast were harvested by centrifugation at 2,000rpm for 5 min and the remaining pellet resuspended in 1ml of 0.9M LiOAc/TE. The yeast were again harvested by centrifugation at 8,000rpm for 30 secs and resuspended in 50-100µl of 0.9 LiOAc/TE. 8µl of DNA (from mini pp) was added to 12µl of competent yeast, 45µl of sterile 50% PEG and 5µl 10mg/ml denatured Salmon sperm. Following incubation at 30°C for 1 hour the yeast were then heat shocked at 42°C for 5 min before plating onto selective media.

2.3.10 Plasmid DNA preparation.

2.3.10.1 Small scale preparations.

Plasmid DNA was routinely isolated from 2ml overnight cultures using the QIAprep Spin Miniprep Kit protocol (QIAGEN) or alternatively by the alkaline lysis method (Maniatis *et al*, 1989).

2.3.10.2 Large scale preparations.

Large scale plasmid preps and BAC preps were completed with the QIAGEN plasmid midi kit from 50ml overnight cultures of single colonies.

2.3.11 End-filling restriction endonuclease digested DNA.

Both 5' and 3' overhangs were end-filled with T4 DNA polymerase. 1µg of restricted DNA was incubated with 0.2mM dNTP's, 1 X T4 DNA polymerase buffer and 2.5 units of the polymerase at 37°C for 1 hour. The enzyme was heat inactivated at 68°C for 10 min and the end product purified by phenol/chloroform extraction and ethanol precipitation.

2.3.12 Southern analysis of DNA.

Digested samples were mixed with ficoll loading dye and loaded onto an appropriate percentage agarose gel. Electrophoresis was carried out at 50-60mA in 1 X TAE until the dye was $^3/_4$ of the length down the gel. The gel was stained with ethidium bromide, photographed next to a fluorescent marker and then soaked in 1-2 volumes of 0.25M HCl with gentle agitation for 10-20 min. Following rinsing in Milli-Q water the gel was soaked in 0.4M NaOH with agitation for 20 min. The gel was rinsed in Milli-Q water and placed into 2 X SSC. Transfer of the DNA to the filter was then accomplished by placing the gel into a tray with the well openings facing down. Nylon membrane was placed onto the gel ensuring no bubbles between the gel and the membrane. Whatman 3mm paper was placed on top of the filter followed by a stack of pre-cut paper towels. 2 X SSC was then poured around the base of the gel and the capillary transfer was left for at least 6 hrs. DNA was then fixed to the filter by UV treatment in a cross linker.

Filters were prehybridised in an appropriate volume of 7% SDS, 0.5M Na_2HPO_4 and 1mM EDTA at 65°C for at least one hour. The probe was labelled as described in Section 2.3.8, denatured at 100°C for 5 min and added to the prehybridisation mix. Filters were left to hybridise for at least 6 hrs at 65°C for same species hybridisation and at 42°C for cross-species hybridisation. Excess probe was removed by washes in variable solutions ranging from the lowest stringent 2 X SSC, 0.1% SDS to the highest stringent 0.1 X SSC, 0.1% SDS (at either room temperature and or 65°C). Filters were covered in plastic and exposed to Hyperfilm with 1-2 intensifying screens at -80°C. Bound probe was stripped from the filters by washing in boiling 0.1% SDS.

2.3.13 Sequencing of double stranded DNA templates.

2.3.13.1 Preparation of template DNA.

20µl (1µg) of plasmid DNA was incubated at 37°C for 15 min with 5µl of 1M NaOH and 1mM EDTA. The denatured DNA was purified by centrifugation through a Sepharose CL-6B column as described in Section 2.3.8 and the 25µl of single-stranded template DNA was stored on ice prior to use.

2.3.13.2 Sequencing reactions.

The dideoxy chain termination reaction was performed using the Sequenase Version 2.0 kit and [α^{32}P]dATP, as described by the manufacturer.

2.3.13.3 Preparation of sequencing gels.

Sequencing gels consisted of either 5% or 6% (w/v) acrylamide in a final volume of 60ml following the protocol supplied by Sequagel (National Diagnostics). Following addition of 480µl of APS (10%) and 24µl TEMED, the gel was mixed and poured between clean, clamped glass plates, separated by 0.2mm spaces.

2.3.13.4 Denaturing gel electrophoresis.

Sequencing reactions were run on a Model S2 sequencing gel electrophoresis system (BRL). The gel was pre-electrophoresed at 47mA for 30 min, using 1 X TBE as the running buffer. Following denaturation for 2 min at 75°C, 1.2µl of each DNA sequencing reaction was loaded into the wells and electrophoresis continued until the first tracking dye had reached the bottom of the gel plates. The loading process was repeated for medium and short-length runs. The gel was run at 47mA (1900V). Following electrophoresis, the sequencing gel was fixed to 3mm Whatman paper and covered with plastic, taking care not to get any air bubbles. The gel was exposed to Hyperfilm for at least 10 hrs at -80°C.

2.3.13.5 Automated sequencing of PCR products.

All automated sequencing runs were completed at the IMVS Molecular Pathology Sequencing Unit, University of Adelaide, South Australia. Automated sequencing reactions were carried out using 7-8µl of terminator ready reaction mix, 5µl of Template (30mg/µl), 3.2 pmole primer and approximately 4-5 µl of water. The cycles completed on the DNA engine were: 96°C - 15 secs, 50°C - 5 secs, 60°C - 4 min, and completed 25 times.

2.3.14 Polymerase Chain Reaction (PCR).

PCR's were performed in 50µl volumes containing 0.5mM dNTP's, 1 X PCR reaction buffer, 5mM $MgCl_2$, 0.7-1.0µM each primer, 1.5U of *Taq* DNA polymerase and

template DNA. Amplification was performed in a Peltier Thermal Cycler 200 programmed with an initial template denaturation at 94°C for 3 min followed by 35-45 cycles of denaturation at 94°C for 1 min, a primer annealing step and extension at 72°C. Annealing temperature and time varied depending on the primer pairs.

2.3.15 Preparation of PCR products for cloning.

PCR products were ethanol precipitated as detailed in Section 2.3.1, resuspended in water and then digested with the appropriate enzyme. The digest was gel purified as detailed in Section 2.3.4, again resuspended in water and an appropriate amount of the purified fragments used in ligation reaction as detailed in Section 2.3.6.

2.3.16 Screening cDNA and genomic libraries.

2.3.16.1 Preparation of cells.

Cells that were competent to phage entry were produced by inoculating a 50ml culture of L-Broth + 0.2% maltose + 10mM $MgSO_4$ with a single bacterial colony and grown at 37°C overnight. The cells were pelleted for 5 min at 3,000rpm in a bench centrifuge and then resuspended in 10ml of 10mM $MgSO_4$ and kept on ice. From this stock another 10ml of 10mM $MgSO_4$ was diluted to approximately OD_{600} = 1 and kept on ice.

2.3.16.2 Titration of phage libraries.

Phage libraries were titred by making serial dilutions of 1 X $10^{-1/-2/-3/-4}$ and $^{-5}$ of the original stock. 10µl of each dilution was added to 100µl of *E.coli* (LE392) at OD_{600} of 1 in 10ml disposable tubes and incubated at 37°C for 10min. 3ml of melted L-Broth and 0.7% agarose was dispensed to each tube, mixed and poured onto preheated agar plates. After the plates had set they were incubated at 37°C for 12-15 hrs. The number of phage colonies growing on each plate was counted to determine the original concentration of the stock solution.

2.3.16.3 Screening of libraries.

Sixteen large agar plates were pre-warmed at 37°C. Appropriate amounts of phage were added to each of 16 10ml tubes to allow between 6 X 10^4 and 8 X 10^4 phage per tube. 500µl of the cells resuspended in 10mM $MgSO_4$ (OD_{600} = 1) were added to each tube and left for 30 mins at 37°C to allow the phage to absorb to the bacteria. 8ml aliquots of melted L-broth + 0.7% agar were dispensed into each of the 16 tubes containing cells pre-absorbed to the phage. This was mixed and immediately plated onto the pre-warmed plates. After the plates had set, they were incubated at 37°C for 12-15 hrs. The plates were cooled at 4°C for at least 1 hour to firm the agar. Pre-cut Hybond^{TM} - N+ nylon filters (134mm) were then placed on the agarose from the centre outwards and keyed to the plates. The filters were left on the plates for 1 min before being lifted off and dried between 3mm Whatman paper. Duplicate filters were obtained by repeating the lifts and leaving the sec group of filters on the plates for 3 mins. The phage were lysed and fixed to the filter by treating with denaturing solution for 2 mins and neutralising solution for 2 mins. Filters were then soaked in 2 X SSC, placed between two pieces of Whatman 3MM paper and baked for 2 hrs at 55°C. Hybridisation of DNA probes to the filters was completed as described in section 2.3.8. Following removal of excess probe the filters were exposed to Hyperfilm with two intensifier screens at -80°C for three to four days. The autoradiography film was aligned with the plates and a plug of agarose corresponding to the position of positive signals on the film removed using the wide end of a sterile pasteur pipette. The plug was then placed in 1ml of SM buffer plus 50µl chloroform to elute the phage at either 4°C overnight or shaking at room temperature for one hour. Subsequent plating of positive plaques to isolate a single phage was completed using serial dilutions of 1 X $10^{-3/-4/-5}$ of the phage eluted in SM buffer. 10µl of these dilutions were added to 100µl of cells and incubated at 37°C for 15 min and plated on small agar plates. These were incubated at 37°C for 12-15 hrs. Pre-cut 80mm nitrocellulose filters were then placed on the agarose and keyed to the plates. Filters were then treated as per the first screening.

2.3.17 Phage DNA preparation from eluted plugs.

50µl of eluted phage (in SM buffer plus chloroform) was added to 500µl of previously prepared OD_{600}=1 LE392 cells (see section 2.3.16.1). The phage were allowed to pre-absorb for 30 mins at 37°C. Pre-absorbed phage were then added to 37ml of L-Broth supplemented with 0.2% Maltose and 10mM $MgSO_4$ and grown at 37°C for 12-15 hrs with shaking (200rpm). Following growth, cultures were transferred to 37ml tubes before addition of 100µl chloroform, 370µl of nuclease solution (50mg DNase, 50mg RNase A in 10ml of 50% glycerol, 30mmole NaAc at pH 6.8) and incubation at 37°C for 30 mins. 2.1g of NaCl was then added and gently dissolved. The cell debris was pelleted by spinning at 10,000rpm at 4°C for 20 mins and the supernatant transferred to new tubes containing 3.7g PEG (MW = 8000). The tubes were then placed on ice for one hour and spun at 10,000rpm at 4°C for 20 mins. After the supernatant was removed the phage were resuspended in 500µl SM buffer and transferred to microfuge tubes. 500µl of chloroform was added and the supernatant transferred to new tubes after spinning at 15,000rpm for 5min. 20µl of 0.5M EDTA, 5µl of 20% SDS and 10µl proteinase K (2.5mg/ml) were added and incubated at 65°C for 30 mins. The supernatant was then subjected to extraction with an equal volume of phenol/chloroform. DNA was precipitated by the addition of 200µl 5M ammonium acetate and 700µl of isopropanol, washed with 100µl of 70% ethanol and resuspended in 200µl of TE.

2.3.18 DNA preparations from paraffin-embedded tissue.

Three fine slices of paraffin embedded tissue were placed into a 1.5ml microfuge tube. 500µl of xylene was added and vortexed gently. Following centrifugation at 14,000 rpm for 5 min, xylene was removed and replaced with 500µl absolute EtOH. The mixture was spun for 5 min at 14,000rpm and desiccated for 10 min. A detergent lysis buffer was added (0.5mM KCl, 0.1mM Tris-HCl (pH8.3), 0.15mM $MgCl_2$, 0.1% gelatin, 0.45% NP40, 0.45% Tween 20) at approximately 1µl/2mm^2 of tissue. 2µl of Proteinase K (10mg/ml) was added/50µl of detergent lysis buffer and digested for 1hr at 65°C, following which the preparation was

stored at 4°C. Before use in PCR the preparation was spun for 1min in a microfuge to pellet any cellular debris.

2.3.19 Fixing grid colonies onto filters.

To screen large numbers of bacterial colonies for specific plasmid inserts the colonies were replica-plated using Grunstein grids on ampicillin-containing agar overlain with Hybond™-N+ membrane and grown at 37°C overnight. The filters were taken off the agar and dried for no more than two mins. Trays were lined with Whatmann paper and all solutions required for the fixing process were poured into the trays until just covering the paper. The filters (with colonies always face up) were placed in 10% SDS for three mins, blotted on dry Whatmann and left in denaturing solution for three to five mins depending on the size of the colonies. After blotting, the filters were placed in neutralising solution for five to seven mins and then briefly removed to 2 X SSC. The filters were baked in an oven at 70-80°C for one hour and probed as detailed in section 2.3.12.

2.3.20 Maintaining cultured cell lines.

All cultured cell lines were routinely grown in 75-150cm3 flaks (Falcon) at 37°C in an atmosphere of 5% CO_2. Cell lines were maintained by subculturing approximately 1:10-1:20 dilutions every 3-4 days. Harvesting and subculturing adherent cells was completed by first removing the culture media, washing twice with PBS before the addition of 1-2ml of trypsin/EDTA solution. The cells were left at room temperature until they began to detach from the surface of the flask, after which time 7ml of culture media was added and the flask washed to remove any remaining cells. Harvested cells were washed twice in PBS and pelleted by centrifugation at 1,200 X g for 5 min before being resuspended in the appropriate buffer.

2.3.21 Transfection of cultured cells with Fugene.

Cells were seeded into appropriately sized dishes to approximately 60-80% confluency in growth media. The cells were allowed to attach to the surface of the flask or

inserted coverslip for at least 4 hrs and transfected with a mixture of Fugene (Roche) diluted with DMEM and the appropriate DNA construct (as per manufacturers recommendations). Following at least 24 hrs of expression, cells were utilised for either protein extraction or immunofluorescence.

2.3.22 Non-denaturing protein extraction from cultured cells.

10cm plates containing either transfected or untransfected cells that were 80-90% confluent were rinsed twice with ice-cold PBS. Cells were collected by physical removal with a cell scraper in 1ml of ice-cold non-denaturing lysis buffer and transferred to a microcentrifuge tube. Following a brief vortex for 10 sec the cells were incubated on ice for 30 min and stored at -20°C.

2.3.23 Immunofluorescent analysis of cultured cells.

24 hrs post transfection cells plated on coverslips were rinsed twice PBS and fixed with 3.5% PFA in PBS. Following permeabilisation with 0.2% Nonidet-P40 in PBS, mitochondria were stained with the appropriate dilution of primary antibody for 1 hr. Excess primary antibodies were washed off with PBS and attached antibodies were then detected with appropriate dilutions of conjugated secondary antibodies. The coverslips were inverted and mounted onto glass slides for visualisation under appropriate wavelength light on an Olympus AX70 microscope and images captured using a Photometrics CE200A cooled CCD camera.

2.3.24 Protein gel electrophoresis and western blotting.

All SDS-PAGE of protein samples and subsequent western transfer to nitrocellulose or nylon membranes, Coomassie blue staining of gels and Ponceau S staining of blots was performed exactly as described by (Harlow and Lane, 1988). Nitrocellulose and Nylon blots were washed thoroughly with PBST and then blocked for 1 hr in PBST 5% Blotto. Primary and Secondary antibody incubations were carried out overnight at 4°C or for 45 min at room

temperature with the appropriate dilutions of antibody in the aforementioned blocking solution. All secondary antibodies were conjugated to horseradish peroxidase (Amersham) and detected by Enhanced Chemiluminescence (Amersham).

2.3.25 Protein concentration: Bradford assay.

Bradford reagent (Biorad) was diluted 1:5 with Milli-Q water. Between 1-5µl of protein was made up to 200µl with dilute Bradford reagent and mixed by pipetting. The assay solution was placed into a 96 well plate and the absorbance at 590nm was measured on a UV spectrophorometer. BSA protein standard assays were obtained between the range 0-40mg/ml. Approximate concentration of the test sample was determined against a linear plot produced by the BSA standard. All assays were completed in duplicate and the mean result determined.

2.3.26 Isolation of mitochondria.

2.3.26.1 Ball bearing homogenisation.

Subconfluent Cos-1 cells were transfected with GFP fusion constructs using the Fugene transfection reagent. After 48 hr expression cells were collected in growth media and washed twice with cold PBS. Cells were harvested with trypsin/EDTA following 2 washes in PBS. Trypsin/EDTA was inhibited by resuspension in complete growth media. The cells were then lysed by resuspension in mitochondria buffer and passed 5-6 times through a ball-bearing homogeniser (5mm ball diameter; kindly supplied by Dr B. Wattenberg, Institute of Medical and Veterinary Science, South Australia). Unbroken cells and nuclei were pelleted by centrifugation twice at 3,000rpm for 5 min at 4°C in a Beckman JA-10 centrifuge. Post-nuclear supernatant was then centrifuged in a Beckman JA-10 rotor at 15,000 X g for 15 min at 4°C to pellet crude mitochondria. The remaining pellet was washed twice in buffer B before final resuspension in the same buffer. These mitochondria were used immediately after isolation.

2.3.26.2 Buffer A homogenisation.

Cos-1 cells were transfected with GFP or 6myc fusion constructs using the Fugene transfection as previously mentioned. The mitochondria fraction in this method was then obtained as previously described (Wu *et al*, 2000). In brief, 10^7cells were lysed in 1ml of buffer A for 30 min on ice. Following homogenisation with a Dounce homogenizer B pestle cell lysates were cleared twice by centrifugation at 1,500rpm for 5 min at 4°C in a Beckman CS-6R centrifuge. To obtain mitochondria the supernatant was then spun at 9,000 X *g* for 30 min at 4°C. The pellet containing the mitochondria was resuspended in buffer A and recentrifuged at 9,000 X *g* for 30 min at 4°C. Mitochondria were again resuspended in buffer A and aliquots (500µg/tube) were stored at –70°C.

2.3.26.3 Mitochondrial purification by percoll gradient.

Mitochondria isolated in the 2.3.26.2 were layered on top of 30% Percoll (diluted with PBS) placed into 10ml heat sealable ultra-centrifuge tubes to fit a Sorvall T-1250 centrifuge. Following centrifugation at 90,000 X g at 4°C for 30 min the gradient was collected in 2ml fractions. To collect fractions the bottom of the tube was pierced with a 20g syringe and the drops collected in 10ml plastic tubes. The fractions were then diluted with 2 volumes of cold buffer A and protein was pelleted by centrifugation at 9,000 X g for 10 min at 4°C. The pellet was washed twice in buffer A before final resuspension in 100µl of the same buffer before addition of SDS load buffer and use in western blot.

2.3.27 Fractionation of mitochondria.

2.3.27.1 Digitonin fractionation.

To selectively disrupt the outer mitochondrial membrane purified mitochondria were pelleted by centrifugation at 13,000rpm at 4°C for 10 min. The pellet was then resuspended in extraction buffer (mitochondria buffer) at a concentration of 50ug/µl. Digitonin was added to the mitochondrial suspension between 1-5µl of digitonin/µg mitochondrial protein both with and without 1µg/ml ProK. The protein mixture was incubated for 30 min on ice with

agitation. ProK was inhibited by pelleting the remaining mitochondrial protein followed by resuspension in SDS load buffer containing 1mM PMSF.

2.3.27.2 Osmotic shock fractionation.

Mitoplasts consisting of proteins located in the mitochondrial inner membrane and mitochondrial matrix were prepared essentially as described by Nobumoto *et al* (Nobumoto *et al*, 1998). Mitochondria (100µg) were recovered by centrifugation at 13,000rpm at 4°C and resuspended in 60µl of 20mM HEPES-KOH (pH 7.4) containing 1mM BSA and placed on ice for 30 min. Mitoplasts were then obtained by centrifuging at 10,000rpm for 5 min at 4°C and resuspended in 50µl 10mM HEPES-KOH (pH 7.4) containing 220mM mannitol and 70mM sucrose. Both mitochondria and mitoplasts were treated with 200µg/ml proteinase K with or without 1% Triton X-100 at 4°C for 30min. Proteinase K was then inhibited with 2 µl of 100mM PMSF and the remaining protein was recovered by centrifugation at 13,000rpm at 4°C. The pellets were immediately dissolved in SDS load buffer and subjected to electrophoresis on 10% or 15% SDS-PAGE gels. After semi-dry transfer to nitrocellulose membrane, the corresponding proteins were detected with appropriate antibodies.

2.3.28 Co-immuno precipitation.

Mitochondria isolated with the buffer A homogenization protocol (2.3.26.2) were centrifuged at 13,000rpm and lysed in mitochondrial lysis buffer for 30 min on ice. 100µl of lysis buffer was used for every 10^7 cells in the starting culture. Following clearing of the lysate with a spin of 13,000rpm at 4°C protein concentration was estimated by Bradford assay. 100µg of mitochondrial protein was incubated with bait antibody and mixed overnight at 4°C with gentle rocking. 40ul of protein A/G-Plus-agarose beads (Santa Cruz) were added to each tube and mixed at 4°C for 2-4 hrs. Beads were pelleted by centrifugation at 4,000rpm for 5 min and washed 4 times with buffer A followed by one wash with PBS. Remaining pellets were boiled at 95°C for 5 min in SDS load buffer and used for SDS PAGE and western blot analysis.

2.3.29 Polyclonal antibody production.

2.3.29.1 Expression and extraction of bacterial fusion protein.

An overnight culture of cells carrying the GST expression construct was diluted 100 fold into fresh L-broth containing amp and incubated at 37°C for approximately 3 hrs. Cells were pelleted by centrifugation at 3,500 X g for 10 min, and then resuspended in 1/100 volume of PBS. Cells were lysed by incubation with 50ug/ml lysozyme for 15 min, followed by sonication 3 times for 30 sec on ice ensuring samples remained cold. The insoluble and soluble fractions were separated by centrifugation at 3,500 X g for 10 min. The insoluble fraction was solubilised in PBS + 1% Triton X-100.

2.3.29.2 Generation of anti-murine CTS antiserum.

Murine CTS was separated by SDS-PAGE (12%) and protein was visualised by staining the gel with Coomassie prepared in water (Harlow and Lane, 1988), and the appropriate gel slice excised. The slice was homogenised in an equal volume of PBS by passage through a G-20 needle. The gel slurry was then mixed with Freund's adjuvent and administered to New Zealand White rabbits as previously described (Casanova *et al*, 1989). In brief, approximately 100μg of protein was injected to the rabbit at each injection. In total 3 injections were completed over a 1 month period. Following the third round of injection antiserum was tested on native HCCS and also HCCS over-expressing cell lines before the final bleeding of the animal. The crude anti-serum was used without further purification. Pre-immune serum was harvested and used as a negative control.

2.3.30 Benzidine H_20_2 staining procedure.

Yeast colonies were fixed to the surface of YPD plates by spraying with common hair spray. 15ml of benzidine reagent (1g benzidine hydrochloride, 20ml glacial acetic acid, 30ml Milli-Q water, and 50ml 95% EtOH) was then added to the surface of the plates and incubated at room temperature for under 1 min. After removing the benzidine reagent a 5% solution of H_20_2 was placed onto the plate until colonies had developed a sufficient blue colour.

2.3.31 Karyotype analysis.

Mouse ES cells were seeded into 10cm dishes 24 hrs prior to replacement of media with fresh growth media containing 0.02ug/ml colcemid and incubation for an hour at 37°C. Cells were washed twice with PBS and collected by trypsinisation for around 5-10 min. Trypsin was then inhibited by resuspension in DMEM with 10% FBS followed by centrifugation at 1,000rpm for 3 min to collect the cells. 1ml of 0.56% KCl was then added drop-wise and resuspended by gentle flicking. Another 4ml of 0.56% KCl was added to the mixture and incubated at room temperature for 6 min. The cells were then pelleted at 500rpm for 5 min before addition of 1ml of fix (3:1 methanol:acetic acid) and flicking to resuspend. A further 4ml of the fix was added and incubated for another 5 mins at room temperature. The cells were washed a further three times in fix and finally resuspended in only 1ml of the same solution. 2-3 drops of the cells were dropped onto glass slides (prepared by being rinsed in fix and then soaked in ice cold water until ready for use) from at least 30cm height. The slides were air dried before staining with a 1:20 dilution of Giemsa for 15 min and washing with water. Coverslips were placed over the spread on 90% glycerol and photographed with a light microscope.

Chapter Three: Functional analysis of mammalian *CTS.*

3.1 Introduction.

Oncocytic cardiomyopathy (OC) is a severe disorder that often results in sudden infant death. Morphologically, OC resembles the well characterised mitochondrial myopathies (i.e. mitochondrial hyperplasia in affected tissue) and the finding of decreased activity of respiratory complexes III and/or IV in a number of cases supports the conclusion that a primary respiratory chain defect underlies the disorder. Interestingly, OC presents predominantly in females which led to the initial hypothesis that it may be an X-linked embryonic male lethal disorder. Although a recent publication detailed the mutation of *cytochrome b* in a patient with an OC like phenotype, this case likely indicates the expected genetic heterogeneity of the disorder. Indeed, the presence of sporadic male patients may also support this theory.

Giving some insight to the possible underlying X-linked genetic fault was the identification of a number of patients with a normal karyotype that co-present with both OC and MIDAS syndrome (Bird *et al*, 1994; Cox *et al*, 1998). Retrospective investigations add further support for the Xp location of the OC causative gene; over 10% of OC patients also present with MIDAS related features, while the same proportion of MIDAS patients also show a dilated cardiomyopathy consistent with OC.

Correlations between various X chromosome abnormalities and patient phenotypes have been utilised to delineate a small chromosomal segment that is likely to contain the causative gene(s) for the MIDAS (and thus also OC) phenotype (Fig 1.1; Wapenaar *et al*, 1994; Cox *et al*, 1998). In 1996, Schaefer and colleagues identified a gene from within this region whose predicted protein product exhibited ~35% and ~33% amino acid identity with the primary sequences of the yeast holocytochrome c synthase (HCCS; referred to as *Cyc3p*) and holocytochrome c1 synthase (HCC1S; referred to as *Cyc2p*), respectively (Fig 1.3). In *S.cerevisiae* and *N.crassa,* the c-type synthases (CTS's) are required for the activation of both apocytochromes c and c1. Consequently, the mature cytochromes c and c1 allow the transition of electrons from complex III to complex IV in the mitochondrial respiratory chain. Deficiencies within both of these complexes have previously been shown to cause various

forms of cardiomyopathies (Bohles *et al*, 1987; Papadimitriou *et al*, 1984; Otani, 1995; Andreu *et al*, 2000).

Due to the primary sequence similarity, this human gene is likely to encode a mammalian holocytochrome c-type synthase (CTS; Schaefer *et al*, 1996). This putative *CTS* is one of three genes found to map within the originally described ~570 kb critical interval. However, Cox *et al* (2001) provided support for a refinement of this region to ~260 kb. This alteration was based on the lack of any phenotype from mutations within the other two genes from this region, *MID1;Mid1* and *ARHGAP6;Arhgap6* (Cox *et al*, 2001). Notably, the putative *CTS* is the only known gene located completely within the refined ~260 kb interval.

Like most mitochondrial proteins, the c-type cytochromes are encoded within the nucleus, synthesised on cytosolic ribosomes and translocated to their correct mitochondrial compartment (Wang *et al*, 1996; Nicholson *et al*, 1989). While the translocation of cytochrome c1 into the inter-membrane space has been well documented, little is known about the passage of cytochrome c to the same compartment as it has no characteristic targeting signal(s). Results suggest that apocytochrome c is able to reversibly cross the outer mitochondrial membrane and is only sequestered within the inter-membrane space by either heme attachment or binding to HCCS (Steiner *et al*, 1995). Given that mutant forms of HCCS are unable to catalyse heme attachment to the apocytochrome but still retain the protein within the mitochondria, implies that binding to HCCS is the determinant. Indeed, complete removal of HCCS has been found to eliminate any mitochondrial localisation of cytochrome c (Mayer *et al*, 1995).

Interestingly, cytochrome c has become the focus of recent research due to its secondary role in programmed cell death. Upon initiation of apoptotic signalling cascades from the mitochondria, mature cytochrome c is relocated from the inter membrane space to the cytosol where it interacts with apoptotic protease activating factor 1 (Apaf1) and pro-caspase 9 to form the "apoptosome". The apoptosome then promotes cleavage of effector caspases (caspase-3, -6 and –7) that activate substrates required for apoptotic degradation. Initiation of apoptosis may also result from cell membrane signalling through other upstream caspases (caspase-2, -8 and –10) that also utilise common effector caspases (reviewed in Green & Kroemer, 1998).

The work in this chapter has aimed at investigating whether the putative human CTS is a true orthologue of the yeast CTS genes with which it shares high sequence similarity. For this study a number of yeast mutants have been obtained and utilised in a phenotypic rescue experiment, while the visual properties of the Green Fluorescence Protein (GFP) (Prasher, 1995) have also been applied to address protein localisation in the cell. These experiments have been undertaken to provide additional support for the notion that abnormalities of *hCTS* cause OC and other features associated with MIDAS syndrome.

3.2 Results.

3.2.1 Analysis of a human CTS-GFPS65T fusion construct.

To investigate the similarity of the putative mammalian CTS further, a construct encoding the entire human *CTS* ORF fused in-frame with GFP was generated prior to the initiation of this project (pBSK-CTS-GFP; Schwarz, 1997). Creation of a C-terminal GFP fusion protein was chosen because of the possibility that the CTS protein, if indeed involved within the respiratory chain, might possess an N-terminal mitochondrial targeting pre-sequence that could be enzymatically cleaved upon translocation to that organelle.
Within this construct the TAA stop codon of human CTS was removed by PCR amplification with the primers HKpnI and CCHL1 that concomitantly introduced a *Kpn*I restriction site that allowed in-frame fusion with GFPS65T[6].

In order to analyse localisation of this fusion protein within cells, the cassette was first placed into both yeast and mammalian expression vectors. For these purposes, a yeast expression vector was generated by directionally cloning a 700bp *Hin*dIII / *Eco*RI fragment of the constitutively expressing alcohol dehydrogenase (ADH) promoter from *S.pombe* into the yeast CEN cloning vector pRS314 (Sikorski & Hieter, 1989) (obtained from Dr S. Dalton, University of Adelaide, South Australia). An *Xba*I / *Bam*HI fragment containing the fusion of CTS-GFPS65T was then ligated into a similarly digested yeast expression vector to yield pADH-CTS-GFP. For localisation of the fusion protein to be analysed in mammalian cells

[6] GFPS65T is a red-shifted variant of GFP that promotes increased fluorescence as a result of a serine to threonine mutation at amino acid 65.

the pRc/RSV expression vector was chosen. This vector contains the constitutively expressing Rous sarcoma virus (RSV) promoter that has previously been used in cell lines available for these studies (i.e. Cos-1 and HeLa cell lines; Lober *et al*, 2002). A *Hin*dIII / *Xba*I cassette from pBSK-CTS-GFP was inserted in to appropriately digested pRc/RSV to generate RSV-CTS-GFP. GFPS65T was also placed into the *Bam*HI / *Eco*RI site of the yeast expression vector (pADH-GFP) to be used as a control for transfection, expression and intracellular localisation. All constructs were confirmed by restriction enzyme analysis and sequencing.

The yeast expression vectors containing CTS-GFP and GFP alone were transformed into a Δ*Cyc3p* (Δ*HCCS*) strain, B-8025, (obtained from Prof. F. Sherman, University of Rochester, New York) under selection for Tryptophan auxotrophy. Following analysis of live cells under appropriate wavelength ultraviolet light there was minimal fluorescence noticed (results not shown) on either the Olympus AX70 microscope or Confocal microscope, suggesting that the GFPS65T ORF in these constructs would not be appropriate for yeast studies. To address whether expression and fluorescence were readily detectable in mammalian cells the pRSV-CTS-GFP construct was transiently introduced to Cos-1 cells by electroporation. After multiple transfections, only low levels of fluorescence were detected from the pRSV-CTS-GFP vector (results not shown). The pEGFPC$_2$ (Clontech) vector that encodes the enhanced GFP ORF optimised for brighter fluorescence and higher expression in mammalian cells was subsequently obtained and transfected to determine whether any observed targeting was conferred by this construct. Live cells were stained with the mitochondria selective dye Mitotracker CxMRos (Molecular Probes) and again analysed on the Olympus AX70 microscope. In striking contrast to the S65T variant, the EGFP control had bright fluorescence from a high percentage of cells, suggesting that either the pRSV-CTS-GFP construct was not being expressed efficiently, or that fluorescence from this pGFPS65T was not strong in the mammalian cells used.

3.2.2 Generation and analysis of a human CTS-EGFP fusion construct.

To analyse localisation of the putative hCTS in mammalian cells, EGFP was fused to the C-terminus of hCTS as a marker protein. For these studies, the $pEGFPN_1$ vector (Clontech) was utilised as it facilitates insertion of an ORF 5' of the GFP cDNA. A *Hin*dIII / *Kpn*I fragment from pBSK-CTS-GFP was placed into similarly digested $pEGFPN_1$. In-frame fusion between *CTS* and *EGFP* was then obtained by removal of the *Kpn*I site by restriction enzyme digestion, Klenow end-filling and re-ligation (hCTS-EGFP-K). Restriction digestion was used to identify clones with removal of *Kpn*I while sequencing confirmed the fusion of the two ORF's.

The expression construct, hCTS-EGFP-K, and the control vector $pEGFPN_1$ were transfected into various cell lines (i.e. HeLa, Cos-1 and NIH3T3) to investigate the intracellular localisation of the protein. Unlike the even cytoplasmic distribution of green fluorescence that was observed for the EGFP control, the hCTS-EGFP-K transfected cells showed fluorescence that was restricted to distinct regions throughout the cytoplasm. Co-staining with Mitotracker clearly demonstrated that these fluorescent regions co-localised, indicating that the hCTS-GFP fusion protein was targeted to mitochondria. Example cells expressing these constructs are represented in figure 3.1.

3.2.3 Localisation of native CTS using CTS-specific antibody.

Although the expected localisation to mitochondria was observed for the over-expressed hCTS-GFP it was important to confirm that this reflected the localisation of the endogenous (native) protein. To this end, and to facilitate future studies of endogenous mammalian CTS, a polyclonal antibody to murine CTS was raised. A full-length mouse CTS EST (# 413678) was obtained from the IMAGE consortium and confirmed by sequence analysis with mCCHL1 and T3 / T7 vector primers. To enable synthesis of purified full-length mCTS protein for the inoculation of animal hosts, the inducible bacterial expression vector pGEX4T-2 that contains a Glutathione S-Transferase (GST) tag was chosen. Appropriate restriction sites allowing in-frame fusion of murine CTS with GST were introduced by first removing the ORF from EST# 413678 with *Nco*I / *Kpn*I and ligating to pLIT28 (pLIT28-mCTS). By then removing a *Bam*HI / *Xho*I fragment from this vector and

placing into similarly digested pGEX4T-2 an in-frame fusion was created with GST (GST-mCTS). Sequencing of this construct confirmed the correct orientation and continuity of the reading frame.

GST-CTS was over-expressed in DH5α and purified as detailed in section 2.3.29 before being used to inoculate one New Zealand White Rabbit (Institute of Medical and Veterinary Science, South Australia). Anti-serum was analysed against endogenous and over-expressed hCTS-EGFP protein by SDS-PAGE. The serum was found to be specific to CTS and active in multiple species including human, mouse and monkey with an optimal dilution of 1:15,000 – 1:20,000 for western blot, and 1:50 – 1:100 for immunofluorescence (Fig 3.2A and 3.2B). Western blot analysis identified an approximate 35 kDa endogenous protein and, as expected, also recognised the hCTS-EGFP-K fusion protein. Localisation of endogenous CTS within cells was also found to co-localise with Mitotracker CxMRos, confirming the localisation also observed with the hCTS-EGFP construct. Mitochondrial localisation of this putative mammalian CTS is consistent with the predicted respiratory chain function of the mature protein.

3.2.4 Functional analysis of human CTS in yeast mutants.

3.2.4.1 Production of CTS yeast expression vectors.

Cytochrome c molecules from such diverse organisms as man and yeasts still retain a high level of sequence conservation, suggesting that even mammalian heme lyases might be able to specifically replace their yeast counterpart, as has been found for *C.albicans* (Cervera *et al*, 1998). To therefore determine if the putative hCTS shares the same function as either of the yeast proteins with which it shares sequence similarity, a rescue of the respective yeast mutants was attempted. Deficiencies in the mitochondrial respiratory pathway, such as *Cyc-3* and *Cyt-2* mutants, show diminished growth on all non-fermentable carbon sources. Lactate, in particular, does not support growth of even partial deficiencies within this pathway. The reasons for this are unclear, but may reflect an increased requirement of cytochrome c (Sherman *et al*, 1974). In contrast, glycerol, another non-fermentable carbon source is able to support growth of partial cytochrome deficiencies that are unable to grow on lactate (Dumont *et al*, 1990).

Figure 3.1

Mitochondrial localisation of the putative human CTS
Cos-1 cells were electroporated with either the human pCTS-EGFP fusion construct or pEGFPN1 alone (green). The same cells were counter-stained with the mitochondrial selective dye MitoTracker Red CXMRos (red). Images were captured with an Olympus AX70 microscope using a Photometrics CE200A cooled CCD camera under the appropriate wavelength UV light. Overlaying the two images (Merge) highlights a mitochondrial localisation of the hCTS protein. The EGFP expressing cells were also stained with the DNA specific dye DAPI (blue).

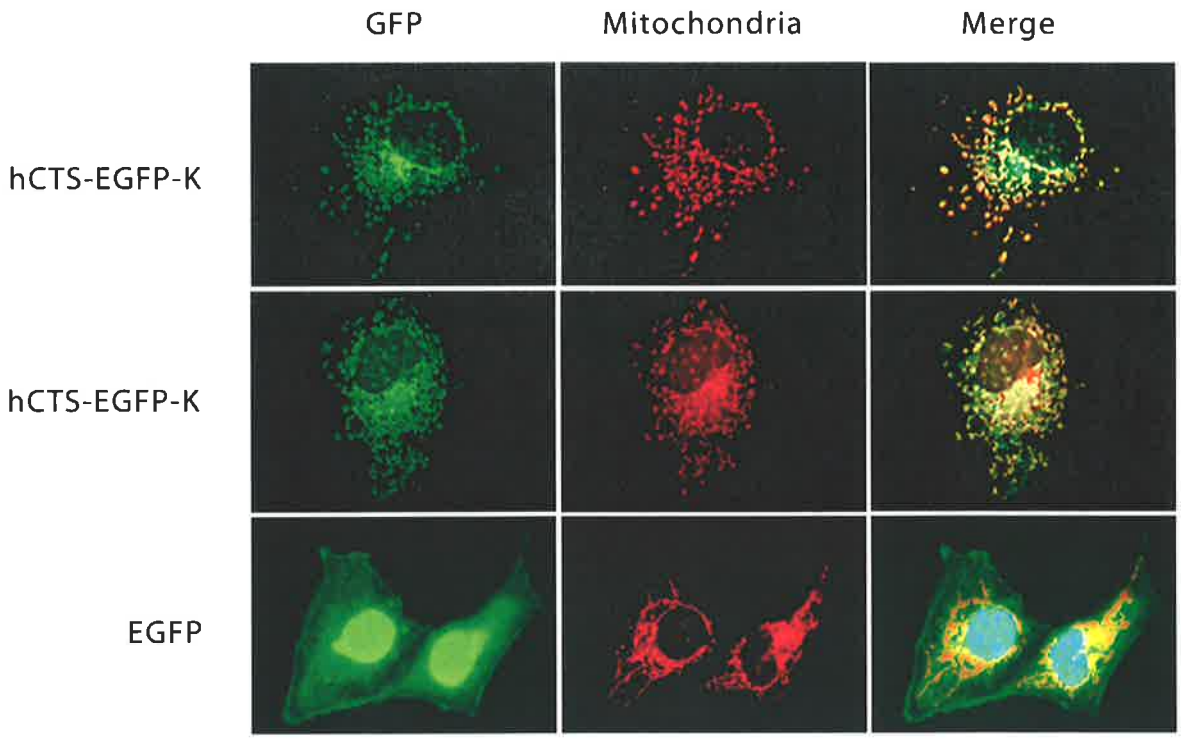
GFP
Mitochondria
Merge
hCTS-EGFP-K
hCTS-EGFP-K
EGFP

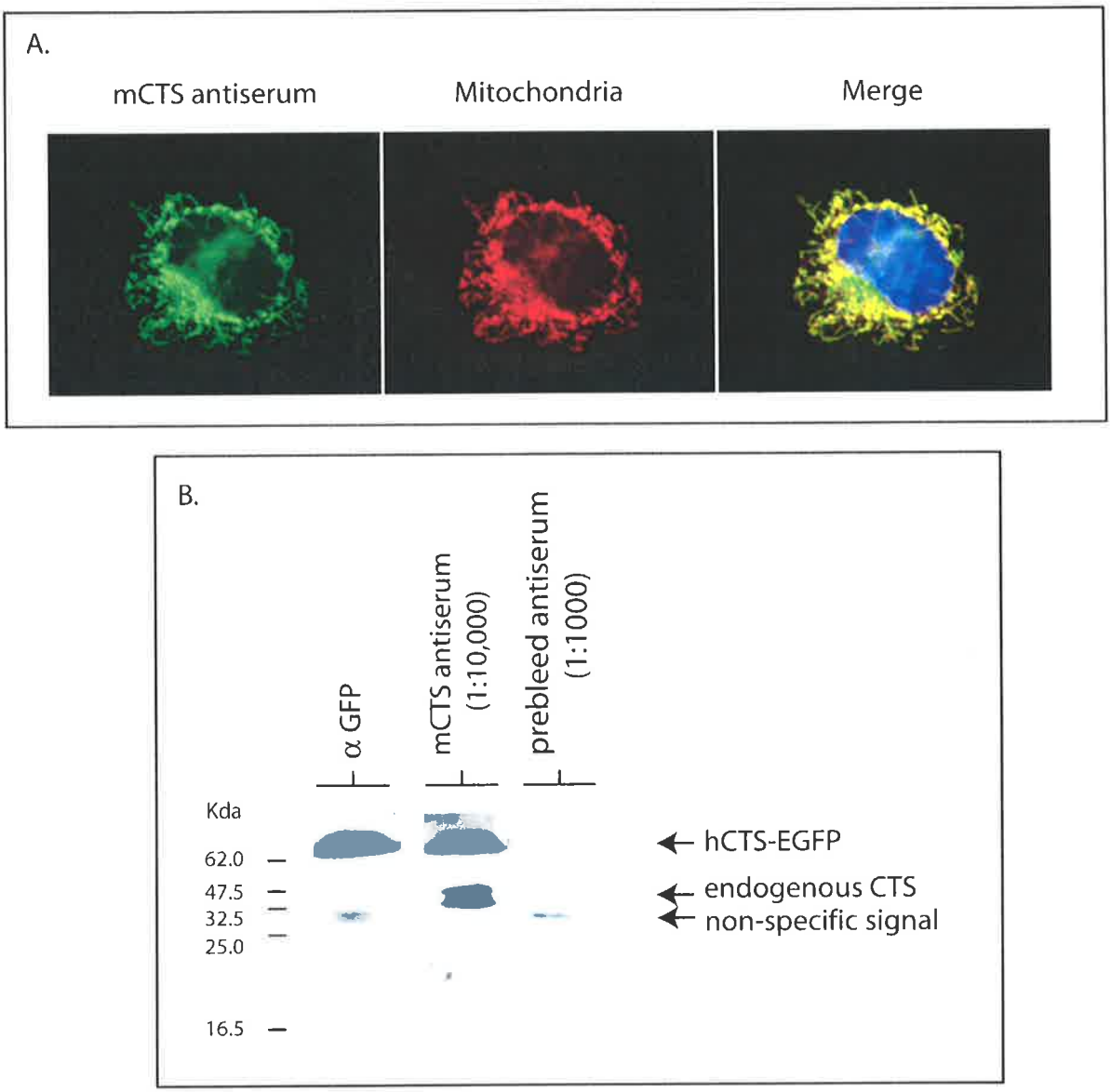

Figure 3.2

A. Immunofluorescent analysis of mammalian CTS antibody
Fixed and permeabilised Cos-1 cells were incubated with a 1:50 dilution of antiserum obtained from NZ white rabbits injected intramuscularly with purified mCTS protein. The same cells were counter-stained with the mitochondrial selective dye MitoTracker Red CXMRos (red) and the DNA specific dye DAPI (blue). Cells were mounted on slides and images captured with an Olympus AX70 microscope using a Photometrics CE200A cooled CCD camera under the appropriate wavelength UV light. Overlaying the two images (Merge) highlights the mitochondrial localisation of the native CTS protein.

B. Immunohistochemical analysis of mammalian CTS antibody
Whole cell protein extracts were made from human HEK-293T cells transiently transfected with hCTS-EGFP-K. 20μg of protein was subjected to SDS PAGE and transferred to nitrocellulose. Filters were treated with either a 1:10,000 dilution of anti mCTS antiserum, 1:1,500 dilution of anti GFP antibody or 1:1000 dilution of pre-bled rabbit serum. Both endogenous CTS and over-expressed CTS-EGFP were readily detected by the mCTS antiserum. A non-specific band detected by the pre-bled serum was also detected at lower levels by the mCTS serum. A band was also detected with the mCTS antibody but was non consistent between western blots.

To enable these studies, an *S.cerevisiae Cyc3p* deficient strain, B-8025, was obtained from Prof. F. Sherman (University of Rochester, New York). Likewise, a *Cyt2p* mutant strain, YS-10, was obtained from Prof. R. Lill (University of Marburg, Marburg) with the control strain, YS-51, that contains a functional copy of Cyt2p in the same genetic background as YS-10. For expression of hCTS in these yeast strains the pRS314 and pRS316 cloning vectors were utilised. As previously mentioned, the ADH promoter from *S.pombe* was cloned into the *Eco*RI / *Hin*dIII site of pRS314 (pRS314-ADH) and also into the same sites of pRS316 (pRS316-ADH) to drive expression of inserted ORF's. hCTS was then inserted into both vectors as a *Bam*HI cassette from pGEM7-hCTS (Schwarz, 1997) and digested with *Eco*RI to identify correctly oriented clones (pRS314-ADH-hCTS and pRS316-ADH-hCTS, respectively). To generate controls with appropriate selection markers, a pRS316-ADH-CYC3 vector was constructed by insertion of a 1kb *Sal*I / *Eco*RI fragment from pAB790 (Dumont *et al*, 1991) into pRS316-ADH. Similarly, a pRS314-ADH-CYT2 control vector was constructed by insertion of a 1.4kb *Not*I / *Eco*RI fragment from the plasmid BS4 that contains the full length *Cyt2* ORF (Zollner *et al*, 1992) into pRS314-ADH. Restriction analysis and DNA sequencing were used to confirm all constructs.

3.2.4.2 Transfection and growth rescue of mutant yeast strains.

Following transformation of the pRS-ADH-hCTS vectors and control constructs to the mutant *S.cerevisiae* strains, a partial rescue of the *Cyc3p* mutant was observed on glycerol. This rescue experiment was repeated several times with various dilutions of cells and in each case partial rescue of *Cyc3p* was seen but no growth rescue of the *Cyt2p* mutant was noticed (Fig 3.3A). Further analysis of these constructs on lactate media (results not shown) identified no growth rescue of either strain as may be expected from Sherman's original findings (Sherman, 1974). Although this restoration of growth was not as efficient as that seen when rescuing the phenotype with native *S.cerevisiae* Cyc3p (see Fig 3.3A) it does demonstrate that the human protein is able to catalyse the attachment of heme to apocytochrome c. Expression of *hCTS* within these strains was confirmed by western blot analysis of whole cell protein with the aforementioned polyclonal antibody (results not shown).

3.2.4.3 Maturation of cytochrome c in the B-8025 partial rescue.

Growth restoration of the B-8025 mutant importantly demonstrates that constitutive, low level expression of putative hCTS was able to replace Cyc3p. Given that the activity of each lyase is directed only at a specific apocytochrome (Dumont *et al*, 1987), it is therefore likely that this mammalian gene (hereafter referred to as *HCCS*) is indeed orthologous to yeast *Cyc3p*.

To confirm this phenotypic growth rescue at the molecular level, an antibody recognising both the apo- and holo-forms of *S.cerevisiae* cytochrome c (Cyc7p) (9624; Dumont *et al*, 1991) was obtained from Mr T. Cardillo (University of Rochester, New York). In the absence of HCCS both isoforms of apocytochrome c are proteolytically processed soon after synthesis and are therefore undetectable by western analysis (Dumont *et al*, 1989). Hence, only the stabilised holo-protein is detected by western blot. Consequently, this antibody was expected to be informative in detecting increased levels of the holo-cytochrome c protein. Immunohistochemical analysis of protein extracts from the transformed B-8025 strain grown in suspension at varying temperatures and with either glycerol or glucose as the primary carbon source identified an increase, albeit minor and variable, in the production of holocytochrome c when compared to untransformed B-8025 (Fig 3.3B). The minor increase detected on numerous occasions is consistent with only the partial restoration of the growth phenotype of this strain.

Further studies to confirm the increase in holocytochrome c were attempted with the benzidine-H_2O_2 stain detailed in Sherman *et al* (1968). This technique relies on the peroxidatic oxidation of benzidine catalysed by all heme and heme proteins. The assay is detected by blue colour staining of the cell colonies with intensity correlating to the amount of total cellular cytochromes. Of all the heme containing enzymes, cytochrome c has the largest effect on benzidine oxidation and therefore maturation of this protein can be readily analysed with this method (Downie *et al*, 1977). Although no consistent differences were detected with this assay (results not shown), increases in the mature protein indicated by partial growth rescue and immunohistochemistry nevertheless suggest that the putative human *CTS* is indeed the orthologue of *Cyt3p*. Therefore this gene has been referred to as *HCCS* for the remainder of this thesis.

Figure 3.3

A. Putative human CTS complements the *S.cerevisiae* Cyc3p growth deficiency
Yeast strains deficient for Cyt2p (HCC_1S) and Cyc3p (HCCS) were grown on minimal media and transformed with the putative full-length human CTS cDNA under the control of the *S.pombe* ADH promoter (pRS314/316-ADH-hCTS). The ability to complement the loss of either yeast CTS activity was assayed by re-plating different amounts (determined by optical density at 600 nm) of the transformed cells on glycerol containing media. Note the partial restoration of the poor growth phenotype of the B-8025 strain (deficient for Cyc3p) but not the YS-10 strain (deficient for Cyt2p) following tranformation with hCTS. Strain YS-51 was plated as a wild-type growth control of the YS-10 mutant strain.

B. Immunohistochemical analysis of Cyc7p maturation
The B-8025 yeast strain deficient for Cyc3p (HCCS) was transformed with either pRS314-ADH-CTS or pRS316-ADH-CYC3. Protein extracts were obtained from each strain grown at 30°C with 1:1 glucose : glycogen mix as the primary carbon source. Maturation of apocytochrome c to holocytochrome c was assayed by detection of the mature protein with a Cyc7p (CYT-C) specific antibody (9624; Dumont *et al*, 1991).

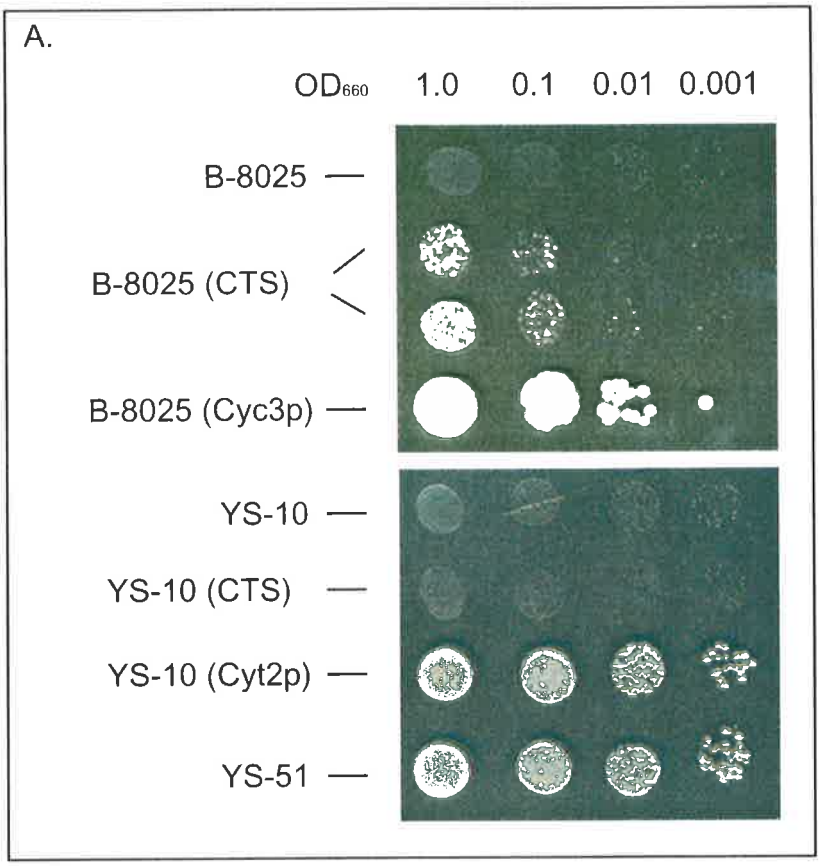
A.
OD660
1.0
0.1
0.01
0.001
B-8025
B-8025 (CTS)
B-8025 (Cyc3p)
YS-10
YS-10 (CTS)
YS-10 (Cyt2p)
YS-51

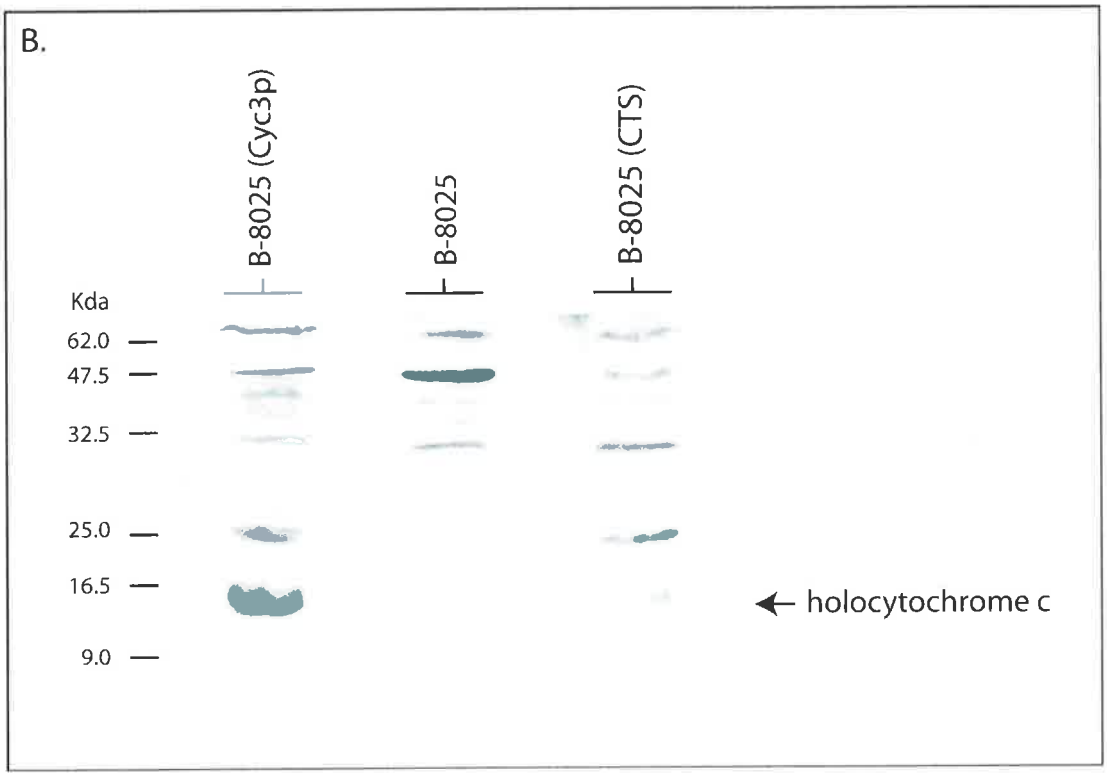
B.
B-8025 (Cyc3p)
B-8025
B-8025 (CTS)
Kda
62.0
47.5
32.5
25.0
16.5
9.0
holocytochrome c

3.2.5 Interaction of human HCCS and cytochrome c.

In yeast, Cyc3p (HCCS) interacts with apocytochrome c (Cyc7p) to catalyse the covalent addition of a heme moiety to the precursor protein (Dumont *et al*, 1991). HCCS also has the additional function as a high affinity binding site for the correct import of apocytochrome c to the mitochondrial inter-membrane space (Mayer *et al*, 1995).

3.2.5.1 Yeast two hybrid analysis of HCCS – CYTC protein interaction.

To determine whether this mammalian HCCS is also able to interact with cytochrome c (CYTC), the yeast two-hybrid system that is routinely used for the detection of protein-protein interactions was initially adopted. The yeast two-hybrid system allows interactions between two proteins to be detected by fusion of one protein to a DNA binding domain (the "bait") and the other protein to a trans-activation domain (the "prey"). Interaction between the two proteins therefore tethers the DNA binding domain to the activation domain to allow activation of reporter gene expression. Within the lab, the ProQuest^{TM} two-hybrid system (GibcoBRL) that uses three reporter genes (*His3*, *Leu2* and *LacZ*) to verify protein interactions was available. This system also contains five control strains of varying interaction strength that allow comparisons to be drawn with the test proteins. For this analysis fusion constructs containing the human *HCCS* or human *CYTC* ORF were generated with both the GAL4 DNA binding domain (BD) and GAL4 activation domain (AD). An in-frame fusion of *HCCS* with BD was generated by placing a *Not*I / *Nco*I fragment from pBS-HCCS (Schwarz, 1997) into similarly digested pDBLeu (provided with the ProQuest system) to produce pHCCS-BD. To generate a fusion between HCCS and the AD a *Not*I / *Sal*I fragment from pHCCS-BD was placed into similarly digested pPC86 (provided with the ProQuest system) to produce pHCCS-AD. A complete cDNA of *CYTC* was identified and obtained as an EST (IMAGE clone number 50907). The ORF was excised with *Hin*dIII / *Not*I and ligated to pBS (pBS-CYTC) to enable sequencing with vector primers. In-frame fusion with the AD was then produced by amplification of the ORF using Pfx polymerase and the primers cytc5'Sal and cytc3'BglII, followed by ligation to *Sal*I / *Bgl*II digested pPC86 (pCYTC-AD). CYTC was then placed in frame with the BD by removal from this vector with *Sal*I / *Not*I and ligation to similarly digested pDBLeu (pCYTC-BD). All constructs were confirmed by sequencing.

To detect an interaction between the two proteins the fusion constructs were transformed to the *S.cerevisiae* strain MaV203 that contains the three reporter genes at different loci. Initially, the fusion constructs were transformed with various combinations of pDBLeu (BD) or pPC86 (AD) to analyse self-activation of the *HIS3* reporter gene (summarised in table 3.1). As MaV203 has basal levels of expression from the *HIS3* promoter, these transformants were analysed on plates containing various amounts of 3-amino triazole (3AT[7]) to identify stronger activation of this reporter and hence an appropriate concentration to detect a bonafide interaction.

Plasmid 1	Plasmid 2	Selection media (SC-)	10mM 3AT	25mM 3AT	50mM 3AT	100mM 3AT
CYTC-AD	-	T	+	-	-	-
CYTC-BD	-	L	-	-	-	-
HCCS-AD	-	T	+	-	-	-
HCCS-BD	-	L	-	-	-	-
CYTC-AD	BD	L, T	+	-	-	-
CYTC-BD	AD	L, T	-	-	-	-
HCCS-AD	BD	L, T	+	-	-	-
HCCS-BD	AD	L, T	-	-	-	-
Control Strains						
A		L	+	+	-	-
B		L, T	+	+	+	-
C		L, T	+	+	+	+
D		L, T	+	+	+	+
E		L, T	+	+	+	+

Table 3.1 - Analysis of self activation of various HCCS / CYTC fusion constructs. + indicates growth on the detailed plate, - indicates no growth following replica cleaning. L, leucine; T, tryptophan.

[7] 3AT reduces background expression of *HIS3* by inhibiting histidine biosynthesis.

Following analysis of these strains, the minimal amount of 3AT identified to reduce background growth on media lacking histidine was found to be 25mM and was therefore used on all *His* selection plates. Any interaction between HCCS and CYTC was then analysed with co-transformation of the various BD and AD fusion constructs. Analysis of all selection markers was completed on appropriate media with no interaction between the two proteins being observed in either orientation (results not shown). Protein extracts from the strains expressing the human HCCS and human CYTC fusion constructs were analysed with anti-CYTC, anti-Hccs and anti-GAL4AD antibodies (obtained from Prof. R.Saint, Adelaide University, South Australia) which confirmed that the fusion proteins were indeed being expressed. This suggested that no growth on the selection plates indicated a lack of interaction between the two proteins in this system. This may have been due to interference by the fusion component in each case as the AD and BD portions are much larger than the CYTC protein. Alternatively, as these are single copy vectors, expression of endogenous yeast CYTC may be able to compete for binding to hHCCS and thereby significantly reduce reporter activation.

3.2.5.2 Co-immunoprecipitation analysis of HCCS – CYTC protein interaction.

The interaction between Cyc3p (HCCS) and Cyc7p (CYTC) in *S.cerevisiae* was initially detected by Cyc3p co-immunoprecipitation (co-IP) of *in vitro* transcribed and radioactively labelled apocytochrome c (Nicholson *et al*, 1988; Dumont *et al*, 1988). Therefore, to address this further a co-IP approach was also used in an attempt to show an interaction of the corresponding human proteins. To increase cellular protein levels for this experiment, both HCCS and CYTC were over-expressed from the cytomegalovirus (CMV) promoter. A pCMV expression vector was generated by *Bam*HI / *Xba*I excision of the *EGFP* ORF from pEGFPN$_1$ followed by T4 blunting and religation (made by Dr. B.Hopwood, University of Adelaide, South Australia). Subsequently, a pCMV-hCYTC vector was produced by excision of a *Sac*I / *Kpn*I fragment from pBSK-hCYTC and ligation to similarly digested pCMV. A *Hin*dIII fragment of the *HCCS* ORF from pGEM7-HCCS was placed into similarly digested pCMV to generate pCMV-HCCS. Correct orientation of the insert was identified by digestion with *Kpn*I. Both constructs were confirmed by sequencing before being co-transformed into HeLa cells.

Mitochondrial protein was purified from these cells and treated with either anti-CYTC antibody (2ug/ml; Wu *et al*, 2000) or anti-Hccs antiserum. Following precipitation with protein A &/or G agarose beads, antigens were detected by western blot analysis (Fig 3.4). Several different concentrations of the polyclonal anti-Hccs antibody (ranging from 4-10 µl) were tested and able to recognise and precipitate the native protein in all cases. Importantly, anti-CYTC antibody was also able to detect a band in the HCCS pull-down, confirming an interaction between the two proteins, and supporting the likelihood of this gene being the orthologue of *Cyc3p*. The detection of an interaction between the two proteins by Co-IP but not by the yeast two-hybrid system may be for reasons highlighted in the previous section. Alternatively, this may be because the environment of the inter-membrane space is necessary for the correct folding of HCCS and hence an interaction with CYTC. Indeed, the results presented by Dumont *et al* (1991) showing that HCCS is peripherally associated with the outer surface of the mitochondrial inner-membrane may be interpreted as support for this suggestion.

3.2.6 Do cells over-expressing HCCS undergo apoptotis?

Curiously, transient transfection of Cos-1 cells with the hCTS-EGFP-K fusion construct as opposed to pEGFP alone, resulted in a smaller proportion of cells exhibiting fluorescence. Furthermore, many of those cells appeared to clump together 48 hours post transfection. As release of holocytochrome c from mitochondria has been implicated in the initiation of programmed cell death (Garland & Rudin, 1998), it is feasible that over-expression of HCCS might result in over production of the cytochrome c holoenzyme that could subsequently be released from the mitochondria and signal apoptosis. As previously mentioned, release of CYTC into the cytosol promotes interaction with apoptotic protease activating factor 1 (Apaf1) and pro-caspase 9 to form the "apoptosome" that initiates caspase mediated apoptosis. This process begins with the cleavage and subsequent activation of the effector caspases, including caspase-3, -6 and -7, that are involved in cleaving substrates required for apoptotic degradation. Initiation of apoptosis may also result from cell membrane signalling through upstream caspases (caspase-2, -8 and –10) that also utilise common effector caspases.

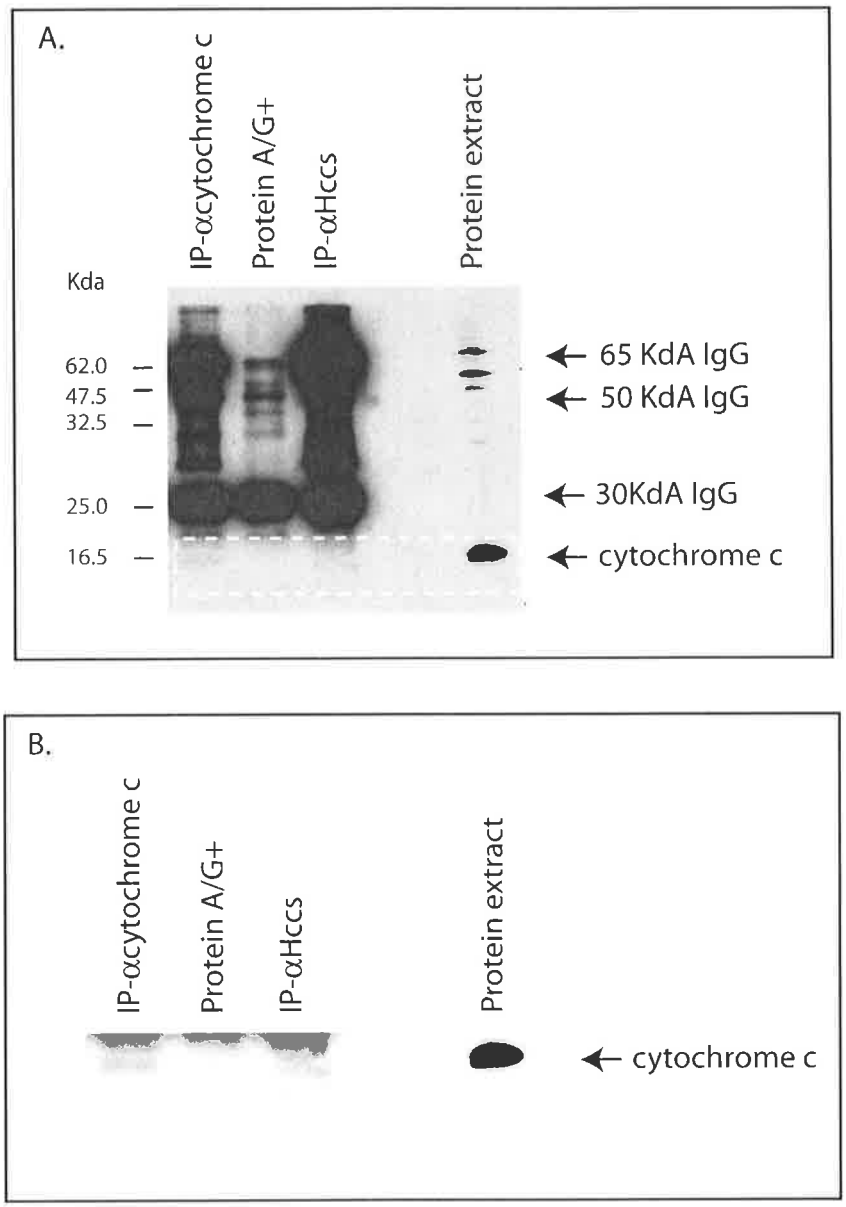

Figure 3.4

Co-immunoprecipitation of cell extracts over-expressing hHCCS and hCYTC
Mitochondrial protein was extracted from human (HeLa) cells transiently over-expressing HCCS and CYTC (pCMV-hHCCS and pCMV-hCYTC, respectively). Anti-Hccs rabbit antiserum and anti-CYTC rabbit antibody were used to immunoprecipitate native proteins (as indicated) that were separated using 15% PAGE. Protein extracts treated with protein A/G+ beads alone were used as a negative control while untreated extract was used as loading control. (A) Western blot analysis with anti-CYTC antibody. (B) The dashed box in A has been enhanced to highlight the bands in the CYTC and Hccs immunoprecipitation. Note the presence of a band corresponding to CYTC in the anti-Hccs immunoprecipitation.

To investigate if over-expression of HCCS was indeed inducing apoptosis, the localisation of cytochrome c within cells was initially analysed. No gross differences were seen between normal and over-expressing cells suggesting that cytochrome c was still localised to the inter-membrane space (results not shown). Whole cell protein extracts were then obtained from a human cell line (HEK-293T) over-expressing hCTS-EGFP-K, pEGFP and pCaspase-2-EGFP, a known inducer of apoptosis (obtained from Dr K. Harvey, Institute of Medical and Veterinary Science, South Australia). In comparison to the caspase-2 control, no cleavage of caspase-3 (32 kDa inactive and 20 kDa active) was identified by western blot in the hCTS-EGFP-K extracts (Fig 3.5) indicating that the cells were not undergoing a cytochrome c/caspase-3 mediated apoptosis. Anti GFP antibody was used on the same membranes to confirm expression of the constructs. Furthermore, morphological analysis of DAPI stained NIH3T3 cells over-expressing the same constructs also failed to indicate any initiation of apoptosis through nuclear condensation (results not shown). Together, these results suggest that the unhealthy appearance of the cells may be due to an alternative form of cell death such as necrosis. Correspondingly, this analysis was not pursued further at this stage.

3.3 Summary.

In this chapter, analysis of a hCTS-EGFP-K fusion construct in mammalian cells has shown that the protein is indeed localised to the mitochondria. Although the intra-mitochondrial sub-compartment of this enzyme is unable to be determined by immunofluorescence alone, this result is consistent with a presumed role in the mitochondrial respiratory chain. Previous studies of both human and mouse putative CTS further support this finding by detailing highest expression of the gene in adult heart and skeletal muscle (Schaeffer *et al*, 1996; Schwarz & Cox, 2002), a profile that is similar to other OXPHOS enzymes (Larsson *et al*, 1998).

In the complementation studies, the ΔCyc3p yeast strain expressing hCTS showed a partial rescue of the growth phenotype on a non-fermentable carbon source. In contrast, the hCTS was unable to complement the Cyt2p mutant. Given that each CTS in yeast is only able to catalyse the addition of heme to its corresponding apocytochrome (Dumont *et al*,

1987), these results suggest that the putative mammalian CTS is likely to be orthologous to yeast Cyc 3 (HCCS), albeit with only 35% amino acid identity.

Interestingly, a holocytochrome c1 synthase (*Cyt2p*) has not been identified in any other species apart from the yeasts. Even extensive searches of the EST databases and the genomes of *C.elegans*, *D.melanogaster, H.sapien* and *M.musculus* have failed to identify more than one species of c-type synthase. Based on the functional data presented here, mammals may only encode the single gene that is orthologous to *Cyc3p*. There are a number of possible explanations for these observations: 1) that in all organisms other than yeasts, one holocytochrome c-type synthase catalyses the insertion of heme into both cytochrome c and c1. Although this would be inconsistent with the complementation assay, it remains feasible that the marginally greater sequence difference between the human protein and yeast Cyt2p is sufficient to prevent interaction with the yeast apocytochrome c1; 2) That the insertion of heme into apocytochrome c1 occurs spontaneously at a sufficient level within higher eukaryotes; or 3) That the insertion of heme into apocytochrome c1 is catalysed by a different enzyme in higher eukaryotes, or at least one that is considerably more divergent from *Cyt2p* such that more sensitive search parameters may be required for detection of similarity.

To confirm that human HCCS is indeed catalysing heme attachment to apocytochrome c, matutration of the enzyme was analysed at the molecular level with an antibody specific for *S.cerevisiae* cytochrome c. Detection of increased levels of the holoprotein further support the phenotypic growth rescue. In yeast, HCCS has the additional function of acting as a binding site for correct import of apocytochrome c to the inter-membrane space. That an interaction between human HCCS and cytochrome c was detected by co-imunoprecipitation suggests that this process may be recapitulated in mammals. Taken together, these results confirm the catalytic function of this *HCCS* gene product.

Any mutation in human *HCCS* could feasibly give rise to a nuclear encoded respiratory chain defect that would have expected complications in tissues also affected in the mitochondrial myopathies (i.e. those requiring highest amounts of energy). Removal of a gene such as HCCS within OC or MIDAS patients could therefore account for the paucity of male patients and the associated muscle defects in females. This data and the accompanying

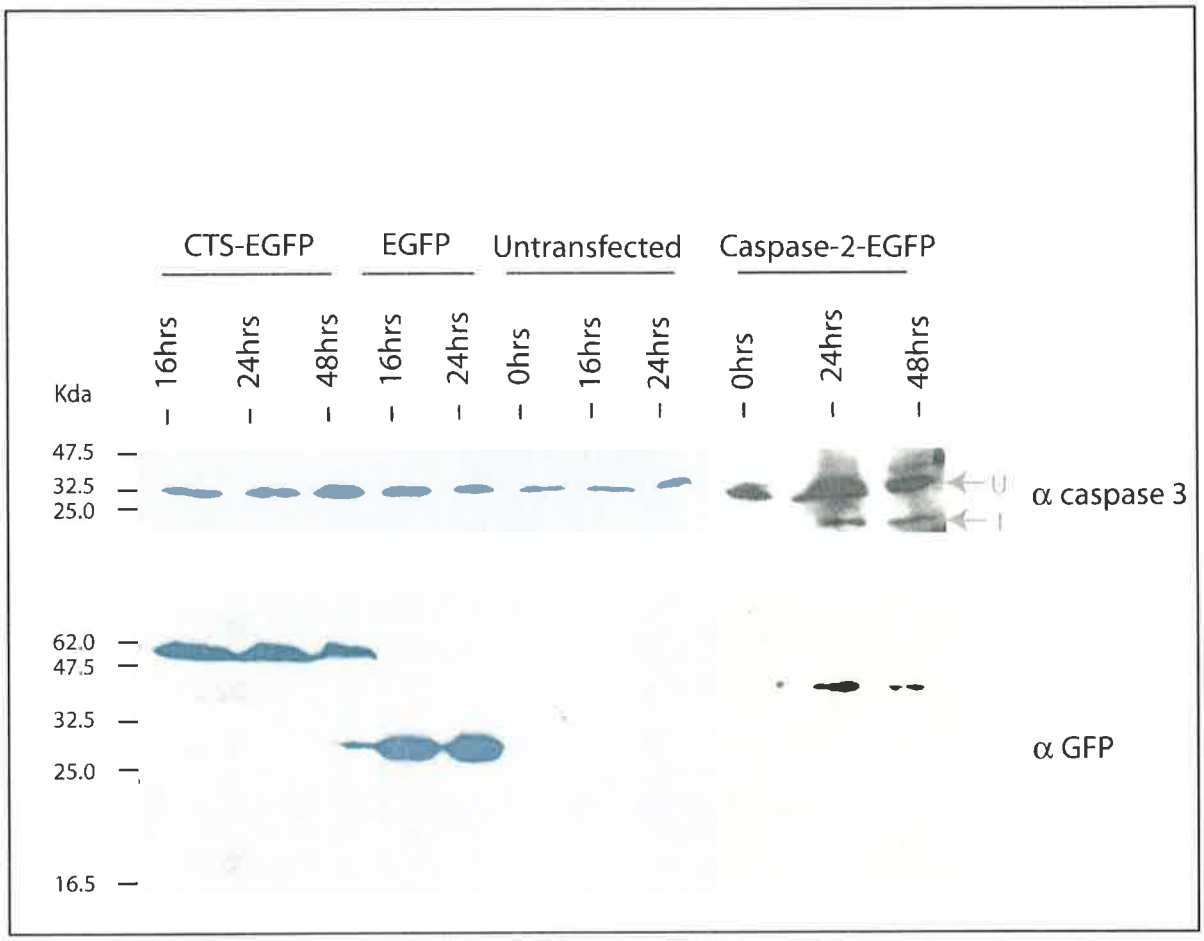

Figure 3.5

Analysis of possible CYT-C mediated apoptosis in cells over-expressing HCCS
Human HEK-293T cells were transiently transfected with either pCTS-EGFP, pEGFP or pCaspase-2-EGFP. Protein extracts were collected at 16hrs, 24hrs and 48hrs post transfection and separated by 15% PAGE. (Top) Western blot analysis with anti-caspase-3 antibody detects cleavage and activation of caspase-3 protein in the caspase-2 expressing cells but not in cells over-expressing HCCS. (Bottom) Western blot analysis with anti-GFP antibody shows correct expression of all constructs in transfected cells (Caspase-2-EGFP blot was exposed for a shorter time than for EGFP and CTS0EGFP alone).

information have led to the proposal that this gene may be a significant factor in the clinical presentation of MIDAS and OC. Later chapters show work toward identifying any role that HCCS may partake in the pathogenesis of these disorders.

Chapter Four: Analysis of human HCCS mitochondrial import.

4.1 Introduction.

4.1.1 Mitochondrial import.

The majority of mitochondrial enzymes (90%; Pfanner *et al*, 1997) are encoded in the nucleus, synthesised on cytosolic ribosomes and then targeted to the mitochondria. Before being directed to their correct location, the pre-proteins must be held in an unfolded state by cytosolic chaperones in an ATP dependent manner (Pfanner & Geissler, 2001). Once directed to the mitochondria, proteins are then translocated to their correct mitochondrial sub-compartment. These sub-compartments include the outer and inner membrane (OM and IM respectively), matrix, and the inter-membrane space (IMS).

Most proteins utilise either N-terminal signal sequences or internal sequences that form amphipathic helices with an overall positive charge to achieve correct targeting (see Omura, 1998 for review). These structures are recognised by receptors on the surface of mitochondria that form part of the translocase machinery used to mediate traffic across the OM (Transfer Outer Membrane or TOM protein complexes). In lower eukaryotes, TOM is composed of three receptor proteins, Tom20, Tom22 and Tom70, the main part of the import pore, Tom40, and three smaller proteins thought to be involved in the specificity of both recognition and transfer (Tom6, Tom7 and Tom8) (Deitmer *et al*, 1997).

Proteins destined for the IM have characteristic pre-sequences which allow them to be transported to the translocase machinery of the inner membrane, the TIM complex. TIM functions independently of TOM and consists of five proteins; Tim17 and Tim23 constitute the main pore through which trafficking occurs, while Tim44, Tim22 and Tim11 are involved in more specialised roles (Segui Real *et al*, 1993). To cross the inner membrane, the $(\Delta)\Psi$ established by a proton gradient across the inner membrane is essential. The overall negative charge within the matrix exerts an electrophoretic effect on the positively charged amphipathic helix driving it across the inner membrane with the aid of internal chaperones. From this position, most proteins are then sorted to their final destination by internal sorting sequences (Pfanner & Geissler, 2001). The best characterised examples of proteins localised to the IMS are that of cytochrome c1 and cytochrome b2 (van Loon *et al*, 1988; Baker *et al*,

1996). Both proteins are encoded in the nucleus and targeted to the mitochondria through the use of bipartite signal motifs. Initially, matrix targeting signals direct the proteins across the OM to the translocase machinery of the IM where the matrix processing peptidase (MPP) removes the matrix signal sequence. Two models are currently proposed for the final mechanism of transport. The first is the "conservative sorting" model in which the precursor protein is completely translocated across the IM into the matrix and then re-exported to its final destination within the IMS by an internal sorting sequence. Alternatively, the "stop-transfer" model proposes the arrest of the internal sorting sequence in the IM that is able to direct the protein to the IMS, never crossing the IM. Recent findings add support for the latter in at least cytochrome b2 localisation (Esaki *et al*, 1999). In both cases, the initial matrix targeting sequence is composed of a characteristic signal sequence which is able to form an amphipathic helix with an overall positive charge. This signal sequence is then cleaved to form an intermediate protein. Internal sorting signals that mediate transportation to the IMS are also removed to form the mature protein. These sorting signals are composed of a hydrophobic stretch preceded by positively charged residues (Pfanner & Geissler, 2001).

While most proteins utilise these signalling motifs to identify their final mitochondrial destination, a number of nuclear encoded pre-proteins do not contain typical targeting sequences yet still utilise the same import machinery (i.e. all proteins of the OM and some proteins of the IM (Diekert *et al*, 1999)). Analysis of the mechanisms involved in the localisation of these proteins has shed light on the dynamic nature of the mitochondrial protein translocases (see Pfanner & Geissler, 2001 for recent review). From varied studies in yeast, this sub-group of proteins also includes the holocytochrome c-type synthases (CTS's) that function within the IMS.

4.1.2 The holocytochrome c-type synthases (CTS's).

From extensive mutational analysis completed in yeast, the role of the CTS family in the biogenesis of the c-type cytochromes has been well documented. In this species, both HCCS (Cyc3p) and HCC1S (Cyc2p) are encoded in the nucleus and are only active once translocated to the IMS. From this position they are able catalyse the addition of heme to their corresponding apocytochrome. Furthermore, HCCS has the additional function of acting

as a high affinity binding site for the correct import of apocytochrome c into the IMS (Mayer *et al*, 1995).

Sequence analysis of the CTS family has failed to identify any region possessing the characteristics of a typical signal that could be responsible for correct targeting. The usual site of signal sequences, the N-terminus, is essentially charge neutral, has few hydrophobic residues (Fig 4.1) and as a consequence has little propensity to form an amphipathic helix. Intriguingly then, Cyc3p is localised to the mitochondria through a unique mechanism that still requires the general import machinery and Tom22 as a receptor protein. However, unlike most nuclear-encoded proteins this targeting event does not require any external ATP, the use of TIM, or the $(\Delta)\Psi$ (Lill *et al*, 1992; Segui-Real *et al*, 1993). Indeed, *in vitro* studies have also shown that movement across the outer membrane can occur in the native folded state (Steiner *et al*, 1995).

In the previous chapter a CTS-EGFP fusion construct (now referred to as HCCS-EGFP) was expressed in mammalian cells to show that the human protein is indeed localised to the mitochondria, a finding also supported by analysis of endogenous protein with the Hccs antibody. This chapter details the work completed to investigate the specific mitochondrial sub-compartmental localisation of human HCCS. In addition, fusion constructs of various HCCS deletions were generated to identify the minimal sequences involved in correctly targeting the mammalian protein to the mitochondria. Primary investigations have also been completed to analyse the mechanism by which mammalian HCCS completes this targeting.

4.2 Results.

4.2.1 Intra-mitochondrial localisation of human HCCS.

To investigate the intra-mitochondrial localisation of human HCCS, a fractionation technique was designed to allow purification of mitochondria from other cellular organelles and cell debri, followed by sub-fractionation of the mitochondria. As the production of stable cell lines can be quite time consuming, transient over-expression of HCCS-EGFP in Cos-1 and Hela cells was chosen for this experiment. Following over-expression of this construct for 24 hrs, cells were processed with modifications to a technique previously used on murine

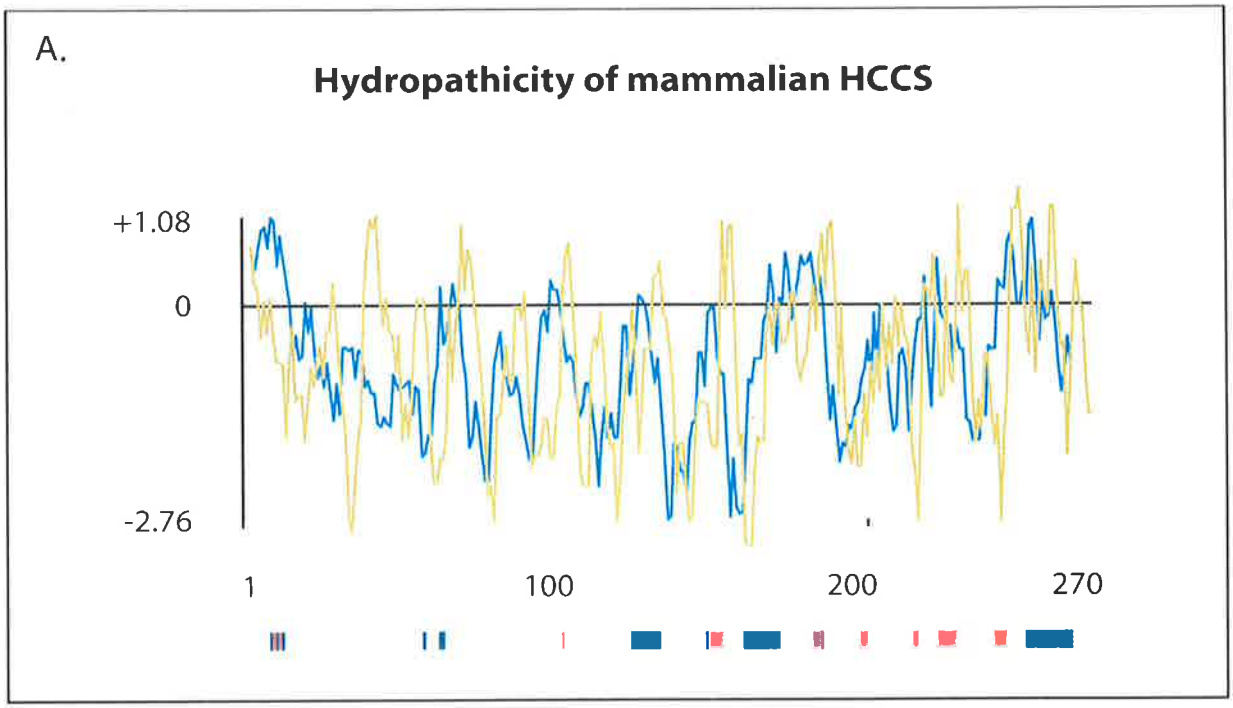

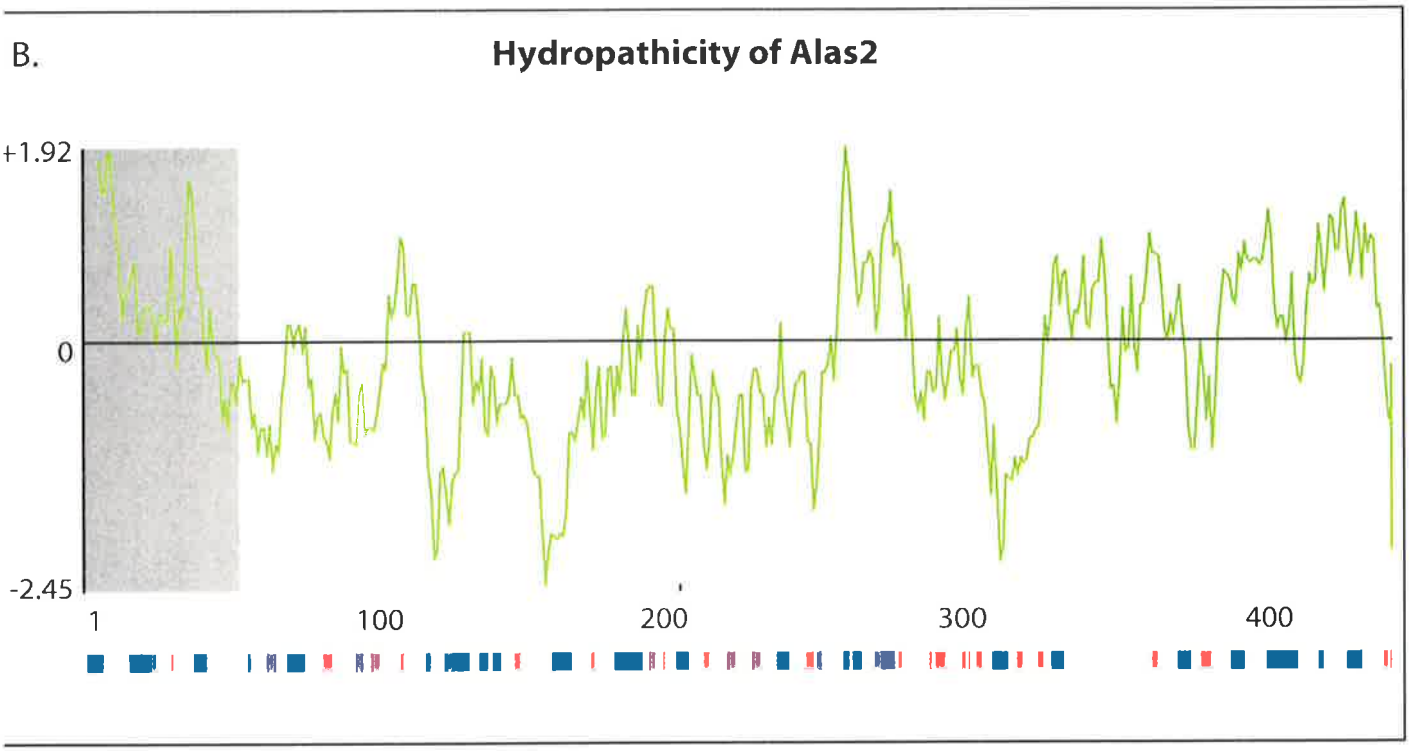

Figure 4.1

Hydropathicity plot of mammalian HCCS and human ALAS2

The hydropathicity of human and murine HCCS, represented as blue and brown lines, respectively (A), and of human ALAS2 (B) were determined using the parameters detailed by Kyte & Doolittle (1982). Positive readings indicate hydrophobic residues while negative readings indicate hydrophilic residues. The secondary structure is shown below the plot and was determined using the NNPREDICT program (Kneller *et al*, 1990). Blue boxes, α-helical; red boxes, ß-strands. The predicted mitochondrial targeting sequence for ALAS2 (B) is shaded grey (Cox *et al*, 2003).

liver tissue (section 2.3.26.1; obtained from Dr. B. Wattenberg, Institute of Medical and Veterinary Science, South Australia). In this technique, cells were homogenised with the use of a ball bearing homogeniser in mitochondrial extraction buffer (containing 20mM Hepes, pH7.5, 220mM Mannitol, 70mM Sucrose, 1mM EDTA and 0.5% BSA) with the addition of protease inhibitors. Cell debris and nuclei were removed by low speed centrifugation and crude mitochondria were then isolated by differential centrifugation. The crude mitochondrial fraction obtained by this method is isolated according to its velocity of sedimentation which is a factor based on the size of the organelle. Given that other cytoplasmic particles have similar sedimentation velocities (i.e. lysosomes, peroxisomes and some endoplasmic reticulum) this mitochondrial fraction will be contaminated to varying degrees depending on speeds of centrifugation (lower spin speeds increase the percentage of heavy mitochondria compared to contaminants).

Based on previous studies in yeast it was expected that HCCS would localise to the IMS. Therefore the mild detergent, digitonin, was used in initial fractionation attempts because at low concentrations this reagent selectively disrupts the outer membrane of the mitochondria leaving the inner membrane intact (Howell *et al*, 1986). Treatment of the crude mitochondrial fraction would allow IMS proteins to leach into the buffer and separate from the remaining mitochondrial protein. To confirm the sub-compartment fractions of the mitochondria, a number of antibodies recognising proteins in differing fractions were obtained for use in western blot analysis: Cpn60 (matrix localised; Prof. N. Hoogenraad, LaTrobe University, Victoria), Tom20 (OM; Dr. B. Wattenberg, Institute of Medical and Veterinary Science, South Australia) and cytochrome c (IMS, Santa Cruz Biotechnology, California). Various centrifugation speeds (ranging from 5,000 – 10,000 X g) and concentrations of digitonin (ranging from 0.3mg – 4mg digitonin / mg of mitochondrial protein) were used on multiple occasions with little effect on protein removal from the mitochondria, as addressed with all control antibodies (results not shown). In an attempt to cleave any remaining protein that was potentially attached to the outer surface of the mitochondria or within the inter-membrane space, trypsin was added to the mitochondria both prior to and after digitonin treatment. Various concentrations were again tested with some degree of degradation of HCCS-EGFP being detected in the expected fractions for an IMS localised protein. However, none of these treatments were satisfactory to obtain conclusive results.

As the initial fractionation technique did not allow the intra-mitochondrial localisation of HCCS to be determined, an alternative method was sought. Following extensive literature reviews, a technique previously used on NDK11 cells was identified (Wu *et a.l*, 2000). The major parameters changed with this method are the use of alternative buffers and an altered homogenisation technique (see section 2.3.26.2). To obtain sub-fractions of the mitochondria, an osmotic shock protocol also identified in the literature review was followed (Nobumoto *et al*, 1998; section 2.3.27.2). With this approach, crude mitochondria are treated with a hypo-osmotic solution which selectively breaks the outer membrane to form a mitoplast (matrix proteins surrounded by IM and the IM proteins). Addition of dilute proteinase K (ProK) to the mitoplast degrades all OM and IMS proteins (i.e. only IM and matrix proteins are left after this treatment). Hence, western blot analysis of different fractions allows intra-mitochondrial localisation to be ascertained.

To overcome any effect that EGFP may have on the specific localisation of HCCS, the HCCS-pCMV expression vector was utilised (detailed in section 3.2.8.2). Mitochondria were obtained from Cos-1 cells transiently over-expressing this construct and subjected to osmotic shock treatment. The results of the control antibodies confirm that this approach was effective (Fig 4.2A): lack of Cpn60 in only the sample treated with Triton X-100 (TTX)[8] and ProK is consistent with this protein being located within the matrix, while the presence of Tom20 in only crude mitochondria that is removed following treatment with ProK is consistent with the highly hydrophobic profile of an outer membrane protein (Abe *et al*, 2000). Under these conditions HCCS was detected with the anti-Hccs antiserum within the fractions of crude mitochondria, crude mitochondria with ProK and the mitoplast alone (Fig 4.3B). Following multiple attempts, however, HCCS was never detected in the mitoplast treated with ProK or mitoplast treated with both TTX and ProK. This profile is consistent with HCCS localisation in the inter-membrane space. That HCCS was not removed from the mitoplast sample alone suggests that the protein is not in a soluble form in the supernatant and may therefore be peripherally associated with the outer surface of the inner membrane, supporting previous findings by Dumont *et al* (1991).

[8] Triton X-100 is a strong detergent that disrupts both the mitochondria IM and OM. Treatment of the crude mitochondria with this reagent and ProK is expected to cleave all proteins localised to the IM and matrix.

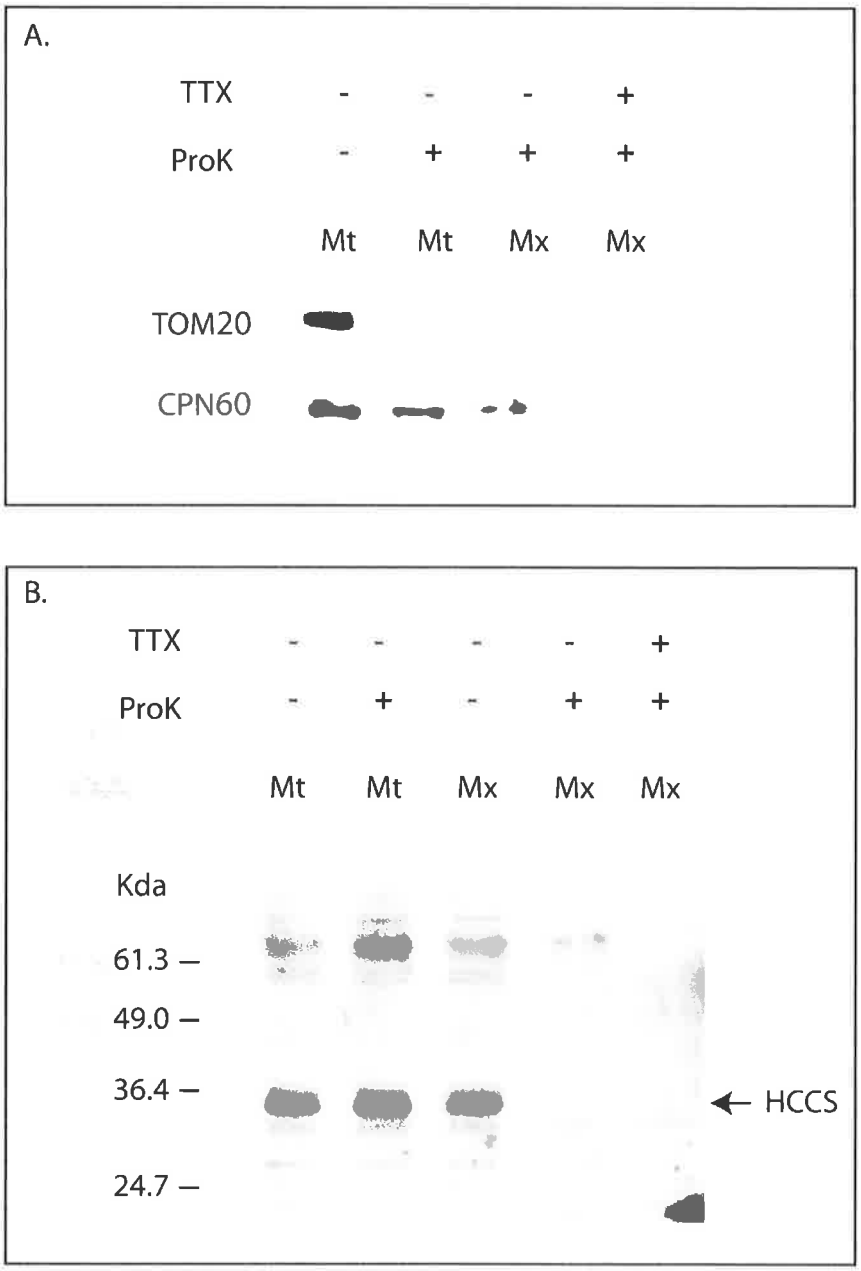

Figure 4.2

Mitochondrial sub-fractionation of Cos-1 cells expressing HCCS-pCMV
Mitochondria (Mt) and mitoplasts (Mx) were prepared from Cos-1 cells transfected with the pCMV-HCCS expression construct. Where indicated (+) fractions were treated with 10μg proteinase K (ProK) and 1% Triton X-100 (TTX). Antibodies to Tom20 (localised to the outer membrane) and Cpn60 (localised to the matrix) were used to confirm the various mitochondrial sub-compartments (A). The approximately 34kDa HCCS protein was identified with the anti-Hccs antiserum (B).

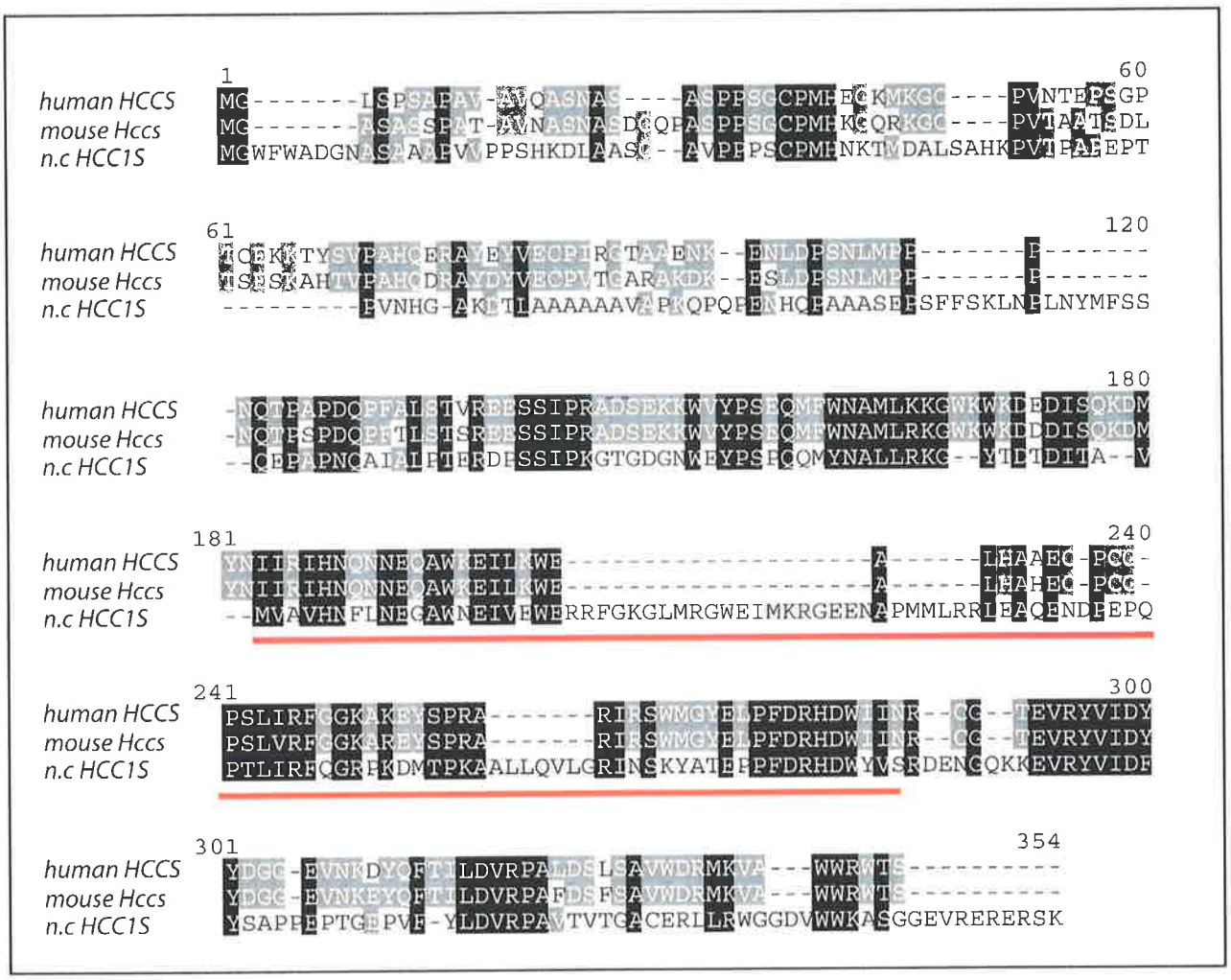

Figure 4.3

Amino acid alignment of mammalian HCCS and N.crassa HCC1S

Complete protein sequences were obtained from the following accession numbers: *H.sapien* HCCS - P53701; *M.musculus* HCCS - P53702; *N.crassa* Cyc2p - P14187 and aligned using the ClustalW program (Thompson *et al*, 1994). Black boxes highlight complete conservation between all proteins; light grey boxes indicate similarity between 2 species. Dashed lines indicate a gap in the alignment. The Cyc2p mitochondrial targeting signal identified in *N.crassa* by Diekert *et al* (1999) is underlined.

4.2.2 Identification of mammalian HCCS mitochondria targeting signal.

4.2.2.1 Generation of HCCS N- and C-terminal EGFP fusion constructs.

Diekert *et al* (1999) recently reported the identification of a mitochondrial localisation signal within the third quarter of *N.crassa* HCC1S (Cyc2p), a region that encodes two highly conserved signature motifs found in all c-type synthases. Notably, however, protein alignments of mammalian HCCS and the c-type synthases of *N.crassa,* highlight a major difference over this region (Fig 4.3). This ambiguity is essentially composed of an insertion into the *N.crassa* HCC1S that largely represents the internal signal. This suggests that mammalian HCCS is likely to be localised to mitochondria through use of an alternative signal. In view of this, sequence comparisons of human and mouse HCCS with other species also reveal extensive differences over the N-terminal sequence. Between human and mouse however, this region has high identity consistent with a functional importance. It is therefore possible that mammalian HCCS may possess a novel localisation signal within its N-terminal region.

To identify the regions of HCCS that are involved in the targeting of the full-length protein to the mitochondrial IMS, a series of deletion constructs were designed. At the time of initiating this experiment the Hccs antiserum used for the localisation studies of HCCS in the previous section was not available. Therefore, as the HCCS-EGFP construct had previously allowed mitochondrial localisation to be determined by immunofluorescence, all deletion constructs were fused to the amino terminus of EGFP for use as a marker protein (Fig 4.4). Initially, primers were designed to amplify the coding regions corresponding to the N- (mHCCS11 and mHCCS 13) and C- (mHCCS12 and the vector primer EBFP-199r) terminal halves of the protein to address if either of these regions could target EGFP to mitochondria (Fig 4.4A). mHCCS12 was designed over an ATG methionine codon corresponding to amino acid 147 such that insertion of this fragment into pEGFP produced a kozak consensus translation initiation site thus theoretically optimising translational initiation. As Diekert *et al* (1999) had recently identified the 3rd quarter of *N.Crassa* Cyc2p to be responsible for correct localisation, the corresponding region of human HCCS was also amplified (mHCCS12 and mHCCS14). Both mHCCS13 and mHCCS14 were designed to introduce a *Kpn*I site upon amplification from the HCCS ORF that allowed in-frame fusion with EGFPN$_2$, while a *Bam*HI site in the 5' primer facilitated directional cloning in to *Bgl*II /

*Kpn*I digested vector. In contrast, the region encoding the C-terminus was amplified from the HCCS-EGFP construct to allow digestion with *Bam*HI for insertion into similarly digested $EGFPN_1$. Correct orientation of this insert was identified with *Eco*RI digestion. These constructs were confirmed by sequence analysis and labelled pEGFP-HCaa1-149 (N-terminus), pEGFP-HCaa147-270 (C-terminus) and pEGFP-HCaa147-171 (3rd quarter), respectively. All constructs produced by PCR based cloning detailed in this chapter were amplified with the use of high fidelity Pfx DNA polymerase (Gibco, BRL).

4.2.2.2 Immunofluorescent analysis of HCCS N- and C-terminal EGFP fusion constructs.

The N and C terminal *HCCS* constructs fused in frame to EGFP were analysed in both Cos-1 and HeLa cells to address localisation within the cell. Following transient expression for 24hrs, cells were fixed and counterstained with the α mitochondria-specific antibody Tom20 (Fig 4.5). The HCaa147-270-EGFP produced a speckled appearance within the cytoplasm that did not correspond to mitochondria. As would be expected from this finding, the HCaa147-171-EGFP construct also did not localise to mitochondria. Interestingly, the HCaa1-149-EGFP construct did localise to mitochondria suggesting that mammalian HCCS does indeed utilise a different signal sequence to *N.crassa*.

4.2.2.3 Generation of HCCS N-terminal deletion constructs.

To delineate a minimal region within the first half of the protein that allows correct targeting of HCCS to mitochondria, further deletion constructs of this region were designed (Fig4.4B). HCCS encodes three CPX (X= I, V, M) putative heme binding motifs within the first 70 amino acids that are likely to be essential for protein function. While yeast CTS's encode only two CPX motifs, studies involving removal or mutation highlight their necessity for enzymatic activity (Steiner *et al*, 1995). Other protein families have also been shown to utilise these CPX motifs for heme binding (Diekert *et al*, 1999). Of note is the mitochondrial matrix enzyme 5-aminolevulinate synthase (ALAS) protein which has both ubiquitous and erythroid specific isoforms encoded by different genes (May *et al*, 1995). Interestingly, localisation of ALAS to the mitochondria is thought to be regulated by excess cytoplasmic heme binding to the CPX motifs (May *et al*, 1995; Lanthrop & Timko, 1993).

Figure 4.4

Schematic representation of various N- and C- terminal HCCS-EGFP deletion constructs

(A) Full-length HCCS cDNA is represented at the top as a blue box. Purple shading indicates the region corresponding to the *N.crassa* Cyc2p targeting signal. cDNA corresponding to the N- and C- terminal halves as well as the region equivalent to the *N.crassa* targeting signal were amplified with the specified primers. (B) N-terminal deletion constructs were also amplified with specific primers shown beneath the cDNA. Introduction of non-native ATG codons by PCR are represented at the start of the cDNA. All fragments generated by PCR were cloned to the corresponding EGFP vector (green box) with the restriction sites indicated; B, *Bam*HI, K, *Kpn*I.

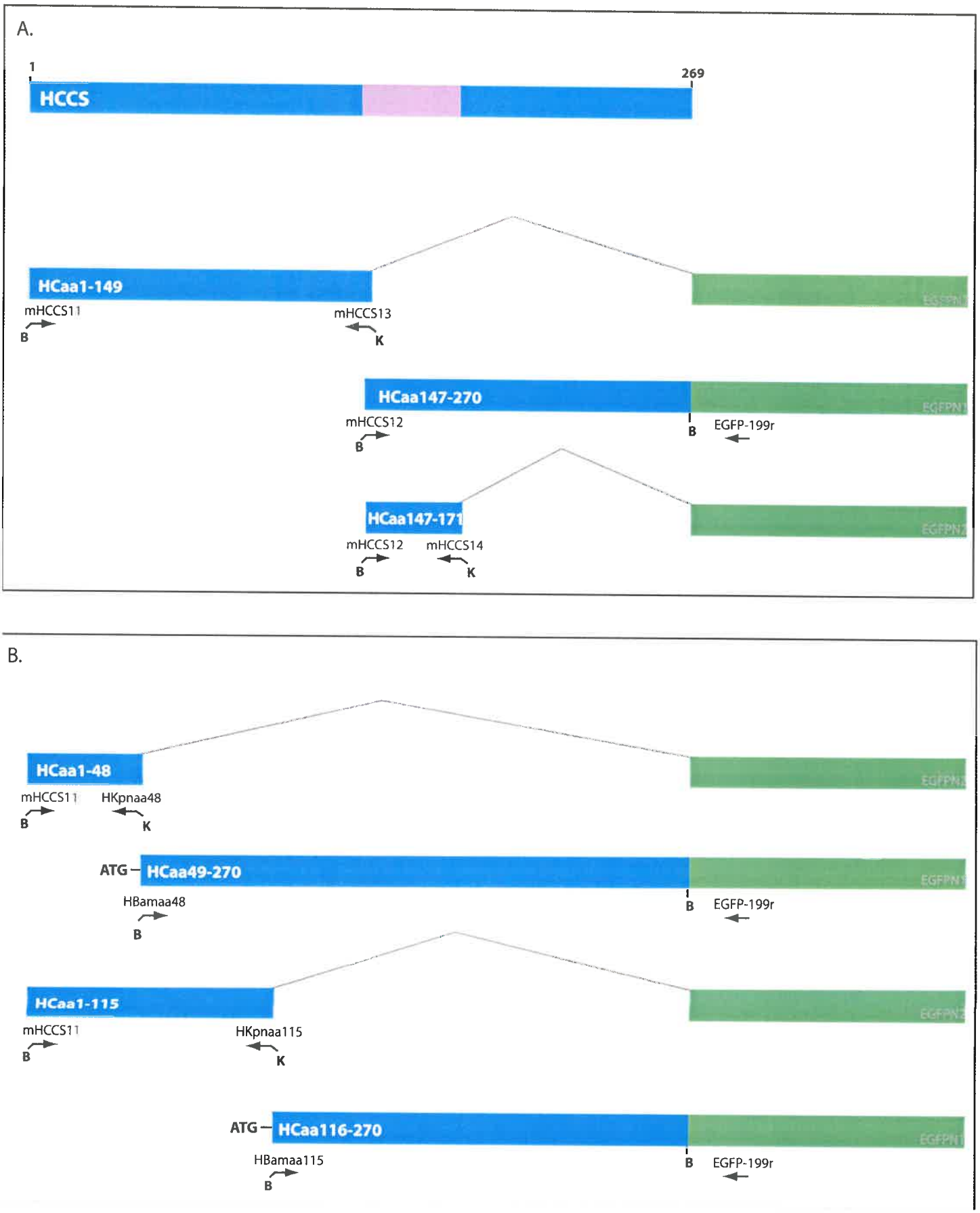
A.
1
269
HCCS
HCaa1-149
mHCCS11
B
mHCCS13
K
HCaa147-270
mHCCS12
B
B
EGFP-199r
HCaa147-171
mHCCS12
B
mHCCS14
K
B.
HCaa1-48
mHCCS11
B
HKpnaa48
K
ATG
HCaa49-270
HBamaa48
B
B
EGFP-199r
HCaa1-115
mHCCS11
B
HKpnaa115
K
ATG
HCaa116-270
HBamaa115
B
B
EGFP-199r

Figure 4.5

Immunofluorescent analysis of N- and C-terminal HCCS-EGFP fusion constructs
Cos-1 cells were transfected with HCaa1-149-EGFP, HCaa147-270-EGFP or HCaa147-171-EGFP deletion constructs as indicated. Cells were counter-stained with a mitochondrial specific anti-Tom20 antibody (red) and the images merged to detect mitochondrial localisation (yellow). The nucleus has been stained with DAPI (blue).

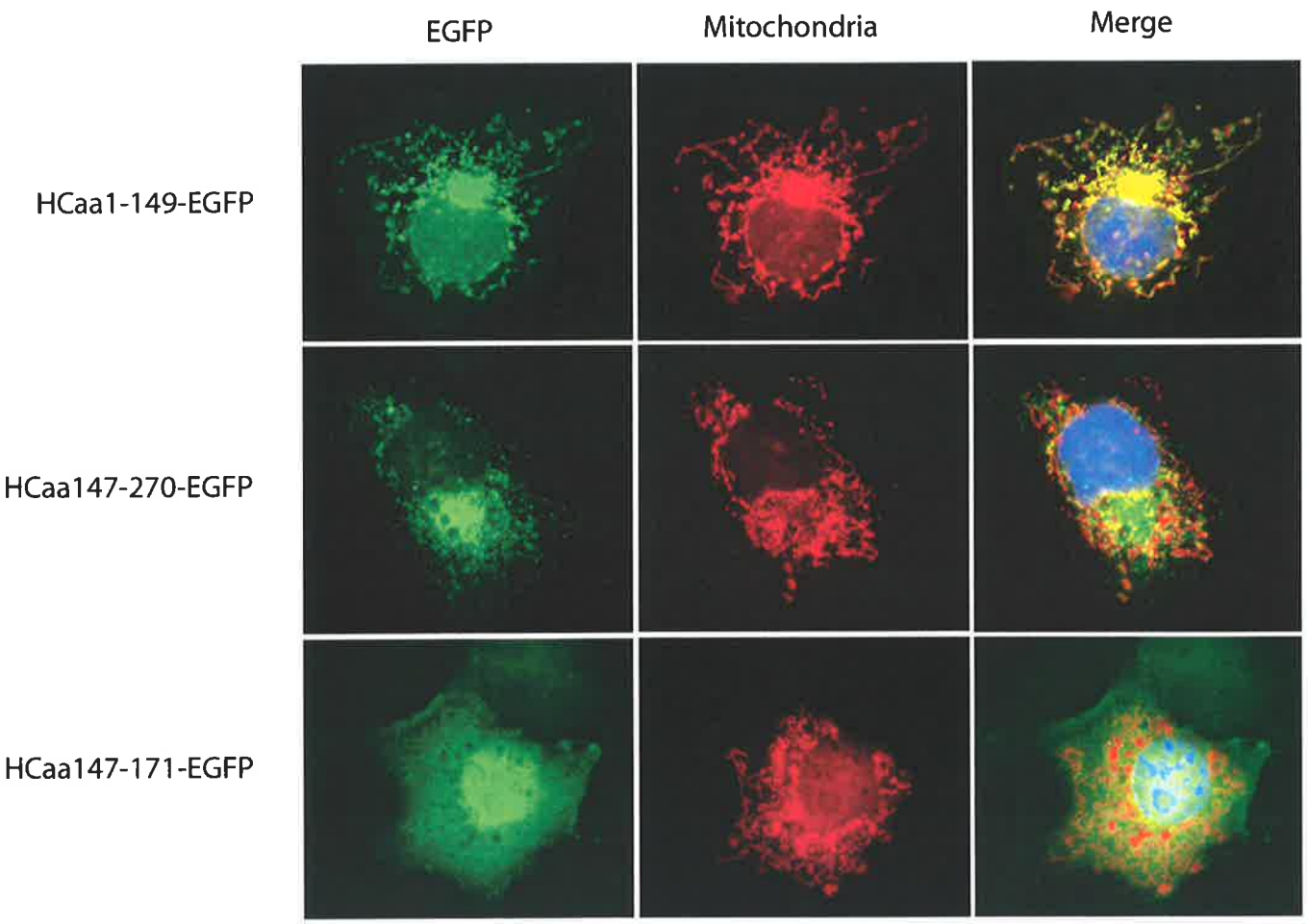
EGFP
Mitochondria
Merge
HCaa1-149-EGFP
HCaa147-270-EGFP
HCaa147-171-EGFP

The cDNA region encoding the first 48 amino acids was amplified with mHCCS11 / Hkpnaa48 and the region encoding the first 115 amino acids amplified with mHCCS11 / Hkpnaa115. The first 48 amino acids was chosen as this region has two of the CPX heme binding motifs also present in other CTS's. Likewise, the first 115 amino acids were amplified as they possess all three CPX motifs unique to human and mouse as well as additional N-terminal sequence that also seem to be specific to the mammalian synthase (see Fig 4.3). Both fragments were placed into *Bgl*II / *Kpn*I digested $EGFPN_2$ to yield pEGFP-HCaa1-48 and pEGFP-HCaa1-115, respectively. Primers were also designed to amplify the adjacent sequence containing aa49-270 (Bamaa48 / EGFP-199r) and aa116-270 (Bamaa115 / EGFP-199r) to allow comparisons between these regions and the remainder of the protein. These primers were also designed to introduce ATG methionine start codons. Following amplification of the aa49-270 and aa116-270 regions from HCCS-EGFP the fragments were digested with *Bam*HI and ligated into *Bam*HI digested $EGFPN_1$ (pEGFP-HCaa49-270 and pEGFP-Hcaa116-270, respectively). Correct orientation of inserts were detected by *Eco*RI digestion and all constructs were confirmed by sequencing.

4.2.2.4 Immunofluorescent analysis of HCCS N-terminal deletion constructs.

The N-terminal deletion constructs were analysed in both Cos-1 and HeLa cells to address localisation within the cell. Following transient expression, again for 24hrs, cells were fixed and counterstained with the α mitochondria-specific antibody Tom20 (Fig 4.6). The aa1-115-EGFP construct had a localisation pattern highly similar to the mitochondrial antibody. While the aa1-48-EGFP construct also had mitochondrial localisation, there was additional background cytosolic fluorescence. In comparison, the adjacent region of aa116-170 did not appear to target EGFP to the mitochondria. However, the region of aa49-270 did show a low degree of fluorescence associated with mitochondria. Example immunofluorescence results are represented in figure 4.6. Taken together these results indicate there is a signal encoded within the first 115 amino acids that is both necessary and sufficient for mediating mitochondrial targeting of these fusion constructs. Furthermore, as the constructs encoding aa1-48 and aa29-270, but not aa116-270 are able to co-localise with the mitochondria, the signal is likely to span the aa48 and aa49 region. An alternative

explanation may be that the presence of a bipartite signal within each construct could be sufficient by themselves to target inefficiently to the mitochondria.

4.2.2.5 Fractionation analysis of HCCS-EGFP deletion constructs.

Importantly, the preliminary immunofluorescent experiments detailed above show a clear mitochondrial localisation. They are, however, unable to definitively show import of the constructs across the outer mitochondrial membrane. To therefore address if these constructs do indeed localise correctly within the IMS fractionation, studies were carried out as previously described (4.2.1).

4.2.2.5-1 Production of an ALAS2 control.

The erythroid specific isoform of 5-aminolevulinate synthase (ALAS2) is involved in the synthesis of ALA for the formation of haemoglobin (May *et al*, 1995). Like most nuclear encoded mitochondrial proteins ALAS2 is synthesised in the cytoplasm and is thought to be targeted to the mitochondrial matrix through the use of an N-terminal pre-sequence. While little is known about the movement of ALAS2 through the outer and inner membranes the process may be regulated by heme as excess hemin inhibits the transport of ALAS2 *in vitro*. As mentioned, this regulation is thought to be mediated through the binding of heme to CPX heme binding motifs located in the pre-sequence that is presumably cleaved (Lathrop & Timko, 1993). Although the role, if any, of the two CPX motifs in HCCS is not known, I have now shown that the first 48 aa of HCCS are involved in mitochondrial localisation. To address if fractionation of cells expressing the HCCS-EGFP deletion constructs would be informative, a number of deletion constructs of ALAS2 that had been made previously in the lab were first analysed (provided by L. Cox, University of Adelaide, South Australia). This study was also undertaken to further characterise the mechanism of ALAS2 localisation to the mitochondrial matrix for assistance with interpretation of findings for HCCS.

4.2.2.5-2 Generation of human ALAS2-EGFP fusion constructs.

Various cDNA fragments of ALAS2 were amplified from the respective pET3a ALAS2 clones previously generated by Dr T. Cox (Conboy *et al*, 1992; Cox *et al*, 2003). All constructs are diagrammatically represented in figure 4.7. Full-length ALAS2 was amplified

Figure 4.6

Immunofluorescent analysis of N-terminal HCCS-EGFP deletion constructs
HeLa cells were transfected with HCaa1-48-EGFP, HCaa1-115-EGFP, HCaa49-270-EGFP or HCaa116-270-EGFP deletion constructs as indicated. Cells were counter-stained with a mitochondrial specific anti-Tom20 antibody (red) and the images merged to detect mitochondrial localisation (yellow). The nucleus has been stained with DAPI (blue).

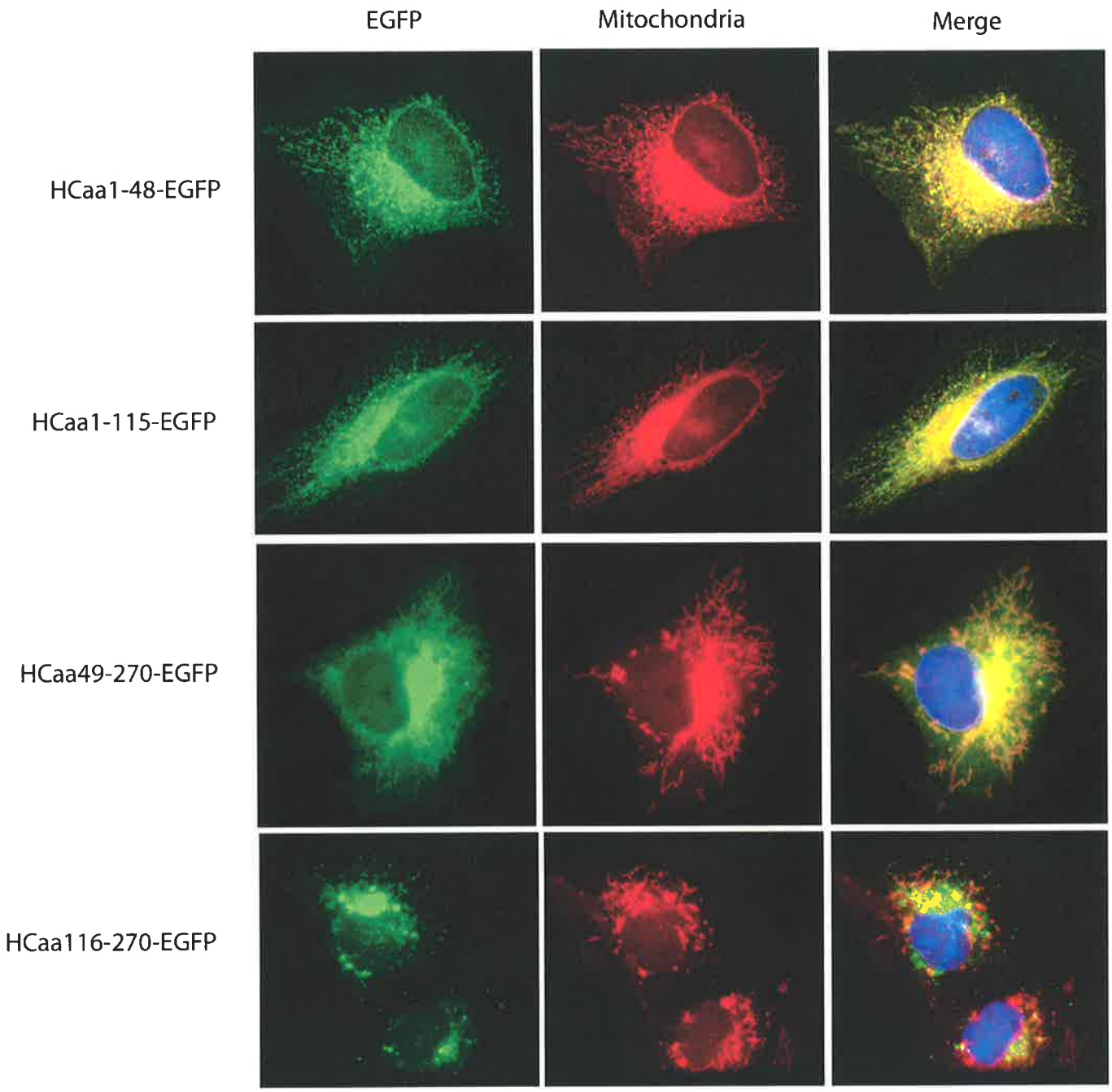
EGFP
Mitochondria
Merge
HCaa1-48-EGFP
HCaa1-115-EGFP
HCaa49-270-EGFP
HCaa116-270-EGFP

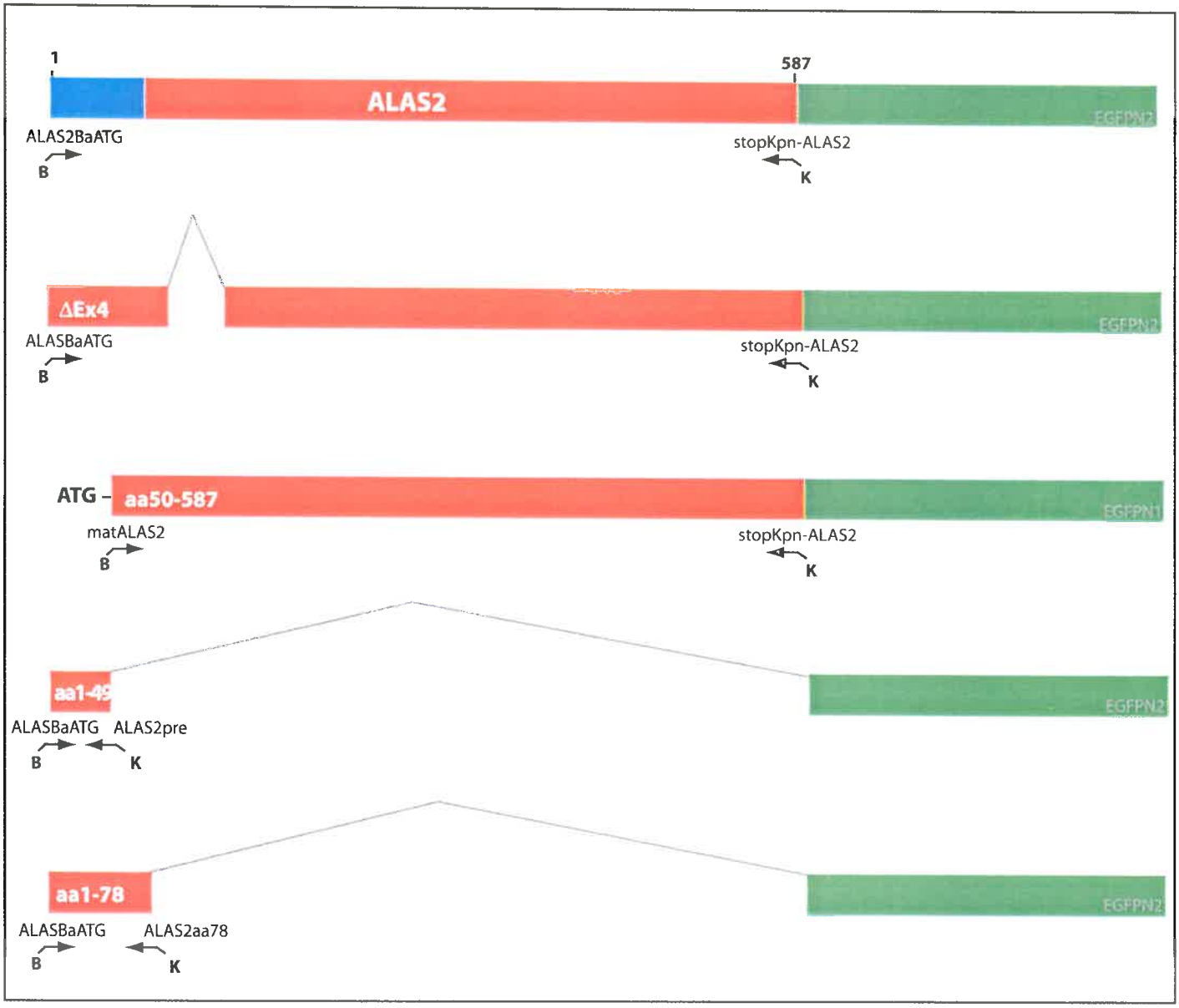

Figure 4.7

Schematic representation of ALAS2-EGFP deletion constructs

Full-length *ALAS2* cDNA and various deletions are represented as red boxes. A blue box at the amino terminus indicates the region corresponding to the previously predicted targeting signal (Cox *et al*, 1991). Introduction of non-native ATG start codons by PCR are represented at the start of the cDNA. Fragments were generated with primers shown beneath the cDNA and cloned to EGFPN2 (green box) with the restriction sites indicated; B, *Bam*HI, K, *Kpn*I.

with primer pair ALAS2BaATG / stopKpn-ALAS2 while the major isoform of ALAS2 that lacks exon 4 (ΔEx4) was amplified from pET3a-delEx4 with the same primers. To generate a cDNA fragment that would encode a protein beginning at amino acid 50 (aa50-587), the primer pair mat-ALAS2 / stopKpn-ALAS2 was used to amplify a 1.6 kb fragment from the full-length clone that concomitantly introduced an ATG start codon. Primer ALAS2BaATG together with primer ALAS2pre or ALAS2aa78 were used to generate sequences encoding the first 49 or 78 amino acids, respectively. All fragments were digested with *Bam*HI / *Kpn*I and cloned into the appropriately restricted $pEGFPN_2$ vector to give: pEGFP-ALAS2 (full-length); pEGFP-ALASDEx4 (Δexon4); pEGFP-ALASaa50-587 (aa50-587); pEGFP-ALASaa1-78 (aa1-78); and pEGFP-ALASaa1-49 (aa1-49). All clones were confirmed by sequencing to ensure the correct orientation and reading frame. The rationale behind the regions of ALAS2 chosen in these constructs is based on a number of observations in the literature. The amino acids encoded by aa1-49 and aa1-78 were utilised to clarify the debate over the true mitochondrial targeting signal (Cox *et al*, 1991; Goodfellow *et al*, 2001; May *et al*, 1995; Schoenhaut and Curtis, 1986). While not expected to have any affect on mitochondrial localisation due to the targeting signal being encoded by exons 1-3, the Δexon4 construct was utilised to address any disruption to localisation of this specific isoform.

4.2.2.5-3 Analysis of human ALAS2-EGFP fusion constructs.

To address if the regions within the deletion constructs of ALAS2 are able to target EGFP to mitochondria, the EGFP fusions were first analysed by immunofluorescence in Cos-1 cells (Fig 4.8). Expression of both full-length ALAS2 and the DEx4 isoform resulted in the complete co-localization of fluorescence signals with Tom20, showing that both protein isoforms are targeted to mitochondria. In contrast, expression of the aa50-587 construct showed no co-localization with Tom20 suggesting that the N-terminal 49 amino acids are required for targeting. Consistent with this, both the aa1-49 and aa1-78 fusion proteins efficiently directed EGFP to mitochondria with no non-specific background fluorescence. This indicates that the first 49 amino acids of ALAS2 are sufficient for mitochondrial targeting as predicted by Cox *et al* (1991).

As immunofluorescence confirmed that the ALAS2 fusion proteins were efficiently targeted to mitochondria they were then utilised to verify that the fractionation technique

would also be informative when using over-expressed minimal signal sequences. Mitochondria were isolated using the differential centrifugation approach found to work for full-length HCCS (section 4.2.1). Following sub-fractionation of the mitochondria with the hypo-osmotic solution, the full-length, Δexon4 isoform and the aa1-49 fusion proteins were efficiently translocated to the matrix side of the inner mitochondrial membrane (Fig 4.9). Given the hydrophobic nature of this 49 amino acid sequence and the likelihood of the secondary structure forming an alpha helix (see fig 4.1B) this region is likely to form a traditional amphipathic helix that has an overall positive charge. This result confirms that targeting of ALAS2 to the matrix of the mitochondria is dictated by a classic N-terminal signal sequence.

4.2.2.5-4 Fractionation of Cos-1 cells expressing HCCS-EGFP deletion constructs.

All deletion constructs were over-expressed in Cos-1 cells and mitochondrial fractions obtained by differential centrifugation. As the HCCS deletion constructs had background cytoplasmic fluorescence not seen with the ALAS2 fusion proteins, EGFP alone was used as a negative control. Immunofluorescence studies with EGFP suggested localisation within the entire cytoplasm, hence, some EGFP protein was expected to be present in the crude mitochondrial fraction. Following the initial sub-fractionation of the mitochondria, EGFP protein was detected in the mitoplast. Given the crude nature of the mitochondria obtained from differential centrifugation it is possible that other organelles are also present in this pellet. Indeed, as mentioned previously, both the endoplasmic reticulum (ER) and golgi complex overlap with the size of mitochondria and as they are similar densities would precipitate at similar centrifugal speeds. In an attempt to overcome this issue another purification step was analysed to address if the EGFP within the mitoplast fraction could be removed. Crude mitochondria were therefore run through a density gradient established with Percoll (section 2.3.26.3) and 1ml aliquots collected. The aliquots were then analysed by western blotting with anti-GFP and anti-Tom20 antibodies to identify the fractions containing mitochondria. Following this experiment the GFP antibody was only detected in the specific mitochondria containing aliquots (Fig 4.10) suggesting the EGFP clone may have a propensity to enter mitochondria, although only a small proportion of the protein was

Figure 4.8

Immunofluorescent analysis of ALAS2-EGFP deletion constructs
Full-length ALAS2 and deletion fragments fused to EGFP were expressed in Cos-1 cells. Full-length and Δexon4 isoforms of ALAS2 show co-localisation with the staining for mitochondrial Tom20 protein. The aa50-581 region showed a general cytoplasmic distribution that did not co-localise with the mitochondrial marker. Both aa1-49 and aa1-78 protein fragments from the N-terminus of ALAS2 also target the mitochondria as demonstrated by the co-localisation with Tom20. Green, EGFP fluorescence; red, anti-Tom20; blue, DAPI nuclear stain. Co-localisation is indicated by yellow colouration in merged images.

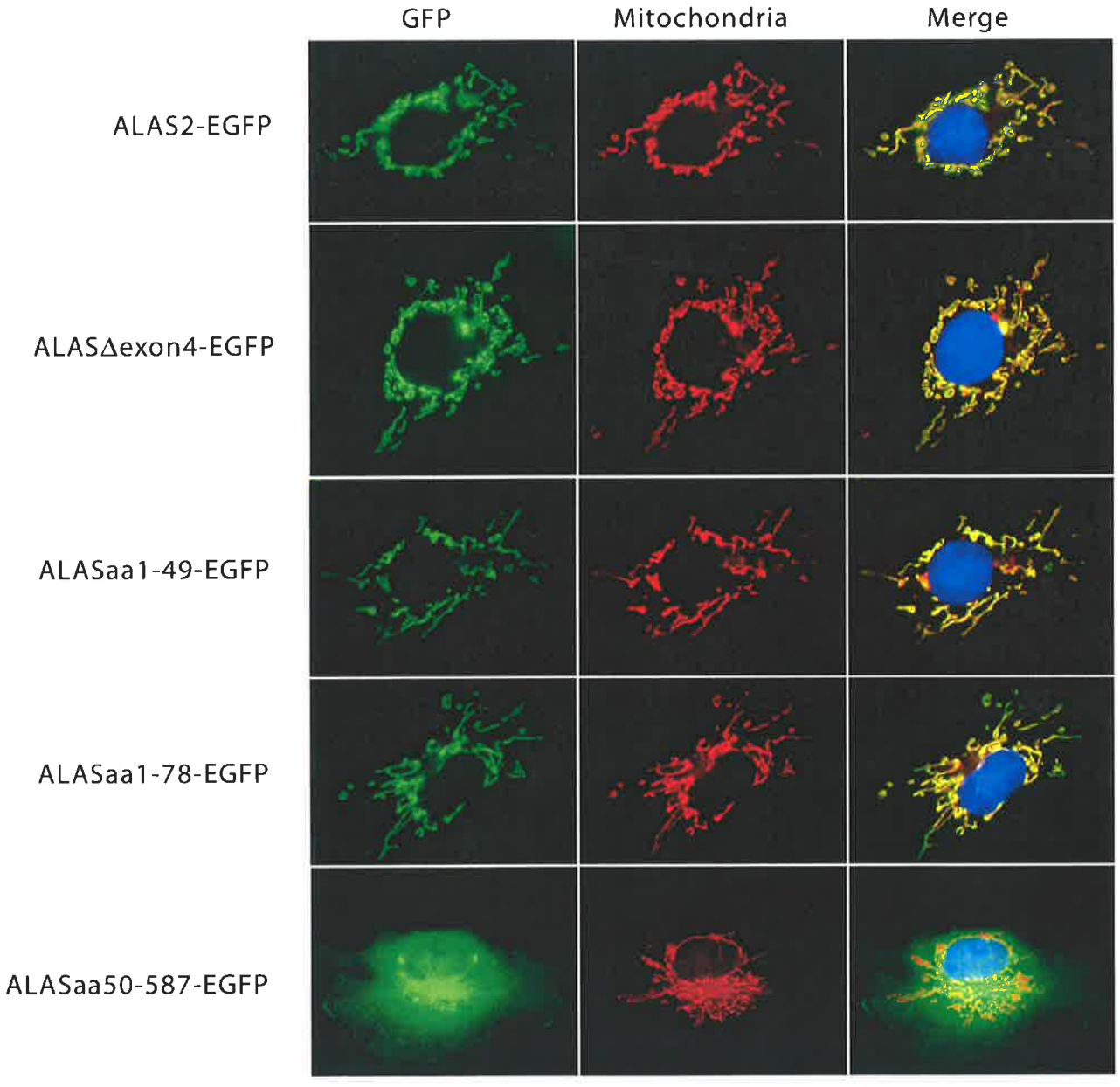
GFP
Mitochondria
Merge
ALAS2-EGFP
ALASΔexon4-EGFP
ALASaa1-49-EGFP
ALASaa1-78-EGFP
ALASaa50-587-EGFP

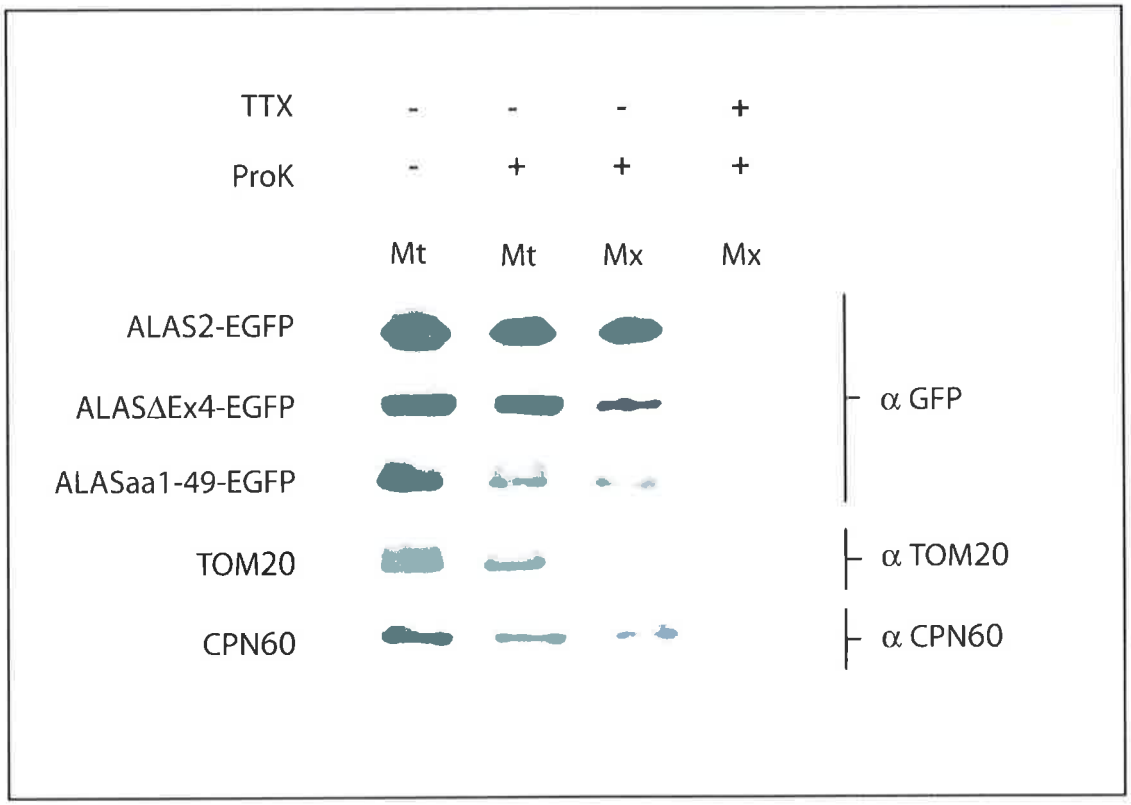

Figure 4.9

Mitochondrial sub-fractionation of Cos-1 cells expressing ALAS2-EGFP deletion constructs

Mitochondria and mitoplasts were prepared from Cos-1 cells that were transfected with various ALAS2-EGFP fusion constructs. Where indicated (+) fractions were treated with 10μg proteinase K (ProK) and 1% Triton X-100 (TTX). An anti-GFP polyclonal antibody was used to detect the various over-expressed ALAS2-EGFP fusion proteins. Antibodies to Tom20 (localised to the outer membrane) and Cpn60 (localised to the matrix) were used to confirm the various mitochondrial compartments.

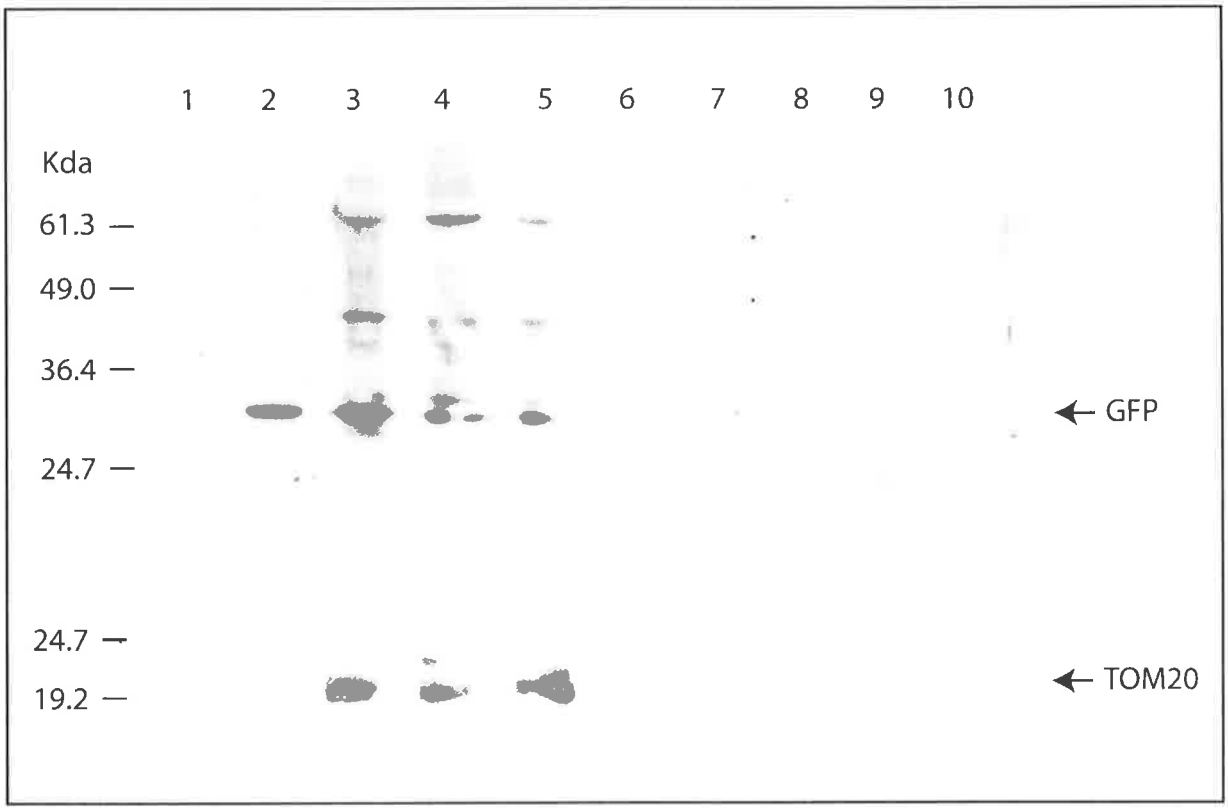

Figure 4.10

Percoll purification of crude mitochondria
Mitochondria were prepared from Cos-1 cells over-expressing EGFP by differential centrifugation. Each lane represents separate fractions collected from Percoll gradient purification. Fractions containing mitochondria were detected with anti-Tom20 antibody. Inclusion of EGFP in the fraction was detected with anti-GFP antibody. All fractions containing EGFP were identified as mitochondria.

within this organelle. Nevertheless, this approach with EGFP fusions may not necessarily be informative for the various HCCS deletions.

4.2.2.6 Generation of HCCS deletion constructs in pCMV.

The HCCS deletion fragments were placed into the pCMV expression vector to minimise any effect that EGFP has on their localisation. This approach relies on recognition of the truncated proteins by the Hccs polyclonal antibody. The 3' primers used to amplify the HCCS deletion regions for insertion to EGFP (section 4.2.2.3) were re-designed to introduce a stop codon at the C terminus. These primers were also designed to allow ligation into the *Bgl*II / *Kpn*I sites of pCMV following amplification from the corresponding EGFP vectors. The resulting constructs were labelled pHCCS-aa1-48-CMV (aa1-48), pHCCS-aa1-115-CMV (aa1-115), pHCCS-aa49-270-CMV (aa49-270), pHCCS-aa116-270-CMV (aa116-270), pHCCS-aa1-149-CMV (aa1-149) and pHCCS-aa147-270-CMV (aa147-270). Following over-expression in Cos-1 cells the Hccs antibody was tested on each of the extracts. Unfortunately, only the aa49-270 and aa1-149 protein fragments could be detected suggesting the antibody recognises epitopes composed of sequence spanning aa115. To therefore address the intra-mitochondrial localisation of the deletion constructs, an alternative protein tag (other than GFP) was required.

4.2.2.7 Generation of 6-Myc tagged HCCS deletion constructs.

As the Hccs antibody was unable to recognise all of the deletion constructs, an available 6-myc epitope-tag was chosen. The 6-myc tag vector was constructed in the backbone of $EGFPN_1$ with 6-myc placed into the *Hin*dIII restriction site following removal of the EGFP ORF (obtained from Dr. B. Hopwood, University of Adelaide, South Australia). Prior to the generation of HCCS deletion constructs in this vector, mitochondrial fractionations of cells expressing 6-myc alone were tested. Over-expression of 6-myc was not detected within any of the mitochondrial fractions and was therefore suitable as a tag for these studies (results not shown).

To generate in-frame fusion of the deletion constructs to the N-terminus of the 6-myc tag, primers were designed to introduce a *Xho*I site at the 3' end of the amplification products for the regions corresponding to aa1-48, aa1-115 and aa1-149. Following amplification by

PCR using the respective EGFP constructs as templates with the vector primer CMV-40 and the relevant 3' HCCS primer, these products were digested with *Nhe*I / *Xho*I and ligated into similarly digested pCMV-6myc. The cDNA cassettes of both aa49-270 and aa116-270 were removed from the corresponding EGFP vectors with *Bam*HI and ligated in-frame to pCMV-6myc digested with *Bgl*II. Correctly oriented clones were identified by PCR with CMV-40 and HKpnaa115. As a positive control for this study, full length HCCS was also fused to the 6-myc tag by ligation of a *Bam*HI / *Bgl*II HCCS fragment from HCCS-EGFP to the *Bgl*II site of pCMV-6myc. Correctly oriented HCCS ORF was determined with an *Eco*RI digestion. Vectors were labelled p6myc-HC-aa1-48, p6myc-HC-aa1-115, p6myc-HC-aa1-149, p6myc-HC-aa49-270, p6myc-HC-aa116-270 and p6myc-HC, respectively. All vectors were confirmed by sequence analysis.

4.2.2.8 Analysis of mammalian cells expressing HCCS-myc deletion constructs.

The myc-tagged deletion constructs were initially expressed in HeLa cells and analysed by immunofluorescence to confirm expression of the cDNA and to also confirm the results obtained with the EGFP fusions. Myc-tagged deletion constructs were detected with a mouse anti-myc monoclonal antibody (9E11) and counterstained with the anti-cytochrome c antibody (Fig 4.11). As expected, full-length HCCS-myc and the N-terminal regions contained in the aa1-48-myc, aa1-115-myc and aa1-149-myc constructs showed mitochondrial localisation. The aa1-48-myc region again targeted less efficiently than the extended region of aa1-115-myc. Intriguingly, the aa49-270-myc construct showed increased targeting in comparison to the EGFP fusion and likewise, the aa116-270-myc construct also showed low levels of mitochondrial co-localisation not detected with EGFP.

To further analyse the mitochondrial localisation of these fusion proteins mitochondrial sub-fractionation studies were again employed. Crude mitochondria were obtained as previously described and further sub-fractionated with hypo-osmotic shock. Using the myc-epitope antibody for western analysis on these fractions, the full length HCCS-myc, aa1-48-myc, aa1-115-myc and aa1-149-myc constructs were identified within the IMS (Fig 4.12). Conversely, the adjacent regions encoded by the aa147-270-myc and aa49-270-myc were unable to direct the myc tag across the outer membrane as shown by complete removal from the mitochondria plus ProK sub-fraction, suggesting that in the case

Figure 4.11

Immunofluorescent analysis of HCCS-myc deletion constructs
HeLa cells were transfected with HCaa1-149-myc, HCaa1-48-myc, HCaa1-115-myc, HCaa49-270-myc or HCaa116-270-myc deletion constructs as indicated (red). Cells were counter-stained with mitochondria specific antibodies (green) and the images merged to detect mitochondria localisation (yellow). Nucleus has been stained with DAPI (blue).

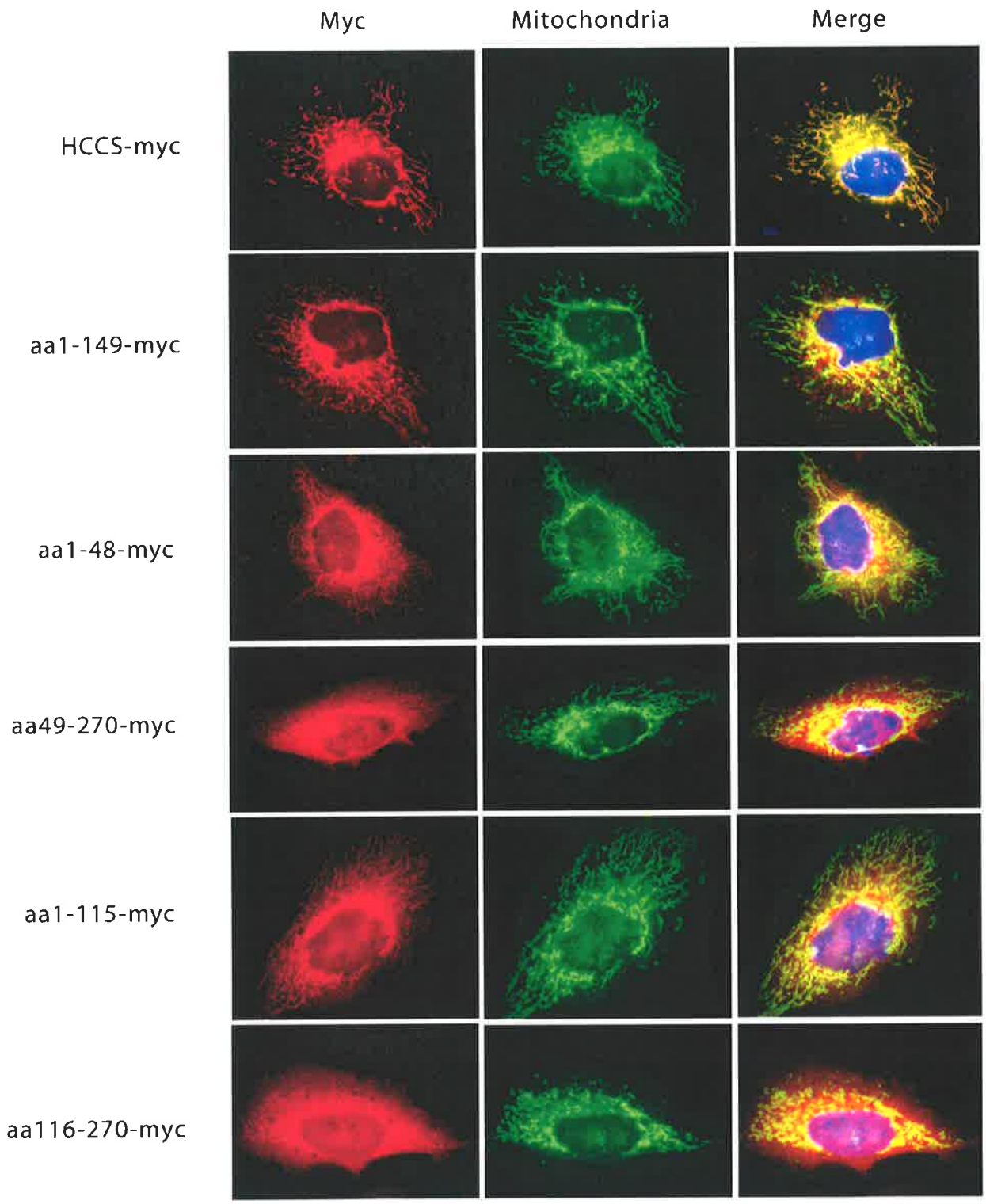
Myc
Mitochondria
Merge
HCCS-myc
aa1-149-myc
aa1-48-myc
aa49-270-myc
aa1-115-myc
aa116-270-myc

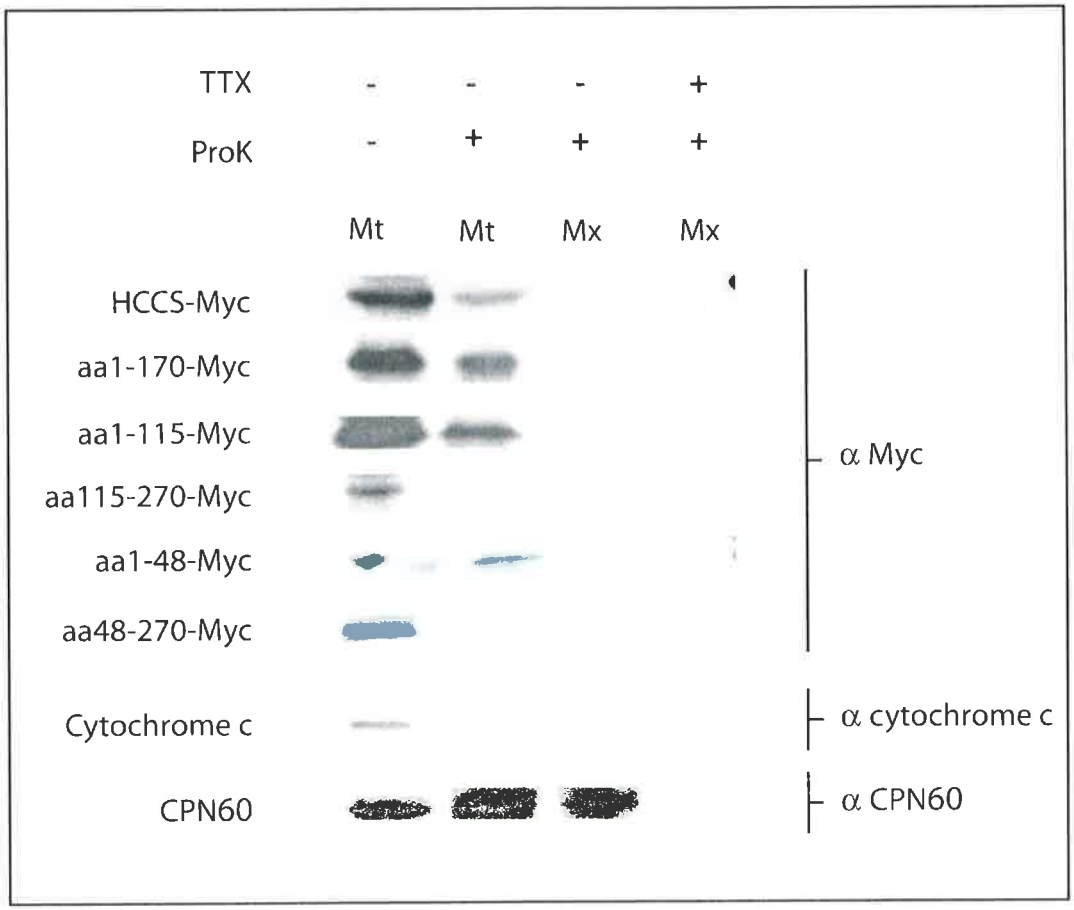

Figure 4.12

Mitochondrial sub-fractionation of HeLa cells expressing HCCS-myc deletion constructs

Mitochondria and mitoplasts were prepared from HeLa cells that were transfected with various HCCS-myc fusion constructs. Where indicated (+) fractions were treated with 10μg proteinase K (ProK) and 1% Triton X-100 (TTX). An anti-myc monoclonal antibody was used to detect the various over-expressed HCCS-myc fusion proteins. Antibodies to cytochrome c (localised to the IMS) and Cpn60 (localised to the matrix) were used to confirm the various mitochondrial compartments.

of these constructs the IF results may show partial outer membrane association. Together these results confirm the targeting potential of the N-terminal region of HCCS. Furthermore, this also suggests that the first 48 aa are both necessary and sufficient to allow IMS localisation although additional sequence may improve targeting efficiency.

4.2.3 The mechanism of mammalian HCCS mitochondria import.

The best characterised IMS proteins, cytochrome c1 and cytochrome b2, localise to this region through the use of a bi-partite signalling sequence. As mentioned previously, these motifs first direct the precursor proteins to the IM by a direct passage across the outer membrane. An internal sorting sequence then directs the intermediate protein to the correct sub-compartment. The Cyc3p of yeast have been shown to target the IMS without the requirement of TIM or $(\Delta)\Psi$, suggesting that the protein does not cross the IM and correspondingly may not utilise internal sorting sequences. However, in light of recent findings that mammalian HCCS utilises an alternative signal sequence to direct the protein to the mitochondria, it may also be possible that this targeting occurs via a different mechanism. To therefore address if human HCCS encodes an internal sequence(s) that may also be acting as a sorting signal, the minimal matrix targeting sequence identified for ALAS2 (section 4.2.2.5-4) was placed in-frame with the full length ORF of HCCS. This fusion protein would be expected to target the mitochondria through the characteristic pathway of most matrix proteins. However, if this protein does indeed encode an internal sorting sequence similar to that located within cytochrome b2 and cytochrome c1, following removal of the matrix targeting sequence at the IM, the HCCS signal might then direct localisation of HCCS to the IMS, or alternatively prevent passage across the IM.

4.2.3.1 Generation of an ALAS-aa1-55-HCCS construct.

In an attempt to allow cleavage of the ALAS2 signal sequence from such a fusion protein the first 55 amino acids of ALAS2 were amplified and fused to HCCS. As the predicted site of cleavage is suggested to be between aa 49-50 (Cox *et al*, 1991) the addition of a further 6 aa was chosen to increase the likelihood of including the correct cleavage recognition sequence. The HCCS ORF was removed from HCCS-EGFP with *Nco*I / *Bam*HI digestion and placed into similarly digested pLIT28 cloning vector. The first 55 amino acids

from ALAS2 were then amplified from the full-length cDNA with ALAS2XbATG and ALAS2aa55 that introduced an *Xba*I site directly upstream of the 5' ATG start codon and an *Nco*I site at the 3' end. Ligation of *Xba*I / *Nco*I digested ALAS2-aa1-55 to the *Xba*I / *Nco*I sites of HCCS-pLIT28 then placed the two regions in-frame. To fuse this ORF with EGFP an *Xba*I / *Bam*HI cassette of ALAS2-aa1-55-HCCS was ligated into the *Nhe*I / *Bam*HI site of $EGFPN_1$ to yield pEGFP-ALAS-HCCS. Continuity of all regions was confirmed by sequencing. To minimise any affect of EGFP on the intra-mitochondrial localisation of ALAS-HCCS the complete ORF was amplified with the primer pair ALASXhATG / HCCSstop and ligated to the PCR cloning vector pGEMT (pGEMT-ALAS-aa1-55-HCCS-TAA) to introduce appropriate restriction sites at the 3' end of the clone. This PCR importantly introduced *Xho*I restriction site at the 5' end of the clone and a stop codon at the 3' end of HCCS to allow correct termination of transcription. A *Xho*I / *Sal*I cassette was then placed into similarly digested pCMV (pCMV-ALAS-aa1-55-HCCS) and confirmed by sequencing.

To address if the ALAS2 precursor sequence was indeed being cleaved from this construct, the fusion of ALAS2-aa1-55-HCCS was amplified from ALAS2-aa1-55-HCCS-EGFP with ALAS2XbATG and the vector primer EGFP-60r. This fragment was digested with *Bam*HI and inserted into appropriately digested pET3a (pET-ALAS2-aa1-55-HCCS), a bacterial expression vector that harbours codons encoding an 8 amino acid T7 tag at the N-terminus of the introduced cDNA and an additional 21 amino acids at the C-terminus before the inclusion of a TAA stop codon. Cleavage of the pre-sequence can then be addressed by comparing the size of the native protein from bacteria (i.e. no post-translational modification) alongside a similar fusion construct expressed in mammalian cells. Correct orientation of inserts was detected with *Eco*RI digestion and confirmed by sequence analysis.

4.2.3.2 Analysis of mammalian cells expressing the ALASaa1-55-HCCS construct.

To detect if the fusion of ALAS2-aa1-55-HCCS to EGFP was indeed allowing localisation to mitochondria the construct was over-expressed in Cos-1 cells and analysed by immunofluorescence. Following counter-staining with anti-Tom20 antibody the EGFP signal was found to be efficiently targeted to mitochondria. The localisation pattern differed to the

full-length HCCS-EGFP construct (as there was a lack of background cytoplasmic expression) and, in fact, more closely resembled that of full-length ALAS2-EGFP (Fig 4.13).

Analysis of the ALAS-aa1-55-HCCS protein expressed from the bacterial expression vector pET3a alongside the same fusion protein expressed in mammalian cells confirms that the signal sequence of ALAS is removed from the fusion protein following mitochondrial targeting (Fig 4.14A). The increased size of the mature ALAS-aa1-55-HCCS protein in comparison to endogenous HCCS detected in this study can be attributed to the 6 aa of ALAS (i.e. residues 50-55) not expected to be cleaved from the pre-sequence, while the increased size of ALAS-HCCS in bacteria is accounted for by the additional 29 aa introduced with the pET3a vector. This provides for the first time, solid support that the ALAS2 pre-sequence is proteolytically removed from the mature matrix protein. Fractionation studies of mitochondria from HeLa cells expressing this construct also show that internal HCCS sequences are unable to direct the mature protein to the inter-membrane space (Fig 4.14B). Taken together these results show that the ALAS-aa1-55-HCCS protein is localised to the mitochondrial matrix, and may suggest that HCCS either does not encode any internal sorting signal or that any sorting signal can not override the matrix targeting signal of ALAS2. This latter point should be addressed in future experiments utilising a known internal sorting signal (i.e. from cyt b2 or c1) with the first 55 aa of ALAS2.

4.3 Summary.

The work in this chapter has confirmed that mammalian HCCS, like the yeast proteins with which it shares amino acid similarity, is indeed localised to the mitochondrial IMS. HCCS deletion constructs fused to various reporter genes have subsequently been used to identify a minimal region conferring correct mitochondrial localisation. The first 48 amino acids were found to be necessary and sufficient for correct IMS targeting as the aa49-270-myc deletion protein was unable to be imported across the OM. In striking contrast to the majority of mitochondrial targeting signals, this region of HCCS does not contain any elements that would be considered to allow the formation of an alpha helix (Fig 4.1) and is essentially charge neutral. The sequence is not conserved across the eukaryotes but is, however, between humans and mice and therefore represents a novel topogenic signalling sequence. That none of the other c-type synthases share similar N-termini suggests that they

may also utilise similar sequences to that of *N.crassa* within the C terminus. This result further highlights the versatility of the mitochondrial import machinery and the ability of both the TOM and TIM enzyme complexes to function independently. As previously mentioned, the targeting region identified in *N.crassa* also harbours the two highly conserved motifs that form the characteristic signatures of all c-type synthases. These motifs are also present in mammalian HCCS. From the results presented here, it is unlikely that these regions have any function in targeting the mammalian orthologue to the IMS, although an influence on efficiency of targeting or retention is still possible. Rather, it is likely that these motifs encode the catalytic domain of the enzyme as previously suggested (Steiner *et al*, 1996). Interestingly, Maurer Stroh and colleagues (2002) recently proposed the presence of a N-myristolation site on the N-terminal Glycine within the HCCS protein. As N-myristolation promotes binding to lipids, this N-terminal region also presents as an ideal region to allow attachment of HCCS to the outer surface of the IM and hence act as a binding site for the correct import of apocytochrome c.

Signalling sequences encoded within HCCS were unable to allow correct IMS localisation of the ALAS-aa1-55-HCCS fusion protein, possibly inferring that there is no internal sorting sequence for retention within the IMS. Indeed, sequence analysis of the HCCS protein is unable to identify any region that would act in a similar way to the bi-partite signals of cytochrome b2 or cytochrome c1 (i.e. a hydrophobic stretch preceded by a number of positively charged residues). This further suggests that mammalian HCCS does not utilise the TIM complex in targeting the mitochondria; rather, the mechanism of localisation may be similar to that of the *S.cerevisiae* and *N.crassa* CTS, albeit with the utilisation of an alternative signal. This result is consistent with the experiments of Segui-Real *et al* (1993) in which the signal peptide of the yeast precursor F_1-ATPas β subunit ($pF_1\beta$) was fused to Cyc3p (HCCS) (Segui-Real *et al*, 1993). With elegant experiments removing the $(\Delta)\Psi$ of purified mitochondria these researchers were able to conclude that yeast HCCS lacks both matrix targeting information and signals for sorting the protein back into the IMS. From recent results presented in this chapter, it is also likely that mammalian HCCS does not encode matrix targeting information.

Like the family of ALAS proteins, the CTS's also contain two CPX heme binding motifs in the first 48 aa. Although we have recently obtained results showing conflicting

Figure 4.13

Immunofluorescent analysis of ALAS2-HCCS-EGFP fusion construct
A construct containing ALAS2aa1-55 fused in-frame with full-length HCCS-EGFP was over-expressed in Cos-1 cells (green). Cells were counter-stained with the mitochondrial anti-Tom20 antibody (red) and overlayed to show co-localisation (yellow). Control cells in which either HCCS-EGFP or full-length ALAS2-EGFP have been expressed are also represented. The nuclei have been stained with DAPI (blue).

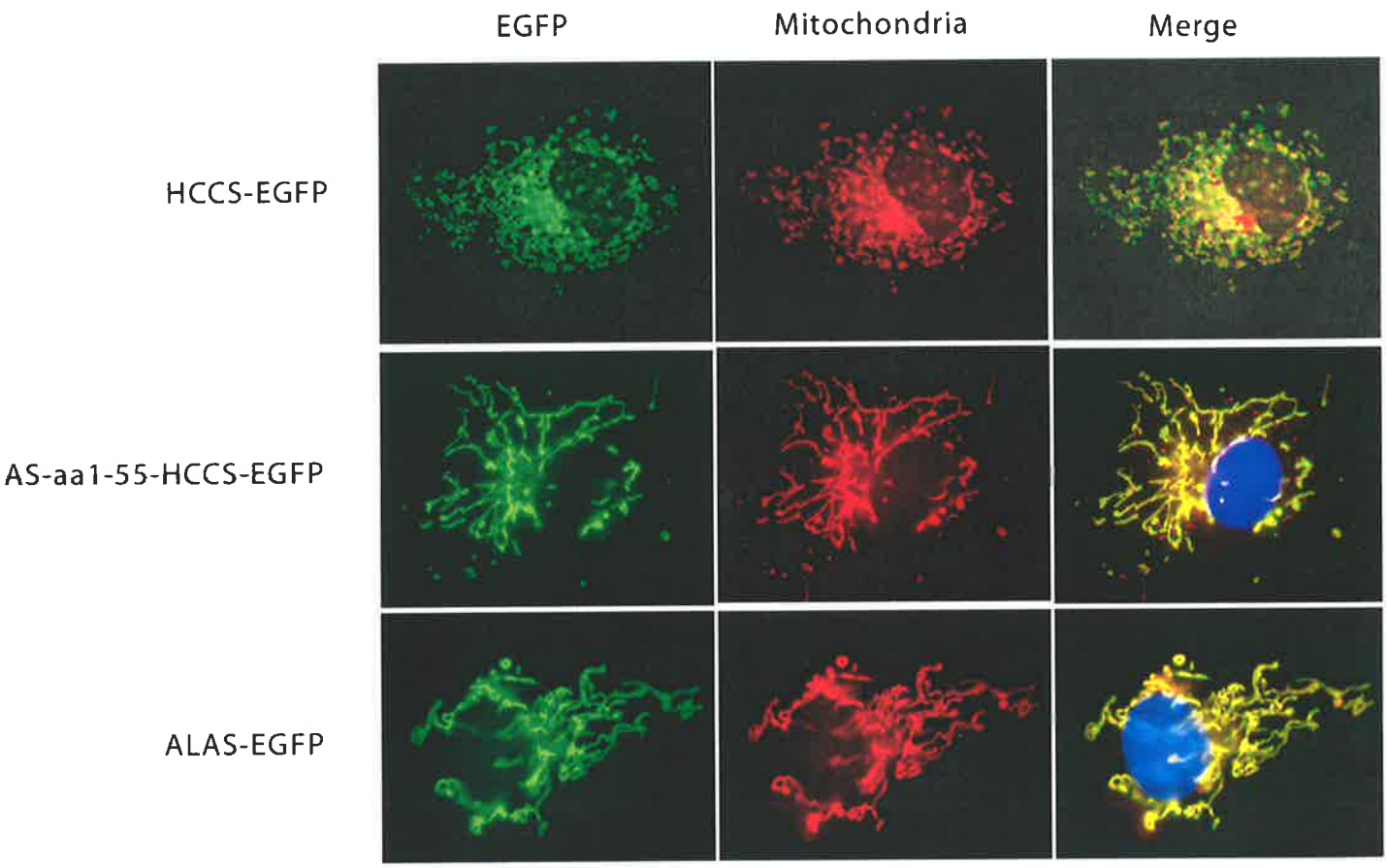
EGFP
Mitochondria
Merge
HCCS-EGFP
AS-aa1-55-HCCS-EGFP
ALAS-EGFP

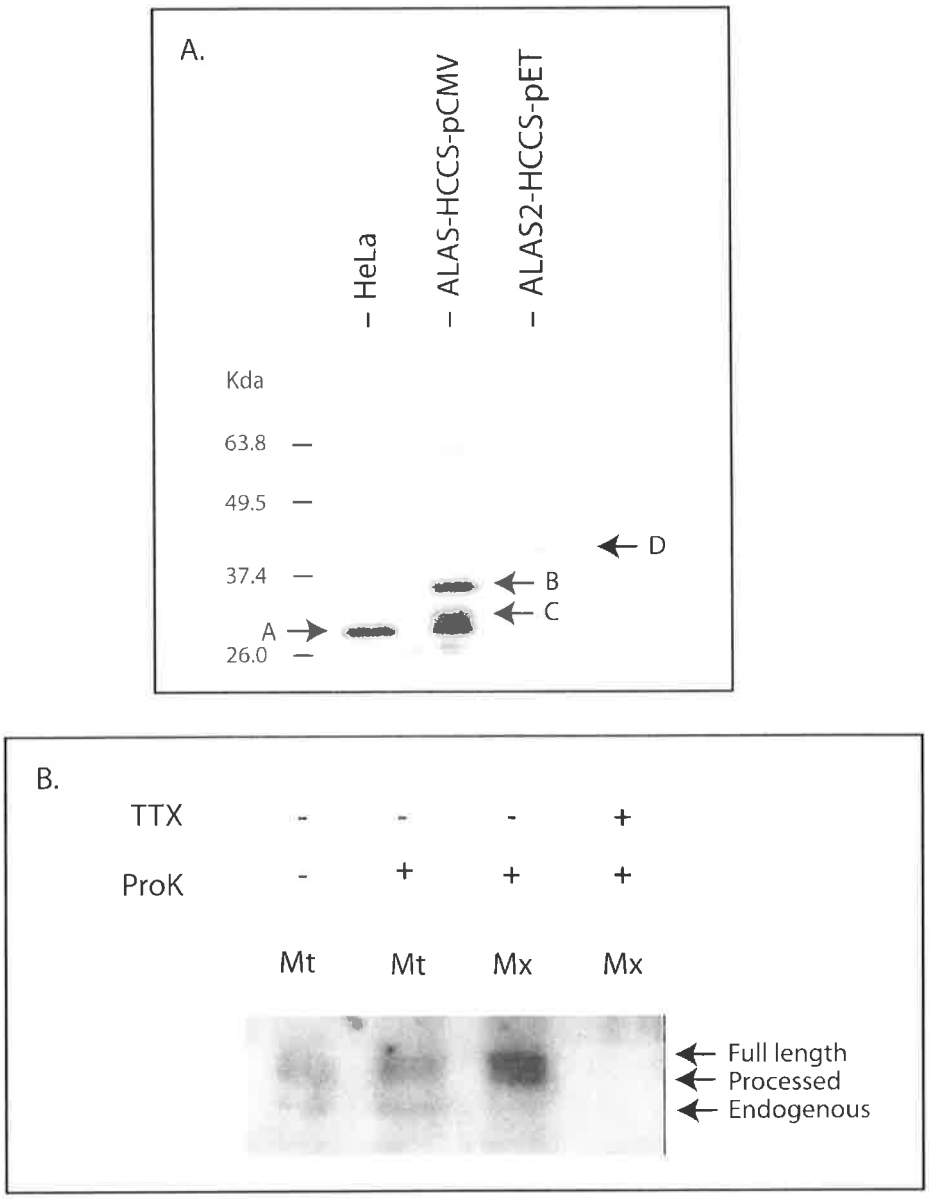

Figure 4.14

A. Cleavage of the ALAS2 pre-sequence
Mitochondria were obtained from HeLa cells with and without the over-expression of the pCMV-ALAS-aa1-55-HCCS fusion construct. Whole cell protein was also extracted from bacteria expressing pET-ALAS-aa1-55-HCCS and separated by 10% PAGE. All fusion proteins were identified with anti-Hccs antiserum. Endogenous HCCS is detected within the mitochondria from both HeLa protein extracts (arrow A). Unprocessed ALAS-aa1-55-HCCS is detected at approximately 37 kDa (arrow B) while the mature form produced from cleavage of the pre-sequence, is slightly larger than the endogenous protein (arrow C). The fusion protein expressed in bacteria is identified at approximately 41 kDa (arrow D), consistent with the introduction of an additional 29 aa by the pET3a vector.

B. Mitochondrial sub-fractionation of HeLa cells expressing ALAS2-aa1-55-HCCS
Mitochondria and mitoplasts were prepared from HeLa cells transfected with pCMV-ALAS-aa1-55-HCCS. Where indicated (+) fractions were treated with 10μg proteinase K (ProK) and 1% Triton X-100 (TTX). Anti-Hccs antiserum was used to detect the over-expressed fusion protein. Note the removal of endogenous HCCS from the mitoplast fraction treated with ProK, while the full length fusion and the processed form remain in the matrix.

results in transient transfection assays, at least in the case of ALAS2 (results not shown), Lathrop and Timko (1993) found the inhibition of mitochondrial localisation of ALAS in the presence of high heme concentrations *in vitro*. This effect was specified by heme binding to the CPX motifs. In a similar way, Steiner *et al* (1996) were able to show the import inhibition of Cyc2p in the presence of exogenous heme *in vitro*. This finding prompted the suggestion that it may be possible for heme to have a regulatory effect in the biosynthesis of c-type cytochromes by the control of heme lyase import. If indeed true, then the requirement of the first 48 aa for mitochondrial targeting of mammalian HCCS would also allow another mechanism by which this regulation could occur (i.e. in presence of heme the targeting signal may not be functional). With this in mind it may therefore be interesting to repeat the experiments of Steiner *et al* (1996) in the mammalian system to address the requirement of the CPX heme binding motifs in mitochondrial targeting *in vivo*. To date only a number of the TOM proteins have been identified in higher eukaryotes, even with the recent completion of a number of genome projects. In contrast, nearly all of the inner membrane translocase proteins have been cloned.

Interestingly, a novel protein localised to the outer membrane, Tom34, has also been identified in mammals (Mori & Terada, 1998) possibly suggesting that higher eukaryotes may have alternative mechanisms for mitochondrial import. With this in mind, it would perhaps be worthwhile addressing the involvement of the TOM proteins in the translocation of mammalian HCCS across the OM. As previously mentioned, yeast Cyc3p is recognised by the receptor protein, TOM22, which directs the pre-protein to the general import pore. With the additional TOM proteins identified in mammals it remains feasible that the alternative targeting signal of mammalian HCCS could also utilise these additional proteins. Indeed, the use of an alternative localisation signal may also explain the partial rescue of the yeast mutant detailed in the previous chapter.

To address the exact mechanism of transport across the OM, further experiments studying the requirement of both $(\Delta)\Psi$ and the need for ATP are imperative. This, as well as the requirement of the TOM subunits, should be followed with the use of *in vitro* import assays of isolated mitochondria in the absence of ATP, removal of TOM and also the ablation of $(\Delta)\Psi$ through the addition of carbonyl cyanide n-chlorophenylhydrazone (CCCP).

Chapter Five: Analysis of patient samples.

5.1 Introduction.

Oncocytic cardiomyopathy (OC) is a severe disorder that is associated with sudden infant death that often results from cardiac arrhythmia (Ferrans *et al*, 1976). Morphologically, the disorder is characterised by the accumulation of uniquely altered cardiac myocytes that have the appearance of large unstructured cells. The affected cells usually form foci and have the appearance of fatty tissue due to their yellowish colour and increased lipid content. On close examination these cells are found to have granular cytoplasm's representing mitochondrial hyperplasia (Bleistein & Zierz, 1989).

Like various other forms of myopathies that are known to result from deficiencies of the mitochondrial respiratory chain, some cases of OC have also been shown to result from these same abnormalities. Specifically, deficiencies in the activities of the cytochrome complexes III and IV of the electron transport chain have been reported in three separate cases (Papadimitriou *et al*, 1984; Bohles *et al*, 1987; Otani *et al*, 1995). Indeed, Andreu and colleagues (2000) recently identified a mutation within the mitochondrial encoded *cytochrome b* gene, a major component of the Coenzyme Q - cytochrome *c* reductase complex (complex III). In this case the mutation was heteroplasmic and found to fulfil all criteria for pathogenicity (Andreu *et al*, 2000). As the respiratory chain is made of five complexes that are composed of multi-enzyme subunits (i.e. complex III alone is composed of one mitochondrial-encoded subunit and 10 nuclear-encoded subunits), deficiencies of one complex can arise through a number of alternate ways. Due to this phenomenon, many myopathies that result from defects in the respiratory chain are genetically heterogeneous (Bleistein & Zierz, 1989). Likewise, it must be considered that OC may also be genetically heterogeneous.

As mentioned previously, OC has been observed in association with the MIDAS syndrome phenotype (Bird *et al*, 1994) and consequently supports the original hypothesis that it may be caused by an X-linked gene (Bruton *et al*, 1977). Further support for this is the finding that over 10% of patients for which a sole diagnosis of OC was made also show MIDAS related symptoms (Malhotra *et al*, 1994; Bird *et al*, 1994). The foci of abnormal appearing cells in the heart may also be due to clonal expansion following the random nature

of X-chromosome inactivation early in cardiac development. These associations are the basis for the proposal that the gene(s) affected in these patients are also encoded within the proposed MIDAS critical region.

As I have demonstrated in the earlier chapters, the only complete gene residing in the refined MIDAS critical interval encodes the human orthologue of *S.cerevisiae* HCCS and therefore mediates the addition of heme to cytochrome c that in turn transfers electrons between complex III and IV of the mitochondrial respiratory chain. We have thus considered *HCCS* as an ideal candidate for the OC associated with MIDAS syndrome.

The focus of the research in this chapter has been aimed at the analysis of *HCCS* in patients with a suspected diagnosis of OC. The *cytochrome b* gene that has recently been shown to harbour a mutation in an OC patient has also been analysed. To facilitate this work, a number of samples from OC patients have been sought with the identification of a skin fibroblast cell line established from one individual. Initial experiments have been completed in attempts to characterise the function of HCCS in this cell line.

5.2 Results.

5.2.1 Human HCCS gene structure and design of exon boundary primers.

Prior to the initiation of this research the gene structure of human *HCCS* was determined by restriction enzyme characterisation and sequencing of the intron/exon boundaries from the cosmid U163G9 (Schwarz, 1997; Cox *et al*, 1998). This gene structure revealed that *HCCS* is composed of six coding exons and one 5' untranslated exon spanning approximately 15kb on the short arm of the X-chromosome (Xp22.3). During the course of this research the entire genomic interval on the X-chromosome was published as a result of the human genome project and confirms these earlier findings. As detailed in the following chapter this organisation is also conserved in mice (Fig 6.2; Schwarz & Cox, 2002).

The human *HCCS* gene encodes three separate transcripts of approximately 1.2kb, 2.6kb and 5.2kb that appear to arise from differential use of polyadenylation signals (Schaeffer *et al*, 1996). Each *HCCS* transcript shows an identical open reading frame of 1.01kb, encoding a protein of 268 amino acids. Studies on mice have also identified a single

2.6kb transcript in all tissues that encodes a protein of 272 amino acids (Schwarz & Cox, 2002).

Primers were designed in the intron sequence around each of the exons to allow amplification of the entire coding exon complement in 7 separate fragments (table 5.1). Where possible, these primers were designed within 150bp of the boundary and with 50 - 60% GC content. Primers were labelled HE-*F, HE-*R, representing the gene *hHCCS*, the corresponding exon (* being the exon number), and also the 5' (F-Forward) or 3' (R-Reverse) boundary. To allow specific re-amplification from primary products obtained off paraffin embedded archival samples, nested PCR was used with internal primers for each fragment. Various combinations of these primers were used to amplify their respective regions at the detailed temperature. Interestingly, sequencing of the 5′ UTR in humans identified a $(GGC)_n$ trinucleotide repeat within exon one that exhibits a low level of polymorphism. Analysis in 50 control samples shows the largest uninterrupted stretch is ten repeating units and the shortest seven (Attard, 1998). As discussed later, a comparable sequence in the mouse 5' untranslated region has not been identified.

Exon	PCR length (bp)	Name	Forward Primer	Name	Reverse Primer	Temp (°c)
1	295	HE1Fa	GAAGTCCCGCCTTCTAAAAAGG	HE1R	GAGAAGCTGCCAAGTGTCTTCCC	55
	377	HE1Fb	CTCCGTGATTGACGGAAAATATTAC	HE1Rb	GAATTCGAAGAAACGAAGGGACAC	55
2	206	HE2Fb	GAGTCCAGAGACATTAATCTGTC	HE2R	ATTTTCTAGGCAAAGGGCCGAT	50
	298			HE2Rb	TCCTGAGCTCAAGCAATCCAC	50
3	248	HE3Fa	AGATGTCCTGCCTTCATGGTGAC	HE3Ra	ACCCTGCATAAAAAGCTCCAG	55
	334	HE3Fb	CCTATGGTGGTAATCATTGGTCAG	HE3Rb	GCAACTTGTCTTGGGAGTCTG	55
4	241	HE4Fa	TATATCCTATAAAAGCAAATCTGTT	HE4Ra	ATAACTCTTGGATATTCTGAC	55
	375	HE4Fb	TATATCCTATAAAAGCAAATCTGTT	HE4Rb	TGAAGGTAAAAAATCTCTTTAGC	55
5	206	HE5Fa	TGGCATTATCAGGAACAGTTGTC	HE5Ra	AGATGCTTGAAACATTTAAGATCTC	55
	258	HE5Fb	GTGGATTAACTTTATGGCATTATC	HE5Rb	GAATGTTAAAACTCTAGAAAGCTG	55
6	152	HE6Fa	ACAGACTTTTCTTATTTGGGGA	HE6R	GATGGTGAAACAACACTTCTGCG	56
	288	HE6Fb	GAACTTACCTTTCTCTGTAAATGT			55
7	254	HE7F	CAAGCATTTTAACACTCAGTGG	HE7Ra	CCATCTGAAACAGTGCTTTACG	58
	355			HE7Rb	AGTGTGATTACCCACTTGAAGTTC	55

Table 5.1 PCR Primers used for amplification of the coding exons of *HCCS*. The (b) primers were used for first round amplification, while (a) primers were used for internal (nested) PCR.

5.2.2 Cytochrome b amplification primers.

Mutations in *cytochrome b* were first detailed in 1988 and have since been highlighted in several mitochondrial disorders including mitochondrial myopathy, complex III deficiency in muscle and cardiomyopathy (see Fisher & Meunier, 2001 for recent review). In all pathogenic cases, the severity of the defect is suggested to correlate with the levels of mutant mitochondrial heteroplasmy. Importantly, mutations have also been shown in an isolated case of OC (Andreu *et al*, 2000). As *cytochrome b* is encoded in the mitochondrial genome, it contains no intronic sequences and therefore allows amplification of the full reading frame directly from genomic DNA. Published human mitochondrial sequence (Genbank accession #J01415) was used to design primers to the 5' (CytBF) and 3' (CytBR) regions adjacent to the ATG start codon and TAA[9] stop codon, respectively. These primers allowed efficient amplification of an approximate 1.1 kb fragment from genomic DNA prepared from whole blood; however, no product was amplified from genomic DNA samples prepared from paraffin embedded tissue. As the majority of patient samples for these experiments were in the form of archival paraffin embedded tissue obtained at necropsy, primers were also designed to allow amplification in four smaller overlapping segments (Table 5.2).

Primer Pair	PCR length (bp)	Name	Forward Primer	Name	Reverse Primer	Temp (°c)
1	455	CytBF	CGCACGGACTACAACCACGA	CytB#5	CCTATGAAGGCTGTTCCGTA	55
2	327	CytB#2	TGCAAGAATAGGAGGTGGAG	CytB#6	TCTGCCTCTTCCTACACATC	55
	473	NlaIII-CytB	GGAGGTCTGGTGAGAATAGTG TTAATGTCATTAAGGAGAG**CA**			55
3	302	CytB#1	TTCACTTCATCTTGCCCTTC	CytB#3	GGAGAATTGTGTAGGCGAAT	55
4	369	CytB#4	GATATTTCCTATTCGCCTACAC	CytBR	GGGTGCTAATGGTGGAGTTA	58

Table 5.2 PCR primers used for amplification of cytochrome b. Underlined and bold text represents base pairs altered to engineer diagnostic restriction sites for quantitation of heteroplasmy.

[9] The TAA stop codon of cytochrome b is completed by the addition of the polyadenylation signal to the end of the mRNA.

5.2.3 Analysis of hHCCS and cytochrome b from patient samples.

5.2.3.1 Collection of patient samples.

MIDAS syndrome is a developmental disorder associated with complete Xp22.3 monosomy usually resulting from translocations or large deletions (Ballabio & Andrea, 1992). Consequently, although some MIDAS patients have OC as an additional feature, the chromosome anomalies prohibit the possibility for conventional mutation analysis of individual genes. To complete mutational analysis on patients suffering from OC and hence analyse *HCCS* as a candidate gene for this disorder, a number of DNA samples from OC patients that do not harbour large chromosome abnormalities have been obtained. As mentioned, the presentation of OC may arise from mutations within more than one gene and therefore analysis would be most informative from patients that also show X-linked features of the MIDAS syndrome (i.e. microphthalmia and sclerocornea). Fortuitously, specimens have been made available from the female patient (referred to as HB) presented by Bird *et al* (1995) that has the diagnostic MIDAS facial skin lesions as well as OC. Detailed molecular analysis of this patient has found no deletion greater than 100kb within and around the MIDAS critical region (Cox *et al*, 2001), possibly indicating that only a single gene may be affected by either point mutation or small deletion. Throughout the course of this project collaboration was also sought with Professor Bahig Shehata (Toledo Children's Hospital, Ohio, USA) who has established a registry of patients diagnosed with OC. While this registry now consists of around 40 cases, only 5 (HC1-5) were made available for this project as institutional regulations did not allow shipment of many patient samples. Patient history was not received for all cases, however, from personal communication with Dr Shehata it was evident that at least two were siblings (male [HC1] and female [HC2]) and that one female had additional eye defects (HC3). No further information was obtained for either HC4 or HC5. As mentioned previously, males are only infrequently encountered in the literature (Silver *et al*, 1980), therefore suggesting that OC in the case of the siblings may not be X-linked. In all five cases OC was diagnosed at autopsy by the identification of characteristic foci in the heart. Perhaps most significantly, a skin fibroblast cell line established from another male patient presented to Dr Kenneth Maclean (Westmead Children's Hospital, Australia) was also obtained (HC6). This patient died as a result of a hypertrophic cardiomyopathy first diagnosed at five and a half months of age. Electron

microscopy of cardiac biopsies highlighted the characteristic presence of mitochondrial hyperplasia. Cytological analysis was unable to identify any gross chromosome alterations, while no OXPHOS deficiencies were detected by standard enzyme assays (Dr. J. Chritodoulou, personal communication). Although genotypically male, this cell line represented an ideal resource to study the pathogenicity of any identified mutation(s).

5.2.3.2 Amplification and analysis of patient samples.

For mutational analysis to be completed on these patients both genes were initially amplified off genomic DNA prepared from available samples. As OC results in only small regions of the heart being affected, DNA was prepared from tissue showing the characteristic disease morphology in an attempt to overcome the possibility that this disorder may arise from genetic mosaicism[10]. Primers were used to amplify each of the exons and fragments constituting *HCCS* and *cytochrome b* independently. Due to the low numbers of patients and relatively few exons / fragments from these genes, automated sequencing of the PCR products was used to identify any possible mutations or polymorphisms. Sequencing was initially performed with the corresponding forward primer for each fragment. Variations and discrepancies in some of the fragments were then confirmed by sequencing in the opposite direction using the reverse primer. Further confirmation was obtained by additional amplification from genomic DNA and re-sequencing. Even with the use of various combinations of all primers, exon 4 and 7 were unable to be amplified from various patients that was related to the poor quality of DNA prepared from paraffin embedded tissue (table 5.3).

Several possible alterations were detected in the *HCCS* ORF from the seven available patients, however, following reverse strand sequencing no mutations/polymorphisms were confirmed. Preliminary analysis of HC6 identified a variation in the sequence 10-15 bp after the stop codon in exon 7. Any mutation in this region would not be expected to have a direct effect on the protein, but may affect correct expression and / or splicing. Unfortunately, repeated attempts at sequencing this region were unsuccesfull so analysis of the protein has been followed in the available cell culture line (detailed in section 5.2.4).

[10] Genetic mosaicism refers to the non genetic-identity of cells in the same tissue. This may arise from mutations introduced in somatic cells post fertilisation, or indeed from mitochondrial heteroplasmy.

Exon / Frag.	HB	HC1	HC2	HC3	HC4	HC5	HC6
HCCS							
1	++	+	+	+	+	+	+
2	+	+	+	++	+	+	+
3	+	++	+	+	+	+	+
4	+	+	+			++	+
5	+	+	+	+	+	++	+
6	++	++	+	+	+	+	+
7	+	+		+	+	+	++ ?
Cytochrome b							
1	?	?	?	?		+	+
2	?	?	?	?	?	?	++
3	+	+	+	+	+	?	+
4	+	?	?	?	?	+	+

Table 5.3 Summary of exons and fragments sequenced from available OC patients. (+) Indicates sequencing with one primer with no differences identified; (++) indicates sequencing with both primers with no differences identified; (?) indicates discrepancies in the sequence compared to the test genomic sequence. A blank box indicates lack of success in amplification of that exon.

In addition, several alterations were identified and also confirmed in the *cytochrome b* gene (Table 5.4). While a number of these differences have been published previously, several are unique to this study. Four of the base pair changes were found to be non-coding and therefore not expected to have any effect on the mature protein. As the mitochondrial genome is transcribed as a polycistronic message from a common promoter in the D-loop region, these variations would also not be expected to have any effect on mRNA splicing or expression levels. The A15326G exchange identified in 5 patients introduces an alanine in place of a threonine at amino acid 194, a polymorphism previously reported in a number of studies with no expected effects on OXPHOS (Andreu *et al*, 1999). Interestingly, HC2 also harboured another two polymorphisms (see Table 5.4) previously reported by the same researchers. All of these substitutions introduce semi-conservative amino acid changes in positions not predicted to have major structural effects on the protein (Fisher & Meunier, 2001). Indeed, the amino acids altered in these examples are also found in this position in other species (Esposti *et al*, 1993).

		HB	HC1	HC2	HC3	HC4	HC5	HC6
non-coding variation	Previous	T15115C	T15115C					
	New		**A15373G** **T15850C**		T15850C			
coding variation	Previous	A15326G *(T194A)* (P)	A15326G *(T194A)* (P)	A15326G *(T194A)* (P) T15693C *(T316I)* (P) A15758C *(I323V)* (P)	A15326G *(T194A)* (P)		A15326G *(T194A)* **C15452A** ***(L236I)***	
	New					**G15431A** ***(A229T)***		

Table 5.4 Mutations / polymorphisms identified in *cytochrome b* from OC patient samples. Previously reported polymorphisms / mutations were identified from the Mitomap website (www.mitomap.org) and are represented with (P). Numbering and comparison of the gene was taken from the standard human Mitochondrial DNA "Cambridge" reference sequence (Genbank accession #J01415). Potential mutations have been highlighted in bold.

Of particular interest however, was the C15452A substitution found in HC5. This introduces an isoleucine at amino acid 236 in place of a leucine (Fig 5.1), a variation that has previously been reported in a case of ischaemic cardiomyopathy and was suggested to be a pathogenic mutation based on the overall reduction of complex III activity by over 50% (Marin-Garcia *et al*, 1996). In addition, the G15431A alteration in HC4 results in the substitution of alanine 229 by a threonine; a relatively conservative change but nevertheless one that could be pathogenic.

In comparison to nuclear genes, the genes encoded within the mitochondria are present in hundred's of copies per cell. As mutations may not be present in all mitochondrial genomes the levels of heteroplasmy are likely to have a critical role in the presentation and severity of the disorder. To therefore quantify the levels of heteroplasmy of the two potential mutations identified in these experiments, RFLP analysis was completed on the respective PCR fragments. For these purposes a primer was designed to the region

harbouring the C15452A mutation (NlaIII-CytB) to introduce an *Nla*III informative restriction site in the presence of the variant. Following amplification with CytB#6, the product was digested with the corresponding restriction enzyme and separated by 2% agarose gel electrophoresis (Fig 5.2A). Interestingly, the C15452A change was found to be present in high copy numbers in both heart and liver of HC5 while not evident at all in the control case. The G15431A variant was also quantified by digestion of *cytochrome b* fragment 3 with *Bsa*HI. In this case, the variation removes the *Bsa*HI recognition site such that only wt (G15431) is cleaved. Heteroplasmy levels of the G15431A variant were analysed from heart samples of HC4 as amplification was not possible from liver tissue. Following digestion of cytochrome fragment 3 with *Bsa*HI, the G15431A mutation was also found to be present in high copy numbers. Restriction analysis completed on a further 21 control samples (Fig 5.2B) was unable detect this change in the general population.

5.2.4 Characterisation of OC cell line.

As mentioned previously, sequence analysis of *HCCS* from HC6 detected a discrepancy after the TAA stop codon in the 3' UTR. To therefore address if this change had any affect on HCCS protein synthesis, a number of experiments were completed on the available cell line. With recent results in mind, a deficiency of HCCS function would be expected to reduce levels of mature cytochrome within the mitochondria, hence prohibiting the efficient transfer of electrons between complex III and IV. Although preliminary mitochondrial respiratory chain enzyme assays on this cell line were unable detect any substantial variations that suggest involvement of this system in the presentation of the disorder, perhaps minor deficiencies of HCCS may have gone unnoticed. If HCCS is indeed altered in these cells, a phenotype similar to the cytochrome c KO fibroblasts may also be expected (Li *et al*, 2000). Mutant $cytc^{-/-}$ cells are unable to grow in normal dulbeco's modified eagles medium (DMEM), most likely resulting from their defect in mitochondrial respiration. When grown in media supplemented with pyruvate and uridine, however, these mutant cells adopt a normal growth rate in a similar way to cells completely devoid of mitochondrial DNA (King & Attardi, 1989). To therefore address a potential deficiency in either HCCS or cytochrome c, a growth rate assay was completed.

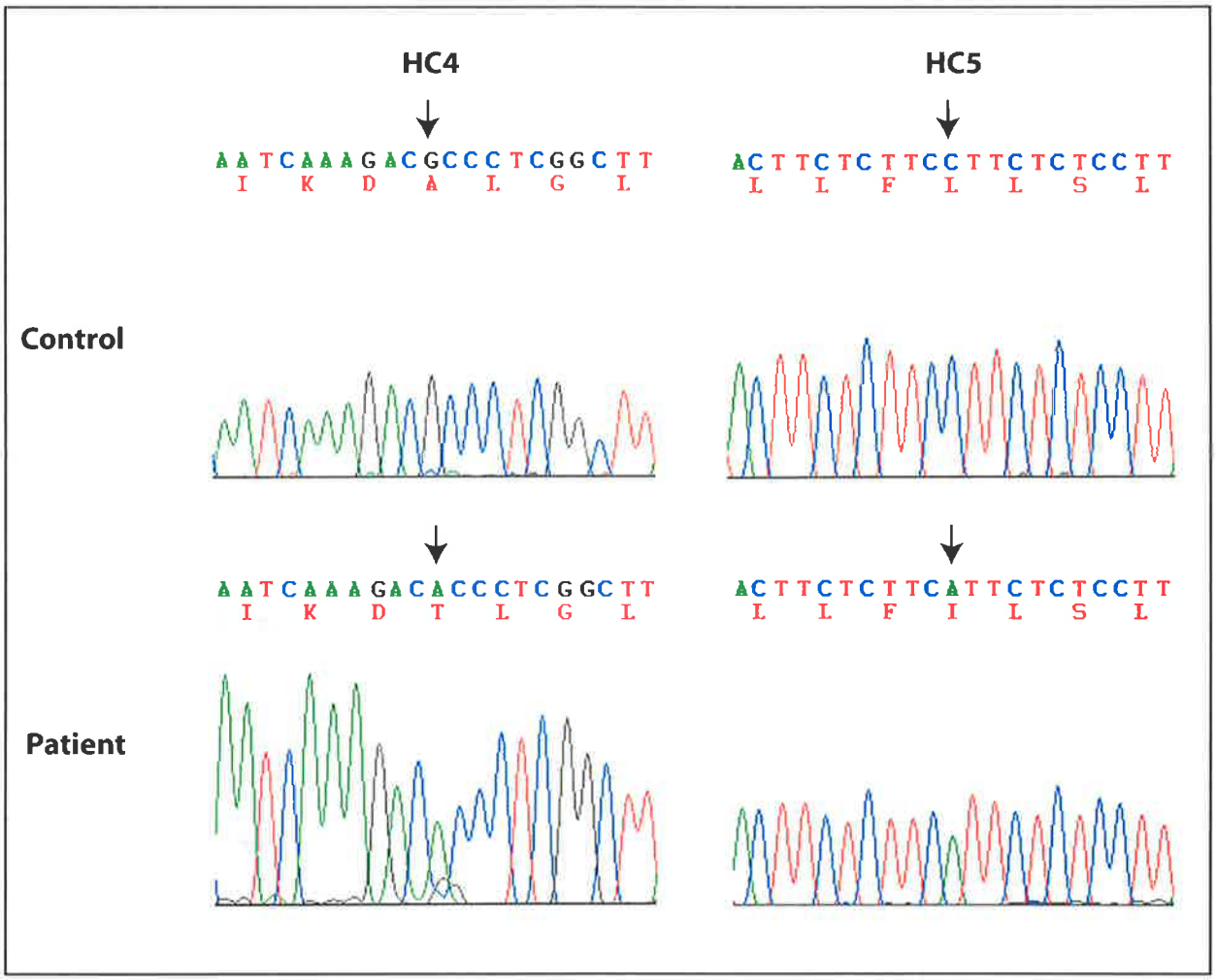

Figure 5.1

Sequence variation in *cytochrome b*

Cytochrome b sequences were obtained from HC4, HC5 and a control patient. Arrows represent the G15431A mutation coding for A229T and the C15452A mutation coding for L236I of HC4 and HC5, respectively. Sequencing was performed using the corresponding forward primer.

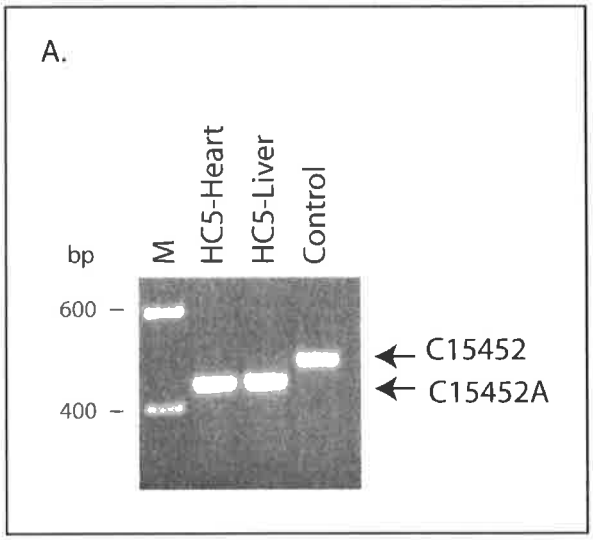

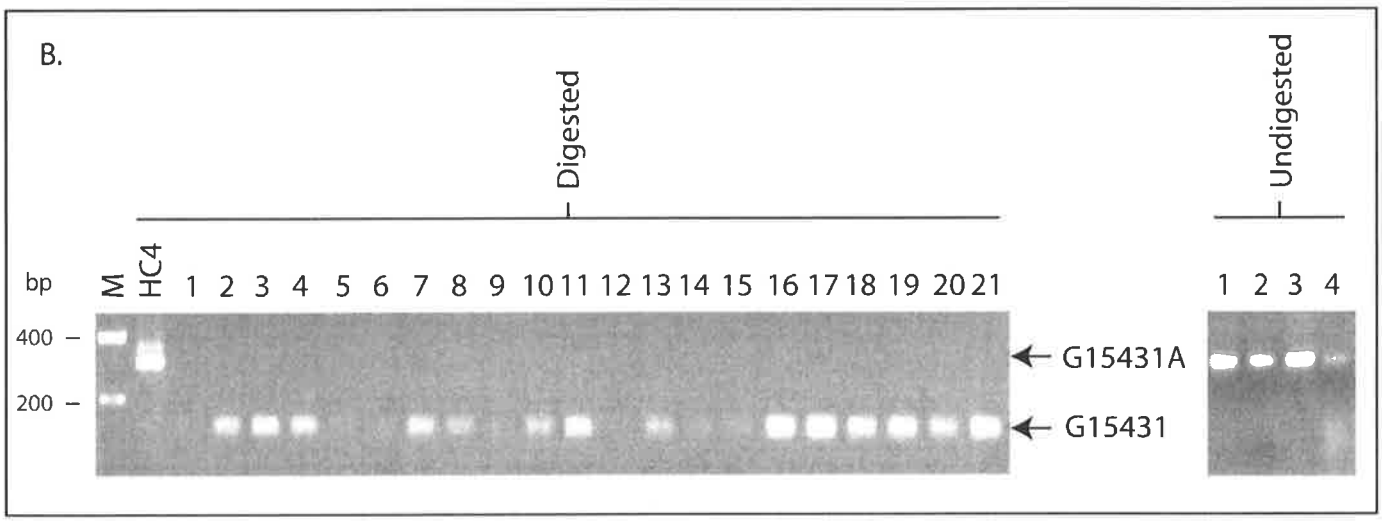

Figure 5.2

A. Quantitation of cytochrome b variation in HC5
Quantitation of the C15452A mutation in HC5 was analysed by *Nla*III digestion of the PCR product from NlaIII-CytB and CytB#6. Reduction in size of all amplified fragments indicates high levels of the mutation in both heart and liver but not in the control sample. Arrows indicate the bands corresponding to the C15452A mutation and wt (C15452) following restriction enzyme digestion, respectively. M refers to the marker lane.

B. Quantitation of cytochrome b variation in HC4
RFLP analysis of the G15431A mutation in HC4 was completed with *Bsa*HI digestion of *cytochrome b* fragment 3 and also from 21 control samples (1-21). Restriction of the fragments occurs in samples not harbouring the mutation and indicates the base change is only present in HC4. Arrows indicate the bands corresponding to the G15431A mutation and wt (G15431) following restriction enzyme digestion, respectively. Undigested controls of controls 1-4 are shown on the right to confirm detectable levels of DNA prior to digestion. M refers to the marker lane.

5.2.4.1 Growth assay.

To address the growth rate of the mutant OC line, 10^7 cells were seeded onto 10cm plates in the presence or absence of 100 µg/ml pyruvate and 50 µg/ml uridine. Cells were harvested from several plates at 24 hr intervals and counted to determine if the subsidised media influenced the noticeably slow growth phenotype. While test lines were not available for this experiment, multiple counts from numerous plates were unable to identify any substantial difference. This suggests that cytochrome c within these cells is normal, or at least functioning at a high enough level not to be detected by this assay (Fig 5.3).

5.2.4.2 Analysis of HCCS protein within the OC cell line.

To address the correct localisation of a number of structural proteins within the OC cell line, available antibodies were utilised for immunofluorescence analysis. Following growth on coverslips, cells were immuno-stained with mitochondrial-specific antibodies (Hccs, Tom20 and cytochrome c) and a microtubule-specific antibody (α-tubulin). Immunofluorescent analysis of these cells was unable to identify any discrepancies that would suggest an alteration to the localisation of these proteins (Fig 5.4A). Given that the first 48 amino acids of HCCS are necessary and sufficient to drive the protein to the mitochondrial IM space, no localisation changes would be expected from a variation outside of this region. That cytochrome c is also localised within the mitochondria suggests no major abnormalities of HCCS function.

Western analysis of protein extracts also shows that the protein is the same molecular size as in control cells, further inferring no post-translational variations in the HCCS protein (Fig 5.4B). Due to the lack of a control line for this patient, quantitation of the extracts was not performed and hence relative levels of HCCS/total protein can not be compared between the two samples. While these preliminary experiments suggest that the protein is adopting a normal function within the cell they are unable to provide conclusive support for normal expression levels of the gene. Further analysis of *HCCS* mRNA will be required to address any alteration of gene expression levels and altered splicing.

5.3 Summary.

This chapter has outlined the analysis of both the *HCCS* gene and the *cytochrome b* gene from available cases of OC that have no large deletions and/or translocations of the short arm of the X chromosome. No mutations were found in the *HCCS* gene; however, a number of patients harbouring variants of the *cytochrome b* gene were identified. While a number of these have been found to be non-coding and previously identified polymorphisms, two remain rather intriguing. The first is a C15452A substitution in HC5 that introduces an alanine at amino acid 236 in place of a leucine. This variation has previously been reported in a case of ischaemic cardiomyopathy and was suggested to be a pathogenic mutation based on the overall reduction of complex III activity by over 50% (Marin Garcia *et al*, 1996). Interestingly, this amino acid is not well conserved in other species, and is indeed an isoleucine in some cases (Fig 5.5). This reason as well as the recent structural prediction of cytochrome b have been cited in arguments against this mutation affecting the formation of the Coenzyme Q - cytochrome *c* reductase complex (Fisher & Meunier, 2001). L236 is located within a transmembrane region of the protein that is not involved with heme or quinone binding. Both of these regions are found to be essential for function in many studies of yeast mutants (Fisher & Meunier, 2001). It remains interesting, however, that this same mutation has now been identified in two separate cardiomyopathies. Furthermore, Marin Garcia *et al* (1996) observed this same mutation in 2 of the 42 controls tested that in each case also had the same reduction of complex III activity. While ischaemic cardiomyopathy is not usually associated with OC it is possible that either of these cases could have been mis-diagnosed.

The second mutation unique to this study was a G15431A alteration that encodes a relatively conservative amino acid substitution of A229T. Amino acid 229 is reasonably well conserved in all species with the presence of an isoleucine in most examples. While an alanine exists at this location in humans, a threonine is only noted in one case (Fig 5.4). This alteration occurs in the same transmembrane domain as the aforementioned case and accordingly, may not be expected to have any deleterious effects on the formation of complex III. However, that only one other species harbours a threonine at this position does not exclude a role for this variant in the presentation of OC.

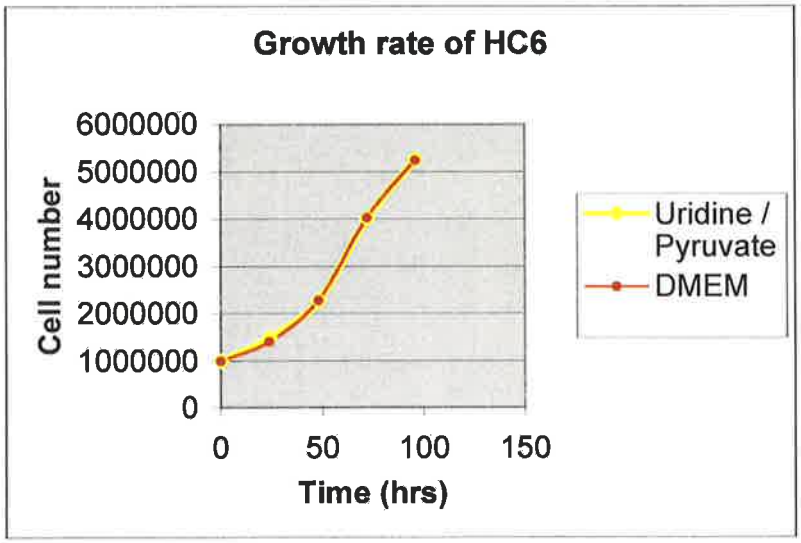

Figure 5.3

Growth rate of HC6 skin fibroblasts
1 X 10^7 cells of the HC6 skin fibroblast cell line were grown in normal DMEM (red line) or with DMEM supplemented with 50 µg/ml Uridine and 100 µg/ml Pyruvate (yellow line). Cells were collected at 24hr time intervals, stained with trypan blue and counted. The supplemented media had no affect on the HC6 cell line.

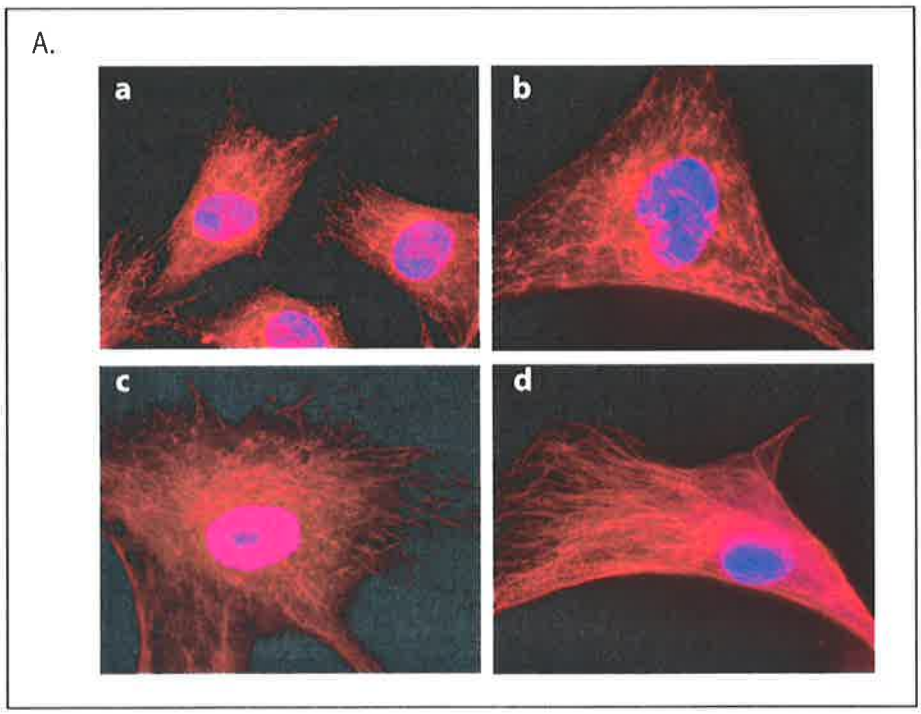

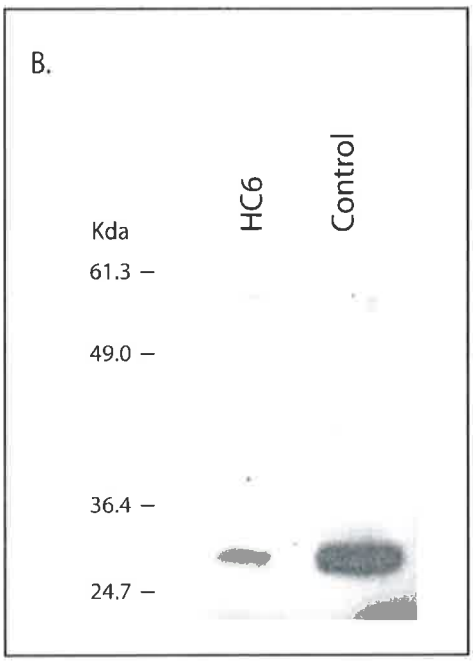

Figure 5.4

A. Immunofluorescent analysis of mitochondria proteins in the OC cell line (HC6)
Mutant cells from the OC patient were immuno-stained with either (a) Hccs, (b) Tom20, (c) cytochrome c or (d) α-tubulin (red). Nucleus has been stained with DAPI (blue).

B. Western analysis of HCCS in the OC cell line (HC6)
Whole cell protein extracts were obtained from the OC cell line and control human HeLa cells. 20µl of protein extract was subjected to SDS PAGE and transferred to nitrocellulose. Filters were treated with anti Hccs antiserum. Endogenous HCCS was detected in both samples at the same height.

Figure 5.5

Protein alignment of cytochrome b

Cytochrome b protein sequences were obtained from Genbank and aligned using the ClustalW program (Thompson *et al*, 1994). This diagram represents the first 350 amino acids of the proteins. Black boxes highlight complete conservation in over 75% of the species. Residues at which alteration in HC4 and 5 were identified are represented with an arrow. (*) A previously reported mutation identified in another case of OC (Andreu *et al*, 2000).

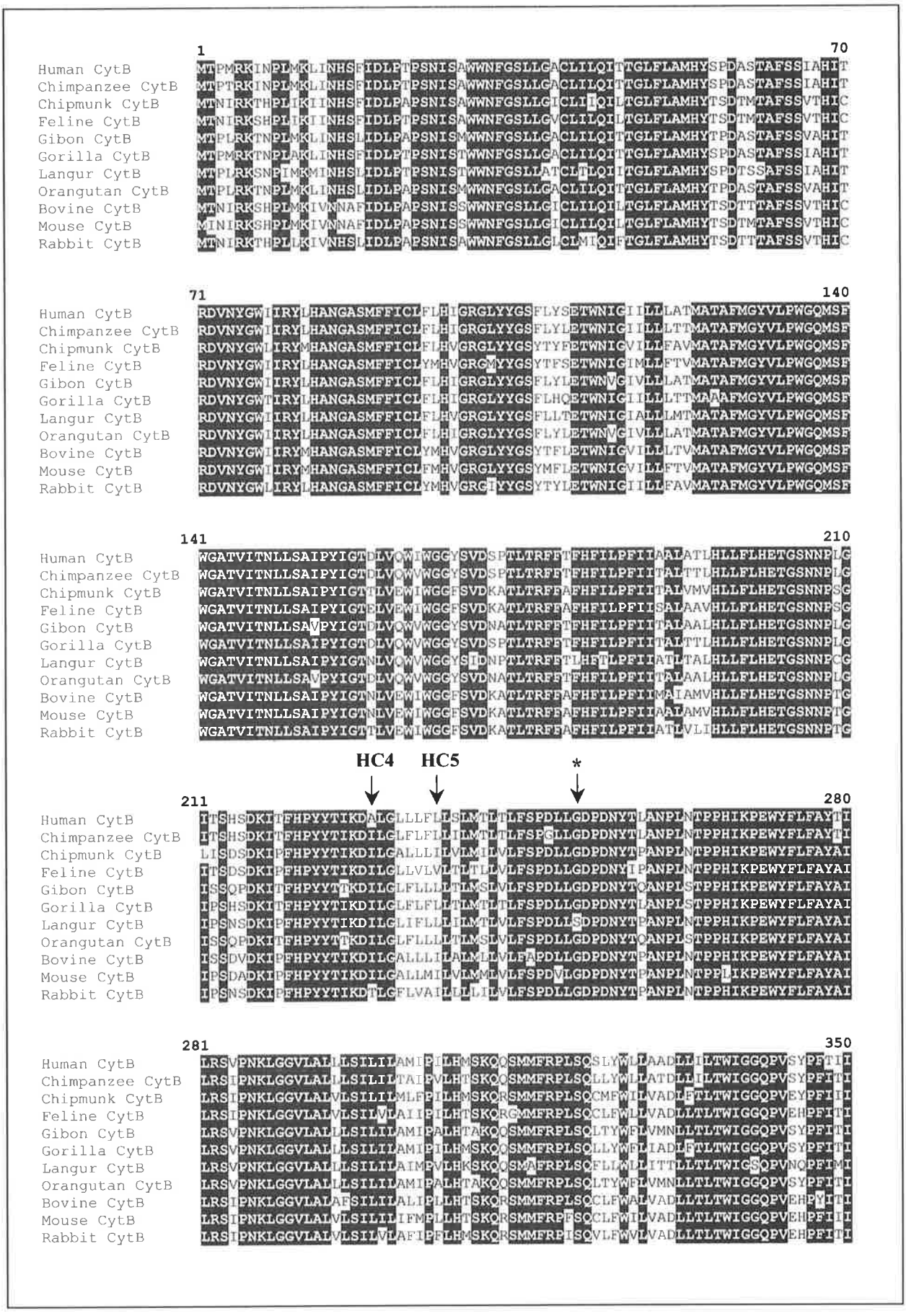
1
70
Human CytB
Chimpanzee CytB
Chipmunk CytB
Feline CytB
Gibon CytB
Gorilla CytB
Langur CytB
Orangutan CytB
Bovine CytB
Mouse CytB
Rabbit CytB
71
140
141
210
HC4
HC5
*
211
280
281
350

Both variants were analysed to detect levels of mutation heteroplasmy which is likely to have a major effect on the presentation and severity of the disorder (i.e. high levels of mutant mitochondria within a cell would be expected to present with a more severe phenotype). Heteroplasmic changes have previously been suggested to indicate pathogenic mtDNA mutations rather than simple polymorphisms (Andreu *et al*, 2000). The reasoning for this suggestion is based on the introduction of mutations post fertilisation as opposed to inheritance of a polymorphism that is more likely to be homoplasmic. While this argument remains very weak, familial members should be studied to address the mode of inheritance of both base changes. That low levels of heteroplasmy of the mutations have been revealed in both cases may suggest inheritance from their mother. In particular, the G15431A mutation was unable to be detected in any of the 21 control samples analysed, therefore suggesting that the coding change of A229T is not a common polymorphism. Screening of additional control samples will add further support to the suggestion that it may be a pathogenic mutation

Interestingly, none of the patients in this study were identified as harbouring the same mutation as that of the Andreu *et al* (2000) patient. In their case, mitochondrial respiratory chain deficiencies of complex III and IV were highlighted by enzyme assays completed on available patient samples. As the cases in the study presented here were obtained from deceased patients identified at necropsy these same enzyme assays are not possible. To overcome this potential problem, available relatives should be analysed to address if these mutations are inherited. If indeed identified, informative respiratory enzyme assays could also be completed.

With the cases presented here and that of the Andreu *et al* (2000), three separate mutations have now been highlighted as potential pathogenic mutations in the presentation of OC. As mentioned previously, the mitochondrial respiratory chain is composed of 5 multi-enzyme complexes encoded by the mitochondrial genome and the nuclear genome that facilitate the production of energy through the transfer of electrons to oxygen. Deficiencies in the respiratory chain can therefore occur through mutation in either genome that could potentially present with similar clinical features (see Shoubridge, 2001 for recent review). That mutations within *cytochrome b* have been identified in only 3 of the 7 patients further supports the notion of genetic heterogeneity in OC. Interestingly, deficiencies of complex III

and IV have now been reported in several cases. With the identification of mutations in *cytochrome b*, the only mitochondrial-encoded sub-unit of complex III, this implicates a respiratory deficiency of these complexes as the underlying genetic fault in all cases.

Complex III is composed of 11 polypeptide sub-units (one mitochondrial encoded), while complex IV is composed of 13 sub-units (three mitochondrial encoded). If indeed deficiencies in these complexes allow the presentation of OC, then mutations in any of the subunits could conceivably give rise to the disorder. Furthermore, any of the enzymes required for correct targeting and post-translation modifications could also be involved. With the recent confirmation of HCCS mediating maturation of cytochrome c, further screening of *HCCS* may be warranted in other female cases of OC that also show MIDAS related features.

With respect to the involvement of *HCCS* in the presentation of OC, several explanations can be put forward as to why no mutations have been identified in this study. As mentioned previously, 3 of the 4 patients not found to have *cytochrome b* mutations have been diagnosed with OC but do not actually present with any other X-linked related features. However, because of the presentation with the characteristic MIDAS facial lesions, the patient of Bird *et al* (1994) which has no detectable deletion over 100kb on the X chromosome is likely to have a defect within the proposed critical region. Due to the possibility that the MIDAS syndrome is a multigene disorder, it is plausible that this patient may have a small deletion under 100kb in size, yet still affect more than one gene in this region. Indeed, all other cases of MIDAS syndrome result from large chromosome disruptions at Xp22.3. In the case that there is a deletion of the region covering *HCCS*, amplification would still occur off the normal X chromosome, hence explaining the lack of detectable sequence change in this patient. Indeed, the paucity of male patients with OC without other MIDAS features is consistent with removal of the only copy of *HCCS* in males (i.e. embryonic lethality). Affected females, who have two copies of the X chromosome but only one functional copy of the affected gene, may then allow the characteristic OC phenotype (i.e. the aggregation of unstructured cells with excess mitochondria) to arise as a result of random X-inactivation in the heart of affected patients. Likewise, the phenotype among female patients could also be explained via an Xp mosaic mutation that arises after fertilisation.

As two male patients have been analysed in this study (HC1 and HC6), OC in either case may not be expected to arise from an X-linked mutation; rather, they may result from a related deficiency within the mitochondrial respiratory chain. As the sibling of HC1, HC2 might also not be expected to harbour a mutation within *HCCS*. While no mutations were identified in the mitochondrial *cytochrome b* gene in either of these siblings, another deficiency of the respiratory chain that is also encoded within the mitochondria could potentially be involved. For example, several other components of complex IV are also encoded in the mitochondrial genome and may represent an ideal target to begin mutation analysis. Although extremely unlikely in siblings, a mutation that occurred in the nuclear genome after fertilisation could also give rise to this phenotype through genetic mosaicism.

Due to the small number of patients analysed in this study, no conclusive results have been obtained regarding the role of HCCS in the presentation of OC. Further studies on patients that have been diagnosed with both OC and the aforementioned X-linked features of MIDAS syndrome need to be completed. Ultimately, these studies will allow us to elucidate any role that this gene may have in the pathogenesis of OC.

Protein alignments of the CTS family highlight a number of regions in which pathogenic point mutations could conceivably occur. As detailed in earlier chapters the amino terminus of HCCS is not well conserved apart from the CPX heme binding motif found in all species. Heme binding motifs are found to be essential for the correct functioning of the holocytochrome c-type synthases in yeast as removal renders the remaining protein non functional. In addition, the carboxy terminus of the protein encodes the characteristic catalytic domain of the enzyme that is largely conserved. Mutation to any of these conserved residues would also be expected to have drastic effects on protein function.

Given that X-linked cases of OC with associated MIDAS features are only expected to be female, a mouse KO may be the most direct way to detect any role that *HCCS* may have in the presentation of the disorder. Indeed, the conditional removal of *Hccs* has been initiated in the following chapter. Mouse models would be an ideal way to also analyse the pathogenesis of the *cytochrome b* mutations presented in this study. However, the uncertainty of mitochondrial genetics in mice and the inability of targeted homologous recombination in the mitochondrial genome make this impossible at present. Indeed, this would also be influenced by the fact that murine cytochrome b has alternative amino acids at

these same positions (Fig 5.4). As neither of these amino acids are conserved in yeast, functional studies in this organism are also not possible (Esposti *et al*, 1993).

A remaining, although perhaps less likely possibility for involvement of *HCCS* in OC, might involve the trinucleotide repeat identified within exon 1 of human *HCCS*. Trinucleotide repeat expansions have been well documented in a number of disorders, including Myotonic Dystrophy, Spinocerebellar Ataxia, Fragile-X Syndrome and Huntington's Disease (Usdin & Grabczyk, 2000). The mechanisms by which these disorders occur vary immensely depending on the location of the repeat. However, in all cases the repeat is susceptible to expansion that eventually leads to the disease phenotype. While unlikely, it is interesting to speculate that a similar mechanism could perhaps lead to disruption of the *hHCCS* gene. Indeed, the *HCCS* repeat is mildly polymorphic and is at the lower end of the range of repeat sizes that have the capacity to expand (Lenzemeier & Freudenreich, 2003).

Chapter Six: Production of a *Hccs* conditional mouse KO.

6.1 Introduction.

OC is a severe disorder that morphologically resembles the well-characterised mitochondrial myopathies. Indeed, the finding of decreased activity of respiratory complexes III and / or IV in a number of cases support the conclusion that a primary respiratory chain defect underlies the disorder. Interestingly, OC presents predominantly in females and often results in sudden infant death, which has led to the hypothesis that it is an X-linked embryonic male lethal disorder (Bruton *et al*, 1977).

Giving some insight to the possible underlying genetic fault in OC was the identification of a patient that co-presented with the X-linked (Xp22.3) deletion defined disorder MIDAS syndrome (Bird *et al*, 1994). Retrospective investigations add further support for the Xp location of the OC causative gene with the finding that over 10% of patients for which a sole diagnosis of OC was made also present with MIDAS related features; whilst the same proportion of MIDAS patients also show a dilated cardiomyopathy consistent with OC. While Andreu *et al* (2000) have reported a mutation in the *cytochrome b* gene from an isolated case of OC, the disorder is likely to be heterogeneous as this has not been found in all cases.

Correlations between various X chromosome abnormalities and patient phenotypes have been used to delineate a small chromosomal segment that is likely to contain the causative gene(s) for the MIDAS (and therefore OC) phenotype. Within this region we have identified an expressed sequence sharing ~60% amino acid sequence similarity (35% identity) to the *S.cerevisiae* enzyme, CYC3 (holocytochrome *c* synthase: HCCS).

As highlighted in the previous chapter we have been unable to identify any definitive mutation in the *HCCS* genomic region of available OC patients. However, there are several explanations for the lack of detectable HCCS abnormalities. The most likely means of determining the role of HCCS, if any, in the pathogenesis of OC may therefore be through gene targeting in mice.

Due to the similar physiology and genome size of mice and humans, the mouse is an ideal model organism to study the pathogenesis of many human mutations. The ability to

engineer specific germline mutations in the mouse genome with the use of techniques such as homologous recombination and ES stem cell culture make it possible to address specific alterations in any gene. Furthermore, with recent advances in the understanding of developmental pathways and cell differentiation, ES stem cells also offer an ideal model for studying gene function *in vitro*.

Traditional gene silencing requires the removal of an entire gene or coding exon that results in a null allele. This technique, however, is unable to be utilised for genes that are essential for organism survival such as those in the respiratory chain, as complete removal of these genes is usually incompatible with embryonic development and viability (Li *et al*, 2000).

Recent advances in mouse KO's have seen the introduction of recombinases to produce conditional silencing of target genes in a temporal and spatial manner. Two systems are currently used in mice: cre / loxP and flp / frt. The 38-kDa protein encoding cre recombinase was identified in coliphage P1 and is able to catalyse recombination between two similarly oriented loxP sites without the need for any other co-factors (Sauer, 1998). In comparison, flp recombinase (45-kDa) is able to recognise and promote recombination between two similarly oriented frt sites also without the requirement of additional co-factors (Fiering *et al*, 1993). Given the higher efficiency of the cre / loxP system compared to the flp / frt system, most current conditional KO's are designed to utilise cre / loxP. Both approaches require the production of two independent mouse lines; one with the gene of interest being surrounded either partially or in full by loxP sites (referred to as a floxed gene) or frt sites, and another harbouring the recombinase under a cell type specific promoter. Following crossing of the two lines, the gene will only be removed in the regions expressing the recombinase while expression of the gene will remain unaffected in all other tissues.

Both loxP and frt sites are composed of unique 34 bp sequences that contain two 13 bp inverted repeats separated by an 8 bp core sequence conferring orientation. When placed in the same orientation, cre and frt are able to recognise the sequences and catalyse recombination between them, thus removing the intervening sequence. Alternatively, when the sites are in opposing orientations the recombinase is able to mediate inversion of the sequence.

6.1.1 Considerations for experimental design.

Gene targeting is achieved by the design of a vector harbouring DNA homologous to the target sequence with the inclusion of selectable markers to enable detection of loci that have undergone integration into the host genome by homologous recombination. The targeting vector is introduced into an ES cell line by transfection (usually electroporation) and homologous recombinants selected by PCR or Southern analysis of G418[11] resistant colonies. The targeted cells are then injected into mouse blastocysts where they are inserted into the inner cell mass thus contributing to the animal proper. The resulting chimeric animals are then bred to generate mouse lines homozygous at the target allele (see Melton, 1994 for review).

Targeting vectors are typically designed to allow homologous recombination by replacement or insertion (see Bronson & Smithies, 1994 for review). Replacement vectors are preferred for conditional gene silencing as minimal changes are made to the targeted locus. Prior investigations by many researchers have identified a number of parameters affecting the efficiency of homologous recombinations. Initial experiments found an increase in recombination with the use of isogenic sequence to the ES cells (van Deursen & Wieringa, 1992; Zhou *et al*, 2001. However, recent unpublished findings suggest that non-isogenic sequences also have a similar recombination efficiency (Dr F. Koentgen, Ozgene, Western Australia) provided the length of homology between the target vector and target gene is sufficient. While the use of as little as 0.5kb has been reported, a minimum of 2kb is suggested on each arm for successful recombination (Hasty *et al*, 1991). Moreover, Deng & Capecchi (1992) also reported the exponential dependance of targeting efficiency on the homology length.

Most ES cells are derived from male mice of a 129 background for reasons largely based on coat colour genetics. Male ES cells have the advantage of allowing large numbers of progeny to be produced from a single animal composed of these cells, hence, decreasing the time to produce and detect germline transmission. Many parameters have also been identified to affect germline transmission of ES cells, of which increased passage number[12] is possibly the most important (Nagy *et al*, 1990). Also of importance is the decrease in efficiency

[11] Neomycin expression in cells confers resistance to G418.
[12] Passage number refers to the number of times the derived ES cell line has been trypsinised and replated.

associated with chromosomal abnormalities (Suzuki *et al*, 1997) that can be detected by karyotyping cells prior to injection.

As *Hccs* is located on the X chromosome, traditional gene silencing would therefore remove the only functional copy of the gene. Functionally, the removal of Hccs would be predicted to decrease if not abolish the mature form of cytochrome c within the cell. A recent mouse model in which cytochrome c has been removed by creation of a null allele has shown survival until only E10.5 (Li *et al*, 2000). A similar outcome might therefore be anticipated with Hccs, thus necessitating the use of a conditional approach to model the deficiency of this gene.

The high level of overall conservation between human and mouse HCCS enzymes (85% identity) supports the use of the mouse as a potentially informative model system in which to study the functional role of this enzyme in cardiac physiology. The work in this chapter has involved the production of a mouse line harbouring a floxed *Hccs* allele with the goal of addressing the role, if any, of this gene in the pathogenesis of OC associated with the MIDAS phenotype. Supporting the essential role of this protein, preliminary attempts to remove *Hccs in vitro* have been unable to allow isolation of viable cells.

6.2 Results.

6.2.1 Isolation of Hccs genomic clones.

Toward the goal of constructing a tissue specific mouse knock out of Hccs, two positive phage clones (λ1 and λ13) were isolated from a mouse genomic library prior to the initiation of this project (Schwarz, 1997; Schwarz & Cox, 2002). The mouse genomic library used for this screening was constructed with genomic DNA extracted from a male 129 strain that has successfully been used in previous gene knockouts (T.Cox, personal communication). Partial restriction analysis of each clone was completed using various combinations of *Eco*RI, *Pst*I, *Sal*I and *Xba*I. Following Southern analysis with corresponding human exons (all with high homology to mouse) and various *Hccs* cDNA fragments, these digestions consequently revealed that both phage clones were in fact distinct from each other. The entire gene was encoded within λ13 that spans approximately 10-11kb of the genome. In

contrast, the λ1 clone encoded only exon 7 of the gene and likely spans approximately 10-15 kb further 3′ of λ13.

At the time of starting this project the mouse genome project was not underway so the genomic sequence of the corresponding region was unavailable. To therefore identify further restriction sites that might have been useful in constructing a targeting vector, restriction analysis was completed with various combinations of *Xho*I, *Spe*I, *Sal*I, *Nhe*I, *Eco*RI, *Nde*I and *BamH*I. Southern analysis with human exons and various *Hccs* cDNA fragments allowed precise positioning of exons within the map (Fig 6.1).

To fascilitate the production of a 5' probe for screening of homologous recombinants in later sections (see section 6.2.4.2-1), a 600bp *Nco*I / *Nsi*I fragment of the EST #44663 that contained the 5' most region of *Hccs* cDNA was used to screen a C57BL/6J female mouse BAC library. This fragment contains cDNA that maps further 5' to λ13 and was expected to allow detection of genomic clones containing this region. The 600bp fragment was first analysed by Southern analysis on digests of mouse genomic DNA. As only single bands were detected in each of the digests the fragment was therefore sent to Dr P. Farley (Murdoch Children's Research Institute, Melbourne) for use as a probe. Following standard protocols (Kim *et al,* 1994), this screen identified 12 positive BAC's that were recovered and amplified. PCR with primers located within exons 3 and 4, respectively, were utilised to identify two of these clones that harboured the *Hccs* genomic interval, BAC#266F20 and BAC#348M22, respectively (see Fig 6.1). Both BAC's were digested with *Eco*RI and found to have similar banding patterns suggesting that both were probably derived from the same locus. Further digestion with various enzymes and Southern analysis with regions of *Hccs* cDNA conclusively showed that these BAC's extended sequence further 5' than λ13.

6.2.2 Characterisation of Lambda and BAC clones.

During the course of this project the entire sequence of the *Hccs* locus was sequenced with primers designed within the genomic region (see Fig 6.3). This sequence demonstrates that the murine *Hccs* gene consists of seven exons (six coding exons and one 5' untranslated exon) spanning approximately 11 kilobases (Fig 6.2). The ATG start codon was located within exon 2 and was preceded by a site that is consistent with Kozak's consensus

sequence (Kozak, 1984). The TAA stop codon was identified within exon 7 while most exon-intron boundaries conform well to the consensus splice junction sequences (Aebi *et al,* 1986) (Table 6.1). Interestingly, this structural organisation is comparable to that determined for the human gene (Van den Veyver *et al,* 1998) with the only notable change being the considerable size difference of intron 3.

To provide confirmation of the chromosome localisation of the *Hccs* gene, PCR analysis of the BAC clones was completed with primers designed to amplify various exons of the murine homologs of human genes that flank *HCCS* and *Hccs* (Prakash *et al,* 2000). Amplification products were identified for exons located at the 3' end of the *Arhgap6* gene that had previously been localised to band 73 of the murine X chromosome (Van den Veyver *et al,* 1998). PCR with primers designed to exons of the *Amelogenin* (*Amg*) gene that, in humans, resides within the first intron of *ARHGAP6* (Kayserili *et al,* 2001) did not show any amplification from BAC's (detailed in section 6.2.4.2-1) but did, however, from genomic controls. Likewise, specific primers to *Midline 1* (*Mid1*) that is located over the pseudo-autosomal boundary distal to *Arhgap6* and *Amg* (Perry & Ashworth, 1999), also failed to amplify this gene sequence from the BAC clone. Taken together, these data indicate that in mice *Hccs* is also located between *Mid1* and the 3' region of the *Arhgap6* gene, and that *Hccs* and *Arhgap6* are convergently transcribed from band 73 on the mouse X chromosome.

Exon		5' Splice donor		Intron		3' Splice acceptor	
No.	**Size (bp)**	**Exon Seq**	**Intron Seq**	**No.**	**Size (bp)**	**Intron Seq**	**Exon Seq**
1	75[a]	AGTCGGCGAG	gtgacttggg	**1**	524	gctttggcag	CTGGGTATTT
2	153	CAAAGGAAAG	gtaacttgtc	**2**	2292	ataatttcag	GCTGTCCAGT
3	152	TTCAAACCTG	gtaatccacc	**3**	291	tattctatag	ATGCCACCAC
4	149	TACGGAAAGG	gtgagtgaac	**4**	824	tctttcttag	GTGGAAGTGG
5	120	TTCATGCTCA	gtaagtatgt	**5**	1927	gcattttcag	TGAGTGTCCT
6	87	CCTGGATGGG	gtaagtgtca	**6**	565	ttcattacag	GTATGAATTG
7	1478[a]						

Table 6.1 Intron - exon boundary sequences and sizes of the murine *Hccs* gene. (a) Sizes of exon 1 and 7 have been determined from the comparison of available genomic and cDNA sequences. Note that the transcriptional start site has not been experimentally determined.

Figure 6.1

A. Restriction enzyme map of λ13 and λ1
Genomic lambda clones harbouring the *Hccs* gene were identified from a mouse 129/Sv library (946308). Southern analysis on various combinations of restriction enzymes probed with human exons were used to position the corresponding murine exons within the map. λ13 contains all of the 7 exons while λ1 contains only the last exon. Cloned *Eco*RI fragments used for the construction of HccsKO#1 are shown below λ13. Restriction sites contained in the vector are highlighted in bold.

B. Diagrammatic representation of the *Hccs* genomic interval
The entire genomic locus of *Hccs* has been constructed from the partial restriction maps of both λ13 and λ1. For clarity, not all restriction sites have been represented in this figure. In all maps open boxes represent 5' and 3' UTRs while shaded boxes represent coding regions of *Hccs*. B, *Bam*HI; Sa, *Sac*I; Sp, *Spe*I; E, *Eco*RI; Xb, *Xba*I; Xh, *Xho*I; H, *Hin*dIII; Nh, *Nhe*I; No, *Not*I; K, *Kpn*I; P, *Pst*I; S, *Sal*I; Nd, *Nde*I.

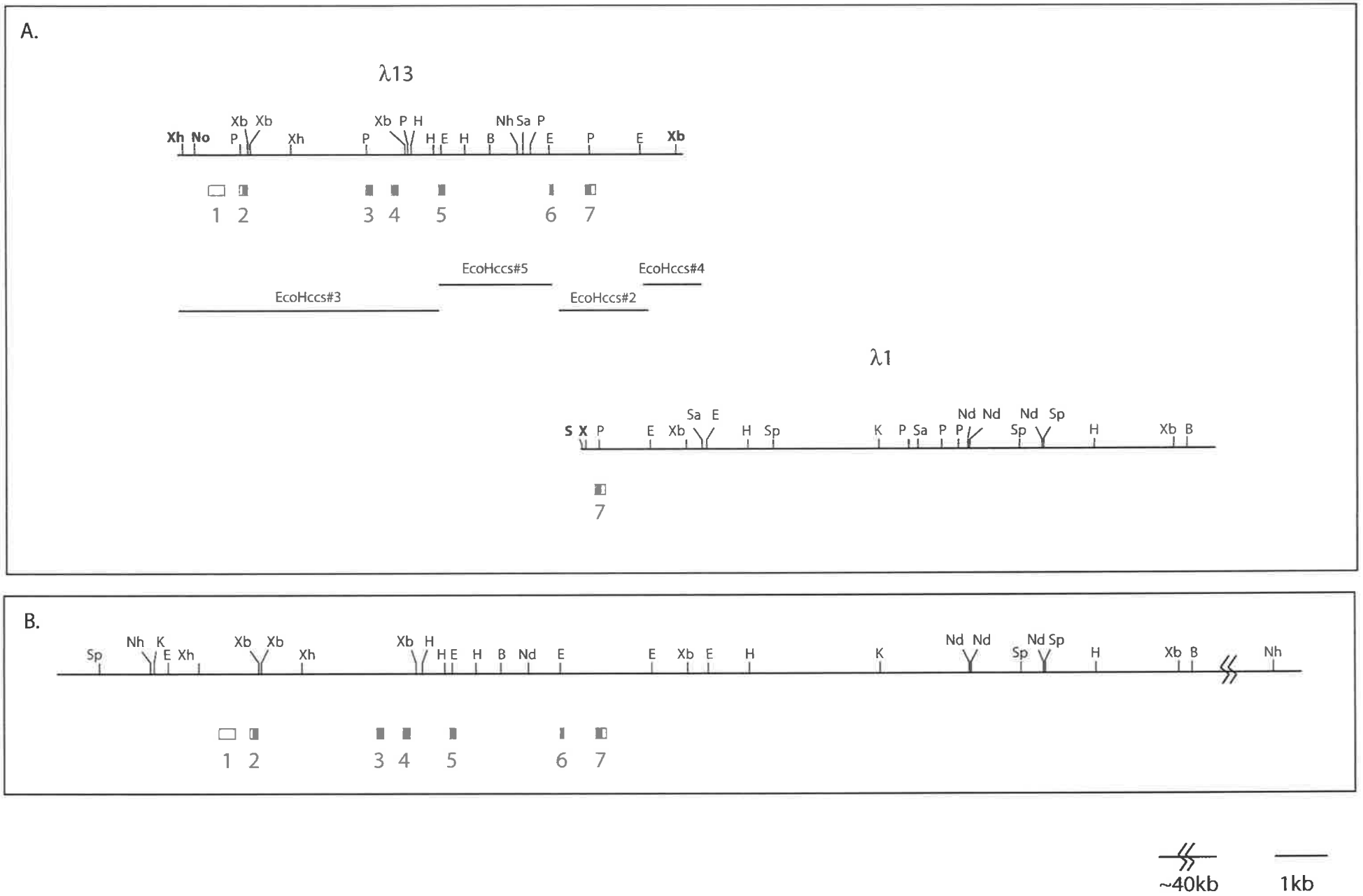
A.
λ13
Xh No P Xb Xb Xh P Xb P H H E H B Nh Sa P E P E Xb
1 2 3 4 5 6 7
EcoHccs#5
EcoHccs#4
EcoHccs#3
EcoHccs#2
λ1
S X P E Xb Sa E H Sp K P Sa P P Nd Nd Sp Nd Sp H Xb B
7
B.
Sp Nh K E Xh Xb Xb Xh Xb H H E H B Nd E E Xb E H K Nd Nd Sp Nd Sp H Xb B Nh
1 2 3 4 5 6 7
~40kb
1kb

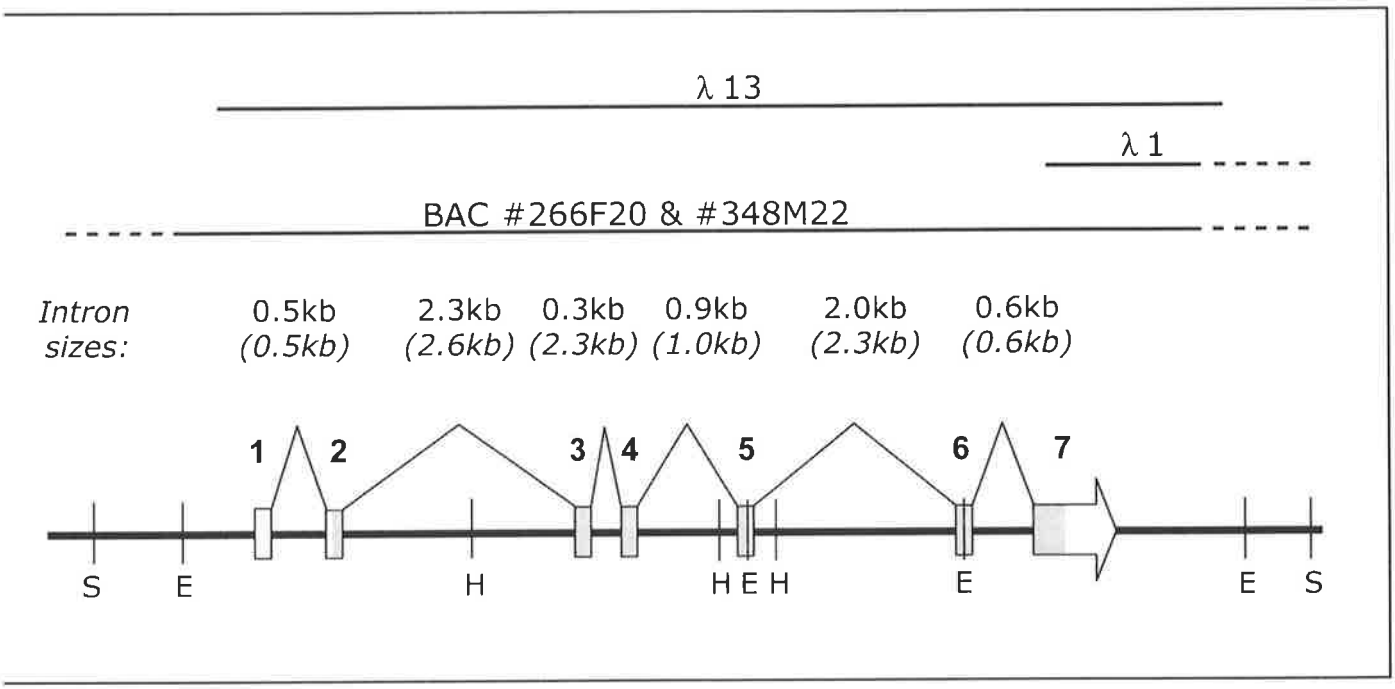

Figure 6.2

Structural organisation of the murine *Hccs* gene

Overlapping λ phage (λ13 & λ1) and BAC clones (BAC#266F20 & BAC#348M22) were isolated and used to generate a restriction map of the mouse *Hccs* gene. E, *Eco*RI; S, *Spe*I; H, *Hin*dIII; B, *Bam*HI. Solid lines represent the region of the murine locus covered by the clones. Dashed lines indicate that the extent of coverage of the respective ends of the relevant clones was not precisely determined. Relative sizes and positions of exons are indicated as boxes. Unshaded and shaded regions of the boxes refer to untranslated and coding sequence, respectively. The approximate sizes of the murine *Hccs* introns are indicated. For comparison, the sizes of the human introns are shown in brackets beneath the respective murine intron sizes.

6.2.3 ES cells for homologous recombination.

For the purposes of producing targeted ES cells, available stocks of the W9.5 cell line were initially chosen (Department of Biochemistry, Adelaide University). W9.5 ES cells are a feeder dependent adherent cell line that were importantly derived from a 129/Sv strain (isogenic to DNA library). These cells had been used previously within the Department and had successfully formed high percentage coat colour chimeras that subsequently colonised the germline (Tim Sadlon, personal communication). As the cells harbour no deletions or selection markers, and are susceptible to low levels of Geneticin (G418), the *Neomycin* gene under the control of the phosphoglucokinase (pgk) promoter was chosen as a positive selection marker for the following experiments. Likewise, the *Thymidine Kinase* gene under the expression of herpes simplex virus (hsv) that confers cell death in the drug 1-(2-deoxy 2-fluoro-B-D-arabinofluranosyl)-5-iodouracil (FIAU) was also employed as a negative selection marker to decrease the selection of flase positive ES colonies. Both of these markers have been used routinely for KO experiments with minimal effect on germline transmission (Colbere-Garapin *et al*, 1981; Borelli *et al*, 1988).

6.2.4 Construct design for removal of exon 3 and 4 of Hccs.

The detailed restriction map produced above was used to design a cloning strategy to insert the loxP sites, positive Neomycin selection marker (*Neo*^{r}) and negative Thymidine Kinase selection marker (*TK*) within and around the *Hccs* gene. Both selection markers and loxP sites were provided in the p18 vector constructed in the pBS KS$^+$ backbone kindly donated by Dr D. Pennisi (Centre for Molecular and Cellular Biology, University of Queensland). The markers and recognition sites in this vector had previously been used for a conditional KO (Andras Nagy, personal communication). A vector with only *Neo*^{r} surrounded by loxP sites (ploxPNeo) was also obtained from Dr D. Pennisi. To identify further restriction sites, both ploxPNeo and p18 were sequenced with vector primers and marker specific primers designed to sequences downloaded from the National Centre for Biotechnology Information (NCBI) website.

Over the course of this project a number of targeting constructs have been produced in attempts to obtain homologous recombination in ES cells. Each construct was made with current suggestions for increased efficiency of homologous recombination in mind. Initially,

exon 3 and 4 were chosen to be targeted as excision of these coding exons upon cre expression would remove the CPX heme binding motifs of Hccs. Furthermore, this deletion would also create a frame shift in the remaining ORF that introduces a premature stop codon in the remaining mRNA if produced. As the mRNA from this deletion does not contain any of the regions essential for gene function, this design was expected to abolish any function in tissues expressing cre and hence would be expected to show a phenotype. To keep the targeting construct at a manageable size for production in pBS KS^+, this design included the *Neo*^{r} gene between exon 2 and 3 and the *TK* gene at the 5' end of the construct (Fig 6.3). The orientation of the *Neo*^{r} was placed in the opposite transcription orientation to *Hccs* as this was suggested to reduce interference of exon splicing (Nagy, 1996). The negative selection marker was placed at the 5' end of the construct as the 5' homology arm was the smaller region for recombination to occur (see Fig 6.3).

For the purposes of these experiments a mouse line expressing cre recombinase from the Nkx2-5 promoter was identified in the literature and obtained from Dr R. Harvey (Victor Chang Research Institute, New South Wales). Nkx2-5, a homologue of the Drosophila *tinman* gene (Bodmer, 1990), is expressed in early cardiac progenitor cells before cardiogenic differentiation. Expression is also seen in pharyngeal endoderm, tongue, spleen, and the distal stomach (Lints *et al*, 1993). As Nkx2-5 is the earliest known marker of the cardiac lineage it is likely that it is regulated in direct response to signalling pathways activated by cardiogenic inducers (Schwartz & Olsen, 1999). While expression extends to other regions apart from the developing heart, the use of cre expression from this promoter was expected to be useful in addressing the role of Hccs in the presentation of OC. In contrast, the use of cardiogenic inducers that are expressed in a wide range of cells (such as those encoded by the BMP family) may remove the floxed gene in multiple regions and affect the extent of conclusions that could be drawn from these experiments.

6.2.4.1 Generation of a targeting construct for removal of exon 3 and 4 of Hccs.

To facilitate the production of floxed *Hccs(3-4),* the λ13 clone was digested with *Eco*RI and sub-cloned into pBS KS^+. The resulting fragments were then excised and probed with exons from human *HCCS* to identify clones containing useful fragments. This resulted in the identification of 4 separate fragments labelled EcoHccs#2-5 containing all the exons of

Figure 6.3

HccsKO#1 targeting strategy

A partial restriction map of HccsKO#1 details all of the sites used to construct the vector. Enzymes separated by – were cloned together to remove both restriction recognition sites. Thick lines in the targeting construct (top) indicate genomic sequence and thin lines indicate vector backbone. Green arrow heads show loxP sites with their relative orientation. Both *hsvTK* and *pgkNeo*^{r} have been inserted in the opposite transcriptional orientation of *Hccs* to minimise the use of potential splice sites within *Neo*^{r}. Restriction enzyme digestion with *Sal*I (S) was devised to linearise the construct while *Spe*I (Sp) was used for screening both 5' and 3' external probes (relative positions indicated on sequence below vector). Relative fragments used for the construction of the targeting vector are indicated below the construct. Primers designed to various regions within the vector are represented below the target construct. The position of primers allowing introduction of the 3' LoxP site to be confirmed are also shown (mHCCS#3 and mHCCS#4). Homologous recombination in both homology arms would yield floxed *Hccs* with the inclusion of *Neo*^{r} between exon 2 and 3. Addition of cre recombinase to the floxed allele would result in recombination between the two loxP sites that effectively removes CPX heme binding motifs and creates a frame shift in the remaining mRNA that also introduces a premature stop codon. In all maps open purple boxes represent 5' and 3' UTRs while purple shaded boxes represent coding regions of *Hccs*. Red boxes indicate a frame shift and introduction of a premature stop codon. B, *Bam*HI; Sa, *Sac*I; Sp, *Spe*I; E, *Eco*RI; Xb, *Xba*I; Xh, *Xho*I; H, *Hin*dIII; Nh, *Nhe*I; No, *Not*I; K, *Kpn*I; P, *Pst*I; S, *Sal*I; Nd, *Nde*I.

Targeting construct (HccsKO#1)

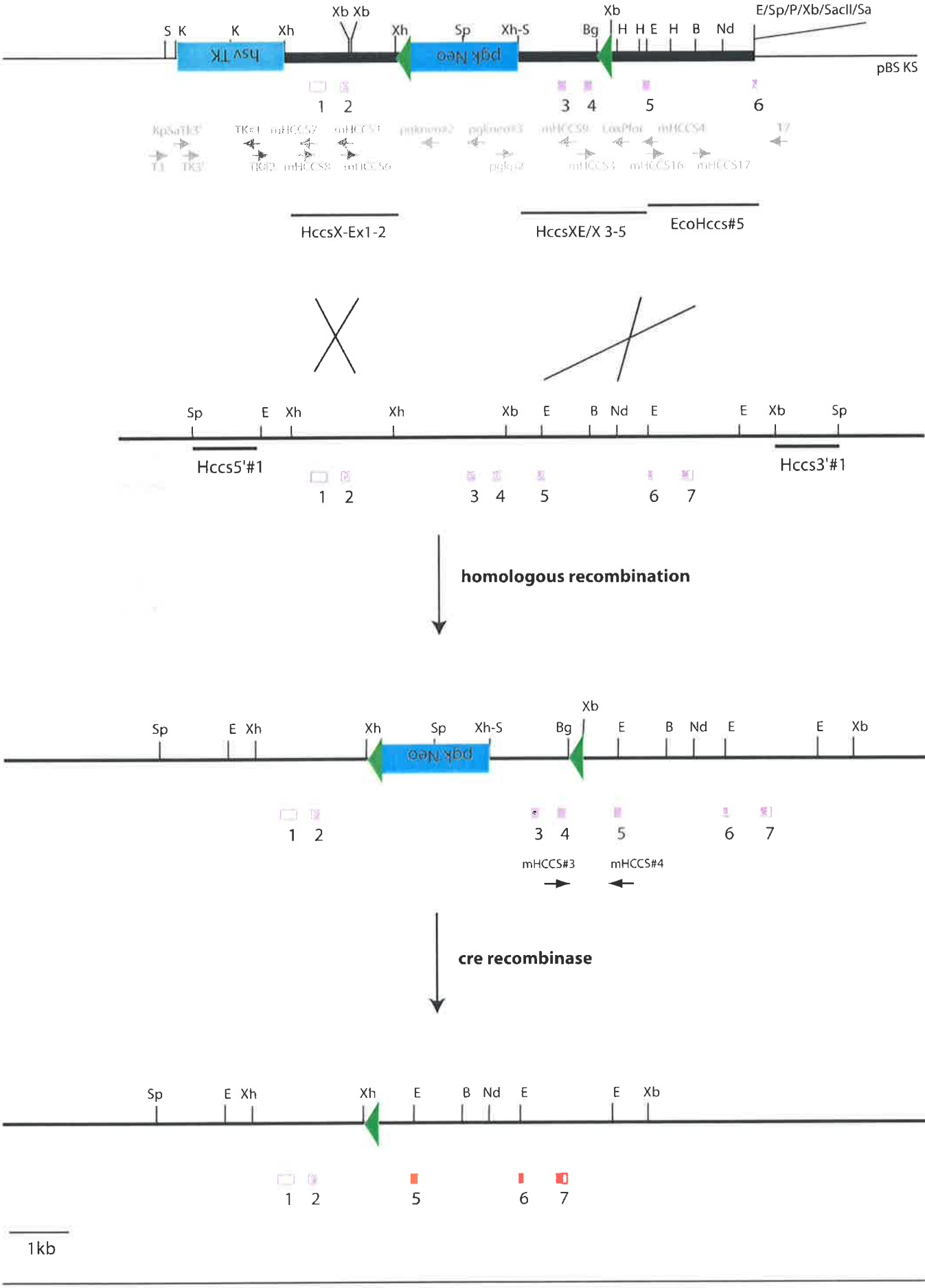

Hccs (Fig 6.1). The vector clones containing exons 1-5 (EcoHccs#3) were digested with *Xho*I to identify a clone with the correct orientation for use in subsequent steps. Following removal and re-cloning of the *Xho*I fragment encoding only exons1-2 into pBS KS^+ for later use, the remaining DNA from the EcoHccs#3 clone was re-ligated to contain an *Eco*RI / *Xho*I clone with only exons 3-5 (HccsE/X 3-5) (see Fig 6.3). Sequencing of the HccsX-Ex1-2 clone confirmed the correct sequence. To further increase the genomic content of the 3' arm of the construct toapproximately 3.5 kb, the EcoHcc#5 clone encoding only half of exon 5 and 6 was placed into the *Eco*RI site of HccsE/X 3-5 (HccsE3-6) (see Fig 6.1 and 6.3). Correctly oriented clones were detected by digestion with *Hin*dIII and confirmed by sequencing.

Primers were designed to introduce appropriate restriction sites around loxP for insertion into the vector upon amplification from ploxPNeo. loxPfor introduced an *Xba*I site immediately 5' of loxP upon PCR amplification with the pgkp2 primer that binds in the *pgkNEO*^{r} promoter region, while an *Nhe*I site within the vector was used as the 3' restriction site. The 700bp product from this reaction was digested with *Nhe*I / *Xba*I to obtain an ~70bp fragment. To facilitate insertion of loxP into the targeting vector HccsE3-6 was digested with *Xba*I that also removed a fragment encoding exons 5-6 that was kept for re-cloning into this same vector. loxP was then introduced into the *Xba*I site of the remaining vector containing exons 3-4. Ligation of loxP in the correct orientation was detected by PCR with loxPfor and mHCCS3 that is localised in exon 3 to yield a 700bp product (see Fig 6.3). As only one functional *Xba*I site remained after this ligation the fragment containing exons 5-6 was reintroduced into this vector, yielding pHccsE3-6+loxP. Interestingly, ligation of any fragment that contained a loxP site either in the vector or insert was quite problematic and consequently no dephosphorylation of any vectors in the remaining cloning steps was performed. To overcome background religation, high numbers of colonies were screened by colony hybridisation (section 2.3.19) with the inserted fragment as a probe. The positive selection marker *pgkNeo*^{r} along with one loxP site were removed from ploxPNeo with *Xho*I / *Sal*I double digestion and ligated into the *Xho*I site of the above vector (HccsE3-6+loxP-Neo). To identify the correct orientation of *Neo*^{r} and loxP, in which the transcription of *Neo*^{r} was in the opposite orientation to that of *Hccs*, the construct was digested with combinations of *Xho*I that remained at only the 3' end of *Neo*^{r} and *Not*I / *Eco*RI. As the design of the targeting vector had only ~2kb of sequence in the 5' homology arm, a negative selection

marker was placed at the end of the construct in an attempt to aid selection of homologous recombinants. For this purpose *hsv-TK* was amplified from p18 with ploxpNeo#2 and TK3' that introduced a *Sal*I site at the 3' end of the gene. With the use of an internal restriction site this fragment was digested with *Xho*I / *Sal*I and inserted to the *Xho*I site of HccsE3-6+loxP-Neo (HccsTKE3-6+loxP-Neo). Digestion with combinations of *Xho*I / *Not*I / *Eco*RI allowed detection of clones with the remaining *Xho*I site between *TK* and *Neo*^{r}. The 5'homolgy arm consisting of the *Xho*I fragment of exon 1-2 was then introduced to the *Xho*I site to yield HccsTKex1-6+loxP-Neo. Correct orientation of this insert was identified by *Xba*I digestion.

6.2.4.1-1 Insertion of SalI for linearisation.

To increase efficiency of homologous recombination, targeting constructs are required to be electroporated as linearised fragments. This is usually achieved with the use of a unique restriction site at one end of the construct, or alternatively at both ends to allow removal of the vector backbone sequence. The inclusion of vector sequence in the linearised vector has previously been found to have no effect on targeting efficiency (Deng & Capecchi, 1992) and therefore a single unique restriction site was chosen for these experiments. During the identification of fragments for the construction of the above vector, *Sac*II sites were initially thought to be ideal for linearisation as no sites were detected within the marker genes or genomic sequence being used. *Sac*II was also left in the pBS KS$^+$ MCS of the targeting vector for these purposes. Multiple digests with various combinations of enzymes were used to confirm correct ligation of the above vector. After multiple digests with *Sac*II, at least one previously undetected internal site was identified, hence this site could not be used for linearisation. From the digestions completed, single restriction sites were identified for *Nde*I and *Bam*HI, however, both removed around 1kb of the 3' homology arm. This removal might therefore be expected to decrease recombination efficiency if used for linearisation in the subsequent targeting experiments. As *Sal*I did not cut within the entire construct, a strategy was designed to insert this restriction site at the 3' end of TK.

To introduce a unique *Sal*I site, a primer was designed over the 3' end of TK with a *Kpn*I-*Sal*I linker (KpSaTK3'). By PCR amplification with this primer and a previously synthesised primer in the promoter region of TK, TK#1, the resulting fragment contained two *Kpn*I sites that were used for insertion of this fragment back into the pHccsTKex1-

6+loxP-Neo vector. Digestion of the vector with *Kpn*I removed a 1kb fragment of TK from pHccsTKex1-6+loxP-Neo which when replaced with the PCR fragment coded for the entire TK gene, and also introduced the unique *Sal*I site. Inclusion of this site and correct orientation of the insert was detected with *Sal*I / *Xho*I restriction analysis. The resulting vector has been referred to as HccscKO#1.

6.2.4.1-2 Confirming the construct.

To confirm that the construct had been placed together correctly, restriction analysis was completed with combinations of *Eco*RI / *Hin*dIII / *Xho*I / *Sal*I / *Sac*I and *Xba*I. Following analysis of these fragments, the primers designed within the construct (Fig 6.3) were also used in PCR amplification to show correct orientation of all inserted fragments. To then check that no errors had been introduced into the coding regions of either *Hccs* or the selection markers, the primers were also used to sequence all exons and marker ORFs (i.e. *Neo*^{r} and *hsv-TK*).

6.2.4.1-3 Cre recombinase removal of floxed sequence.

As mentioned previously, cre recombinase is able to recognise similarly oriented loxP sequences and is able to promote recombination between the two sites without the need of additional co-factors. To address if the loxP sites placed within the above construct could be recognised by cre and allow excision of the intervening sequence, the pHccsKO#1 vector was transformed into an available *E.coli* strain expressing cre recombinase (strain BNN132). This strain is used in combination with genomic libraries produced by MoBiTec (Goettingen, Germany) to allow rapid cloning of identified fragments from Lambda phage. A number of colonies were analysed from the resulting plate, however, following restriction analysis of the plasmid DNA, no excision could be detected. In further attempts to confirm recognition of the loxP sites, commercially available cre recombinase was obtained from Calbiochem (San Diego, California) and used as detailed previously (Baubonis *et al*, 1993). In this method, purified cre protein is added to linearised plasmid DNA that is transformed to bacteria. Unfortunately, this approach was also unable to detect recombination between the two loxP sites. Given that the loxP sites and selection markers from the p18 and ploxPNeo vectors had

been used previously in conditional KO's (Nozaki *et al*, 1999), use of this construct was still pursued.

6.2.4.2 Strategy for detection of homologous recombinants.

Analysis of genomic DNA extracted from ES cells for the presence of homologously recombined targeting vectors is usually completed with either genomic Southern hybridisation or PCR. Southern analysis has traditionally yielded the most consistent results (Koentgen & Stewart, 1993) and was accordingly chosen as the method of screening ES cells for this experiment. External probes both 5' and 3' of the targeting vector are used on genomic digests with restriction enzymes that have been introduced into the construct such that the wt band will be larger than the targeted band. With this technique, randomly integrating vectors allow only wt bands to be detected as the probe is external to the construct. Internal probes, however, allow detection of varied bands from non-specific insertion that increases the number of false positives. Multiple digests completed on the targeting vector identified a number of introduced restriction sites within the *Neo*^{r} gene that could potentially be used for detection of homologous recombinants. External probes on either end of the construct are able to identify and confirm recombination in both the 5' and 3' homology regions, however, this will not detect insertion of the single loxP site located between exon 3-4. To therefore address if the recombination event in the 3' homology arm had occurred outside of this loxP site, PCR with primers located in exon 4 and exon 5 (mHCCS3 and mHCCS4, respectively) could be used to detect an increase in amplification size (i.e. 70 bp increase) compared to wt genomic DNA.

6.2.4.2-1 Obtaining genomic region further 5' of Hccs.

While the λ1 clone extended sequence further 3' to the target construct and therefore facilitated cloning of a fragment for use as the 3' probe, λ13, however, did not contain further sequence 5' of that used for the targeting vector. As mentioned previously (section 6.2.2), both BAC#266F20 and BAC#348M22 were found to extended sequence further 5' than λ13. Following detailed restriction analysis of these clones, *Spe*I was chosen as the enzyme for screening both 5' and 3' probes. Under these conditions the wt band would be ~15kb with the closest upstream recognition site being around 1.5kb from the *Xho*I site that is 5' of exon

1; the closest downstream site was found to be around 5kb from the 3' most region of the construct. This strategy would allow the 5' and 3' probe to detect a 5.5kb and 9kb band in the homologous recombinants, respectively. The distance of these sites from the construct also facilitated the use of sequence adjacent to the vector as 5' and 3' probes.

6.2.4.2-2 Isolation of external probes for detection of homologous recombinants.

6.2.4.2-2a 5' probe.

Various *Xho*I digests of the BAC clones were probed with the 600bp *Nco*I / *Nsi*I fragment of *Hccs* to identify available restriction sites that could be used for cloning further 5' sequence. This screen identified an ~2.5kb *Xho*I / *Sac*I fragment that could potentially be used as the 5' probe. Following cloning of a number of *Xho*I / *Sac*I fragments between 2 and 4 kb into pBS, the correct clone was identified by Southern analysis with the *Nco*I / *Nsi*I fragment (this clone has been referred to as Hccs5'#1) (Fig 6.3). Interestingly, this clone also contained the closest 5' *Spe*I site to the targeting construct, confirming that the screening strategy devised was correct. Sequencing of Hccs5'#1 with available vector primers highlighted repetitive sequence toward the 3' end of this fragment, hence a 1kb subfragment excised with *Spe*I / *Eco*RI was chosen for assessment by genomic Southern analysis for use as the 5' probe. Multiple mouse genomic digests (obtained from W9.5 ES cells), BAC digests and targeting vector digests were probed with this fragment. As only single bands and minimal background were detected in each digest this clone was used as the 5' probe in the following screens.

6.2.4.2-2b 3' probe.

From digests completed on λ1, an ~1.8kb *Xba*I fragment containing exon7 was identified and cloned into pBS KS^+. Sequencing confirmed that the correct region had been cloned, however, following genomic Southern analysis this region was found to contain repetitive sequence and was not used further. Additional digests of λ1 highlighted an ~1.4kb *Spe*I / *Xba*I fragment further 3' of the previous probe. An *Spe*I / *Not*I fragment containing this region was cloned into pBS KS^+. Restriction analysis and sequencing confirmed the correct region. The 1.4kb *Spe*I / *Xba*I fragment excised from this vector (termed Hccs3'#1) (Fig 6.3)

was found to be specific with only a single band being detected on multiple mouse genomic digests from W9.5 ES cells and BAC digests.

6.2.4.3 Transfection of HccsKO#1 in W9.5 ES cells.

As mentioned previously, W9.5 ES cells were initially chosen to use as hosts for electroporation of the HccscKO#1 construct. At the time this construct was synthesised, a number of problems had been uncovered with the stocks of W9.5 ES cells being used in the Department of Biochemistry (University of Adelaide, South Australia). Most significantly, germline transmission of the unmanipulated ES cell stock was no longer being achieved under standard conditions. Given the large amount of time expected for these experiments to be completed and the high expense of maintaining and screening ES cells, an outside source was sought. The gene KO facility offered at OZGENE (established in 2000 at the animal sciences division of the University of Western Australia) was chosen for the vast experience of the chief investigator, Dr Frank Koentgen. Prior to electroporation, the targeting construct and both 5' and 3' external probes were re-analysed by digestion and Southern analysis.

Based on suggestions in the literature, the original construct was designed to include the *Neo*^{r} gene between exon 2-3 with transcription occuring in the opposite orientation to that of *Hccs* (Nagy, 1996). However, a publication early in 2000 (Nagy, 2000) detailed reports of increased interference of normal splicing by *Neo*^{r} when in the opposite transcriptional orientation to the gene in which it was inserted. This finding is based on the presence of a strong splice acceptor consensus site while in this orientation. However, in the same transcriptional orientation to the gene this acceptor site is only partially used and has been employed to produce hypomorphic alleles of targeted genes (Nagy, 2000). To overcome interference of selection markers within genes, loxP sites (Postic *et al*, 1999) or frt sites (Sun *et al*, 2000) can be placed around the selection marker and used to remove the gene either *in vitro* (prior to injection into blastocysts by transfection of cre expressing vectors) or *in vivo* (after mouse lines have been produced by crossing to lines expressing cre or flp, respectively). Using loxP sites alone for this strategy requires the placement of two loxP sites around the selection marker and a third loxP site around the region to be removed. Transient expression of cre will therefore allow recombination between any of the two loxP sites such that it is possible to select colonies, or mice, that have only the marker removed,

leaving two functional loxP sites within the gene that can be utilised in subsequent conditional gene silencing. Alternatively, frt sites are placed around the marker with one loxP site exterior to frt and a second loxP site around the region to be removed. By then expressing flp in cells, or crossing to a mouse flp line, the marker gene is removed leaving only a single frt site and the two loxP sites that can again be used for conditional gene silencing.

6.2.5 Construct design for removal of exon 3 and 4 of Hccs with frt / loxP.

With the consultation of Dr Koentgen the targeting vector was redesigned to place the *Neo*^{r} selection marker in the same transcriptional orientation as *Hccs*. In an attempt to also overcome any partial reduction of Hccs, both frt and loxP sites were designed for placement around *Neo*^{r} for removal after selection either *in vitro* or *in vivo* (Fig 6.4B).

6.2.5.1 Generation of a construct for removal of exon 3 and 4 of Hccs with frt / loxP.

To generate a construct with the *Neo*^{r} gene surrounded by frt and loxP sites the pK11 vector that contains *Neo*^{r} surrounded by frt sites and a single loxP site at only one end of the ORF was obtained from Prof. G. Martin (UCSF, San Francisco, USA). Unfortunately, the loxP sites in pK11, p18 and ploxPNeo were all in the opposite orientation to the *Neo*^{r} gene and therefore the ORF was required to be flipped to facilitate insertion into HccsKO#1 using the previously positioned 3' loxP site between exon 2-3 (pHccsE3-6+loxP; section 6.2.4.1).

6.2.5.1-1 Construction of Neo^r *frt / loxP.*

An *Xba*I site was initially removed from ploxPNeo by digestion with *Eco*RI / *Not*I and religating the end filled vector (ploxPNeo-Xba; Fig 6.4A).

The frt sites along with *Neo*^{r} were then excised from pK11 with *Sal*I / *Sac*I and introduced to the pEGFPN$_1$ expression vector for addition of convenient restriction sites. The *Xho*I site in the MCS of pEGFPN^1 was then removed by digestion, end filling with Klenow and religation to generate pEGFPN^1-Xho. To introduce frt-Neo between the loxP sites, the corresponding region was digested from pEGFPN^1-*Xho*I with *Sal*I / *Nhe*I and cloned directionally into ploxPNeo-Xba cut with *Xba* / *Sal*I. The *Sal*I site remaining between frt and loxP was removed by end filling the *Sal*I site, and religating. A *Xho*I / *Sal*I *Neo*^{r} fragment with frt and

loxP was obtained by PCR amplification with T7 and the primer Sal-pgkneo that introduced the *Sal*I restriction site at the end.

6.2.5.1-2 Insertion of loxP-frt-Neo into Hccs.

To allow insertion of the *Neo*^{r} gene surrounded by loxP and frt sites, the HccsKO#1 vector was digested with *Spe*I / *Xho*I such that only TK was left in pBS KS^{+}. An *Spe*I / *Xho*I fragment from an earlier ligation step (HccsE3-6+loxP; see Fig 6.3 and 6.4) was then directionally inserted into this to leave a *Xho*I site between TK and Exon 3 (HccsTKE3-6+loxP). The Neo-frt-loxP fragment cut with *Xho*I / *Sal*I was placed into this *Xho*I site (HccsE3-6+Neo-frt-lox) and the correct orientation detected by *Xho*I / *Sal*I digestion. Exons 1-2 were then placed into the available re-created *Xho*I site and again oriented with *Xba*I digestion: The resulting construct has been referred to as HccsKO#2. Various combinations of restriction enzymes were used to confirm correct ligation, while PCR was again used to confirm orientation of all ligation steps. To analyse coding regions of *Hccs* and selection markers, sequencing with available primers was completed.

6.2.5.2 Electroporation of HccsKO#2 in W9.5 ES cells.

The HccsKO#2 vector was also designed with the original 5' and 3' probes to be used for selection of homologously recombined ES cells. The vector was linearised by *Sal*I digestion and electroporated at OZGENE under conditions that minimise cell death and decrease multiple integration of the target vector (Barnett & Koentgen, 2001). Initially, the cells were only placed under G418 selection for the positive marker. Approximately 500 colonies were picked and expanded. Following screening of all colonies with the 3' probe on *Spe*I digested genomic DNA, no homologous recombinants were identified (Fig 6.5). As the targeting vector also contained the negative selection marker, a second round of electroporation was completed with selection for both G418 and FIAU. Approximately 250 colonies were picked and expanded, however, no homologous recombinants were identified using the 3' probe for the screen on *Spe*I digested genomic DNA.

Figure 6.4

A. Construction of Neo^r-frt/loxP
All maps indicate restriction sites used in the cloning steps to flip the *Neo^r* gene from pK11 and also place both frt and loxP sites around the ORF. Bold type represents restriction enzymes used for excision and cloning of fragments in subsequent steps. Restriction enzymes separated by – had compatible ends and were ligated together to remove both recognition sites. Shaded restriction sites indicate removal by digestion and end filling. Relative positions of both the T7 and +salpgkneo primers used to amplify Neo^r-frt/loxP with the inclusion of a SalI site are shown below the vector.

B. HccsKO#2 cloning and targeting strategy
Introduction of Neo^r-frt/loxP to the HccsKO#1 was designed to allow excision of the selection marker either *in vitro* or *in vivo*. Primers designed to various regions within the vector are represented below the target construct. The position of primers allowing introduction of the 3' LoxP site to be confirmed following recombination are also shown (mHCCS#3 and mHCCS#4). Thick lines in the targeting construct (top) indicate genomic sequences and thin lines indicate vector backbone. Green arrow heads show loxP sites with their relative orientation while orange circles indicate similarly oriented frt sites. *pgkNeo^r* has been inserted in the same transcriptional orientation to *Hccs*. Restriction enzyme digestion with *Sal*I (S) was devised to linearise the construct while *SpeI* (Sp) was designed to be used for screening both 5' and 3' external probes (relative positions indicated on sequence below vector). Relative fragments used for the construction of the targeting vector are represented beneath the vector. Homologous recombination in both homology arms would yield floxed *Hccs* with the inclusion of *Neo^r* between exon 2 and 3. Addition of cre recombinase to the floxed allele would result in recombination between any of the two loxP sites that can be used to remove the *Neo^r* selection marker. Likewise, expression of frt will excise this selection marker. Following recombination between the loxP sites surrounding exon 3-4, coding regions for CPV heme binding motifs will be removed to create a frame shift in the remaining mRNA that also introduces a premature stop codon. In all maps open purple boxes represent 5' and 3' UTRs while purple shaded boxes represent coding regions of *Hccs*. Red boxes indicate a frame shift and introduction of a premature stop codon. B, *Bam*HI; Sa, *Sac*I; Sp, *Spe*I; E, *Eco*RI; Xb, *Xba*I; Xh, *Xho*I; H, *Hin*dIII; Nh, *Nhe*I; No, *Not*I; K, *Kpn*I; P, *Pst*I; S, *Sal*I; Nd, *Nde*I.

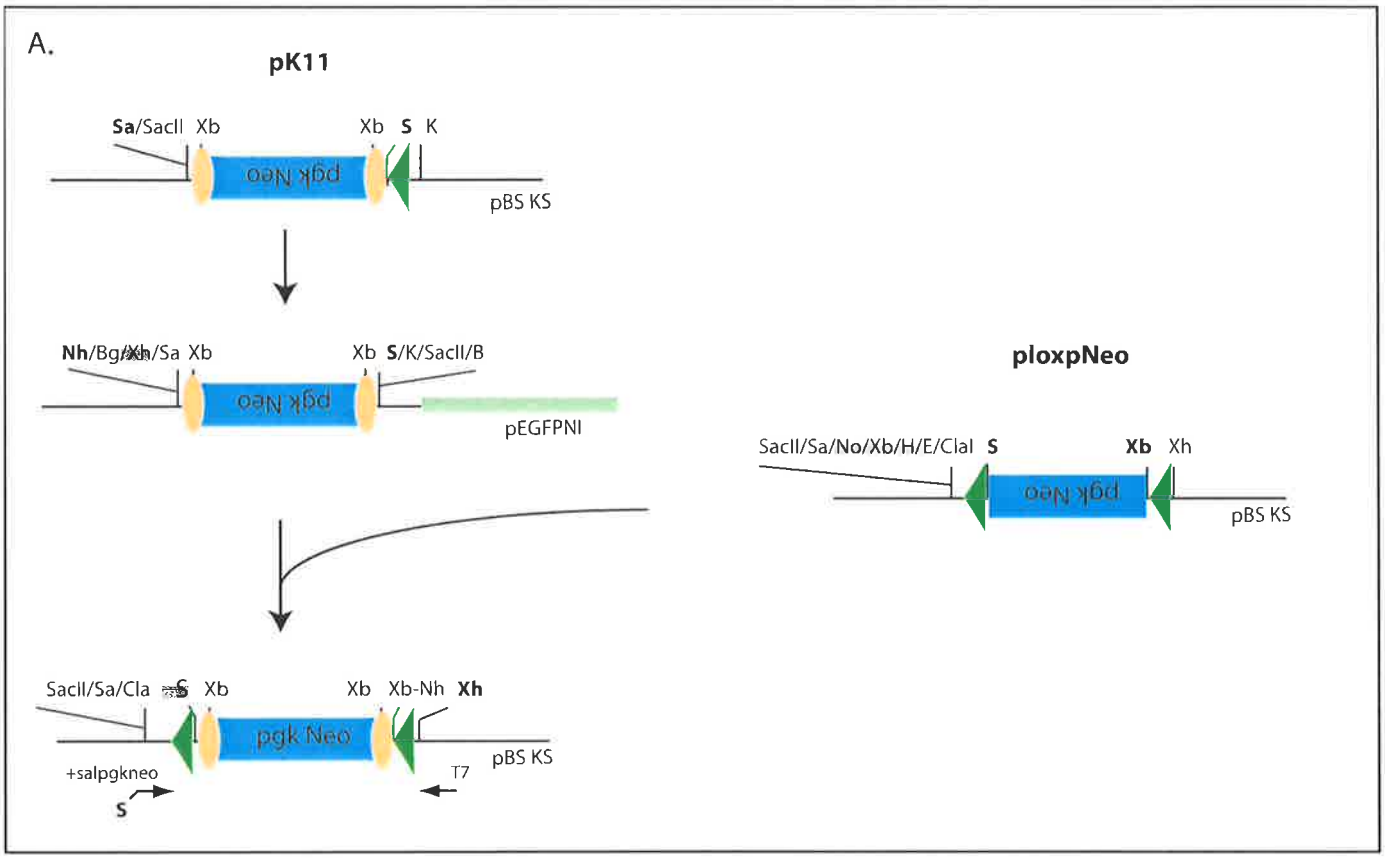
A.
pK11
Sa/SacII Xb
Xb S K
pgk Neo
pBS KS
Nh/Bg/Xh/Sa Xb
Xb S/K/SacII/B
pgk Neo
pEGFPNI
ploxpNeo
SacII/Sa/No/Xb/H/E/ClaI S
Xb Xh
pgk Neo
pBS KS
SacII/Sa/Cla S Xb
Xb Xb-Nh Xh
pgk Neo
pBS KS
+salpgkneo
T7
S

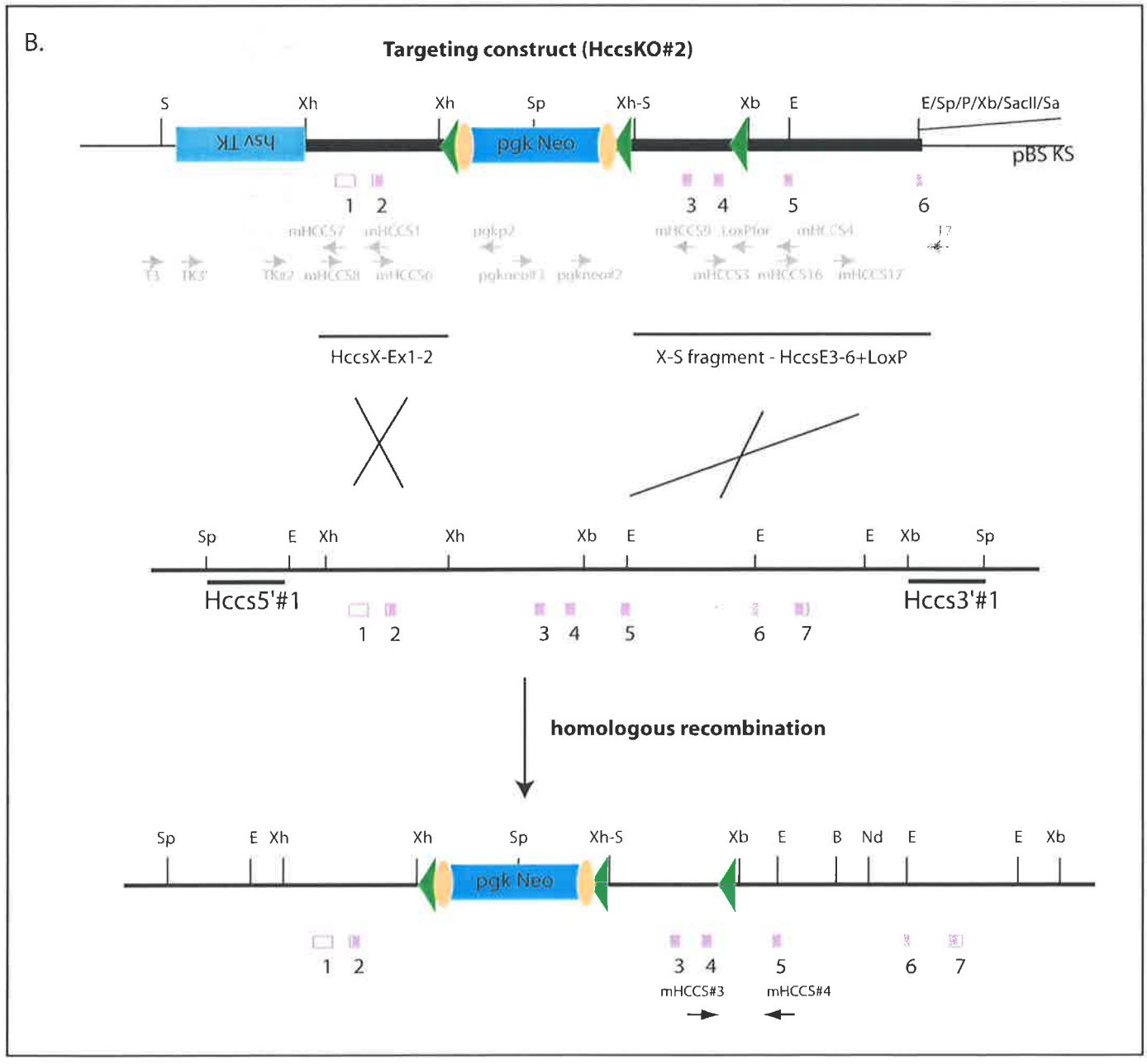
B.
Targeting construct (HccsKO#2)
S Xh Xh Sp Xh-S Xb E E/Sp/P/Xb/SacII/Sa
hsv TK
pgk Neo
pBS KS
1 2 3 4 5 6
HccsX-Ex1-2
X-S fragment - HccsE3-6+LoxP
Sp E Xh Xh Xb E E E Xb Sp
Hccs5'#1
Hccs3'#1
1 2 3 4 5 6 7
homologous recombination
Sp E Xh Xh Sp Xh-S Xb E B Nd E E Xb
pgk Neo
1 2 3 4 5 6 7
mHCCS#3
mHCCS#4

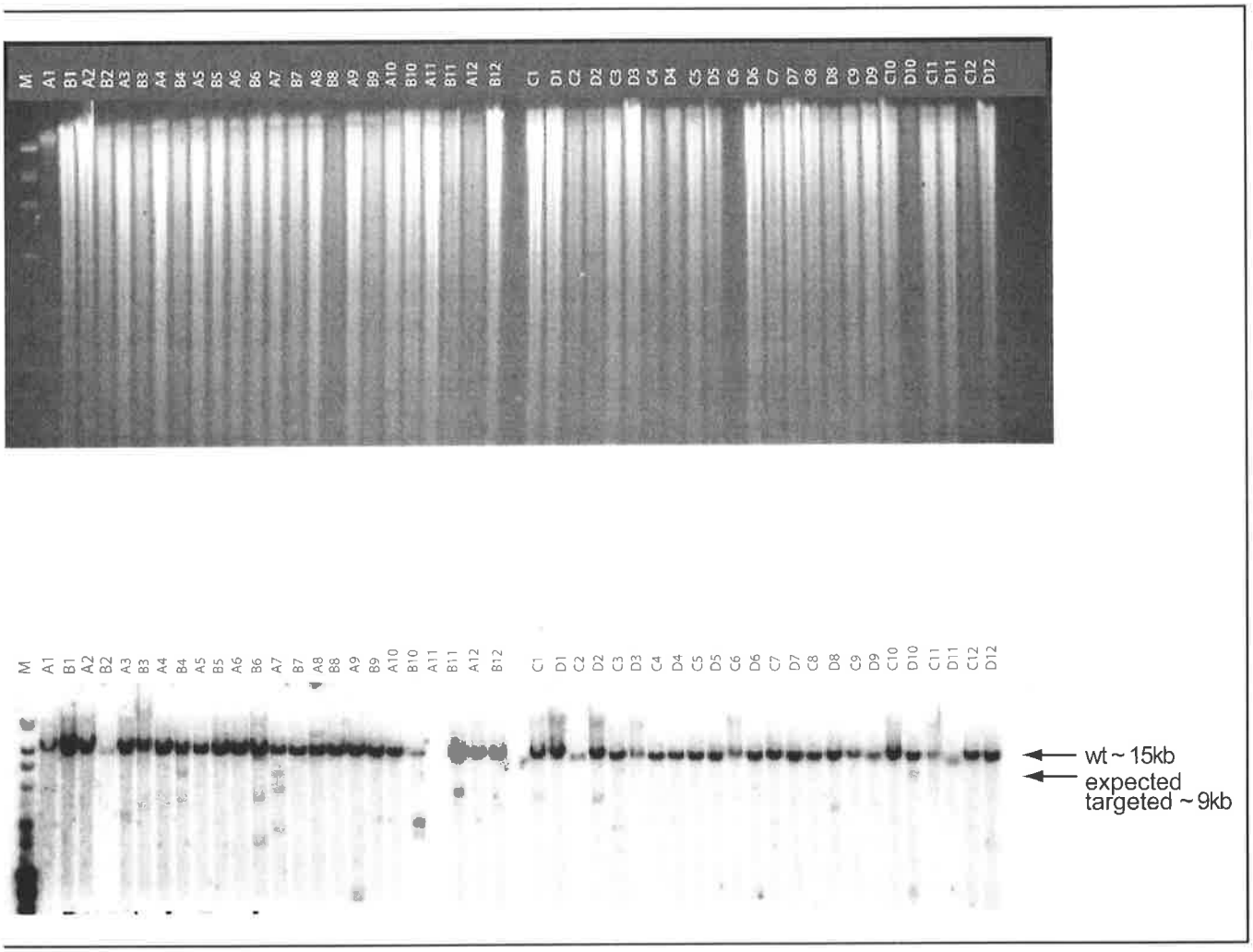

Figure 6.5

Characterisation of HccsKO#2 electroporated ES cells

Genomic DNA was extracted from ES cells, digested with *Spe*I and Southern blot analysis completed with Hccs3'#1. Top box represents an example of DNA digestion and the bottom box represents an example Southern blot. Relative positions of the wt band and the expected targeted band are shown. The well numbers of the ES cell colony are indicated at the top of each lane and M refers to marker lanes.

6.2.6 Increasing size of the 5' homology arm of HccsKO#2.

As the vector used in the aforementioned experiment was unsuccessful in targeting the *Hccs* locus, it was decided that the size of the 5' homology arm of HccsKO#2 should be increased. In the previous vector, the 5' region for recombination was ~ 2kb in length, while the 3' region is 3.5kb. By therefore increasing the 5' region of homology, targeting efficiency would be expected to increase (see Fig 6.6). The 2.5kb *Xho*I / *Sac*I fragment (clone Hccs5'#1) contained an additional 700bp between the internal *Eco*RI restriction site and the 5' *Xho*I site of the targeting vector (see Fig 6.6A). A PCR based strategy to enable ligation of this 700bp fragment into the 5' region of HccsX-Ex1-2 (section 6.2.3.1) was devised from sequence data previously generated (Fig 6.6A). Primers were designed to amplify the 700bp *Eco*RI / *Xho*I region to introduce a *Xho*I site next to *Eco*RI (5'probeXho) and also replace the 5' *Xho*I site with *Hin*dIII (5'probeHind). The primers, Ex1-2Xho and Ex1-2Hind, were also designed to amplify the HccsX-Ex1-2 fragment with replacement of the 5' *Xho*I site with *Hin*dIII (i.e. Ex1-2Hind) (see Fig 6.6A). The 2kb PCR fragment was digested with *Hin*dIII / *Xho*I and ligated into pBS KS^+ (HccsH/X-Ex1-2). The 5' 700bp fragment from pHCCS5'#1 was amplified with the aforementioned primers and then ligated to the HccsH/X-Ex1-2 fragment with *Eco*RI / *Hin*dIII digestion that also introduced a *Xho*I site at the 5' end of the clone. The resulting *Xho*I fragment was then introduced into HccsKO#2 (also digested with *Xho*I) to produce HccsKO#3. Correct orientation of the fragment was addressed with *Hin*dIII digestion. Restriction analysis with multiple enzymes and sequencing were used to confirm that the construct was correct. The introduction of 3 missmatched bases with this PCR based approach was expected to have minimal effects on homologous recombination within this region.

6.2.6.1 Electroporation of HccsKO#3 in W9.5 ES cells.

The HccsKO#3 targeting construct was also sent to OZGENE (Western Australia) for electroporation, expansion and screening. Approximately 500 colonies were analysed with no homologous recombination being detected. This suggests that either the recombination frequency in this region is extremely low (as has been noted for certain regions of the genome) or that the inclusion of the *Neo*^{r} selection marker within the gene is having a deleterious effect on ES stem cell survival and hence only random integration can be selected.

That other genes around *Hccs* have been targeted by homologous recombination (Prakash *et al*, 2000) suggests that the former is not the explanation and that the selection marker may be the primary reason for the lack of recombinants. Further analysis of the construct suggested that the poly A signal of *Neo*^{r} may be prematurely stopping transcription of *Hccs* to an extent that cell survival is severely affected.

6.2.7 Construct design for removal of exon 5 to 7 of Hccs.

As the vector design with *Neo*^{r} within the gene was unable to allow targeting of the *Hccs* locus, an alternative approach was again devised. In this design the selection marker was introduced outside of the *Hccs* gene with the loxP sites surrounding exon 5-7 of the coding region (Fig 6.7). To aid in the identification of restriction sites for the ligation of these fragments, λ1 and the original *Spe*I / *Not*I fragment contained in the 3'probe (section 6.2.4.2-2b) were digested with multiple enzymes and subjected to Southern analysis with the furthest 3' regions previously cloned. The resulting map (see Fig 6.1) and available sequence generated from the previous clones allowed the design of a cloning strategy to produce the new targeting vector. In this strategy, the *Neo*^{r} is placed outside of the *Hccs* transcriptional unit and therefore the inclusion of frt sites or loxP sites around the marker were not adopted. Increased size of both 5' and 3' homology arms in this vector were also expected to increase targeting efficiency. Furthermore, with the use of regions from HccsKO#3, *Sal*I was available for linearisation of the construct and one loxP site had already been cloned between exon 4 and 5.

Using this approach, removal of exon 5-7 with expression of cre recombinase would remove the presumed catalytic domain of Hccs that is conserved among all species (Schaefer *et al*, 1996). While deletion of this region will allow the translation of an 84 amino acid protein that may retain mitochondrial targeting information, removal of this region would be expected to also abolish any function in tissues expressing the recombinase.

6.2.7.1 Generation of a construct for removal of exon 5 to 7 of Hccs.

As mentioned previously, the design of the targeting construct for removal of exon 5-7 utilised a number of characteristics present in the previous construct. The HccsTKE3-

Figure 6.6

A. Construction of HccsX-Ex1-2+5'
Maps indicate the restriction enzyme sites used in the cloning steps to introduce an extra 700bp of genomic sequence into the 5' homology arm of the targeting construct. Enzyme sites in bold type were used for cloning the subsequent step and enzymes separated by – were cloned together to remove both restriction recognition sites. Relative positions of the primers used to join HccsX-Ex1-2 and 700bp from Hccs5'#1 are shown below the corresponding vectors.

B. HccsKO#3 cloning and targeting strategy
Replacement of the 5' homology arm of HccsKO#2 with HccsX-Ex1-2+5' was designed to allow increased targeting efficiency. Primers designed to various regions within the vector are represented below the target construct. The position of primers allowing introduction of the 3' LoxP site to be confirmed are also shown (mHCCS#3 and mHCCS#4). Thick lines in the targeting construct (top) indicate genomic sequences and thin lines indicate vector backbone. Green arrow heads show loxP sites with their relative orientation while orange circles indicate similarly oriented frt sites. *pgkNeo* has been inserted in the same transcriptional orientation to *Hccs*. Restriction enzyme digestion with *SalI* (S) was devised to linearise the construct while *SpeI* (Sp) was designed to allow screening of both 5' and 3' external probes (relative positions indicated on sequence below vector). Homologous recombination in both homology arms would yield floxed *Hccs* with the inclusion of Neo^r between exon 2 and 3. Addition of cre recombinase to the floxed allele would result in recombination between any of the two loxP sites that can be utilised to remove the Neo^r selection marker. Likewise, expression of frt will excise this selection marker. Following recombination between the loxP sites surrounding exon 3-4 coding regions for CPV heme binding motifs will be removed to create a frame shift in the remaining mRNA that also introduces a premature stop codon. In all maps open purple boxes represent 5' and 3' UTRs while purple shaded boxes represent coding regions of Hccs. Red boxes indicate a frame shift and introduction of a premature stop codon. B, *Bam*HI; Sa, *Sac*I; Sp, *Spe*I; E, *Eco*RI; Xb, *Xba*I; Xh, *Xho*I; H, *Hin*dIII; Nh, *Nhe*I; No, *Not*I; K, *Kpn*I; P, *Pst*I; S, *Sal*I; Nd, *Nde*I.

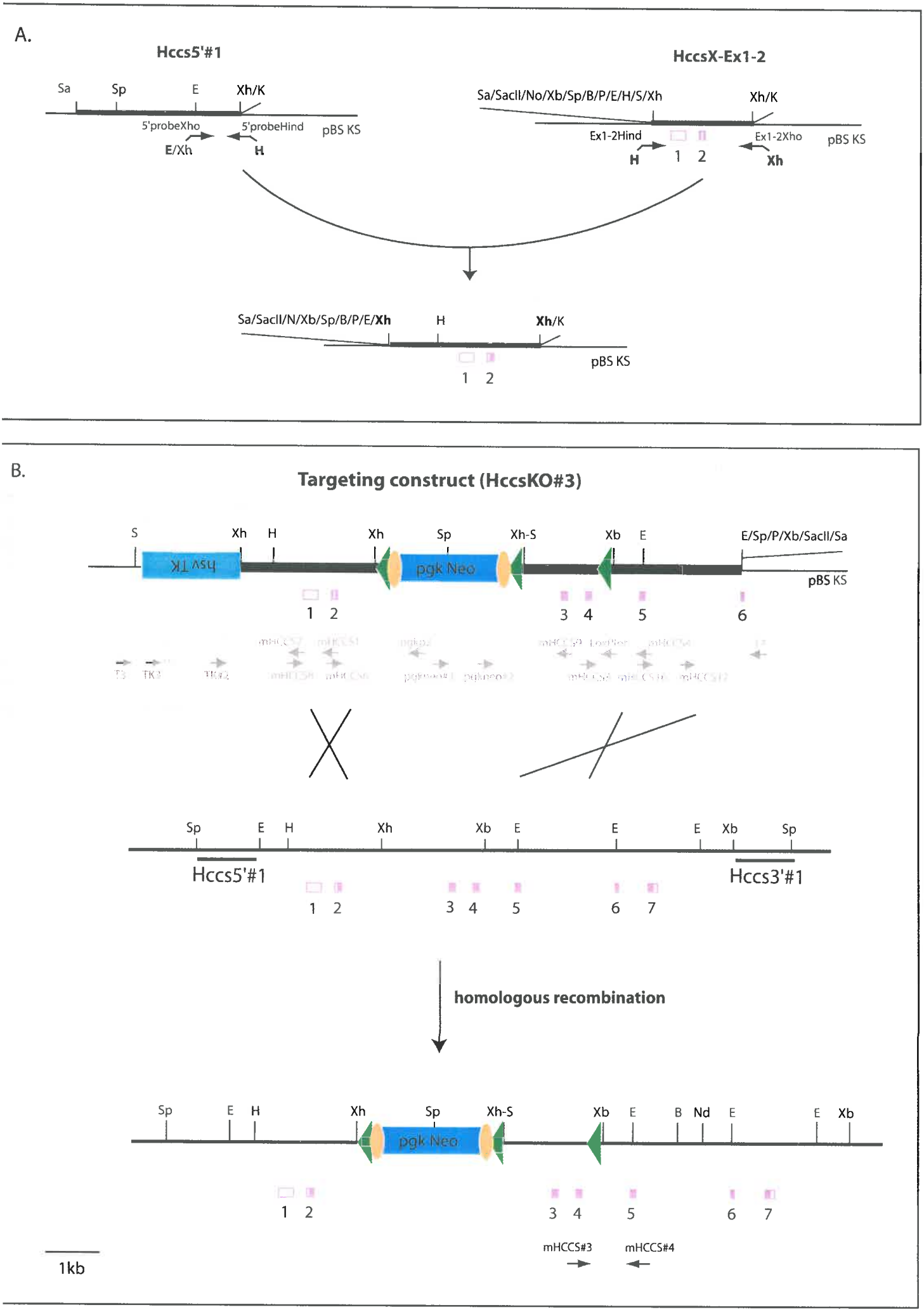
A.
Hccs5'#1
Sa
Sp
E
Xh/K
5'probeXho
5'probeHind
pBS KS
E/Xh
H
HccsX-Ex1-2
Sa/SacII/No/Xb/Sp/B/P/E/H/S/Xh
Xh/K
Ex1-2Hind
Ex1-2Xho
pBS KS
H
1 2
Xh
Sa/SacII/N/Xb/Sp/B/P/E/Xh
H
Xh/K
pBS KS
1 2
B.
Targeting construct (HccsKO#3)
S
Xh
H
Xh
Sp
Xh-S
Xb
E
E/Sp/P/Xb/SacII/Sa
hsv TK
pgk Neo
pBS KS
1 2
3 4
5
6
Sp
E
H
Xh
Xb
E
E
E
Xb
Sp
Hccs5'#1
Hccs3'#1
1 2
3 4
5
6 7
homologous recombination
Sp
E
H
Xh
Sp
Xh-S
Xb
E
B
Nd
E
E
Xb
pgk Neo
1 2
3 4
5
6 7
mHCCS#3
mHCCS#4
1kb

Figure 6.7

HccsKO#4 targeting strategy

A partial restriction map of HccsKO#4 details all of the sites used to construct the vector. Enzymes separated by – were cloned together to remove both restriction recognition sites. Thick lines indicate genomic sequence and thin lines indicate vector backbone. Green arrow heads show loxP sites with their relative orientation. Both *hsvTK* and *pgkNeo* have been inserted in the opposite transcriptional orientation to *Hccs*. Restriction enzyme digestion with *Sal*I (S) was devised to linearise the construct while *Nhe*I (N) and *Bam*HI (B) were designed to be used for screening both 5' and 3' external probes, respectively (relative positions indicated on sequence below vector). Relevant fragments used for cloning this vector are highlighted below the targeting construct. Primers designed to various regions within the vector are represented below the target construct. The position of primers to confirm the introduction of the 5' LoxP site and also the cre mediated recombination in ES cells are also shown. Homologous recombination in both homology arms would yield Floxed *Hccs* with the inclusion of *Neo*^{r} at the end of exon 7. Addition of cre recombinase to the floxed allele would result in recombination between the two loxP sites that effectively removes the catalytic domain of the enzyme. In all maps open purple boxes represent 5' and 3' UTRs while purple shaded boxes represent coding regions of Hccs. B, *Bam*HI; Sa, *Sac*I; Sp, *Spe*I; E, *Eco*RI; Xb, *Xba*I; Xh, *Xho*I; H, *Hin*dIII; Nh, *Nhe*I; No, *Not*I; K, *Kpn*I; P, *Pst*I; S, *Sal*I; Nd, *Nde*I.

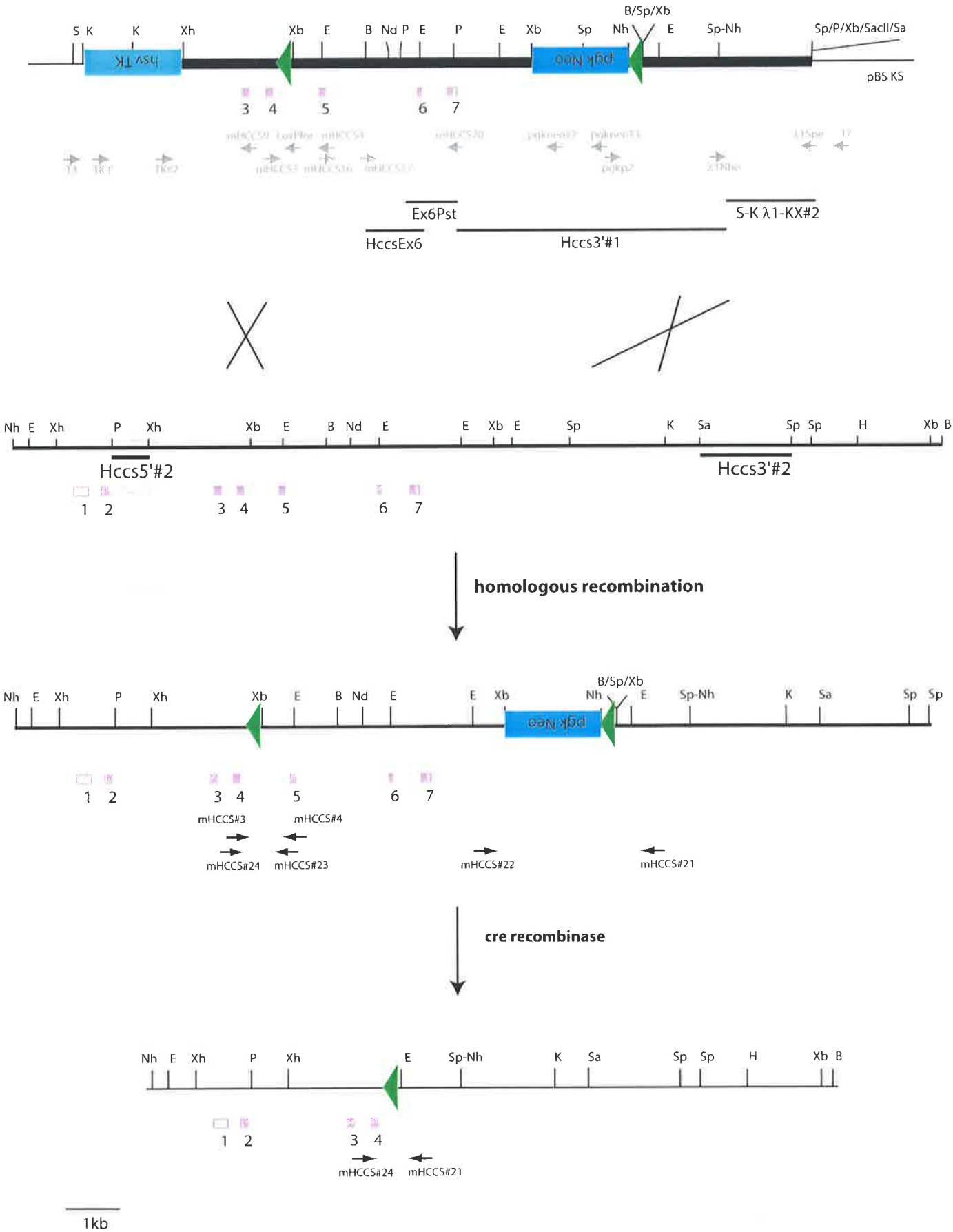
Targeting construct (HccsKO#4)
S K K Xh Xb E B Nd P E P E Xb Sp Nh B/Sp/Xb E Sp-Nh Sp/P/Xb/SacII/Sa
pBS KS
3 4 5 6 7
Ex6Pst
S-K λ1-KX#2
HccsEx6
Hccs3'#1
Nh E Xh P Xh Xb E B Nd E E Xb E Sp K Sa Sp Sp H Xb B
Hccs5'#2
Hccs3'#2
1 2 3 4 5 6 7
homologous recombination
Nh E Xh P Xh Xb E B Nd E E Xb Nh B/Sp/Xb E Sp-Nh K Sa Sp Sp
1 2 3 4 5 6 7
mHCCS#3
mHCCS#4
mHCCS#24
mHCCS#23
mHCCS#22
mHCCS#21
cre recombinase
Nh E Xh P Xh E Sp-Nh K Sa Sp Sp H Xb B
1 2 3 4
mHCCS#24
mHCCS#21
1kb

6+loxP vector (section 6.3.4.1-2) was digested with *Bam*HI / *Eco*RI to clone the 3' half of exon 6 into pLIT28 (Hccs-ex6). To aid in further cloning steps, the *Xba*I site was then removed from the MCS by digestion, end filling and re-ligation (Hccs-ex6-Xb). An *Spe*I / *Pst*I fragment from Hccs3'#1 was then ligated into this to give Hccs-ex7-Xb, as exon 6 was removed with this digest.

To increase the 3' region of this targeting vector, λ1 digests were analysed by Southern hybridisation with the original 1.4kb *Spe*I / *Xba*I fragment of the 3' probe. An approximately 3-4kb *Kpn*I / *Xba*I fragment was identified for use as the 3' homology arm. Following ligation of all *Kpn*I / *Xba*I λ1 fragments into pLIT28, four alternative clones were identified and labelled λ1-KX#1-4. The correct fragment, λ1-KX#2, was then isolated by Southern analysis with the original 3' probe and confirmed with *Spe*I digestion (the correct fragment also contained an internal *Spe*I restriction site). The *Spe*I / *Kpn*I fragment from this clone was excised and ligated into pBS KS^+ to allow sequencing of both ends and the design of primers to replace the *Spe*I site with *Nhe*I for further cloning steps. Following PCR amplification with the synthesised primers, λ1Nhe and λ1Spe, this fragment was inserted into the *Spe*I site of Hccs-ex7-Xb to concomitantly introduce an *Spe*I site in place of *Kpn*I and also destroy the original *Spe*I site with the *Spe*I / *Nhe*I ligation. Correct orientation of this insert was detected by *Xba*I / *Spe*I digestion.

Exon 6 was then introduced into the *Pst*I site of this clone by removal from EcoHccs#6 (section 6.3.4) to produce Hccs-ex6-7BaSp. *Neo*^{r} with one loxP site attached to the 3' region was excised from ploxPNeo by *Xba*I digestion and ligated into similarly cleaved Hccs-ex6-7BaSp. Correct orientation of the insert was determined by *Nhe*I / *Spe*I digestion and confirmed by sequencing with marker primers.

An alternative construct in which *Neo*^{r} was surrounded by loxP sites was also produced. In this vector PCR mutagenesis had been used to remove an *Xba*I site between Neo^r and loxP, however, sequencing identified a number of base changes in the ORF. This altered selection marker was being used by Dr B. Hopwood (University of Adelaide, South Australia) and found to reduce the effectiveness of Neo^r. Therefore, the clone containing only one loxP site was (Hccs-ex6-7Neo-loxP) was used further.

A *Bam*HI / *Spe*I fragment from the above clone was then directionally inserted to similarly digested HccsTKE3-6+loxP (see Fig 6.7). To complete the targeting vector, the

*Bam*HI fragment from Hccs-ex6-7Neo-loxP was placed into this vector yielding HccsKO#4. Correct orientation of all inserts was analysed with restriction enzyme digestion while sequencing also confirmed that the construct was pieced together correctly. This construct was transformed into the bacterial strain BNN132 to address cre recombinase recognition of the loxP sites within the genomic sequence. Restriction analysis of the resulting plasmids conclusively revealed that the region between the two loxP sites was efficiently removed, suggesting that cre does indeed recognised these sequences (Fig 6.8).

6.2.7.2 Strategy for detection of homologous recombinants from HccsKO#4.

Insertion of the loxP-Neo^r fragment into this vector also introduced a number of unique restriction sites that could be used for detecting homologous recombinants. *Bam*HI at the 3' end of *Neo^r* was chosen for a diagnostic test of the 3' probe as the wild type band was found to be 13kb and the targeted band expected to be approximately 9.5kb. Likewise, *Nhe*I, that was also introduced at the 3' end of *Neo^r* was found to be appropriate for the 5' probe as wild type would be approximately 40kb with an expected targeted band of 10kb.

6.2.7.2-1 Isolation of external probes for detection of homologous recombinants from HccsKO#4.

6.2.7.2-1a 5' probe.

As the previously cloned *Xho*I fragment containing exon 1-2 was not used in this construct two different fragments within this region were chosen for an assessment of their suitability as probes. A 1kb fragment from the 3' end of the clone obtained by *Pst*I / *Kpn*I digestion was found to be specific on genomic digested DNA with the hybridisation of a single band and minimal background. This fragment has been referred to as Hccs5'#2 (Fig 6.7).

6.2.7.2-1b 3' probe.

To obtain regions further 3' to those used in the construct, the previously made filters containing λ1 digests were probed with the *Spe*I / *Kpn*I fragment used in the HccsKO#4 vector. An ~5kb *Spe*I fragment was identified, cloned into pBS KS$^+$ (λ1-5kbSpe-pBS) and confirmed by sequencing. Various digests identified an internal *Sac*I site that

Figure 6.8

A. Cre mediated recombination of HccsKO#4 in bacterial cells
Schematic representation of cre mediated removal of the intervening sequence between two similarly oriented LoxP sites. The partial restriction map indicates the restriction enzyme sites used to confirm excision of the sequence. B, *Bam*HI; Sp, *Spe*I; Xh, *Xho*I; S, *Sal*I.

B. Restriction analysis of Cre recombined HccsKO#4
HccsKO#4 was transformed to BNN132 and the resulting plasmid was digested with various restriction enzymes (+cre lanes). To confirm excision of the intervening sequence these were compared to untreated digested vector (enzyme alone) on a 1% gel. Marker sizes are shown in kb.

A.

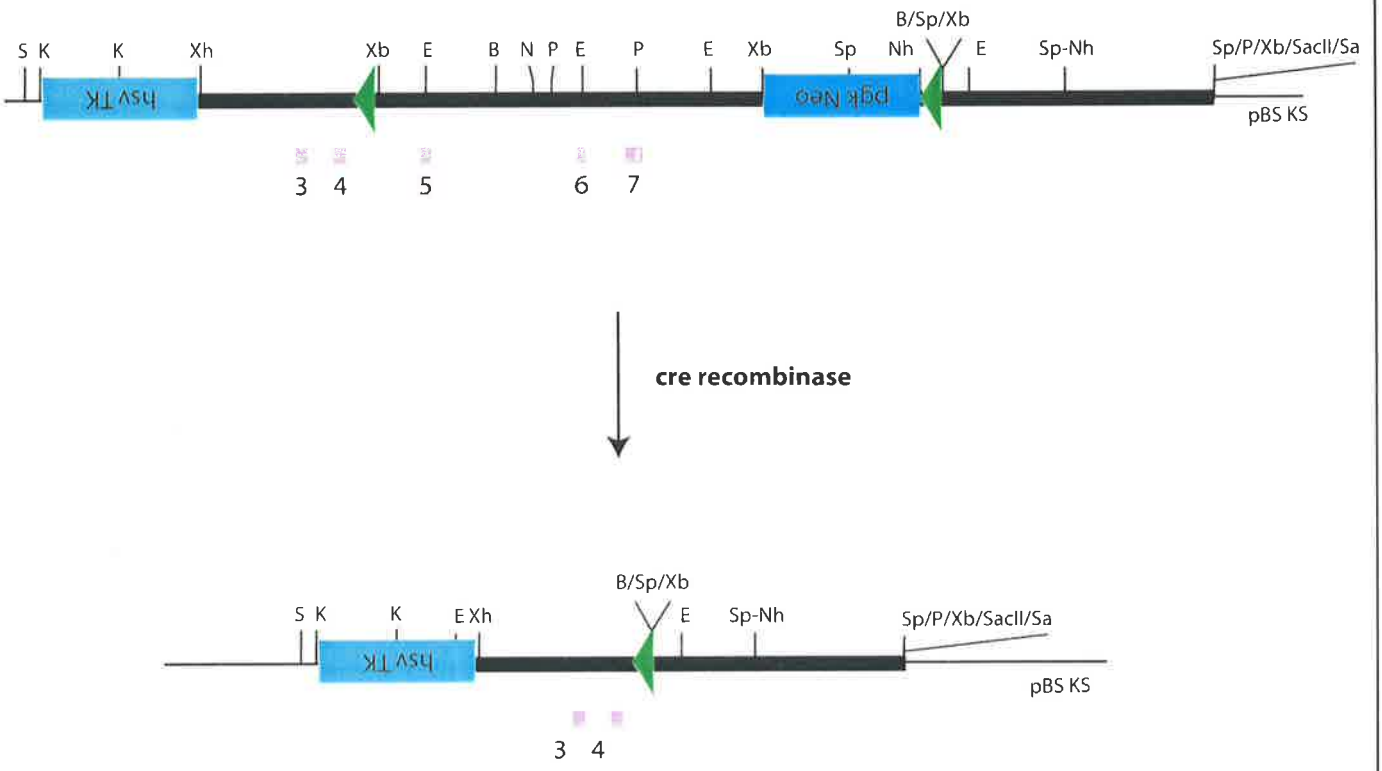
Hccs KO#4
S K K Xh Xb E B N P E P E Xb Sp Nh B/Sp/Xb E Sp-Nh Sp/P/Xb/SacII/Sa
hsv TK
pgk Neo
pBS KS
3 4 5 6 7
cre recombinase
S K K E Xh B/Sp/Xb E Sp-Nh Sp/P/Xb/SacII/Sa
hsv TK
pBS KS
3 4

B.

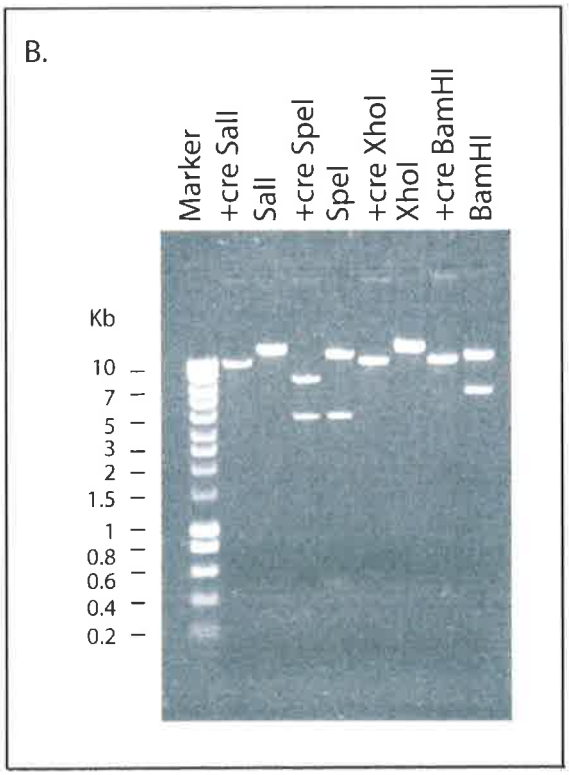
Marker
+cre SalI
SalI
+cre SpeI
SpeI
+cre XhoI
XhoI
+cre BamHI
BamHI
Kb
10
7
5
3
2
1.5
1
0.8
0.6
0.4
0.2

allowed excision of a 1.9kb fragment from λ1-5kbSpe-pBS for use as the Hccs3'#2 probe (Fig 6.7). Various genomic digests probed with this fragment produced single bands with minimal background.

6.2.7.3 Electroporation of HccsKO#4.

As targeted ES cells had not been identified at OZGENE (Western Australia), an alternative source of ES cells was also sought for use in parallel experiments. R1 ES cells that have previously been shown to colonise the germline through ES aggregates or blastocyst injection (Wood *et al*, 1993), were obtained from Dr S. Wood (Children's Health Research Institute, South Australia). These cells are an adherent, feeder dependent cell line derived from a male mouse of 129/Sv background. The cells also require Leukemia Inhibitory Factor (LIF) to prevent differentiation *in vitro*. R1 cells were maintained on either growth-arrested primary Mouse Embryonic Fibroblasts (pMEF) that were obtained from a *Neo* resistant mouse line, or Slow-twitching oxidative (sto^r) cells that were also Neo^r such that they would be viable during G418 selection.

The vector was linearised by *Sal*I digestion and the vector transfected into R1 ES cells following previously published methods (Kwee *et al*, 1995) at GenSA (Institute of Medical and Veterinary Science, South Australia). G418 selection was initiated 24hrs after transfection and maintained for 10 days. Around 480 colonies were picked and expanded in duplicate for Southern blot analysis and storage. Genomic DNA was extracted from the 240 colonies provided and then digested with *Bam*HI. The filters were probed with the Hccs3'#2 probe to detect a targeted band of 9.5kb or wild type band of 13kb. Seven of the colonies were identified to contain correct targeting at the 3' end of the gene (Fig 6.9A). DNA from these positive colonies were then subjected to *Nhe*I digestion and Southern analysis with the Hccs5'#2 probe to detect homologous recombination at the 3' end of the target vector (Fig 6.9B). Hccs5'#2 detects a wild type band at 40kb while targeted alleles are seen at 10kb. To address multiple integration of the target vector, a 700bp *Xho*I / *Sal*I fragment of the Neo^r gene from ploxPNeo was analysed on both *Bam*HI and *Nhe*I digested DNA. This Southern analysis confirmed that all homologous recombinants had indeed only integrated at the target locus. Homologous recombination could have occurred at either side of the 5' loxP site. Therefore, the presence of this site was assessed by PCR amplification with mHCCS3 and

mHCCS4, with the presence of the loxP sitre detected by an approximate 70bp increase in size (Fig 6.9C). Example results of the Hccs5'#2 and Hccs3'#2 Southern analyses as well as the PCR results are shown in figure 6.9. From the 240 colonies screened 9 were detected to be targeted at both the 5' and 3' ends of the construct, however, only 4 of these included the distal 5' loxP site.

Due to contractual reasons, the HccsKO#4 targeting construct was also sent to OZGENE at the same time for electroporation into the same W9.5 ES cells used in previous attempts (project identification code: 178-Rolex). Initially, 200 colonies were analysed with both probes with the identification of 5 targeted clones at both the 5' and 3' ends (labelled 178-1E1, 178-1E3, 178-3E2, 178-1D4 and 178-3G3). PCR amplification with mHCCS3 and mHCCS4 from genomic DNA obtained from OZGENE was again used to confirm the inclusion of the 5' loxP site. Four of the five clones received (178-1E1, 178-1E3, 178-1D4 and 178-3E2) were found to include this site (results not shown) and hence appropriate for blastocyst injections.

6.2.7.4 Karyotypic analysis of targeted R1 ES cells.

Three of the four targeted R1 ES cell clones were retrieved from frozen stocks and expanded (referred to as Hc-flox#1, 2 and 3). Phenotypically, Hc-flox#2 and 3 were noted to form quite flat colonies that had increased levels of differentiated cells compared to Hc-flox#1 that in contrast appeared quite normal (Dr. J. Rathjen, personal communication). As the presence of significant chromosome abnormalities has been suggested to inhibit germline colonisation in chimeric mice (Suzuki *et al*, 1997) all the R1 cell lines were first karyotyped following standard protocols (Section 2.3.31). As detailed in figure 6.10, all three lines were identified to contain high levels of cells with a normal 2n karyotype of 40. However, given the abnormal phenotypic appearance of Hc-flox#2 and 3, only Hc-flox#1 was used in further experiments.

6.2.7.5 Generation of Hc-flox chimeras.

Initially, Hc-flox#1 cells were injected into 83 stage 5 blastocysts that were inserted into 3 pseudo-pregnant C57/Bl6 recipients (Injection was undertaken by GenSA, South Australia). Following gestation, only 6 pups were born with no coat colour chimeras being

Figure 6.9

A. Characterisation of HccsKO#4 targeted ES cells with Hccs3'#2
Genomic DNA was extracted from ES cells, digested with *Bam*HI and Southern blot analysis completed with Hccs3'#2. An example digestion is represented at the top while the bottom shows an example Southern blot. Relative positions of the wt band and the targeted band are shown.

B. Characterisation of HccsKO#4 targeted ES cells with Hccs5'#2
Genomic DNA was extracted from the positive ES cells identified with Hccs3'#2, digested with *Nhe*I and probed with Hccs5'#2. An example digestion and Southern blot are shown. Relative positions of the wt band and the targeted band are also indicated.

C. Analysis of targeted ES cells for inclusion of 5' LoxP
PCR with mHCCS#3 and mHCCS#4 was completed on genomic DNA from targeted ES cells with positive (+) and negative (-) controls. Amplification products were analysed on 1.5% agarose gels. In all figures numbers refer to the ES cell colony being analysed and M is marker lane.

A.

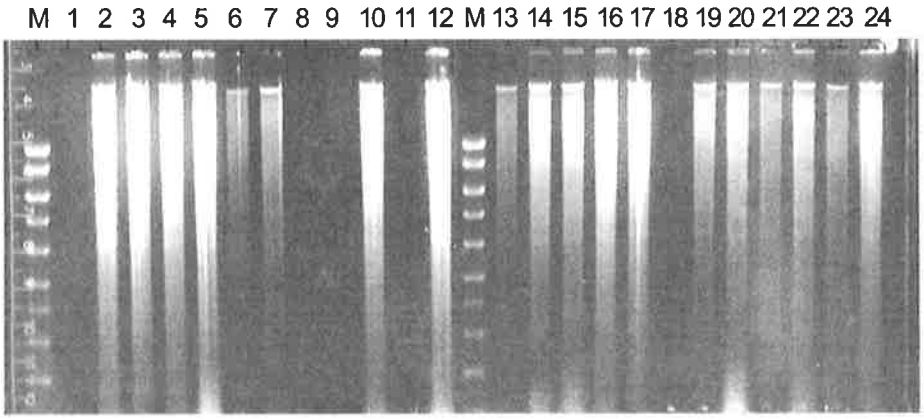
M 1 2 3 4 5 6 7 8 9 10 11 12 M 13 14 15 16 17 18 19 20 21 22 23 24


M 1 2 3 4 5 6 7 8 9 10 11 12 M 13 14 15 16 17 18 19 20 21 22 23 24
wt ~ 13kb
targeted ~ 9.5b

B.

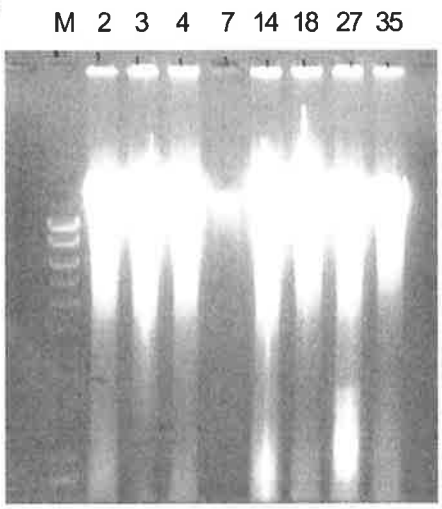
M 2 3 4 7 14 18 27 35

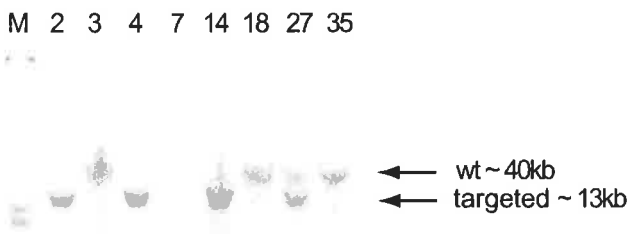
M 2 3 4 7 14 18 27 35
wt ~ 40kb
targeted ~ 13kb

C.

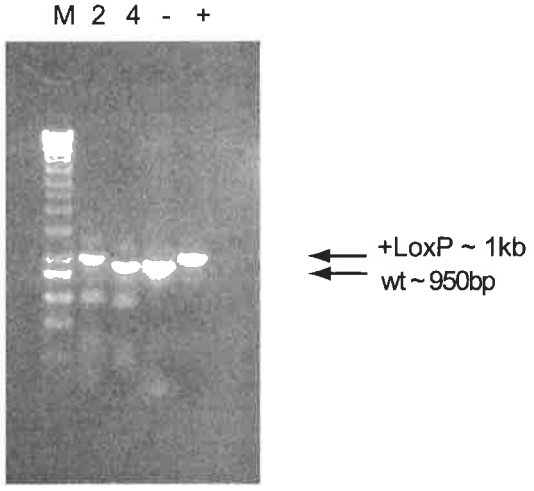
M 2 4 - +
+LoxP ~ 1kb
wt ~ 950bp

Figure 6.10

A. Karyotype analysis of Hc-flox #1-3
Hc-flox#1-3 were grown in feeder free plates and treated with colchicine to arrest cells in metaphase. Following hypo-osmotic swelling cells were mounted on slides. Chromosome numbers were counted from a total of 50 cells of each floxed *Hccs* line and plotted on a bar graph.

B. Example karyotype of Hc-flox#1
Images were taken on an Olympus ATX 70 miroscope with a Fujix HC-1000 3CCD camera. Shown is an example image of a normal cell with 2n = 40.

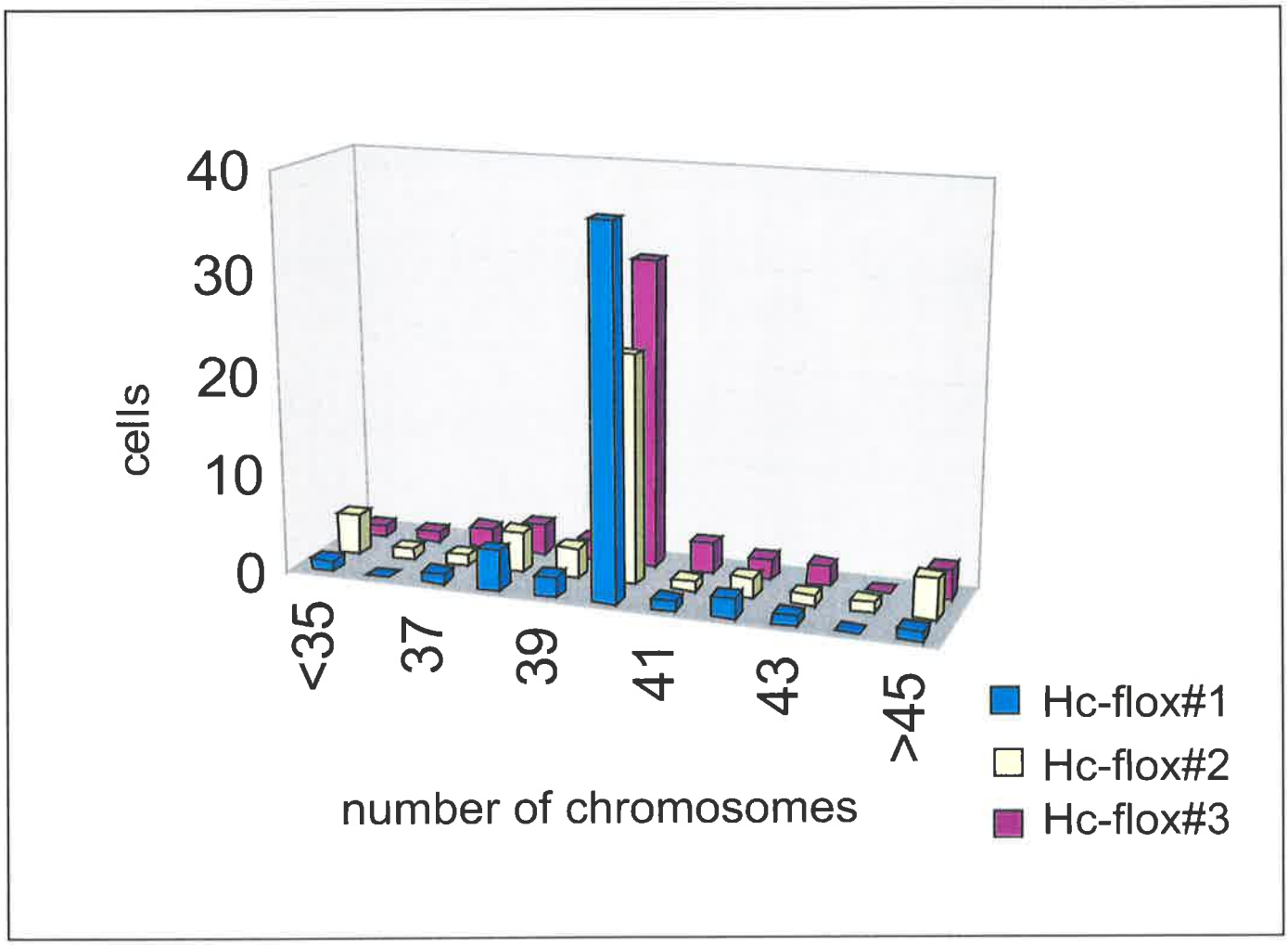
40
30
20
10
0
cells
<35
37
39
41
43
>45
number of chromosomes
Hc-flox#1
Hc-flox#2
Hc-flox#3

identified. A second round of injections into 2 pseudopregnant females also resulted in low birth levels with no coat colour chimeras. Given the normal karyotype of these cells and that the majority of host blastocysts did not implant or reach term suggested a possible problem with the injection procedure itself. Indeed, even unhealthy ES cells are expected to have low levels of colonisation. Interestingly, other attempts at GenSA (South Australia) to inject other ES cells that had previously formed high percentage coat colour chimeras that colonised the germline were also unsuccessful at this time (Dr. R. Keough, personal communication).

In parallel experiments, two of the cell lines identified by OZGENE (178-1E1 and 178-1D4) were injected into C57/Bl6 hosts prior to confirming the inclusion of the 5' most loxP site. Fortuitously, both of the cell lines injected were identified to carry this loxP site. Following gestation, a number of high-level coat colour chimeric pups were identified (Table 6.2) that have subsequently been found to colonise the germline. At the time of writing this thesis, these mice were being bred to obtain homozygous females before genotyping to confirm the presence of the floxed *Hccs* gene.

6.2.7.6 Removal of *Hccs* ex5-7 in ES cells.

One of the many advantages in using ES cells to study gene function is their ability to differentiate into any cell type. Recent advances in the understanding of these processes now allow the continually growing cell population to be directed into almost any specific cell in culture (i.e. cardiomyocytes). Indeed, this approach is often utilised to overcome the problems associated with lethal phenotypes of genes involved in early development and can provide complimentary results more readily than through the production of a mouse KO line. In such an approach, removal of *Hccs* exon 5-7 *in vitro* can be analysed by transiently over-expressing cre recombinase in the *Hccs* floxed cell line. To address any phenotype associated with the removal of *Hccs* in these cells, a vector (pBS185) expressing cre from the CMV promoter was obtained (generously provided by Dr P. Farley, Murdoch Institute, Melbourne). pBS185 had previously been electroporated into three independent ES cell lines by Araki *et al* (1997) with an efficiency of cre-mediated recombination of up to 8%.

ES clone	Chimera #	Sex	Birth date	% chimera
178-1E1	1	M	21-12-2002	90
	2	M	21-12-2002	90
	3	F	21-12-2002	100
	4	F	21-12-2002	100
	5	F	21-12-2002	100
	6	F	21-12-2002	90
	7	F	21-12-2002	90
	8	M	21-12-2002	100
	9	F	21-12-2002	100
	10	F	21-12-2002	100
	11	M	21-12-2002	100
	12	M	21-12-2002	90
	13	M	21-12-2002	90
	14	F	21-12-2002	100
	15	F	21-12-2002	100
	16	F	21-12-2002	100
	17	F	21-12-2002	<25
	18	M	26-12-2002	100
	19	M	26-12-2002	100
	20	M	26-12-2002	100
	21	F	26-12-2002	100
	22	F	26-12-2002	100
	23	F	26-12-2002	100
	24	F	26-12-2002	75
	25	M	26-12-2002	100
	26	M	26-12-2002	100
	27	M	26-12-2002	100
	28	M	26-12-2002	<25
	29	F	26-12-2002	100
	30	F	26-12-2002	100
	31	F	26-12-2002	100
178-1D4	1	F	27-12-2002	100
	2	M	27-12-2002	100
	3	M	27-12-2002	100
	4	M	27-12-2002	100

Table 6.2 Coat colour chimera percentages of the blastocyst injections with two independent *Hccs* floxed cell lines.

Similar to the eventual KO in mice, removal of *Hccs* in cell culture would be expected to result in a lack of functional cytochrome c and therefore effects on the mitochondrial respiratory chain. Similar deficiencies within the various mitochondriopathies have previously been suggested to lead to mitochondrial hyperplasia as a compensatory mechanism to increase energy production (Papadimitriou *et al*, 1984). Recent studies using cells derived from a cytochrome c KO utilised media supplemented with 100 μg/ml pyruvate and 50 μg/ml uridine to allow near normal growth of mutant cells (Li *et al*, 2000). With this in mind, growth media was supplemented with both reagents in the following experiments.

The Hc-flox#1 cell line was electroporated with the plasmid pBS185 following methods established by Araki *et al* (1997). Initially, all the cells were seeded onto 10cm plates in the presence or absence of sto^r feeders. Following 12hrs of expression the cells were collected for genomic DNA preparation to analyse cre mediated recombination by PCR. Primers were designed in the intronic sequence around the positions in which the 5' and 3' loxP sites were inserted (mHCCS21 & 24, respectively) (see Fig 6.7) such that amplification of a 434 bp fragment would result if recombination had occurred (Fig 6.11). Internal primers to each site (mHCCS22 & 23 for use with mHCCS 21 & 24, respectively) were also designed to confirm that mHCCS 21 & 24 did indeed confer PCR aplification under the conditions used (i.e. temperature and extension times). The primer pair mHCCS21/22 amplified a 360 bp fragment over the *Xba*I site in which the *Neo*^{r} gene and the 3' loxP site were placed into wt genomic DNA, while mHCCS23/24 amplified a 380 bp fragment over the XbaI site in which the 5' LoxP site was placed in wt genomic DNA. Amplification with each primer pair confirmed the PCR conditions and importantly demonstrated cre-mediated excision of the intervening sequence between the two loxP sites (Fig 6.11A).

To isolate cells in which exons 5-7 of *Hccs* had been deleted, the Hc-flox#1 cell line was again electroporated with pBS185. Cells were plated onto sto^r feeders at low density in media supplemented with pyruvate and uridine without G418 resistance and grown 7 days to allow formation of single colonies. Given the efficiency of recombination reported by Smith *et al* (1996) only 96 colonies were isolated from the plates. Following expansion of these colonies, replica plates were grown in the supplemented media with and without G418 selection. 18 of the cells found to have decreased growth in G418 media were further expanded from the replica plate for analysis of *Bam*HI restricted genomic DNA with the

Hccs3'#2 probe. If recombination had occurred in these cells Southern analysis would show a normal targeted band at ~ 9.5 kb and a recombined band at ~ 40kb, however, in each line only the targeted band was identified (Fig 6.11B). As recombination has been confirmed by PCR this result suggests that the expected deficiency in complex III and IV of the mitochondrial respiratory chain may be deleterious to survival even with the use of supplemented media. Hence, during the period required for the identification of single colonies, all HccsΔEx5-7 cells may have been lost. Further experiments utilising a shorter growth time may allow these cells to be isolated and thus facilitate further studies on differentiated cells. Indeed, prior guidance into the cardiomyocyte lineage would be ideal to address any role mutant *Hccs* may partake in the presentation of OC (i.e. mitochondrial hyperplasia and deficiencies in the mitochondrial respiratory chain).

6.3 Summary.

This chapter outlines the work that has been completed to produce a conditional mouse KO with the aim of studying the removal of *Hccs* as a potential model for OC associated with MIDAS syndrome. There is considerable identity (85%) between the human and mouse sequences (see Fig 1.3) and, as expected, this level of identity decreases when compared to sequences from species that are more evolutionarily divergent (Steiner *et al,* 1995). Comparison of the genomic clones spanning the murine locus with genomic sequence across the human HCCS locus at Xp22.3 shows that the two genes are similar in their overall size, each being comprised of seven exons with conservation of all splice site positions. As in humans, the mouse gene is located on the X chromosome in a position syntenic to Xp22.3 and is adjacent, and transcribed in the opposite direction, to the *Arhgap6* / *ARHGAP6* gene in both species. This conservation highlights the similarity between the two genes and the potential use of *Hccs* as a model for the removal of *HCCS* in the presentation of OC.

Several attempts to utilise a construct containing loxP sites surrounding exons 3-4 of the gene with the positive selection marker between exons 2-3 failed to produce any homologous recombinants. As *Hccs* is X-linked, only one copy of the gene is present in the male ES cells used in this project. It then follows that any moderate reduction of gene expression which can occur from the insertion of selection markers within a gene, may impact

Figure 6.11

Analysis of cre mediated recombination in Hc-flox#1 ES cells
Hc-flox#1 ES cells were electroporated with pBS185 that expresses cre recombinase from the CMV promoter. (A) Cells were allowed to grow in the presence (+cre-feeder) or absence (+cre) of sto^r feeder cells. Following 12 hrs of growth, genomic DNA was extracted from the cells and analysed by PCR. Relative positions of mHCCS21 (m21), mHCCS22 (m22), mHCCS23 (m23) and mHCCS24 (m24) are shown in figure 6.7. Amplification of a 330bp fragment with m21 and m22 over the *Xba*I site in which *Neo*^{r} and a loxP site from wt DNA confirms PCR conditions. Likewise, amplification of a 360bp or 410bp fragment with m23 and m24 over the *Xba*I site in which the 5' loxP site was placed from wt DNA also confirms PCR conditions. Cre mediated recombination between the two loxP sites was detected by amplification of a 434bp fragment with m21 and m24. Control PCR was completed from Hc-flox#1 and wt genomic DNA. (B) Individual colonies were isolated from electroporated cells and replica plated in media with and without G418 selection. Genomic DNA was extracted from 16 of the 18 cell lines identified to have decreased growth under selection. Following *Bam*HI restriction enzyme digestion Southern analysis was completed with Hccs5'#2. The positions of the wt band and the band expected from cre mediated recombination are highlighted by arrows. M, marker lane; *, *Bam*HI digested genomic DNA from Hc-flox#1 and –ve, no DNA.

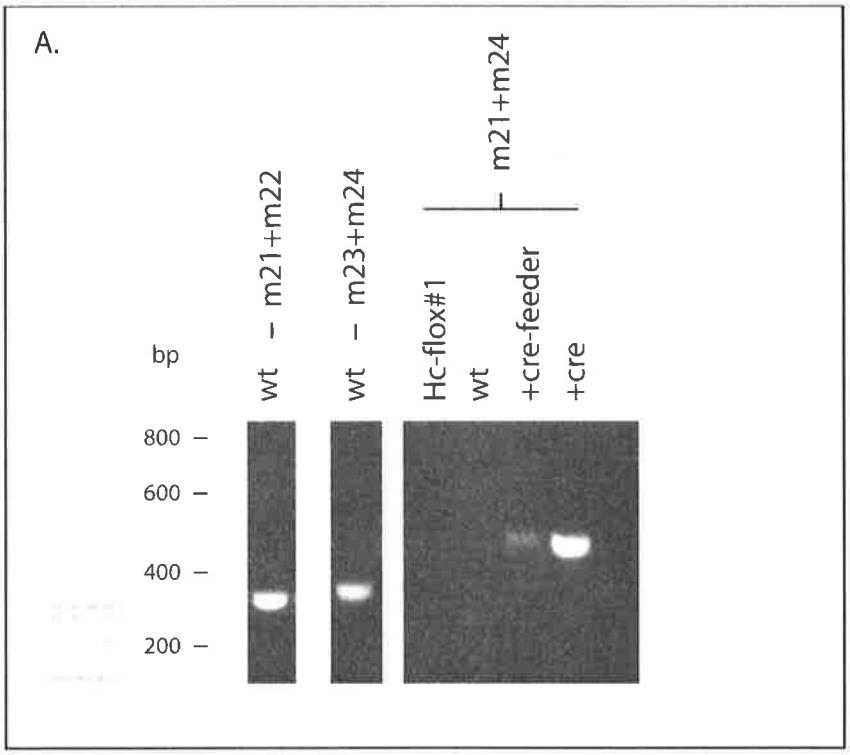
A.
m21+m24
wt – m21+m22
wt – m23+m24
Hc-flox#1
wt
+cre-feeder
+cre
bp
800
600
400
200

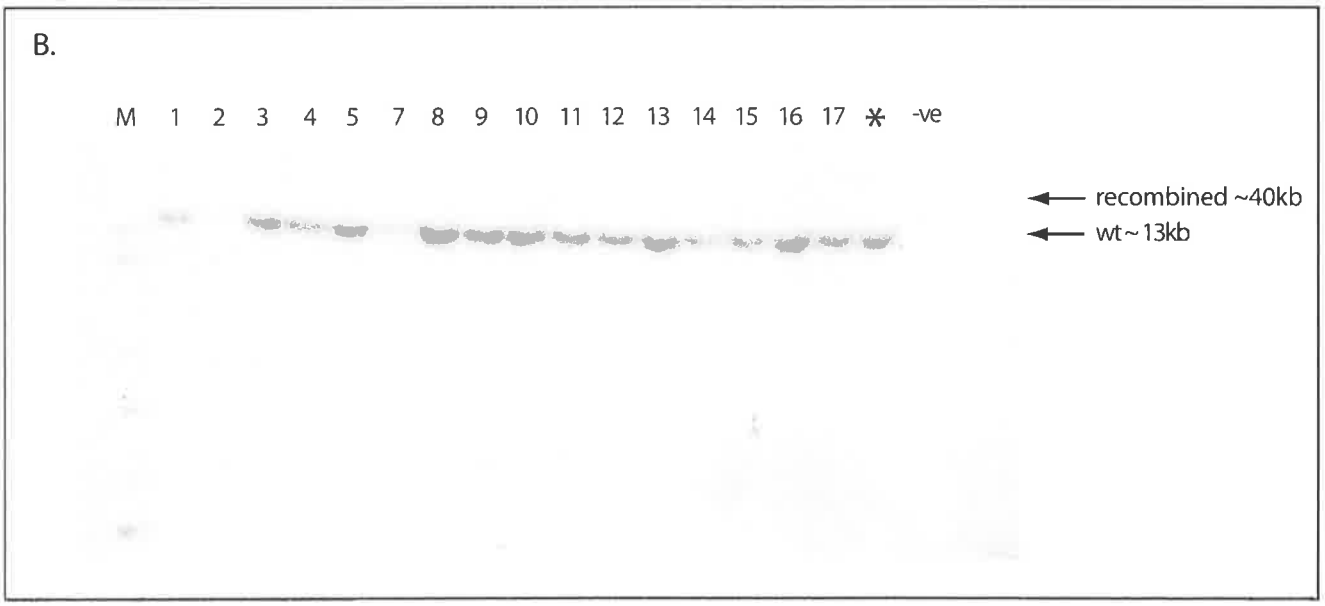
B.
M 1 2 3 4 5 7 8 9 10 11 12 13 14 15 16 17 * -ve
recombined ~40kb
wt ~ 13kb

on cell survival in comparison to autosomal genes. For *Hccs*, the decreased level of mature cytochrome c expected with such a hypomorphic allele could significantly impact on the production of cellular energy through the mitochondrial respiratory chain. Such deficiencies have been reported in many human disorders and also recently in mice (i.e. cytochrome c KO).

As would be expected, cytochrome c deficient mice die *in utero* by mid-gestation (Li *et al*, 2000). Experiments completed on cultured fibroblasts from these mice identified major deficiencies in both OXPHOS and programmed cell death. Decreased levels of *Hccs* are also expected to have similar deficiencies that may be deleterious to ES cell viability and indeed, the conditional KO approach was adopted in the first instance for this reason. During the end stages of this project, Prakash *et al* (2002) detailed the deletion of the entire region corresponding to the human MIDAS critical region in mice as a means of studying the removal of *Hccs in vivo*. This approach was adopted as earlier attempts to create either null or conditional removal of Hccs with insertion of a selection marker within the gene were unsuccessful (Prakash *et al*, 2002). This further supports the view that the reduced levels of *Hccs* from the targeting vectors initially used in this thesis (HccsKO#1-3) may also have had a severe impact on cell survival that did not permit growth of homologous recombinants.

As expected, the "MLS" mice died before birth (Prakash *et al*, 2002); an effect attributed by the authors to the removal of *Hccs*. This result should be taken with caution, however, as the KO removes an ~300kb region of genomic DNA that contains at least three identified genes and a number of incompletely characterised genes. Of the reported full length genes, *Arhgap6*, a Rho type GTPase activating protein, that maps centromeric to *Hccs* has no detectable phenotype in a previously reported null KO (Prakash *et al*, 2000). Likewise, removal of the other gene in this region, *MidI*, a member of the RBCC superfamily of proteins, that maps telomeric of *Hccs* also has no gross phenotype (Dr. T. Cox and Dr. A. Ashworth, personal communication). Loss-of-function mutations in *Mid1* do, however, cause X-linked Opitz syndrome, a disorder that presents only mildly in females (Quaderi *et al* 1998; Cox *et al*, 2000). At least in the latter case, presentation of a phenotype in mice may be affected by gene redundancy. Similar justification was used by Kayserili *et al* (2001) to redefine the MIDAS critical region to an ~260kb interval between the *MID1* and *ARHGAP6* genes. Notably, *HCCS / Hccs* is the only full length gene so far identified in this region. In

addition, preliminary expression data has been obtained from a highly conserved segment of DNA in this region that also suggests other transcripts may be encoded within the ~260kb critical interval (results not shown). Consequently, the conditional removal of only *Hccs* as outlined in this thesis will specifically address whether decreased respiratory chain function is the true reason for the paucity of males with MIDAS syndrome and OC.

Further attempts to create a mouse line with floxed *Hccs* were completed with a construct introducing the selection marker outside of the gene with loxP sites surrounding exons 5-7. Removal of such a region would be expected to reduce all enzymatic function of the protein as this would delete the catalytic domain. From two independent electroporations, eight correctly targeted colonies were identified and used to produce germline transmission of the floxed *Hccs* allele. While these mice have yet to be crossed with cre expressing lines, the tools have now been synthesised to address the specific phenotype associated with removal of only *Hccs*. Expression analysis obtained from adult tissue in both human and mice provide clues to the potential phenotypes that may be expected from removal of this gene. In this respect, northern analysis and semi-quantitative RT-PCR have shown highest expression within adult heart, skeletal muscle, and ocular tissue (Schwarz & Cox, 2002; Schaefer et al, 1996), all tissues that require high levels of energy.

As mentioned previously, the *Hccs* floxed mouse line generated here has been designed to study any effect the removal of this gene may have in the presentation of a heart phenotype. Analysis of such a defect will be addressed with crosses to transgenic lines expressing cre recombinase from the Nkx2-5 promoter. As MIDAS and OC have associated eye defects it is also important to study removal of this gene in ocular tissue. For these purposes a cre transgenic line that expresses the recombinase from the *Pax6* promoter has been identified (Ashery-Padan *et al*, 2000). This transgene is expressed from embryonic day eight before any detectable morphological differentiation of eye tissue. Removal in the eye may be expected to present as microphthalmia that has also been suggested by Prakash *et al* (2002) for their KO. Mice produced from such a cross will allow the analysis of any role that *Hccs* /*HCCS* has in the pathogenesis of OC and the MIDAS syndrome phenotype. Prior to these analyses it is imperative to show stable inheritance of the X-linked floxed gene and that gene activity is unaffected by the insertion of loxP sites and *Neo*^{r} sequences. To this end, expression levels of the gene will be addressed by RT-PCR, while the size of the protein,

correct localisation and also protein levels will be analysed with the Hccs antiserum detailed in previous chapters. Indeed, this should also be analysed on crosses to cre expressing lines to confirm the reduction of functional Hccs protein upon the excision of exons 5-7.

Finally, attempts were made in the presence of pyruvate and uridine supplemented media to isolate an ES cell line with deletion of exons 5-7 of *Hccs*. While this media is sufficient for the growth of a fibroblast cell line lacking cytochrome c (Li *et al*, 2000) it may not have been sufficient for the survival of the ES cells used in these experiments. Indeed, just to promote cell growth and survival, ES cells require the addition of alternative factors in the growth media to that used for the fibroblast cells lacking cytochrome c. An alternative approach to study Hccs removal *in vitro* could perhaps be completed in fibroblasts obtained from the complete KO of Hccs following breeding of the floxed mice to a line expressing cre recombinase from a constitutive promoter (i.e. β-actin cre-transgene; Larsson *et al*, 1998).

Chapter Seven: Final Summary.

7.1 Summary.

The work completed in this thesis was undertaken to address the initial hypothesis that deficiencies within the putative human CTS may lead to the presentation of OC associated with MIDAS syndrome. As mentioned in the introduction chapter, the putative human *CTS* cDNA (Schaefer *et al*, 1996) is the only complete gene so far identified in the MIDAS critical interval refined by Kayserili *et al* (2001) to a ~260 kb region; bounded distally by *MID1* and proximally by *ARHGAP6*. The putative gene was initially suggested to encode a cytochrome c-type synthase (CTS) based on the significant amino acid sequence identity with the primary sequences of the yeast holocytochrome c synthase (HCCS or Cyc3p) and holocytochrome c1 synthase (HCC1S or Cyc2p).

To provide support for a conserved mitochondrial function of human CTS-like protein, localisation within mammalian cells was initially analysed. The work in chapter 3 and 4 has shown that an over-expressed *hCTS* fusion construct, and importantly, the hCTS native protein is indeed localised to the mitochondrial inter-membrane space (IMS). This localisation is consistent with an expected role in the mitochondrial respiratory chain. Subsequent successful complementation of the *S.cerevisiae* Cyc3 mutant conclusively demonstrated that this human protein is able to catalyse the covalent addition of heme to cytochrome c, that in turn allows transfer of electrons from complex III to complex IV of the mitochondrial respiratory chain. As OC has been documented to arise from deficiencies of cytochrome complexes III and IV in several cases, these results provide additional support for the initial hypothesis. Further supporting evidence may be found in previous studies of this gene in human and mouse that highlight increased expression in adult heart and skeletal muscle (Schaefer *et al*, 1996; Schwarz & Cox, 2002), a profile that is similar to other OXPHOS enzymes (Levy *et al*, 2000; Larsson *et al*, 1998).

The inability of mammalian HCCS to rescue the yeast Cyt2p mutant prompted extensive searches of the available EST and genomic databases in attempt to identify a putative holocytochrome c1 synthase (*Cyt2p*) orthologue (based on sequence similarity). The failure to detect such sequences in any species other than yeasts suggested that either: 1) In

all organisms other than yeasts, one holocytochrome c-type synthase catalyses the insertion of heme into both cytochrome c and c1; 2) The insertion of heme into apocytochrome c1 occurs spontaneously at a sufficient level within higher eukaryotes; or 3) The insertion of heme into apocytochrome c1 is catalysed by a different enzyme in higher eukaryotes, or at least one that is considerably more divergent from *Cyt2p* such that more sensitive search parameters may be required for detection of similarity. During the writing of this thesis, Bernard *et al* (2003) presented data that appear to clarify this issue. In contrast to the results presented in this thesis, their paper details the ability of human HCCS to complement both the Cyc3p (HCCS) and Cyt2p (HCC1S) growth phenotypes on non-fermentable carbon sources, and therefore an overlapping specificity of HCCS for both apocytochrome c and c1. The reason for this discrepancy likely resides in the level of expression of the mammalian *HCCS* in the different yeast experiments. For example, their growth rescue results clearly indicate that human HCCS is able to complement the Cyc3p (HCCS) deficiency to the same extent as native yeast protein; whilst also complementing the Cyt2p (HCC1S) deficiency to approximately 50% of normal growth. In the assay completed in this thesis only a partial growth rescue of the Cy3p (HCCS; approximately 5-10%) phenotype was obtained with the human HCCS protein in comparison to native *S.cerivisiae* Cyc3p. Bernard *et al* (2003) suggest that there differences may be attributed to the alternative promoters used in the studies to drive expression of the different CTS enzymes: The heterologous *S.pombe* alcohol dehydrogenase promoter used here may not have been as efficient as the *S.cerevisiae* phosphoglucokinase promoter used in their study. This implies that growth complementation of the CTS mutants may vary due to dosage levels of the HCCS protein. With this in mind then, the same relative reduction of *hHCCS* expression in the Cyt2p complementation assay (as seen in the Cyc3p complementation) may not have been sufficient to overcome any growth deficiency. However, it must also be mentioned that in the assay presented here only 2% glycerol was used as the sole carbon source, while no mention was made of the level of glucose used in their study. Regardless, the combined studies support the notion that a specific human Cyt2p orthologue does not exist, but that hHCCS can perform the covalent attachment of heme to cytochrome c1 (albeit with lower efficiency in yeast). The production of floxed *Hccs* ES cells and a targeted mouse line (as detailed in chapter 6) may enable further biochemical analysis of this possibility.

Targeting of proteins to the mitochondrial IMS is still poorly understood in contrast to matrix and membrane targeting. Chapter 4 detailed the work completed to investigate the minimal sequences involved in correctly targeting the mammalian protein to mitochondria and initial studies into the mechanism by which mammalian HCCS completes this targeting event. The first 48 amino acids of HCCS were found to be necessary and sufficient for correct targeting to the IMS. The presence of an N-terminal targeting sequence is reminiscent of import sequences for matrix enzymes (i.e. ALAS2), however, the amino acids encoded by this region lack any elements that would be considered to allow the formation of an alpha helix typical of matrix targeting sequences. In fact, the HCCS N-terminus is essentially charge neutral. Therefore, the localisation of HCCS to mitochondria is likely to occur by an alternative mechanism to the typical targeting of most mitochondrial proteins.

Not surprisingly, the first 48 amino acids are highly conserved between humans and mice. However, given that this region is not conserved with the yeast CTS enzymes, it therefore represents a novel topogenic signalling sequence. This result also highlights the caution that should be taken when extrapolating data from lower eukaryotes to higher organisms.

The mechanisms of mitochondrial targeting have been investigated for only a few proteins localised to the IMS. From these studies, a consensus of hydrophobic stretches preceded by a number of positively charged residues has been found to be indicative of the sorting signals encoded by such proteins as cytochrome b2 and cytochrome c1. However, sequence analysis suggests that the HCCS protein does not possess such characteristics. To further investigate this, a construct containing the typical mitochondrial targeting signal of ALAS2 fused to full length HCCS was completed and introduced into cultured cells. The targeting of the fusion protein to the matrix suggested that HCCS may not contain internal sorting sequences for retention within the IMS. Consistent with the experiments of Segui Real *et al* (1993), this may also suggest that mammalian HCCS utilises a similar mechanism to that of the *S.cerevisiae* and *N.crassa* CTS's, albeit with the utilisation of an alternative signal.

The work described in chapter 5 has been specifically directed at identifying potential mutations within the *HCCS* gene from a cohort of OC patients. No definitive mutations were identified in *HCCS* from the seven patients available for testing. However, as mentioned,

several problems with these cases were identified and discussed in detail. That most of the patients did not actually present with any other features that would suggest an X-linked basis, and the relatively small numbers analysed, does lend support for the justification of further analysis of the *HCCS* gene in additional cases. Ultimately, these studies will address any potential role that mutations in *HCCS* have in the pathogenesis of OC. As currently hypothesised, any mutation in human *HCCS* could conceivably give rise to a nuclear encoded respiratory chain defect that would have expected deleterious consequences in numerous tissues. Removal of the *HCCS* gene within OC or MIDAS patients would suitably account for the paucity of male patients and the associated muscle defects occasionally described in these conditions.

Despite not finding a mutation in the case of Bird *et al* (1994) which has no deletion over 100 kb, the characteristic MIDAS facial lesions in this patient are nevertheless consistent with a defect in the 260 kb MIDAS critical interval on Xp22.3. Therefore, this case will be an invaluable resource for ultimately identifying the underlying genetic fault. Analysis of recent informative markers within this chromosomal region may therefore aid in resolving this issue.

Chapter 6 also details the analysis of the *cytochrome b* gene from available cases of OC. The sequencing of this gene has identified two patients harbouring variants that may infer a pathogenic mutation. In addition, a number of both non-coding base pair substitutions and amino acid changes unique to this study were found. The first alteration that may be pathogenic is that of the C15452A substitution in patient HC5. This change has previously been reported in a case of ischaemic cardiomyopathy and was associated with a reduction of complex III activity by over 50% in that patient (Marin-Garcia *et al*, 1996). Given that this amino acid is not well conserved in other species, and that this mutation would not be predicted to have any effect on the formation of the Coenzyme Q - cytochrome *c* reductase complex, Fisher & Meunier (2001) have suggested that it may therefore represent a standard polymorphism. Indeed, Marin-Garcia *et al* (1996) observed this mutation in 2 of the 42 controls tested. However, lending support to there argument for a causative role is the fact that the same reduction of complex III activity was detected in each of the cases with the alteration. The second alteration of G15431A in patient HC4 results in the substitution of an alanine at amino acid 229 to a threonine, a change that was unique to this study. This

alteration occurs in the transmembrane region of the protein and therefore may not be expected to have any deleterious affect on the formation of complex III. However, that only one of over 10 other species analysed harbours a threonine at this position indicates that a role of this variant in the presentation of OC can not be excluded. Further analysis of additional family members should shed light on the mode of inheritance of both base changes and potentially identify the more likely contributory variant to the presentation of the disorder.

With the cases presented here, together with that of Andreu *et al* (2000), three separate *cytochrome b* mutations have now been highlighted as potentially pathogenic mutations for the presentation of OC. This further supports the notion of more than one gene being involved in the presentation of the OC phenotype. With this in mind, future experiments addressing the role of *HCCS* may best be limited to only those cases that show a pattern of inheritance consistent with X-linkage and to those having additional features associated with the MIDAS syndrome phenotype.

Given that X-linked cases of OC with associated MIDAS features are only expected to be female, a conditional mouse KO of the *Hccs* gene was initiated and detailed in chapter 6 to address any role HCCS may have in the presentation of OC. While functional studies on a model system such as mice would also be ideal to analyse the possible pathogenic nature of the *cytochrome b* mutations presented in this study, the production of mitochondrial mutants by targeted homologous recombination are not yet possible.

Removal of an essential X-linked gene in male ES cells also poses other problems, hence a conditional approach was deemed most appropriate. Following several unsuccessful attempts to create a conditional KO of exons 3-4 of the *Hccs* gene an alternative approach was devised to specifically target exons 6-7 with inclusion of the positive selection marker outside of the last coding exon. As mentioned, one possible explanation for the lack of selection of targeted ES cells with the initial constructs may have been due to reduction of gene expression from inclusion of the selection marker between exons 2-3: Either from premature transcriptional termination due to recognition of the *Neo*^{r} polyA signal (forward orientation), or utilisation of a cryptic splice site in *Neo*^{r} (reverse orientation). In this scenario a significant decrease in the amount of *Hccs* expression within the cell might therefore be expected. This, in turn, would also decrease the level of functional cytochrome c

within the cell, such as reported for the recently produced cytochrome c KO (Li *et al*, 2000). As expected, cytochrome c deficient mice die *in utero* by mid-gestation from major deficiencies in both OXPHOS and programmed cell death (Li *et al*, 2000). During the course of this project, Prakash *et al* (2002) detailed the deletion of the entire region corresponding to the human MIDAS critical region in mice as a means of studying the removal of *Hccs in vivo*. Similar to the cytochrome c KO, the "MLS" mice died before birth. However, as the "MLS" KO removes an ~300kb region of genomic DNA that contains at least three identified genes and multiple partial genes, the embryonic lethality can not be definitively ascribed to *Hccs*.

Correctly targeted ES cells were, however, ultimately obtained for the construct that introduced the selection marker outside of the coding region for the *Hccs* gene. Furthermore, during the writing of this thesis, these colonies were used to produce germline transmission of the floxed *Hccs* allele. While results from these mice are still being awaited, the resources are now available to address the initial aims of this thesis. Nevertheless, given the expression pattern of *HCCS* and *Hccs* in adult tissue being highest within heart, skeletal muscle and ocular tissue (Schwarz & Cox, 2002; Schaefer *et al*, 1996), removal of this gene is expected to produce a phenotype reminiscent of the mitochondrial myopathies, and will permit a more complete assessment to address the role of *Hccs* in the presentation of OC associated with MIDAS syndrome.

Bibliography.

Abe Y., Shodai T., Muto T., Mihara K., Torii H., Nishikawa S., Endo T., and Kohda D. (2000). Structural basis of presequence recognition by the mitochondrial protein import receptor Tom20. *Cell* **100:** 551-60.

Aebi M., Hornig H., Padgett R., Reiser J., and Weissmann C. (1986). Sequence requirements for splicing of higher eukaryotic nuclear pre-mRNA. *Cell* **47:** 555-65.

Aicardi J., and Chevrie J. (1994). The Aicardi Syndrome. *In* "Callosal Agenesis" (M. Lassonde, and M. Jeeves, Eds.), pp. 7-17, Plenum Press, New York.

Al-Gazali L., Mueller R., Caine A., Antoniou A., McCartney A., Fitchett M., and Dennis N. (1990). Two 46,XX,t(X;Y) females with linear skin defects and congenital microphthalmia: A new syndrome at Xp22.3. *Journal of Medical Genetics* **27:** 59-63.

Allanson J., and Richter S. (1991). Linear skin defects and congenital microphthalmia: A new syndrome at Xp22.2. *Journal of Medical Genetics* **28:** 143-4.

Andreu A., Checcarelli N., Iwata S., Shanske S., and DiMauro S. (2000). A missense mutation in the mitochondrial *cytochrome b* gene in a revisited case with histiocytoid cardiomyopathy. *Pediatric Research* **48:** 311-4.

Andreu A., Hanna M., Reichmann H., Bruno C., Penn A., Tanji K., Pallotti F., Iwata S., Bonilla E., Lach B., Morgan Hughes J., and DiMauro S. (1999). Exercise intolerance due to mutations in the *cytochrome b* gene of mitochondrial DNA. *The New England Journal of Medicine* **341:** 1037-44.

Araki K., Araki M., and Yamamura K. (1997). Targeted integration of DNA using mutant lox sites in embryonic stem cells. *Nucleic Acids Research* **25:** 868-72.

Araki K., Imaizumi T., Okuyama K., Oike Y., and Yamamura K. (1997). Efficiency of recombination by Cre transient expression in embryonic stem cells: Comparison of various promoters. *The Journal of Biochemistry* **122:** 977-82.

Attard M. (1998). Analysis of a candidate gene for MIDAS syndrome. *In* "Department of Genetics", University of Adelaide, Adelaide.

Baker A., Kaplan C., and Pool M. (1996). Protein targeting and translocation; a comparative survey. *Biological Reviews of the Cambridge Philosophical Society* **71:** 637-702.

Ballabio A., and Andria G. (1992). Deletions and translocations involving the distal short arm of the human X chromosome: review and hypotheses. *Human Molecular Genetics* **1:** 221-7.

Barnett L., and Koentgen F. (2001). Gene targeting in a centralized facility. *Methods in Molecular Biology* **158:** 65-82.

Bassi M., Schiaffino M. V., Renieri A., De Nigris F., Galli L., Bruttini M., Gebbia M., Bergen A., Lewis R., and Ballabio A. (1995). Cloning of the gene for ocular albinism type 1 from the distal short arm of the X chromosome. *Nature Genetics* **10:** 13-9.

Baubonis W., and Sauer B. (1993). Genomic targeting with purified Cre recombinase. *Nucleic Acids Research* **21:** 2025-9.

Bernard D., Gabilly S., Dujardin G., Merchant S., and Hamel P. (2003). Overlapping specificities of the mitochondrial cytochrome c and c1 heme lyases. *The Journal of Biological Chemistry* **278:** 49732-42.

Bird L., Krous H., Eichenfield L., Swalwell C., and Jones M. (1994). Female infant with oncocytic cardiomyopathy and microphthalmia with linear skin defects (MLS): A clue to the pathogenesis of oncocytic cardiomyopathy? *American Journal of Medical Genetics* **53:** 141-8.

Bleistein J., and Zierz S. (1989). Partial deficiency of complexes I and IV of the mitochondrial respiratory chain in skeletal muscle of two patients with mitochondrial myopathy. *Journal of Neurology* **236:** 218-222.

Bodmer R., Jan L., and Jan Y. (1990). A new homeobox-containing gene, msh-2, is transiently expressed early during mesoderm formation of Drosophila. *Development* **110:** 661-9.

Bohles H., Singer H., Ruitenbeek W., Trijbels J., Sengers R., Ketelsen U., Wagner Thiessen E., and Wick H. (1987). Foamy myocardial transformation in a child with a disturbed respiratory chain. *European Journal of Pediatrics* **146:** 582-6.

Boissy C., Chevallier A., Michiels J., De Swarte M., Mariani R., Hofman P., and Saint Paul M. (1997). Histiocytoid cardiomyopathy: A cause of sudden death in infancy. *Pathology, Research and Practice* **193:** 589-93; discussion 595-6.

Bonifas J., Morley B., Oakey R., Kan Y., and Epstein E. (1987). Cloning of a cDNA for steroid sulfatase: Frequent occurrence of gene deletions in patients with recessive X chromosome-linked ichthyosis. *Proceedings of the National Academy of Sciences of the United States of America* **84:** 9248-51.

Borelli I., Crepaldi T., Frattasio C., and Curtoni E. (1988). A new duplication at the C4B locus associated with the HLA-Aw68, Cw8, Bw65 haplotype. *Journal of Immunogenetics* **15:** 239-41.

Bronson S., and Smithies O. (1994). Altering mice by homologous recombination using embryonic stem cells. *The Journal of Biological Chemistry* **269:** 27155-8.

Brown C., Hendrich B., Rupert J., Lafreniere R., Xing Y., Lawrence J., and Willard H. (1992). The human *XIST* gene: Analysis of a 17 kb inactive X-specific RNA that contains consereved repeats and is highly localised within the nucleus. *Cell* **71:** 527-542.

Bruton D., Herdson P., and Becroft D. (1977). Histiocytoid cardiomyopathy of infancy: An unexplained myofibre degeneration. *Pathology* **9:** 115-22.

Casanova M., Gil M., Cardenoso L., Martinez J., and Sentandreu R. (1989). Identification of wall-specific antigens synthesized during germ tube formation by *Candida albicans*. *Infection and Immunity* **57:** 262-71.

Chinnery P. (2002). Modulating heteroplasmy. *Trends in Genetics* **18:** 173-6.

Chinnery P., Samuels D., Elson J., and Turnbull D. (2002). Accumulation of mitochondrial DNA mutations in ageing, cancer, and mitochondrial disease: Is there a common mechanism? *Lancet* **360:** 1323-5.

Chinnery P., and Turnbull D. (2001). Epidemiology and treatment of mitochondrial disorders. *American Journal of Medical Genetics* **106:** 94-101.

Colbere Garapin F., Horodniceanu F., Kourilsky P., and Garapin A. (1981). Construction of a dominant selective marker useful for gene transfer studies in animal cells. *Developments in Biological Standardization* **50:** 323-6.

Conboy J., Cox T., Bottomley S., Bawden M., and May B. (1992). Human erythroid 5-aminolevulinate synthase. Gene structure and species-specific differences in alternative RNA splicing. *The Journal of Biological Chemistry* **267:** 18753-8.

Cormier T. A., Prakash S. K., Magner D. B., Zoghbi H. Y., and Van_den_Veyver I. B. (2001). Analysis of *Mid1*, *Hccs*, *Arhgap6*, and *Msl3l1* in X-linked polydactyly (*Xpl*) and Patchy-fur (*Paf*) mutant mice. *Mammalian Genome* **12:** 796-8.

Cox T., Bawden M., Martin A., and May B. (1991). Human erythroid 5-aminolevulinate synthase: Promoter analysis and identification of an iron-responsive element in the mRNA. *The Embo Journal* **10:** 1891-902.

Cox T., Cox L., and Ballabio A. (1998). A very high density microsatellite map (1 STR/41 kb) of 1.7 Mb on Xp22 spanning the microphthalmia with linear skin defects (MLS) syndrome critical region. *European Journal of Human Genetics* **6:** 406-12.

Cox T., Cox L., and Ballabio A. (2001). Development of a very high density microsatellite map (1 STR / 41 kb) in Xp22 reveals two exceptional "non-deletion" cases of microphthalmia with linear skin defects (MLS) syndrome. *European Journal of Human Genetics*.

Cox T., Sadlon T., Schwarz Q., Matthews C., Wise P., Cox L., Bottomley S., and May B. (2004). The major splice variant of human 5-aminolevulinate synthase-2 contributes significantly to erythroid heme biosynthesis. *The International Journal of Biochemistry & Cell Biology* **36:** 281-95.

Darley Usmar V., and Schapira A. (1994). "Mitochondria: DNA, proteins and disease.," Portland Press, London, UK.

De Rosa M., De Brasi D., Zarrilli S., Paesano L., Pivonello R., D Agostino A., Longobardi S., Merola B., Lupoli G., Ogata T., and Lombardi G. (1997). Short stature and azoospermia in a patient with Y chromosome long arm deletion. *Journal of Endocrinological Investigation* **20:** 623-8.

Deng C., and Capecchi M. (1992). Reexamination of gene targeting frequency as a function of the extent of homology between the targeting vector and the target locus. *Molecular and Cellular Biology* **12:** 3365-71.

Diekert K., Kispal G., Guiard B., and Lill R. (1999). An internal targeting signal directing proteins into the mitochondrial intermembrane space. *Proceedings of the National Academy of Sciences of the United States of America* **96:** 11752-7.

Dietmeier K., Honlinger A., Bomer U., Dekker P., Eckerskorn C., Lottspeich F., Kubrich M., and Pfanner N. (1997). Tom5 functionally links mitochondrial preprotein receptors to the general import pore. *Nature* **388:** 195-200.

DiMauro S., and Moraes C. (1993). Mitochondrial encephalomyopathies. *Archives of Neurology* **50:** 1197-208.

DiMauro S., and Schon E. (2001). Mitochondrial DNA mutations in human disease. *American Journal of Medical Genetics* **106:** 18-26.

Downie J., Stewart J., and Sherman F. (1977). Yeast mutants defective in iso-2-cytochrome c. *Journal of Molecular Biology* **117:** 369-86.

Duker J., Weiss J., Siber M., Bieber F., and Albert D. (1985). Ocular findings in a new heritable syndrome of brain, eye, and urogenital abnormalities. *American Journal of Ophthalmology* **99:** 51-55.

Dumont M., Cardillo T., Hayes M., and Sherman F. (1991). Role of cytochrome c heme lyase in mitochondrial import and accumulation of cytochrome c in *Saccharomyces cerevisiae*. *Molecular and Cellular Biology* **11:** 5487-96.

Dumont M., Cardillo T., Hayes M., and Sherman F. (1991). Role of cytochrome *c* in *Saccharomyces cerevisiae*. *Molecular and Cellular Biology* **11:** 5487-5496.

Dumont M., Ernst J., Hampsey D., and Sherman F. (1987). Identification and sequence of the gene encoding cytochrome c heme lyase in the yeast *Saccharomyces cerevisiae*. *The Embo Journal* **6:** 235-41.

Dumont M., Ernst J., and Sherman F. (1988). Coupling of heme attachment to import of cytochrome c into yeast mitochondria. Studies with heme lyase-deficient mitochondria and altered apocytochromes c. *The Journal of Biological Chemistry* **263:** 15928-37.

Dumont M., Mathews A., Nall B., Baim S., Eustice D., and Sherman F. (1990). Differential stability of two apo-isocytochromes c in the yeast *Saccharomyces cerevisiae. The Journal of Biological Chemistry* **265:** 2733-9.

Dumoulin R., Sagnol I., Ferlin T., Bozon D., Stepien G., and Mousson B. (1996). A novel gly290asp mitochondrial *cytochrome b* mutation linked to a complex III deficiency in progressive exercise intolerance. *Molecular and Cellular Probes* **10:** 389-91.

Ellison J., Passage M., Yu L., Yen P., Mohandas T., and Shapiro L. (1992). Directed isolation of human genes that escape X inactivation. *Somatic and Cell Molecular Genetics* **18:** 259-268.

Ellison K., Fill C., Terwilliger J., DeGennaro L., Martin Gallardo A., Anvret M., Percy A., Ott J., and Zoghbi H. (1992). Examination of X chromosome markers in Rett syndrome: Exclusion mapping with a novel variation on multilocus linkage analysis. *American Journal of Human Genetics* **50:** 278-87.

Esaki M., Kanamori T., Nishikawa S., and Endo T. (1999). Two distinct mechanisms drive protein translocation across the mitochondrial outer membrane in the late step of the cytochrome b(2) import pathway. *Proceedings of the National Academy of Sciences of the United States of America* **96:** 11770-5.

Esposti M., De Vries S., Crimi M., Ghelli A., Patarnello T., and Meyer A. (1993). Mitochondrial cytochrome b: evolution and structure of the protein. *Biochimica Et Biophysica Acta* **1143:** 243-71.

Evans M., and Kaufman M. (1981). Establishment in culture of pluripotential cells from mouse embryos. *Nature* **292:** 154-6.

Ferrans V., H. M., and Haese W. (1976). Infantile cardiomyopathy with histiocytoid change in cardiac muscle cells: Report of six patients. *Circulation* **53:** 708-19.

Fisher N., and Meunier B. (2001). Effects of mutations in mitochondrial *cytochrome b* in yeast and man. Deficiency, compensation and disease. *European Journal of Biochemistry* **268:** 1155-62.

Franciosi R., and Singh A. (1988). Oncocytic cardiomyopathy syndrome. *Human Pathology* **19:** 1361-2.

Franco B., Meroni G., Parenti G., Levilliers J., Bernard L., Gebbia M., Cox L., Maroteaux P., Sheffield L., and Rappold G. A. (1995). A cluster of sulfatase genes on Xp22.3: Mutations in chondrodysplasia punctata (*CDPX*) and implications for warfarin embryopathy. *Cell* **81:** 15-25.

Furuyama K., and Sassa S. (2000). Interaction between succinyl CoA synthetase and the heme-biosynthetic enzyme ALAS-E is disrupted in sideroblastic anemia. *The Journal of Clinical Investigation* **105:** 757-64.

Garland J., and Rudin C. (1998). Cytochrome c induces caspase-dependent apoptosis in intact hematopoietic cells and overrides apoptosis suppression mediated by bcl-2, growth factor signaling, MAP-kinase-kinase, and malignant change. *Blood* **92:** 1235-46.

Gelb A., Van Meter S., Billingham M., Berry G., and Rouse R. (1993). Infantile histiocytoid cardiomyopathy- myocardial or conduction system hamartoma: What is the cell type involved? *Human Pathology* **24:** 1226-31.

Gonzales D., and Neupert W. (1990). Biogenesis of mitochondrial c-type cytochromes. *Journal of Bioenergetics and Biomembranes* **22:** 753-68.

Goodfellow B., Dias J., Ferreira G., Henklein P., Wray V., and Macedo A. (2001). The solution structure and heme binding of the presequence of murine 5-aminolevulinate synthase. *Febs Letters* **505:** 325-31.

Green D., and Kroemer G. (1998). The central executioners of apoptosis: Caspases or mitochondria? *Trends in Cell Biology* **8:** 267-71.

Gu H., Zou Y., and Rajewsky K. (1993). Independent control of immunoglobulin switch recombination at individual switch regions evidenced through Cre-loxP-mediated gene targeting. *Cell* **73:** 1155-64.

Happle R., Daniels O., and Koopman R. J. (1993). MIDAS syndrome (microphthalmia, dermal aplasia, and sclerocornea): An X-linked phenotype distinct from goltz syndrome. *American Journal of Medical Genetics* **47:** 710-713.

Harlow E., and Lane D. (1988). "Antibodies: A laboratory manual," Cold Spring Harbor Press, Cold Spring Harbor, New York.

Hasty P., Rivera Perez J., Chang C., and Bradley A. (1991). Target frequency and integration pattern for insertion and replacement vectors in embryonic stem cells. *Molecular and Cellular Biology* **11:** 4509-17.

Howell N., Nalty M., and Appel J. (1986). A digitonin-based procedure for the isolation of mitochondrial DNA from mammalian cells. *Plasmid* **16:** 77-80.

Johns D., Smith K., Savino P., and Miller N. (1993). Leber's hereditary optic neuropathy. Clinical manifestations of the 15257 mutation. *Ophthalmology* **100:** 981-6.

Kauffman S., Chandra N., Peress N., and Rodriguez Torres R. (1972). Idiopathic infantile cardiomyopathy with involvement of the conduction system. *The American Journal of Cardiology* **30:** 648-52.

Kayserili H., Cox T., Cox L., Basaran S., Kilic G., Ballabio A., and Yuksel Apak M. (2001). Molecular characterisation of a new case of microphthalmia with linear skin defects (MLS). *Journal of Medical Genetics* **38:** 411-7.

Kim U., Shizuya H., Birren B., Slepak T., de Jong P., and Simon M. (1994). Selection of chromosome 22-specific clones from human genomic BAC library using a chromosome-specific cosmid library pool. *Genomics* **22:** 336-9.

King M., and Attardi G. (1989). Human cells lacking mtDNA: Repopulation with exogenous mitochondria by complementation. *Science* **246:** 500-3.

Kneller D., Cohen F., and Langridge R. (1990). Improvements in protein secondary structure prediction by an enhanced neural network. *Journal of Molecular Biology* **214:** 171-82.

Koentgen F., and Stewart C. (1993). Simple screening procedure to detect gene targeting events in embryonic stem cells. *Methods in Enzymology* **225:** 878-90.

Kozak M. (1984). Compilation and analysis of sequences upstream from the translational start site in eukaryotic mRNAs. *Nucleic Acids Research* **12:** 857-72.

Kutsche K., Werner W., Bartsch O., von der Wense A., Meinecke P., and Gal A. (2002). Microphthalmia with linear skin defects syndrome (MLS): A male with a mosaic paracentric inversion of Xp. *Cytogenetics and Genome Research* **99:** 297-302.

Kwee L., Burns D., Rumberger J., Norton C., Wolitzky B., Terry R., Lombard Gillooly K., Shuster D., Koentgen F., and Stewart C. (1995). Creation and characterization of E-selectin- and VCAM-1-deficient mice. *Ciba Foundation Symposium* **189:** 17-28; discussion 28-34, 77-8.

Kyte J., and Doolittle R. (1982). A simple method for displaying the hydropathic character of a protein. *Journal of Molecular Biology* **157:** 105-32.

Larsson N., Wang J., Wilhelmsson H., Oldfors A., Rustin P., Lewandoski M., Barsh G., and Clayton D. (1998). Mitochondrial transcription factor A is necessary for mtDNA maintenance and embryogenesis in mice. *Nature Genetics* **18:** 231-6.

Lathrop J., and Timko M. (1993). Regulation by heme of mitochondrial protein transport through a conserved amino acid motif. *Science* **259:** 522-5.

Lee W., Ferrero G., Chinault A., Yen P., and Ballabio A. (1993). A yeast artificial chromosome contig linking the steroid sulfatase and Kallmann syndrome loci on the human X chromosome short arm. *Genomics* **18:** 1-6.

Lenzmeier B., and Freudenreich C. (2003). Trinucleotide repeat instability: A hairpin curve at the crossroads of replication, recombination, and repair. *Cytogenetics and Genome Research* **100:** 7-24.

Li K., Li Y., Shelton J., Richardson J., Spencer E., Chen Z., Wang X., and Williams R. (2000). Cytochrome c deficiency causes embryonic lethality and attenuates stress-induced apoptosis. *Cell* **101:** 389-99.

Lill R., Stuart R., Drygas M., Nargang F., and Neupert W. (1992). Import of cytochrome *c* heme lyase into mitochondria: A novel pathway into the intermembrane space. *The Embo Journal* **11:** 449-456.

Lindor N., Michels V., Hoppe D., Driscoll D., Leavitt J., and Dewald G. (1992). Xp22.3 microdeletion syndrome with microphthalmia, sclerocornea, linear skin defects, and congenital heart defects. *American Journal of Medical Genetics* **44:** 61-65.

Lindsay E., Grillo A., Ferrero G., Roth E., Magenis E., Grompe M., Hulten M., Gould C., Baldini A., Zoghbi H., and Ballabio A. (1994). Microphthalmia with linear skin defects (MLS) syndrome: Clinical, cytogenetic, and molecular characterization. *American Journal of Medical Genetics* **49:** 000-000.

Lints T., Parsons L., Hartley L., Lyons I., and Harvey R. (1993). *Nkx-2.5*: A novel murine homeobox gene expressed in early heart progenitor cells and their myogenic descendants. *Development* **119:** 419-31.

Lober C., Lenz Stoppler C., and Dobbelstein M. (2002). Adenovirus E1-transformed cells grow despite the continuous presence of transcriptionally active p53. *The Journal of General Virology* **83:** 2047-57.

Lyon H. (1961). Gene action in the X-chromosome of the mouse. *Naturwissenschaften* **190:** 372-3.

Malhotra V., Ferrans V., and Virmani R. (1994). Infantile histiocytoid cardiomyopathy: Three cases and literature review. *American Heart Journal* **128:** 1009-21.

Marin Garcia J., Hu Y., Ananthakrishnan R., Pierpont M., Pierpont G., and Goldenthal M. (1996). A point mutation in the *cytb* gene of cardiac mtDNA associated with complex III deficiency in ischemic cardiomyopathy. *Biochemistry and Molecular Biology International* **40:** 487-95.

Maurer Stroh S., Eisenhaber B., and Eisenhaber F. (2002). N-terminal N-myristoylation of proteins: Prediction of substrate proteins from amino acid sequence. *Journal of Molecular Biology* **317:** 541-57.

May B., Dogra S., Sadlon T., Bhasker C., Cox T., and Bottomley S. (1995). Molecular regulation of heme biosynthesis in higher vertebrates. *Progress in Nucleic Acid Research and Molecular Biology* **51:** 1-51.

Mayer A., Neupert W., and Lill R. (1995). Translocaiton of apocytochrome c across the outer membrane of mitochondria. *The Journal of Biological Chemistry* **21:** 12390-12397.

McKusick V., Francomano C., and Antonarakis S. (1995). "Mendelian inheritance in man.," Johns Hopkins University Press, Baltimore.

Melton D. (1994). Gene targeting in the mouse. *Bioessays* **16:** 633-8.

Migeon B. (1998). Non-random X chromosome inactivation in mammalian cells. *Cytogenetics and Cell Genetics* **80:** 142-148.

Mori M., and Terada K. (1998). Mitochondrial protein import in animals. *Biochimica Et Biophysica Acta* **1403:** 12-27.

Nagy A. (1996). Engineering the mouse genome. *In* "Mammalian Development" (P. Lonai, Ed.), pp. 339-371, Harwood Academic Publishers, Amsterdam.

Nagy A. (2000). Cre recombinase: The universal reagent for genome tailoring. *Genesis* **26:** 99-109.

Nagy A., Gocza E., Diaz E., Prideaux V., Ivanyi E., Markkula M., and Rossant J. (1990). Embryonic stem cells alone are able to support fetal development in the mouse. *Development* **110:** 815-21.

Naritomi K., Izumikawa Y., Nagataki S., Fukushima Y., Wakui K., Niikawa N., and Hirayama K. (1992). Combined Goltz and Aicardi syndromes in a terminal Xp deletion: Are they a contiguous gene syndrome? *American Journal of Medical Genetics* **43:** 839-43.

Nicholson D., Hergersberg C., and Neupert W. (1988). Role of cytochrome c heme lyase in the import of cytochrome c into mitochondria. *The Journal of Biological Chemistry* **263:** 19034-42.

Nicholson D., and Neupert W. (1989). Import of cytochrome c into mitochondria: Reduction of heme, mediated by NADH and flavin nucleotides, is obligatory for its covalent linkage to apocytochrome c. *Proceedings of the National Academy of Sciences of the United States of America* **86:** 4340-4.

Nobumoto M., Yamada M., Song S., Inouye S., and Nakazawa A. (1998). Mechanism of mitochondrial import of adenylate kinase isozymes. *The Journal of Biochemistry* **123:** 128-35.

Nozaki M., Ohishi K., Yamada N., Kinoshita T., Nagy A., and Takeda J. (1999). Developmental abnormalities of glycosylphosphatidylinositol-anchor-deficient embryos revealed by Cre/loxP system. *Laboratory Investigation* **79:** 293-9.

Omura T. (1998). Mitochondria-targeting sequence, a multi-role sorting sequence recognized at all steps of protein import into mitochondria. *The Journal of Biochemistry* **123:** 1010-6.

Otani M., Hoshida H., Saji T., Matsuo N., and Kawamura S. (1995). Histiocytoid cardiomyopathy with hypotonia in an infant. *Pathology International* **45:** 774-80.

Panigrahi G., Beatty L., and Sadowski P. (1992). The FLP protein contacts both major and minor grooves of its recognition target sequence. *Nucleic Acids Research* **20:** 5927-35.

Papadimitriou A., Neustein H., Dimauro S., Stanton R., and Bresolin N. (1984). Histiocytoid cardiomyopathy of infancy: Deficiency of reducible cytochrome b in heart mitochondria. *Pediatric Research* **18:** 1023-8.

Perry J., Short K. M., Romer J. T., Swift S., Cox T. C., and Ashworth A. (1999). *FXY2/MID2*, a gene related to the X-linked Opitz syndrome gene FXY/MID1, maps to Xq22 and encodes a FNIII domain-containing protein that associates with microtubules. *Genomics* **62:** 385-94.

Pfanner N., Craig E., and Honlinger A. (1997). Mitochondrial preprotein translocase. *Annual Review of Cell and Developmental Biology* **13:** 25-51.

Pfanner N., and Geissler A. (2001). Versatility of the mitochondrial protein import machinery. *Nature Reviews Molecular and Cell Biology* **2:** 339-49.

Postic C., Shiota M., Niswender K., Jetton T., Chen Y., Moates J., Shelton K., Lindner J., Cherrington A., and Magnuson M. (1999). Dual roles for glucokinase in glucose homeostasis as determined by liver and pancreatic beta cell-specific gene knock-outs using Cre recombinase. *The Journal of Biological Chemistry* **274:** 305-15.

Prakash S., Cormier T., McCall A., Garcia J., Sierra R., Haupt B., Zoghbi H., and Van Den Veyver I. (2002). Loss of holocytochrome c-type synthetase causes the male lethality of X-linked dominant microphthalmia with linear skin defects (MLS) syndrome. *Human Molecular Genetics* **11:** 3237-48.

Prakash S., Paylor R., Jenna S., Lamarche Vane N., Armstrong D., Xu B., Mancini M., and Zoghbi H. (2000). Functional analysis of ARHGAP6, a novel GTPase-activating protein for RhoA. *Human Molecular Genetics* **9:** 477-88.

Prasher D. (1995). Using GFP to see the light. *Trends in Genetics* **11:** 320-329.

Quaderi N., Schweiger S., Gaudenz K., Franco B., Rugarli E., Berger W., Feldman G., Volta M., Andolfi G., Gilgenkrantz S., Marion R., Hennekam R., Opitz J., Muenke M., Ropers H., and Ballabio A. (1997). Opitz G/BBB syndrome, a defect of midline development, is due to mutations in a new RING finger gene on Xp22. *Nature Genetics* **17:** 285-91.

Sambrock J., Fritsch E., and Maniatis T. (1989). "Molecular cloning, A laboratory manual," Laboratory Press, Cold Spring Harbor, New York.

Sauer B. (1998). Inducible gene targeting in mice using the Cre/lox system. *Methods* **14:** 381-92.

Schaefer L., Ballabio A., and Zoghbi H. (1996). Cloning and characterization of a putative human holocytochrome c-type synthetase gene (*HCCS*) isolated from the critical region for microphthalmia with linear skin defects (MLS). *Genomics* **34:** 166-72.

Schaefer L., Prakash S., and Zoghbi H. (1997). Cloning and characterization of a novel rho-type GTPase-activating protein gene (*ARHGAP6*) from the critical region for microphthalmia with linear skin defects. *Genomics* **46:** 268-77.

Schagger H. (2002). Respiratory chain supercomplexes of mitochondria and bacteria. *Biochimica Et Biophysica Acta* **1555:** 154-9.

Schanen N., Dahle E., Capozzoli F., Holm V., Zoghbi H., and Francke U. (1997). A new Rett syndrome family consistent with X-linked inheritance expands the X chromosome exclusion map. *American Journal of Human Genetics* **61:** 634-41.

Schoenhaut D., and Curtis P. (1986). Nucleotide sequence of mouse 5-aminolevulinic acid synthase cDNA and expression of its gene in hepatic and erythroid tissues. *Gene* **48:** 55-63.

Schwartz R., and Olson E. (1999). Building the heart piece by piece: Modularity of cis-elements regulating *Nkx2-5* transcription. *Development* **126:** 4187-92.

Schwarz Q. (1997). Characterisation of a candidate gene for oncocytic cardiomyopathy, a monogenic disorder contributing to the MIDAS phenotype. *In* "Department of Genetics", University of Adelaide, Adelaide.

Schwarz Q., and Cox T. (2002). Complementation of a yeast CYC3 deficiency identifies an X-linked mammalian activator of apocytochrome c. *Genomics* **79:** 51-7.

Segui Real B., Kispal G., Lill R., and Neupert W. (1993). Functional independence of the protein translocaiton machineries in mitochondrial outer and inner memebranes: Passage of preproteins through the intermembrane space. *The Embo Journal* **5:** 2211-2218.

Shehata B., Patterson K., Thomas J., Scala Barnett D., Dasu S., and Robinson H. (1998). Histiocytoid cardiomyopathy: three new cases and a review of the literature. *Pediatric and Developmental Pathology* **1:** 56-69.

Sherman F., Stewart J., Jackson M., Gilmore R., and Parker J. (1974). Mutants of yeast defective in iso-1-cytochrome c. *Genetics* **77:** 255-284.

Sherman F., Stewart J., Parker J., Inhaber E., Shipman N., Putterman G., Gardisky R., and Margoliash E. (1968). The mutational alteration of the primary structure of yeast iso-1-cytochrome c. *The Journal of Biological Chemistry* **243:** 5446-56.

Shoubridge E. (2001). Nuclear gene defects in respiratory chain disorders. *Seminars in Neurology* **21:** 261-7.

Siber M. (1984). X-linked recessive microencephaly, microphthalmia with corneal opacities, spastic quadriplesia, hypospadias and cryptorchidism. *Clinical Genetics* **26:** 453-6.

Sikorski R., and Hieter P. (1989). A system of shuttle vectors and yeast host strains designed for efficient manipulation of DNA in *Saccharomyces cerevisiae*. *Genetics* **122:** 19-27.

Silver M., Burns J., Sethi R., and Rowe R. (1980). Oncocytic cardiomyopathy in an infant with oncocytosis in exocrine and endocrine glands. *Human Pathology* **11:** 598-605.

Steiner H., Kispal G., Zollner A., Haid A., Neupert W., and Lill R. (1996). Heme binding to a conserved cys-pro-val motif is crucial for the catalytic function of mitochondrial heme lyases. *The Journal of Biological Chemistry* **271:** 32605-32611.

Steiner H., Zollner A., Haid A., Neupert W., and Lill R. (1995). Biogenesis of mitochondrial heme lyases in yeast: Import and folding in the intermembrane space. *The Journal of Biological Chemistry* **270:** 22842-9.

Sun X., Lewandoski M., Meyers E., Liu Y., Maxson R., and Martin G. (2000). Conditional inactivation of *Fgf4* reveals complexity of signalling during limb bud development. *Nature Genetics* **25:** 83-6.

Suzuki H., Kamada N., Ueda O., Jishage K., Kurihara Y., Kurihara H., Terauchi Y., Azuma S., Kadowaki T., Kodama T., Yazaki Y., and Toyoda Y. (1997). Germ-line contribution of embryonic stem cells in chimeric mice: Influence of karyotype and in vitro differentiation ability. *Experimental Animals* **46:** 17-23.

Temple I., MacDowall P., Baraitser M., and Atherton D. (1990). Focal dermal hypoplasia (Goltz syndrome). *Journal of Medical Genetics* **27:** 180-187.

Thomas K., and Capecchi M. (1987). Site-directed mutagenesis by gene targeting in mouse embryo-derived stem cells. *Cell* **51:** 503-12.

Thompson J., Higgins D., and Gibson T. (1994). CLUSTAL W: Improving the sensitivity of progressive multiple sequence alignment through sequence weighting, position-specific gap penalties and weight matrix choice. *Nucleic Acids Research* **22:** 4673-80.

Tong J., and Margoliash E. (1998). Cytochrome c heme lyase activity of yeast mitochondria. *The Journal of Biological Chemistry* **273:** 25695-702.

Usdin K., and Grabczyk E. (2000). DNA repeat expansions and human disease. *Cellular and Molecular Life Sciences* **57:** 914-31.

Valnot I., Kassis J., Chretien D., de Lonlay P., Parfait B., Munnich A., Kachaner J., Rustin P., and Rotig A. (1999). A mitochondrial *cytochrome b* mutation but no mutations of nuclearly encoded subunits in ubiquinol cytochrome c reductase (complex III) deficiency. *Human Genetics* **104:** 460-6.

Van den Veyver I. (2002). Microphthalmia with linear skin defects (MLS), Aicardi, and Goltz syndromes: are they related X-linked dominant male-lethal disorders? *Cytogenetics and Genome Research* **99:** 289-96.

Van den Veyver I., Cormier T., Jurecic V., Baldini A., and Zoghbi H. (1998). Characterization and physical mapping in human and mouse of a novel RING finger gene in Xp22. *Genomics* **51:** 251-61.

Van den Veyver I., Subramanian S., and Zoghbi H. (1998). Genomic structure of a human holocytochrome c-type synthetase gene in Xp22.3 and mutation analysis in patients with Rett syndrome. *American Journal of Medical Genetics* **78:** 179-81.

van Deursen J., and Wieringa B. (1992). Targeting of the creatine kinase M gene in embryonic stem cells using isogenic and nonisogenic vectors. *Nucleic Acids Research* **20:** 3815-20.

van Loon A., Eilers M., Baker A., and Verner K. (1988). Transport of proteins into yeast mitochondria. *Journal of Cellular Biochemistry* **36:** 59-71.

Wallace D. (1999). Mitochondrial diseases in man and mouse. *Science* **283:** 1482-8.

Wang X., Dumont M., and Sherman F. (1996). Sequence requirements for mitochondrial import of yeast cytochrome c. *The Journal of Biological Chemistry* **271:** 6594-604.

Wapenaar M., Bassi M., Schaefer L., Grillo A., Ferrero G., Chinault A., Ballabio A., and Zoghbi H. (1993). The genes for X-linked ocular albinism (*OA1*) and microphthalmia with linear skin defects (MLS): Cloning and characterization of the critical regions. *Human Molecular Genetics* **2:** 947-52.

Wapenaar M., Schiaffino M., Bassi M., Schaefer L., Chinault A., Zoghbi H., and Ballabio A. (1994). A YAC-based binning strategy facilitating the rapid assembly of cosmid contigs: 1.6 Mb of overlapping cosmids in Xp22. *Human Molecular Genetics* **3:** 1155-61.

Willard H. (1996). X chromosome inactivation, XIST, and pursuit of the X-inactivation center. *Cell* **86:** 5-7.

Wood S., Allen N., Rossant J., Auerbach A., and Nagy A. (1993). Non-injection methods for the production of embryonic stem cell-embryo chimaeras. *Nature* **365:** 87-9.

Wu H., Rao G., Dai B., and Singh P. (2000). Autocrine gastrins in colon cancer cells Up-regulate cytochrome c oxidase Vb and down-regulate efflux of cytochrome c and activation of caspase-3. *The Journal of Biological Chemistry* **275:** 32491-8.

Zhou L., Rowley D., Mi Q., Sefcovic N., Matthes H., Kieffer B., and Donovan D. (2001). Murine inter-strain polymorphisms alter gene targeting frequencies at the mu opioid receptor locus in embryonic stem cells. *Mammalian Genome* **12:** 772-8.

Zimmermann A., Diem P., and Cottier H. (1982). Congenital "histiocytoid" cardiomyopathy: Evidence suggesting a developmental disorder of the purkinje cell system of the heart. *Virchows Archive* **396:** 187-95.

Zollner A., Rodel G., and Haid A. (1992). Molecular cloning and characterization of the *Saccharomyces cerevisiae CYT2* gene encoding cytochrome-c1-heme lyase. *European Journal of Biochemistry* **207:** 1093-100.

Schwarz, Q.P., and Cox, T.C., (2002) Complementation of a yeast *CYC3* deficiency identifies an x-linked mammalian activator of apocytochrome *c*.
Genomics, v. 79 (1), pp. 51-57.

Cox, T.C., Sadlon, T.J., Schwarz, Q. P., Matthews, C.P., Wise, P.D., Cox, L.L., Bottomley, S.S., and May, B.K., (2004) The major splice variant of human 5-aminolevulinate synthase-2 contributes significantly to erythroid heme biosynthesis. *International Journal of Biochemistry and Cell Biology, v. 36 (2), pp. 281-295, February 2004*